Methods in Molecular Biology 1686

Springer Protocols

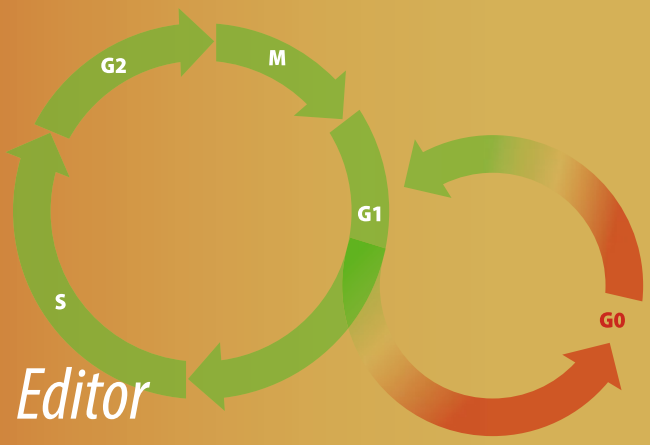


H. Daniel Lacorazza *Editor*

# Cellular Quiescence

## Methods and Protocols

Humana Press

# METHODS IN MOLECULAR BIOLOGY

*Series Editor*
**John M. Walker**
**School of Life and Medical Sciences**
**University of Hertfordshire**
**Hatfield, Hertfordshire, AL10 9AB, UK**

For further volumes:
http://www.springer.com/series/7651

# Cellular Quiescence

## Methods and Protocols

Edited by

**H. Daniel Lacorazza**

*Texas Children's Hospital, Baylor College of Medicine, Houston, TX, USA*

Humana Press

*Editor*
H. Daniel Lacorazza
Texas Children's Hospital
Baylor College of Medicine
Houston, TX, USA

ISSN 1064-3745 ISSN 1940-6029 (electronic)
Methods in Molecular Biology
ISBN 978-1-4939-7370-5 ISBN 978-1-4939-7371-2 (eBook)
DOI 10.1007/978-1-4939-7371-2

Library of Congress Control Number: 2017954401



Printed on acid-free paper

This Humana Press imprint is published by Springer Nature
The registered company is Springer Science+Business Media LLC
The registered company address is: 233 Spring Street, New York, NY 10013, U.S.A.

# Preface

Quiescence is defined as a state of quietness or inactivity. The concept of cellular quiescence has rapidly evolved in recent years from a default state devoid of extracellular nutrients to an actively regulated and reversible cell cycle arrest poised to re-enter the cell cycle in response to a combination of cell-intrinsic and cell-extrinsic factors. Recent technological breakthroughs have allowed the study of the regulation of cellular quiescence in well-defined stem cell subsets by either flow cytometric or tissue detection.

A state of dormancy and inertness has clear implications in the maintenance of tissue-specific stem cells because this state is believed to preserve stemness and prevent the accumulation of genomic aberrations ensuring the regeneration of a healthy tissue during homeostasis or in response to injury. On the other hand, cancerous and leukemic cells have hijacked this property to evade deleterious toxicities caused by cell cycle-dependent chemodrugs. A better understanding of how cells enter a quiescent state during homeostasis and how cells exit quiescence and re-enter differentiating cell divisions to restore damaged tissues is essential for developing new approaches in regenerative medicine in the future.

The main goal of this book is not to give a comprehensive account of all techniques available but rather a broad view of basic and cutting-edge technology to inspire research in this emerging field of cell biology. The chapters in this book are designed to address cellular quiescence in prokaryote and eukaryote organisms, detection of quiescence (Hoechst/pyronin Y, FUCCI, CFSE, BrdU, H2B-GFP, CyTOF), quiescence in stem cells (skin, intestinal, neuronal, hematopoietic), genomic regulation (gene expression, transcription factors, lncRNA, RNA methylation), and finally, an analysis of the heterogeneity of quiescence by computer modeling.

*Houston, TX, USA* *H. Daniel Lacorazza*

# Contents

# Contributors


Hassan Azari • *Neural Stem Cell and Regenerative Neuroscience Laboratory, Department of Anatomical Sciences and Shiraz Institute for Regenerative Medicine, Shiraz University of Medical Sciences, Shiraz, Iran*

Gregory K. Behbehani • *Division of Hematology, Ohio State University and James Cancer Hospital, Columbus, OH, USA*

Holger Bierhoff • *Department of Biochemistry, Center for Molecular Biomedicine (CMB), Friedrich Schiller University Jena, Jena, Germany*

François D. Boussin • *CEA DSV iRCM SCSR; Laboratoire de Radiopathologie, INSERM; Université Paris Diderot, Sorbonne Paris Cité, Université Paris Sud, Paris, France*

Caroline E. Brun • *Regenerative Medicine Program, Department of Cellular and Molecular Medicine, Faculty of Medicine, Sprott Center for Stem Cell Research, Ottawa Hospital Research Institute, University of Ottawa, Ottawa, ON, Canada*

Syed I.A. Bukhari • *Center for Cancer Research, Massachusetts General Hospital, Harvard Medical School, Boston, MA, USA; Center for Regenerative Medicine, Massachusetts General Hospital, Harvard Medical School, Boston, MA, USA; Harvard Stem Cell Institute, Harvard University, Cambridge, MA, USA*

Johanna M. Buschhaus • *Department of Radiology, Center for Molecular Imaging, University of Michigan, Ann Arbor, MI, USA; Department of Biomedical Engineering, University of Michigan, Ann Arbor, MI, USA*

Stephanie Louise Canning • *Flow Cytometry Core Facility, Camelia Botnar Laboratories, UCL Great Ormond Street Institute of Child Health, London, UK*

Tom H. Cheung • *Division of Life Science, Center for Stem Cell Research, State Key Laboratory of Molecular Neuroscience, Center of Systems Biology and Human Health, Institute for Advanced Study, The Hong Kong University of Science and Technology, Clear Water Bay, Kowloon, Hong Kong, China*

Hongbo Chi • *Department of Immunology, St. Jude Children's Research Hospital, Memphis, TN, USA*

Alexandra Chicheportiche • *CEA DSV iRCM SCSR; Laboratoire de Radiopathologie, INSERM; Université Paris Diderot, Sorbonne Paris Cité, Université Paris Sud, Paris, France*

Hilary A. Coller • *Department of Molecular, Cell and Developmental Biology, University of California, Los Angeles, Los Angeles, CA, USA; Department of Biological Chemistry, David Geffen School of Medicine, Los Angeles, CA, USA*

Mathieu Daynac • *CEA DSV iRCM SCSR; Laboratoire de Radiopathologie, INSERM; Université Paris Diderot, Sorbonne Paris Cité, Université Paris Sud, Paris, France; Molecules Circuits Department, Neuroscience Paris-Saclay Institute, CNRS, Université Paris Sud, UMR9197, Paris, France; Department of Neurological Surgery, Helen Diller Comprehensive Cancer Research Center, University of California San Francisco, CA, USA*

Loic P. Deleyrolle • *Lillian S. Wells Department of Neurosurgery, McKnight Brain Institute, University of Florida, Gainesville, FL, USA; Preston A. Wells, Jr. Center for Brain Tumor Therapy, University of Florida, Gainesville, FL, USA*

Jyotsna Dhawan • *CSIR-Centre for Cellular and Molecular Biology, Hyderabad, India*

Ayad Eddaoudi • *Flow Cytometry Core Facility, Camelia Botnar Laboratories, UCL Great Ormond Street Institute of Child Health, London, UK*
Hardik P. Gala • *CSIR-Centre for Cellular and Molecular Biology, Hyderabad, India*
Linda D. Ho • *Department of Molecular, Cell and Developmental Biology, University of California, Los Angeles, Los Angeles, CA, USA*
Jenny Hsieh • *Department of Molecular Biology, University of Texas Southwestern Medical Center, Dallas, TX, USA; Hamon Center for Regenerative Science and Medicine, University of Texas Southwestern Medical Center, Dallas, TX, USA*
Kevin R. Hughes • *Nottingham Digestive Diseases Centre, Queen's Medical Centre, Nottingham, UK*
Emilie Jalbert • *Division of Hematology, Department of Medicine, University of Colorado Anschutz Medical Campus, Aurora, CO, USA*
Claudine S. Kadmon • *Pediatric Infectious Diseases, Stem Cells and Regenerative Medicine Center, Center for Cell and Gene Therapy, Baylor College of Medicine, Houston, TX, USA*
Itaru Kato • *Department of Pediatrics, Kyoto University Hospital, Kyoto, Japan*
Katherine Y. King • *Pediatric Infectious Diseases, Stem Cells and Regenerative Medicine Center, Center for Cell and Gene Therapy, Baylor College of Medicine, Houston, TX, USA; Texas Children's Hospital, Houston, TX, USA*
Jungeun Sarah Kwon • *Department of Molecular and Cellular Biology, University of Arizona, Tucson, AZ, USA*
H. Daniel Lacorazza • *Department of Pathology and Immunology, Baylor College of Medicine, Texas Children's Hospital, Houston, TX, USA*
Gary D. Luker • *Department of Radiology, Center for Molecular Imaging, University of Michigan, Ann Arbor, MI, USA; Department of Biomedical Engineering, University of Michigan, Ann Arbor, MI, USA; Department of Macromolecular Science and Engineering, University of Michigan, Ann Arbor, MI, USA*
Kathryn E. Luker • *Department of Radiology, Center for Molecular Imaging, University of Michigan, Ann Arbor, MI, USA*
Yashwant R. Mahida • *Nottingham Digestive Diseases Centre, Queen's Medical Centre, Nottingham, UK*
Katie A. Matatall • *Pediatric Infectious Diseases, Stem Cells and Regenerative Medicine Center, Center for Cell and Gene Therapy, Baylor College of Medicine, Houston, TX, USA*
Rakesh K. Mishra • *CSIR-Centre for Cellular and Molecular Biology, Hyderabad, India*
Mithun Mitra • *Department of Molecular, Cell and Developmental Biology, University of California, Los Angeles, CA, USA; Department of Biological Chemistry, David Geffen School of Medicine, Los Angeles, CA, USA*
Shradha Mukherjee • *Department of Molecular Biology, University of Texas Southwestern Medical Center, Dallas, TX, USA; Hamon Center for Regenerative Science and Medicine, University of Texas Southwestern Medical Center, Dallas, TX, USA*
Hoang Nguyen • *Department of Molecular and Cellular Biology, Stem Cell and Regenerative Medicine Center, Center for Cell and Gene Therapy, Baylor College of Medicine, Houston, TX, USA; Program in Developmental Biology, Department of Dermatology, Baylor College of Medicine, Houston, TX, USA*
Chun Shik Park • *Department of Pathology and Immunology, Baylor College of Medicine, Texas Children's Hospital, Houston, TX, USA*
Eric M. Pietras • *Division of Hematology, Department of Medicine, University of Colorado Anschutz Medical Campus, Aurora, CO, USA*

Brent A. Reynolds • *Lillian S. Wells Department of Neurosurgery, McKnight Brain Institute, University of Florida, Gainesville, FL, USA*
Christine N. Rodriguez • *Department of Molecular and Cellular Biology, Stem Cell and Regenerative Medicine Center, Center for Cell and Gene Therapy, Baylor College of Medicine, Houston, TX, USA*
Martial Ruat • *Molecules Circuits Department, Neuroscience Paris-Saclay Institute, CNRS, Université Paris Sud, UMR9197, Paris, France*
Michael A. Rudnicki • *Regenerative Medicine Program, Department of Cellular and Molecular Medicine, Faculty of Medicine, Sprott Center for Stem Cell Research, Ottawa Hospital Research Institute, University of Ottawa, Ottawa, ON, Canada*
Wai-Kin So • *Division of Life Science, Center for Stem Cell Research, State Key Laboratory of Molecular Neuroscience, Center of Systems Biology and Human Health, Institute for Advanced Study, The Hong Kong University of Science and Technology, Clear Water Bay, Kowloon, Hong Kong, China*
Marla M. Spain • *Basic Sciences Division, Fred Hutchinson Cancer Research Center, Seattle, WA, USA*
Surabhi Srivastava • *CSIR-Centre for Cellular and Molecular Biology, Hyderabad, India*
Sarah G. Swygert • *Basic Sciences Division, Fred Hutchinson Cancer Research Center, Seattle, WA, USA*
Samuel S. Truesdell • *Center for Cancer Research, Massachusetts General Hospital, Harvard Medical School, Boston, MA, USA; Center for Regenerative Medicine, Massachusetts General Hospital, Harvard Medical School, Boston, MA, USA; Harvard Stem Cell Institute, Harvard University, Cambridge, MA, USA*
Toshio Tsukiyama • *Basic Sciences Division, Fred Hutchinson Cancer Research Center, Seattle, WA, USA*
Shobha Vasudevan • *Center for Cancer Research, Massachusetts General Hospital, Harvard Medical School, Boston, MA, USA; Center for Regenerative Medicine, Massachusetts General Hospital, Harvard Medical School, Boston, MA, USA; Harvard Stem Cell Institute, Harvard University, Cambridge, MA, USA*
Xia Wang • *Department of Molecular and Cellular Biology, University of Arizona, Tucson, AZ, USA*
Yu Xin Wang • *Regenerative Medicine Program, Department of Cellular and Molecular Medicine, Faculty of Medicine, Sprott Center for Stem Cell Research, Ottawa Hospital Research Institute, University of Ottawa, Ottawa, ON, Canada*
Kai Yang • *Department of Immunology, St. Jude Children's Research Hospital, Memphis, TN, USA*
Guang Yao • *Department of Molecular and Cellular Biology, University of Arizona, Tucson, AZ, USA*

# Chapter 1

# Molecular Regulation of Cellular Quiescence: A Perspective from Adult Stem Cells and Its Niches

**Wai-Kin So and Tom H. Cheung**

## Abstract

Cellular quiescence is a reversible growth arrest state. In response to extracellular environment, quiescent cells are capable of resuming proliferation for tissue homeostasis and tissue regeneration. Subpopulations of adult stem cells remain quiescent and reside in their specialized stem cell niches. Within the niche, they interact with a repertoire of niche components. Niche integrates signals to maintain quiescence or gear stem cells toward regeneration. Recent studies provide insights into the regulatory components of stem cell niche and their influence on residing stem cells. Aberrant niche activities perturb stem cell quiescence and activation, compromise stem cell functions, and contribute to tissue aging and disease pathogenesis. This review covers current knowledge regarding cellular quiescence with a focus on original and emerging concepts of how niches influence stem cell quiescence.

**Key words** Cellular quiescence, Stem cell, Niche, Hair follicle stem cell, Bulge, Hematopoietic stem cell, Endosteal niche, Satellite cell, Myofiber, Skeletal muscle, Aging

## 1 A Historical Perspective of Cellular Quiescence

Using the radioactive labeling technique to label newly synthesized DNA in early cell division studies, it was found that a population of cells are negative for the labeling, suggesting the existence of a non-dividing, dormant state [1]. Similarly, some cells are more resistant to ablation in the studies using X-ray to eliminate cycling cells [2]. Within a population, some cells, or the "growth fraction," are cycling continuously whereas other cells exist in a non-proliferative state that they rarely divide during homeostasis. As a matter of fact, majority of cells in adult mammalian body are out of active cell cycle. They are cells that are either terminally differentiated or resided in a quiescence or senescence state [3]. Unlike lower multicellular organisms such as *Caenorhabditis elegans*, cells in its adult body are no longer able to proliferate, quiescent cells in higher multicellular organisms are able to reenter the cell cycle in response to various extrinsic stimuli [4]. For instance, injury reactivates

H. Daniel Lacorazza (ed.), *Cellular Quiescence: Methods and Protocols*, Methods in Molecular Biology, vol. 1686,
DOI 10.1007/978-1-4939-7371-2_1, 

quiescent cells to proliferate for tissue repair and regeneration [5, 6]. Nevertheless, quiescent cells are largely non-dividing under normal circumstance.

It was originally proposed that quiescence is a prolonged G1 phase of the cell cycle [4]. Quiescent and G1 cells share the characteristic of non-replicated 2n DNA content [7]. However, there are striking differences between the two states. For instance, quiescent cells proceed to S phase with a significant delay relative to G1 cells, suggesting that they are fundamentally different states [7]. Quiescence is a non-proliferative state out of the cell cycle, termed G0 phase [8] (Fig. 1). Two additional types of non-dividing cells, senescent and terminally differentiated cells, are also considered to be in the G0 phase. Among these G0 cells, reversibility of cell cycle arrest is a hallmark of cellular quiescence. This characteristic distinguishes quiescent cells from senescent and terminally differentiated cells as they are considered to be irreversibly restricted in the G0 phase and rarely reengage in active cell cycle under normal physiological conditions. It is important to note that certain differentiated cells, like mature hepatocytes, are also considered to be quiescent in normal tissues and are capable of entering the cell cycle in case of injury and stress [4]. Cells adopted quiescence, senescence or differentiation states have similar and also different characteristics. These cells contain similar DNA contents since all of them withdraw from the cell cycle during the G1 phase [9]. Distinctively, quiescent cells are smaller in cell size, metabolically less active with suppressed global RNA and protein synthesis, and display increased autophagy [10, 11].

Most of the early studies about mammalian cells quiescence employ in vitro cell culture quiescence models [4]. Through manipulating the culture conditions: serum deprivation, contact inhibition and loss of adhesion, cultured cells can be effectively driven into quiescence via distinct mechanisms [7, 10, 12–15]. These studies suggest the notion that the extracellular environment has pivotal regulatory roles in cellular quiescence. Such notion is further underpinned by more direct evidence. Mature hepatocytes are largely quiescent in intact liver and they undergo limited rounds of replication after partial hepatectomy [16]. Yet they exhibit more robust proliferative potential in vitro. They are able to proliferate continuously and develop into non-transformed lines [17], implicating that tissue environment tends to maintain cells in a quiescent state.

It is interesting and also important to answer the question that, at which point of the cell cycle, cells make the decision between going into quiescence or proliferation. Zetterberg and Larson demonstrated that only cells in early G1 phase exit the cell cycle and enter quiescence in response to serum starvation whereas growth of cells in late G1 phase is not arrested [7, 18]. The classic model of “restriction point” or “R point” based on the work by

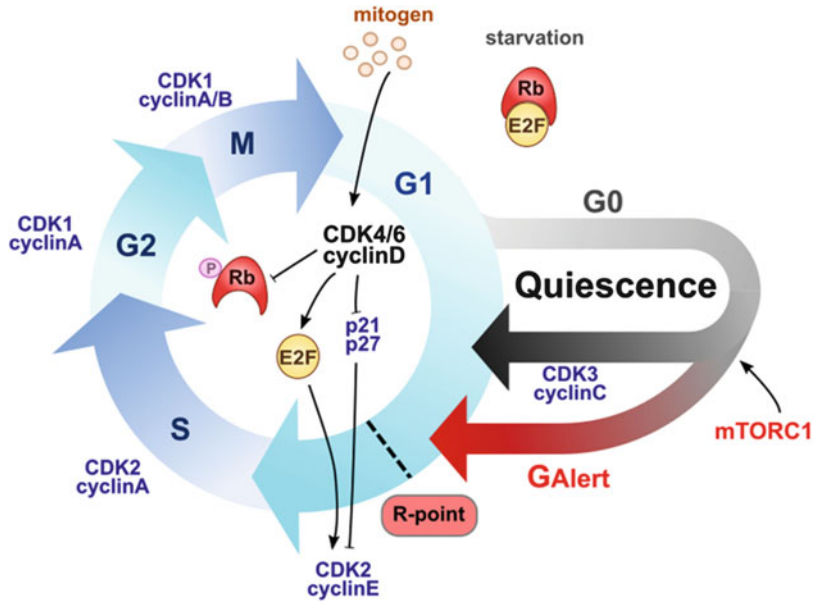


**Fig. 1** Cell cycle progression and cellular quiescence. Each of the four phases of the cell cycle is regulated by a specific complex of cyclin and CDK (cyclin-dependent kinase). The regulatory machinery of G1 progression overlaps with decision mechanism about the commitment to quiescence or proliferation before the restriction point (R point). Under mitogenic condition, CDK4/6/cyclinD complex phosphorylates Rb, thereby releasing E2F from Rb-inhibition. E2F then transactivates cyclin E. CDK2/cyclin E complex drives G1 to S phase transition. CDK4/6/cyclinD complex also removes p21 and p27 inhibition on CDK2. Cells in G1 phase exit the cell cycle and exist in G0 phase as quiescent, senescent, or differentiated cells. In the absence of mitogen, Rb is active and sequesters E2F to render its promoting effect on CDK2/cylin E complex formation. As a result, cell cycle arrest is induced and cells are then driven into quiescence. CDK3/cyclin C complex can drive cells to enter cell cycle from quiescence. In response to mTORC1 signaling, quiescent cells can transit into the GAlert phase and become poised for rapid cell cycle entry

Pardee supports the existence of a decision point in late G1 phase: before the R point, cells are withdrawn from the cell cycle and become quiescent under unfavorable growth conditions, like serum deprivation. When there is stimulation by mitogens, cells in G1 phase continue the cell cycle toward the R point. Once passed the R point, the cell cycle becomes autonomous and it will proceed to S phase and continue until completion regardless of serum availability [19] (Fig. 1). R point guards the proliferation and quiescence in normal, non-transformed cells and the loss of R point control is proposed to lead to uncontrolled replication of malignant cells [19].

## 2 Molecular Regulation of Cellular Quiescence

The molecular mechanism of R point is closely linked to the cell cycle machinery of G1 progression [20], in which the retinoblastoma (Rb) protein serves as the key determinant to enter

quiescence or to progress to S phase. Under mitogenic condition, Rb protein in cells is inactivated by hyperphosphorylation [20]. E2F is then released from Rb repression and promotes CDK2/Cyclin E complex formation, which promotes cell cycle progression to S phase (Fig. 1). Under conditions like serum insufficiency, Rb is hypophosphorylated and becomes active, E2F is sequestered and repressed by this growth-inhibitory form of Rb. Growth is arrested at G1 and cells are driven to quiescence [21] (Fig. 1). Activation of E2F under physiological serum levels is implicated in the reversibility of quiescence [3]. On the contrary, the threshold for E2F activation is greatly raised by high levels of CDK inhibitors, like p21 and p16 in senescent and differentiated cells [22, 23], making cell cycle arrest irreversible under normal growth conditions [3].

In contrast to the decision point in the G1 phase, there is a long-standing thought that commitment decision in whether to proceed to the next cell cycle occurs at the previous G2 phase [24, 25]. An alternative decision point located at late G2/M phase of the preceding cycle has also been proposed recently [26]. Governed by serum availability, cycling cells in late G2/M phases are bifurcated into two populations, defined by high and low CDK2 activities: in mitogenic environment, low p21 activity allows cells to build up CDK2 activity and commit to the next cell cycle whereas active p21 suppresses CDK2 and directs cells to quiescence when serum is insufficient [26].

Quiescent cells are low in metabolic activity and non-cycling. However, is quiescence solely a state of cell cycle arrest? Is quiescence a static or a dynamic cellular state? A recent transcriptional profiling revealed that, in addition to molecular signature of cell cycle arrest, quiescent cells actively express genes to prevent adoption terminal differentiation cell fate and thereby preserve the reversibility of cell cycle arrest [10]. Importantly, these transcriptional and functional aspects of quiescence could not be recapitulated by growth arrest induced by CDK inhibition [10]. Another recent study demonstrates that quiescent adult stem cells can reversibly transit between two distinct functional phases: “deep” quiescence (G0) and quiescence alert (GAlert) [27]. Quiescent stem cells are driven into GAlert in response to mTORC1 signaling elicited by distant injuries (Fig. 1). GAlert is an intermediate state between quiescence and activation, more akin to quiescence. Yet stem cells in GAlert exhibit a set of “alerting” properties that are distinct from quiescent cells: increased cell size, transcriptional activity, mitochondrial metabolism, and accelerated cell cycle entry [27]. Quiescence, once viewed as a static and non-dividing state, is emerging as a cell state that is poised and actively regulated.

## 3 The Evolving Stem Cell Niche Concept

### 3.1 The Classical Stem Cell Niche Hypothesis

The existence of specific microenvironment housing stem cells and regulating their functions was hypothesized based on evidence from early hematologic experiments. Hematopoietic stem cells (HSCs), which regenerate the entire blood and immune system, are difficult to be maintained under in vitro conditions [28]. Dexter demonstrated that HSCs co-culture with bone marrow stromal cells as an efficient mean of preserving HSCs functions [29]. In vivo, HSCs exhibit functional decline if they circulate freely outside the bone marrow, suggesting a dependency of HSCs on specific cues within the bone marrow [30]. Within the bone marrow, it was discovered that there are regions of discrete HSCs and progenitor cell densities, which are associated with the proliferative state of HSCs [31]. This suggests that spatially distinct microenvironments in the bone marrow regulate HSC state and functions [32].

In 1978, Schofield proposed that stem cells are located within tissues in association with other cells. The specialized cellular environment retaining stem cells was coined the term stem cell "niche" [33]. When stem cells are "fixed" in their respective niches, they are restrained from maturation and are capable of replicating indefinitely. Residing in the niche also protects stem cells from mutational errors [33]. An additional property of the niche is that it shapes the fate of stem cells. After a stem cell is divided, the daughter cell that remains in the niche will become a stem cell whereas another daughter cell that cannot occupy the niche will inevitably replicate and differentiate [33].

In *Caenorhabditis elegans*, somatic distal tip cells (DTCs) cap the ends of the gonads and constitute the niche for germline stem cells (GSCs) [34]. Factors from DTCs stimulate adjacent GSCs to proliferate and inhibit meiosis [35], thereby preventing GSC to differentiate into gametes and maintain adult GSCs population. Ablation of DTCs aberrantly shifts GSC self-renewal to differentiation [34]. Moreover, DTC niche maintains the organization of GSCs and gametes within the gonads. The two populations are polarized where GSCs is located at the distal end and gametes are located at the proximal end. Such polarity would be altered accordingly if positions of DTCs are changed during early development [35]. All these findings provide direct evidence to support the notion of the existence of a stem cell niche and laid the framework of the niche theory.

### 3.2 Emerging Concepts About Stem Cell Niche

Thus far, stem cells and their niches have been identified in numerous mammalian tissues. The interplay between stem cells and various niche components has started to be comprehensively elucidated. New dimensions have been proposed in addition to the original stem cell niche concepts. In this section, these new concepts will be discussed in detail.

#### 3.2.1 Stem Cell Progenies as Niche Cells

The list of niche cells contributing to stem cell microenvironment keeps growing. Recently, stem cell progenies have been shown to become niche cells and feedback to regulate stem cell behaviors [36, 37]. These progenies provide feedback cues to maintain quiescence and prevent excessive activation, thereby preserving a functional stem cell pool. Megakaryocytes (MKs) are myeloid lineage progenies of HSCs. MKs can feedback to regulate HSCs indirectly through the modification of the endosteal niche or to constitute as a part of the HSC niche themselves [38–41]. Two individual groups demonstrated that in vivo ablation of MKs resulted in loss of HSC quiescence and led to a marked increase in HSCs proliferation [40, 41]. Similarly, in the skin compartment, removal of terminally differentiation keratin 6 positive (K6+) inner bulge cells from hair follicles prematurely activates quiescent hair follicle stem cells (HFSCs) because signals from K6+ cells counterbalance other activating signals in the niche and maintain neighboring HFSCs in quiescence [42].

#### 3.2.2 Niche as an Integrator of Tissue and Organismal State

Adding to the view that stem cell niches are generated by signals within a local microenvironment of the stem cell, niche is emerging as an integrator of information from tissue as well as from more distant sites. This enables stem cell behaviors to be modulated in a manner that suits the homeostatic, physiological, or reparative needs of a given tissue. Long-range signals are delivered via vascular, immune, and neural inputs and are incorporated into the local milieu to regulate stem cells.

Skin is supplied with a rich milieu of factors from blood capillaries and neurons [43]. Hair follicle activity in rodents is remodeled during different reproductive states [44], presumably due to endocrine hormones. In pregnant and lactating females, systemic level of prolactin is elevated [45] (Table 1). Prolactin is a negative regulator of hair cycle as exogenous prolactin and prolactin receptor knockout delays and advances hair cycle, respectively [46, 47]. Reaching the hair follicle, inhibitory prolactin signal overrides local stimulatory signals and maintains HFSCs in quiescence, thereby stalling the initiation of a new cycle [48]. Niche also translates cues emanated from distant injuries into regulatory signals of stem cells. Muscle SCs are activated in response to blood-borne factors after burn injuries in distant sites [49, 50]. A recent study has revealed that systemic signals produced by remote injuries do not act directly on stem cells. Rather, they are translated into signals that remodel the extracellular matrix surrounding the stem cells and prime quiescent stem cells for more rapid activation [27]. Niche is the hub for these systemic signals being integrated into the local microenvironment. Such integration enables stem cells quiescence and activation to be regulated timely and appropriately according to the state of the organism.

**Table 1**
**Niche factors and their roles in stem cell quiescence**

| Niche factor | Receptor and signaling | Stem cell/ niche | Source in the niche | Effect on quiescence | Reference |
|---|---|---|---|---|---|
| *TGFβ/BMP signaling* | | | | | |
| TGFβ | TGFβRII, SMAD2/3 | HSC/bone marrow | Megakaryocyte, non-myelinated Schwann cell[a] | Maintain quiescence | [84, 102] |
| TGFβ2 | SMAD2/3 | HFSC/hair follicle | Dermal papilla | Exit quiescence | [59] |
| BMP2 | SMAD1/5/8 | HFSC/hair follicle | Adipocyte | Maintain quiescence, lodge aged HFSCs in quiescence | [44] |
| BMP4 | SMAD1/5/8 | HFSC/hair follicle | Dermal papilla, dermal fibroblast, adipocyte | Maintain quiescence | [44, 62] |
| BMP6 | | HFSC/hair follicle | K6+ bulge cell | Maintain quiescence | [42] |
| BMP inhibitors, Noggin | | HFSC/hair follicle | Dermal papilla | Exit quiescence | [56, 58] |
| Myostatin | | SC/skeletal muscle | SC | Maintain quiescence | [150] |
| Follistatin | | HFSC/hair follicle | Adipocyte | Exit quiescence | [144] |
| Notch | | | | | |
| Delta | Notch1, Notch3, canonical Notch signaling | SC/skeletal muscle | Myofiber, interstitial cell | Maintain quiescence | [120–124] |
| *Wnt signaling* | | | | | |
| Wnt5a | non-canonical Wnt signaling | HSC/bone marrow | Bone marrow stromal cell | Maintain quiescence | [100] |
| Dickkopf1 | Wnt/β-catenin | HSC/bone marrow | Osteoblast, stromal cell | Exit quiescence | [92, 94, 151] |
| Wnt inhibitors | Wnt/β-catenin | HFSC/hair follicle | HFSC | Maintain quiescence | [64, 65] |
| *Growth factors* | | | | | |
| FGF2 | FGFR1, FGFR4 | SC/skeletal muscle | Myofiber, connective tissue | Exit quiescence, disrupt quiescence in aged SCs | [127, 128, 146] |
| FGF1, FGF4 | FGFR4 | SC/skeletal muscle | Myofiber, connective tissue | Exit quiescence | [127, 129] |

(continued)

**Table 1**
**(continued)**

| Niche factor | Receptor and signaling | Stem cell/ niche | Source in the niche | Effect on quiescence | Reference |
|---|---|---|---|---|---|
| FGF6 | | SC/skeletal muscle | Myofiber | Exit quiescence | [127] |
| FGF7, FGF10 | FGFR2-IIIb, MAPK | HFSC/hair follicle | Dermal papilla | Exit quiescence | [56] |
| FGF18 | FGFR3 | HFSC/hair follicle | K6+ cell dermal papilla | Maintain quiescence | [42, 56] |
| BTC | EGFR | NSC/ olfactory bulb and dentate gyrus | Endothelial cell | Exit quiescence | [152] |
| HGF | cMet | SC/skeletal muscle | Myofiber, ECM | Exit quiescence | [127, 130, 134] |
| HGF | cMet, PI3K-AKT/ mTORC1 | SC/skeletal muscle, LT-HSC/bone marrow | Myofiber, ECM, connective tissue | $G_{Alert}$ transition | [27] |
| PDGFα | PDGFR | HFSC/hair follicle | Adipocyte precursor | Exit quiescence | [62] |
| *Other* | | | | | |
| Ang-1 | Tie2 | HSC/bone marrow | Osteoblast | Maintain quiescence | [83, 153, 154] |
| Thpo | Mpl | HSC/bone marrow | Osteoblast | Maintain quiescence | [90, 91] |
| CXCL12 | CXCR4 | HSC/bone marrow | CAR cell, osteoblast, endothelial cell, megakaryocyte | Maintain quiescence | [40, 104–106] |
| Prolactin | prolactin receptor, JAK/ STAT5 | HFSC/hair follicle | Circulation | Maintain quiescence | [48] |

*Abbreviations: Ang-1* angiopoietin-1, *BMP* bone morphogenetic protein, *BTC* betacellulin, *CAR cell* CXCL12-abundant reticular cell, *CXCL12* C-X-C motif chemokine ligand 12, *CXCR4* C-X-C chemokine receptor type 4, *ECM* extracellular matrix, *FGF* fibroblast growth factor, *HFSC* hair follicle stem cell, *HGF* hepatocyte growth factor, *HSC* hematopoietic stem cell, *K6+ cell* keratin 6 positive cell, *LT-HSC* long-term hematopoietic stem cell, *NSC* neural stem cell, *PDGFα* platelet-derived growth factor-α, *SC* satellite cell, *TGFβ* transforming growth factor β, *thpo* thrombopoietin.
[a]Latent TGFβ is secreted by stromal megakaryocytes and processed into active form by non-myelinated Schwann cells

## 4 Adult Stem Cell Niche and Stem Cell Quiescence

Collaborate with intrinsic mechanisms, extrinsic signals from niches tightly control adult stem cell quiescence [51]. To understand how a niche microenvironment maintains the stem cells, it is first necessary to determine where the stem cells reside and identify the repertoire of factors from various niche cells and extracellular matrix (ECM) as well as systemic long-range signals. Several adult stem cells and key components in their corresponding niches have been comprehensively defined, including HFSCs in the skin compartment, hematopoietic stem cells in the bone marrow and satellite cells (SCs) in skeletal muscles.

### 4.1 The Bulge Niche and HFSC Quiescence

Using nucleotide pulse-chase experiments, the existence of slow cycling, label-retaining cells (LRCs) was found in the outermost layer of the bulge region of hair follicle in skin [52]. These LRCs are identified as the stem cells responsible for cyclic hair growth and the bulge as the niche hosts of HFSCs [53]. The hair follicle is a tissue that turnovers periodically. The hair follicles undergo unique cycles of bouts of active growth (anagen), rest (catagen), and regression (anagen), which are collectively termed the hair cycle [54]. HFSCs are maintained in a quiescent state during most of the cycle [52, 55]. They are only transiently sensitive to activating signals during late telogen and become activated to proliferate in anagen [56, 57]. At late anagen, HFSCs enter quiescence again, which persists through catagen and HFSCs remain quiescent until late telogen [44] (Fig. 2).

HFSC quiescence maintenance and activation are complex. Intrafollicular components like K6+ cells and the dermal papilla, a regulatory center located beneath the hair follicle [36], extrafollicular fibroblasts and adipocytes secrete numerous quiescent and regenerative signals to control HFSC quiescence [36, 56, 58, 59] (Fig. 2). Among which, the crosstalk between the Wnt signaling and the bone morphogenetic protein (BMP) signaling is central to HFSC quiescence and the hair cycle regulation [44]. Waves of BMP expression in the bulge niche occur out of phase with Wnt/β-catenin signals cycle [44]. The competitive equilibrium of the two signaling determines responsiveness of HFSCs toward regenerative signals and divides telogen into two distinct functional phases [44] (Fig. 2 and Table 1).

During early telogen, the bulge niche is characterized with a BMP-high, Wnt/β-catenin-low microenvironment, restricting HFSCs in quiescence and refractory to activating signals [44]. Active BMP signaling drives HFSCs into quiescence through repressing CDK4 expression [60]. Ablation of BMP receptor IA causes bulge cells to lose quiescence [61]. High BMP levels in the bulge are contributed by BMP4 from dermal papilla, dermal

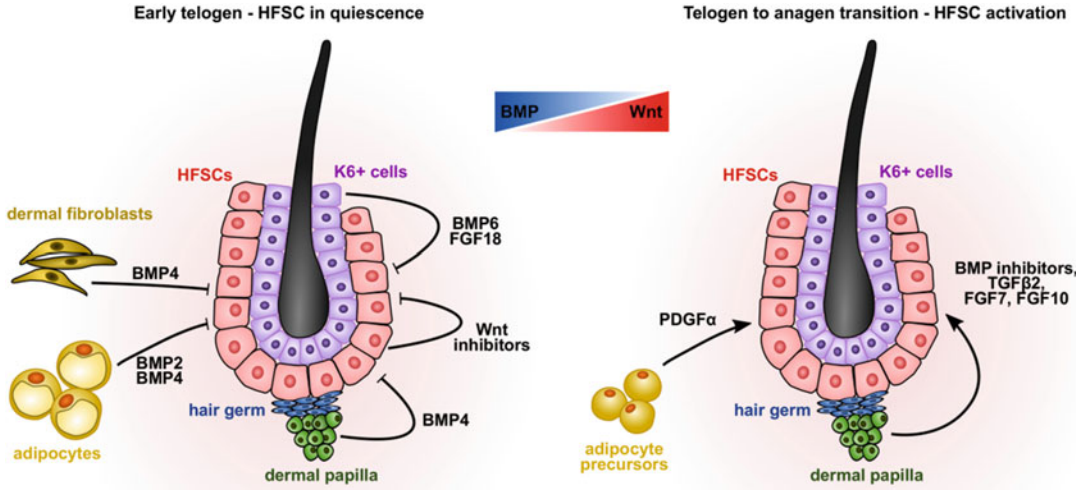


**Fig. 2** Hair follicle stem cell (HFSC) quiescence regulation by the bulge niche. HFSCs are quiescent in early telogen follicles and are activated during anagen induction. HFSC quiescence and activation are regulated by the balance between the Wnt signaling and bone morphogenetic protein (BMP) signaling. (*left*) During early telogen, the BMP-high, Wnt-low niche environment maintains HFSCs in quiescence. Within hair follicles, BMP4, BMP6, and fibroblast growth factor (FGF)18 from dermal papilla and keratin 6 positive (K6+) inner bulge cells act on HFSCs in a paracrine manner. Together with high levels of BMP2 and BMP4 derived from extra-follicular fibroblasts and subcutaneous adipocytes, these factors make HFSCs refractory to stimulation. Wnt ligands are scarce and HFSC-derived Wnt inhibitors keep the Wnt-low microenvironment. (*right*) During late telogen, BMP production from various niche cells ceases. Dermal papilla functions as the activation center and secrete numerous factors, including BMP inhibitors, transforming growth factor-β2 (TGFβ2), FGF7, and FGF10. High levels of these factors antagonize BMP signaling and decrease the threshold for activation. Platelet-derived growth factor-α (PDGFα) from adipocyte precursors also induces exit of HFSCs from quiescence and telogen to anagen transition

fibroblasts, and subcutaneous adipocytes [44, 62]. In addition, adipocytes secrete BMP2 and K6+ inner bulge layer produces BMP6 [42, 44] (Fig. 2). Meanwhile, the Wnt/β-catenin activity reaches its nadir at early telogen of the hair cycle [44, 63], in part due to actions of Wnt inhibitors that prevent premature activation of HFSCs during telogen to anagen transition [64–68]. Fibroblast growth factor (FGF) 18 from K6+ inner bulge cells and dermal papilla also contributes to HFSC quiescence maintenance [42, 53, 56] (Fig. 2 and Table 1).

Approaching the end of telogen, levels of BMP2 and BMP4 in the niche decrease with a concurrent increase in BMP inhibitors Sostdc1, Bambi, and noggin [44, 56, 58] (Fig. 2). Inhibition of BMP signaling has been demonstrated to markedly shorten the refractory phase and induce HFSCs to exit quiescence, thereby accelerating hair follicle cycling and propagation of regenerative wave [44, 61, 69, 70]. BMP signaling is also antagonized by TGFβ2 secretion from dermal papilla, further lowering the overall threshold for HFSC activation [44, 59] (Fig. 2 and Table 1).

The BMP-low microenvironment transits HFSCs from a refractory to a competent state to the activating Wnt/β-catenin signaling [44]. There is a surge in β-catenin activity during anagen induction [44, 63, 67, 71], which is sufficient to break HFSC quiescence and induce hair follicles to enter the anagen of a new hair cycle [66, 67]. During this time, the dermal papilla also releases progressively increased FGF7 and FGF10 to activate HFSCs [56]. In addition, adipocyte precursor cell population increases in number and its platelet-derived growth factor-α (PDGFα) expression peak during anagen induction [62, 72] (Fig. 2 and Table 1). PDGFα further augments HFSC activation and promotes the anagen phase [72]. Activated HFSCs within the bulge divide symmetrically to replenish HFSC pool during early anagen [57]. Until late anagen, they eventually cease proliferation to enter quiescence again, which is possibly driven by the elevated BMP2 and BMP4 signals during late anagen [44]. Together, quiescence and activation of HFSCs are coordinated by intrafollicular and extrafollicular signals HFSCs in the hair cycle.

### 4.2 The Endosteal Niche and HSC Quiescence

The hematopoietic system has a high turnover rate and appropriate quiescence control is critical to maintain stem cell pool for life-long functional hematopoiesis. It is generally accepted that HSC quiescence parallels the self-renewal capacity and repopulation potential [73, 74]. HSCs are mostly quiescent or slowly cycling, with 75% residing within the G0 phase at any one time [75, 76]. They are distributed throughout the bone marrow. Within the bone marrow, two anatomical niches have been proposed: the endosteal niche and the centrally located perivascular niche adjacent to sinusoidal vasculature [77]. These two niches contain different combinations of factors and are believed to play complementary roles in the regulation of HSC quiescence. Quiescent HSCs are preferentially located in endosteal niche that is enriched with osteoblasts and osteoclasts (Fig. 3). Upon activation, cycling HSCs are redistributed to the perivascular niche where factors from sinusoid endothelial cells and perivascular cells are abundant [78–80]. Extensive demonstrations of the endosteal localization highlight the importance of direct contact of HSCs to the endosteal surface in HSC maintenance [78, 81–83]. Disruption of the endosteal niche overcomes HSC quiescence and reduces functional long-term repopulating HSCs [78].

#### 4.2.1 Osteoblasts Are the Key HSC Niche Cells

In the endosteal niche, quiescent HSCs are in close contact with osteoblasts lining the endosteal surface [84]. Osteoblasts are specialized mesenchymal cells responsible for bone formation [85]. Importance of osteoblasts in hematopoiesis has been demonstrated by studies in which conditional ablation of osteoblasts results in significant decrease in the HSC number accompanied by a decrease in marrow hematopoiesis [86], whereas co-

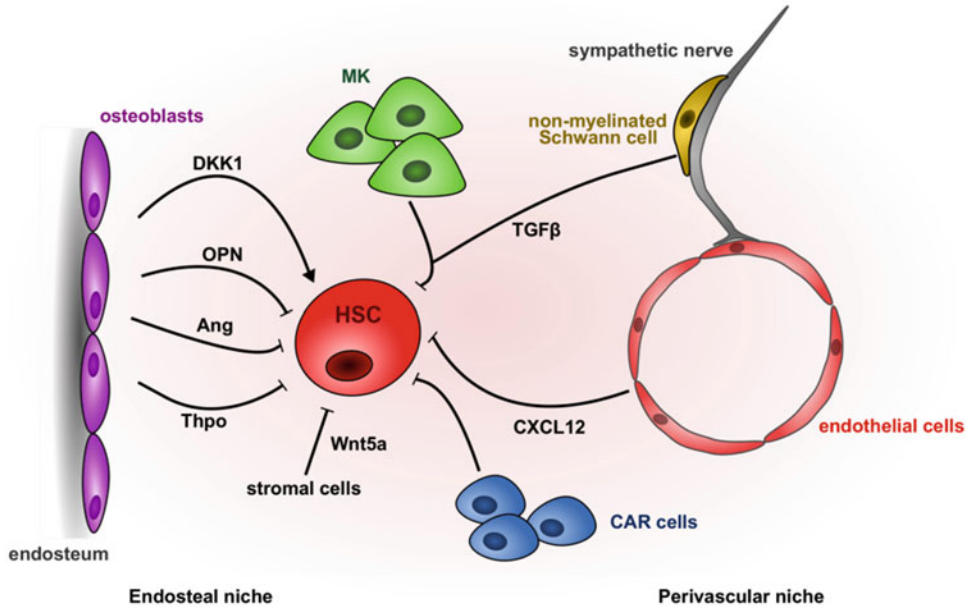


**Fig. 3** Hematopoietic stem cell (HSC) quiescence regulation by the endosteal and the perivascular niches. Within bone marrow, two spatially separated niches with distinct compositions and functions have been proposed. Quiescent HSCs are more concentrated at the endosteum in close proximity to osteoblasts. Osteoblasts are the central niche component to maintain a specialized niche housing quiescent HSCs. They secrete multiple factors such as angiopoietin-1 (Ang-1), osteopontin (OPN), and thrombopoietin (Thpo). Additional niche components have been identified in the stroma, including Wnt5a and CXCL12 from CXCL12 abundant reticular (CAR) cells. Moreover, megakaryocytes (MKs) and non-myelinated Schwann cells cooperate to produce active TGFβ. Although the perivascular niche is thought to be associated with HSC proliferation and differentiation, endothelial cells within the perivascular niche also help to maintain a quiescence-prone microenvironment by contributing CXCL12

transplantation with osteoblasts improves HSC engraftment [87]. Osteoblasts secrete various factors to keep HSCs in quiescence. Within the bone marrow, osteoblasts deposit a matrix glycoprotein osteopontin (OPN) specifically on the endosteal surface [88] (Fig. 3). OPN contributes to HSC trans-marrow migration to the endosteum as evidenced by the failure of transplanted HSCs to locate to the endosteal surface of OPN knockout mice [89]. OPN also promotes HSC quiescence and inhibits HSC cell cycle progression [89]. This notion is supported by the observations of increased number of cycling HSCs and expansion of HSC pool in OPN-deficient mice [88, 89]. In conclusion, osteoblasts serve as a niche component of HSC to promote HSC quiescence [89].

In addition to OPN, several osteoblast expressed soluble ligand-receptor pairs mediate the control of HSC quiescence. Osteoblasts express angiopoietin-1 (Ang-1) and thrombopoietin (Thpo), which interact with the receptors Tie2 and Mpl on HSCs, respectively [83, 90] (Fig. 3 and Table 1). These Tie2+ and Mpl+ HSCs exhibit features of G0 quiescence such as low

Pyronin Y staining, resistance to myelosuppression, and high levels of CDK inhibitors [83, 90, 91]. In the bone marrow transplanted with Ang-1-overexpressing bone marrow cells, percentage of quiescent cells is markedly higher [83]. On the contrary, when Thpo/Mpl signaling is inhibited, HSCs lose quiescence and are redistributed from G0 to G1 and S/G2/M phase [90, 91]. Collectively, both signaling pathways are implicated in the maintenance of HSC quiescence.

Osteoblasts are also a source of endogenous Dickkopf1 (Dkk1), a pan-Wnt inhibitor, which suppresses canonical Wnt signaling in HSCs [92, 93] (Fig. 3). Overexpression of Dkk1 in the osteoblastic niche reduces p21 expression in HSCs and enhances HSC sensitivity to myelosuppression [94]. The loss of quiescence is parallel to the progressive decline in regenerative function of HSCs isolated from Dkk1-overexpressing mice in repopulating irradiated wild-type recipient [94]. However, there are conflicting data regarding the importance of β-catenin on HSCs. For instance, HSCs retain reconstitution capacity even β-catenin is deleted [95]. Ectopic β-catenin expression enhances reconstituting capacity [96]. Furthermore, two individual groups demonstrated a negative role of β-catenin signaling in HSC maintenance. Constitutively active β-catenin leads to loss of HSCs quiescence due to a depletion of long-term stem cell pool, which failed to repopulate irradiated mice [97, 98]. These data make the role of canonical Wnt pathway in HSC quiescence regulation ambiguous [95–98].

#### 4.2.2 *Stromal Cells and the Perivascular Niche*

Away from the endosteum, the stroma contains a heterogeneous population of mesenchymal cells. Stromal cells that are adjacent to sinusoidal vasculature, along with endothelial cells, constitute the perivascular niche [77]. Factors from these compartments are implicated in HSC regulation. It has long been known the stromal compartment is important for preserving HSCs functions [29]. To date, various stromal cells and their roles in HSC quiescence regulation have been identified. Non-canonical Wnt signaling ligand Wnt5a is secreted by bone marrow stromal cells [99] (Fig. 3 and Table 1). In vitro Wnt5a treatment induces p27, restricts HSCs in quiescent state, and inhibits in vitro HSC expansion [100]. In parallel, HSCs transiently incubated with Wnt5a enhance HSC repopulation after engraftment [100, 101]. In addition to Wnt5a, TGFβ has also been shown to be a potent HSC quiescence inducer. Megakaryocytes in the stroma are the major source of TGFβ in the HSC niche and non-myelinated Schwann cells process latent TGFβ into an active form [84] (Fig. 3 and Table 1). In vitro treatment with TGFβ strongly suppresses HSC proliferation and colony formation [102]. In TGFβ type II receptor knockout mice, there is an increase in number of cycling HSCs [84]. TGFβ-induced quiescence is mediated by p57 induction [102, 103] and knockdown of p57 abolished the cell cycle arrest induced by TGFβ [103].

Chemokine CXCL12 is abundantly expressed by multiple cell types in bone marrow, including endothelial cells and various cellular components of stroma [40, 104–106] (Fig. 3 and Table 1). Among which, CXCL12-abundant reticular (CAR) cells secrete a significant level of CXCL12 in both the endosteal and the perivascular niches [106]. Induced genetic ablation of its receptor, CXCR4, in adult bone marrow results in severe reduction in HSC numbers. The remaining HSCs exhibit signs of the loss of quiescence and an increase in the susceptibility to myelosuppressive stress, illustrated by a reduced fraction of Ki67-negative G0 cells and a larger fraction of actively dividing cells [106]. Collectively, HSC quiescence is regulated by factors from the stroma and the perivascular niche in addition to the factors from the endosteal niche.

### 4.3 Basal Lamina and Myofiber Niches and SC Quiescence

In sharp contrast to the hair follicle and the bone marrow, skeletal muscle is a low-turnover tissue under homeostatic conditions. Yet, skeletal muscle has tremendous regeneration potential after injury. SCs are initially identified at the periphery of adult skeletal muscle fibers [107] and later are shown to be the *bona fide* adult stem cells responsible for skeletal muscle regeneration [108]. Anatomically, SCs are sandwiched between basal lamina and myofibers and they lose stem cell characteristics when isolated and cultured in vitro [107, 109] (Fig. 4). Quiescent SCs are characterized by high Pax7

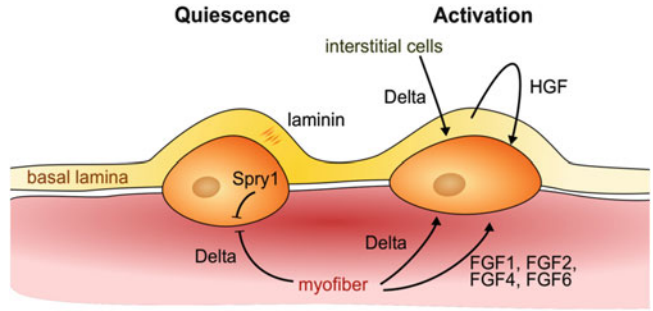


**Fig. 4** Satellite cells (SCs) quiescence regulation by the myofiber and the basal lamina niches. Quiescent SCs are situated juxtaposed to the basal lamina and sarcolemma of myofibers. Tethering of SCs to laminin in basal lamina protects SC quiescence from activating signaling pathways. SC quiescence is also maintained by the Notch-rich environment, with high levels of Notch ligand Delta from myofibers and interstitial cells. Injury-induced SC activation is mainly achieved by elevated levels of activating factors in response to injury, including release of hepatocyte growth factor (HGF) from extracellular matrix ECM and various fibroblast growth factors (FGFs) from the damaged myofibers. These factors promote SCs to leave quiescence and proliferate. FGF also hinders SCs return to quiescence after asymmetric cell division. Inhibiting FGFR signaling in SCs by Sprouty1 (Spry1) is necessary to restore quiescence

expression [110]. The basal lamina and myofibers represent the key niche components for SC quiescence regulation.

Physical tethering to the ECM is critical for SC quiescence. SC is anchored to the ECM laminin through cell surface α7/β1-integrins, which are negative regulators of mechanotransduction [111] (Fig. 4). Extracellular mechanical forces, like during exercise, are transduced into the cells to activate intracellular signaling pathways, including those that are known to break SC quiescence [111–113]. α7/β1-integrins are capable of antagonizing those pathways, making SCs resistance to activation [111]. Underneath the basal lamina, quiescent SCs are closely associated with basal lamina ECM. Biomechanical and biochemical properties of ECM are important for the optimal SC quiescence regulation and functions [109, 114]. SCs cultured on substrates that simulate the physiological stiffness of muscle can improve SC self-renewal and restore in vivo repopulating capability [109]. Collagen VI (ColVI) is an ECM component that affects the elasticity of ECM. Muscles from ColVI null mice display significant decrease in stiffness. Such niche compromises SC-mediated muscle regeneration and SC self-renewal capacity after injury [114].

Equally important is the myofiber niche. It is reported that SCs associated with myofibers remain in the quiescent state and exhibit reduced response to mitogens after isolation [115, 116]. Moreover, selective ablation of myofibers led to extensive SC proliferation [116]. Myofibers are a rich source of Notch ligand, Delta [117] (Fig. 4 and Table 1). Notch pathway has emerged as one of the important regulators of SC quiescence [118–123]. Quiescent SCs express multiple Notch receptors and Notch effectors [119, 121–125], making Notch signaling active in quiescent SCs [119, 124]. Intervening Notch signaling by depleting the intracellular mediator RBPJ or downstream targets of Notch signaling directs SCs to premature quiescent exit and promotes terminal differentiation. As a result, SC number is reduced and muscle regeneration is impaired after acute injury [119–121]. Together, findings from various studies support the notion that physical association or factors emanated from myofibers maintain SCs in a quiescent state.

Interestingly, Notch signaling plays a dual role in maintaining and breaking SC quiescence. The observation that Notch ligand Delta is rapidly upregulated in the interstitial cells, myofibers and the associated SCs upon muscle injury suggests that Notch activity is implicated in SC activation and muscle regeneration [117, 122]. Accordingly, Notch is activated when SCs exit quiescence and become proliferative [122]. Blocking Notch signaling restrains SCs from activation and proliferation and impairs muscle regeneration [117, 122].

In addition to Notch ligand**,** injured muscle tissues, including myofibers, release various members of the fibroblast growth factor (FGF) family as paracrine factors for SC proliferation [126, 127]

(Fig. 4 and Table 1). FGF2 promotes quiescent SC cell cycle entry in culture [128]. In ex vivo culture of isolated myofibers, a condition that mimics muscle injury, FGF2, as well as FGF1, FGF4, and FGF6, promotes SCs to exit quiescence and accelerate cell cycle entry [129]. SCs devoid of syndecan-4, a FGFR co-receptor, are defective in activation and display a delayed onset of proliferation [130, 131]. Paracrine FGF negatively regulates SC quiescence. Sprouty1 (Spry1), a FGFR signaling inhibitor [132], is highly expressed in Pax7+ cells, which regulates FGF signaling and promotes SC quiescence [112, 124]. Accordingly, SC-specific conditional ablation of Spry1 renders SCs fail to reestablish quiescence after muscle injury [112].

Hepatocyte growth factor (HGF) is another key activator of SCs [133–135]. In uninjured fibers, HGF is sequestered within basal lamina ECM in its latent form. Active HGF is released by matrix metalloproteinases upon both local [134, 136] and distant injuries [27] (Fig. 4 and Table 1). HGF can induce exit from SC quiescence and promote cell cycle entry as reflected by elevated DNA synthesis, cyclin D1, and PCNA expression [134, 135, 137]. Injection of HGF into uninjured muscle stimulated SC activation and upregulated myoblast number [133, 134].

## 5 Stem Cell Niche Aging and Stem Cell Quiescence

The ability of stem cells to maintain and regenerate decreases dramatically with age leading to aging of tissues and organism. There is a debate in whether the functional decline of stem cells during aging is contributed by cell-intrinsic or cell-extrinsic changes [138]. In some cases, cell autonomous defects do play an important role. For example, intrinsic functional and molecular changes in aged HSCs contribute to hematopoietic system aging [139]. Changes in stem cell niche also contribute to the compromised functions of aged stem cells [140]. Through heterochronic parabiosis experiments, exposure of old SCs to the young systemic environment rejuvenates their regenerative activity [141, 142]. On the contrary, exposure to old serum hampers regeneration by young SCs. Furthermore, cross-age transplantation experiments rescued aged phenotypes in skin and muscle, suggesting that defects are rooted in extrinsic changes rather than cell-intrinsic defects [143, 144].

In the skeletal muscle, age-related alterations in both systemic inputs and local microenvironment contribute to the loss of stem cell quiescence and diminished regenerative capacity. Circulation of aged mice contains elevated levels of factors that are deleterious to the regeneration process [141, 145]. For example, young SCs express Notch ligand Delta and activate themselves in an autocrine manner [122]. Yet, SCs express a reduced level of Delta in old mice

and therefore SC activation and muscle regeneration are hampered [117]. Regenerative potential is also possibly impaired through alteration of stem cell fates. In both in vitro and in vivo, Wnt ligands can promote fibrogenesis at the expense of myogenic potential of young SCs [142]. Serum content of Wnt ligands mount during aging, which is suggested to associate with poor muscle regeneration and excessive fibrosis in aged muscle [142].

Within the aged local niche, myofibers are the principal source of elevated FGF2 [146], an activator of SCs [128]. In such microenvironment, aged SCs lose their ability to retain a quiescent state, as evidenced by the loss of molecular signatures of quiescence [146]. Counterbalancing FGF2 signal from the aged niche via Spry1 overexpression in SCs has been shown to promote long-term SC quiescence and improve regenerative capacity during aging [146].

Loss of quiescence is obviously deleterious as it accelerates the depletion of stem cell pool. Yet, stem cells can be lodged in quiescence and fail to regenerate tissue if the niche provides excessive quiescence signals. This notion is best exemplified by the aging-related defects in HFSCs. The resting telogen phase of hair follicle becomes increasingly prolonged with age [144, 147]. Interestingly, HFSCs in aged skin are not depleted nor prematurely activated. Instead, aged HFSCs retain their number and have higher propensities of staying in dormancy [144].

In young hair follicle, active BMP signaling keeps HFSCs in quiescence and refractory to Wnt/β-catenin anagen inducing signaling [44]. Such balance is perturbed in aged HFSC niche and quiescent HFSCs become excessively resistant to activation [144, 147]. From adipose tissue in aged skin, elevated levels of BMP proteins and reduced BMP-inhibitor follistatin are secreted into the niche [144, 147]. All these signals set a high threshold for the activation of aged HFSCs and thus delay their response to activation [147]. Meanwhile, activation by Wnt/β-catenin signaling is dampened by aberrant secretion of Wnt pathway inhibitors (Dkk1 and Sfrp4) from aged adipocytes [144], further tipping the balance from activation toward quiescence. Moreover, there is a general elevation of inflammatory cytokines in the niche microenvironment, presumably from extrafollicular T lymphocytes [148]. The downstream JAK/STAT signaling is hyperactive in aged HFSCs and helps in keeping HFSCs in deep dormancy [48, 148]. Together, changes in the stem cell niches deteriorate stem cell functions during aging, opening the avenue to ameliorate aging phenotypes through manipulating stem cell niches.

## 6 Concluding Remarks and Future Directions

Taken all together, quiescence protects adult stem cells from activation and depletion and preserves stem cell properties including regeneration capacity. Adult stem cells reside in specific niches containing a combination of cellular and acellular components. Niche complexity is increased as long-range physiological and pathological information being integrated. Niche microenvironment is central to long-term maintenance of stem cell in the quiescent state and dysregulation of stem cell quiescence by the niche underlies aging and presumably disease pathogenesis. In this vein, a niche can be therapeutically targeted to correct stem cell functions. All these findings support manipulations of stem cell niche to treat stem cell-related diseases as a novel approach of regenerative therapy. The possibility of this notion is only beginning to be understood and is supported by fascinating data from several proof-of-concept studies in recent years [149].

With a tremendous potential to regulate stem cell quiescence as well as other stem cell properties, the manipulation of stem cell niches opens future applications in regenerative medicine and therefore warrants further in-depth research. The first challenge of niche manipulation is to identify critical components among a complex crosstalk between stem cells and various niche components. Sophisticated genetic, imaging, and sequencing approaches will enable a holistic view of the identity, influence, and molecular mechanism of niche components. The extrinsic and intrinsic regulation of cellular quiescence is highly complex and our knowledge is far from complete. A more thorough understanding about cellular quiescence and its regulation is critical to delineate and manipulate its imperative homeostatic and reparative potentials.

### References


1. Howard A, Pelc SR (1986) Synthesis of deoxyribonucleic acid in normal and irradiated cells and its relation to chromosome breakage. Int J Radiat Biol Relat Stud Phys Chem Med 49(2):207–218. doi:10.1080/09553008514552501
2. Hevesy G (1945) On the effect of roentgen rays on cellular division. Rev Mod Phys 17:102–111. doi:10.1103/RevModPhys.17.102
3. Yao G (2014) Modelling mammalian cellular quiescence. Interface Focus 4(3):20130074. doi:10.1098/rsfs.2013.0074
4. Baserga R (1968) Biochemistry of the cell cycle: A review. Cell Prolif 1(2):167–191. doi:10.1111/j.1365-2184.1968.tb00957.x
5. Fausto N (2004) Liver regeneration and repair: hepatocytes, progenitor cells, and stem cells. Hepatol Baltim Md 39(6):1477–1487. doi:10.1002/hep.20214
6. Bischoff R (1990) Cell cycle commitment of rat muscle satellite cells. J Cell Biol 111(1):201–207
7. Zetterberg A, Larsson O (1985) Kinetic analysis of regulatory events in G1 leading to proliferation or quiescence of Swiss 3T3 cells. Proc Natl Acad Sci U S A 82(16):5365–5369
8. Patt HM, Quastler H (1963) Radiation effects on cell renewal and related systems. Physiol Rev 43:357–396
9. Blomen VA, Boonstra J (2007) Cell fate determination during G1 phase progression. Cell Mol Life Sci 64(23):3084–3104. doi:10.1007/s00018-007-7271-z

10. Coller HA, Sang L, Roberts JM (2006) A new description of cellular quiescence. PLoS Biol 4 (3):e83. doi:10.1371/journal.pbio.0040083
11. Valentin M, Yang E (2008) Autophagy is activated, but is not required for the $G_0$ function of BCL-2 or BCL-xL. Cell Cycle 7 (17):2762–2768. doi:10.4161/cc.7.17.6595
12. Temin HM (1971) Stimulation by serum of multiplication of stationary chicken cells. J Cell Physiol 78(2):161–170. doi:10.1002/jcp.1040780202
13. Stoker MG (1972) The Leeuwenhoek lecture, 1971. Tumour viruses and the sociology of fibroblasts. Proc R Soc Lond B Biol Sci 181 (1062):1–17
14. Polyak K, Kato JY, Solomon MJ, Sherr CJ, Massague J, Roberts JM, Koff A (1994) p27Kip1, a cyclin-Cdk inhibitor, links transforming growth factor-beta and contact inhibition to cell cycle arrest. Genes Dev 8 (1):9–22
15. Benaud CM, Dickson RB (2001) Adhesion-regulated G1 cell cycle arrest in epithelial cells requires the downregulation of c-Myc. Oncogene 20(33):4554–4567. doi:10.1038/sj.onc.1204609
16. Fausto N (1997) Hepatocytes break the rules of senescence in serial transplantation studies. Is there a limit to their replicative capacity? Am J Pathol 151(5):1187–1189
17. Wu JC, Merlino G, Cveklova K, Mosinger B, Fausto N (1994) Autonomous growth in serum-free medium and production of hepatocellular carcinomas by differentiated hepatocyte lines that overexpress transforming growth factor alpha 1. Cancer Res 54 (22):5964–5973
18. Zetterberg A, Larsson O (1991) Coordination between cell growth and cell cycle transit in animal cells. Cold Spring Harb Symp Quant Biol 56:137–147
19. Pardee AB (1974) A restriction point for control of normal animal cell proliferation. Proc Natl Acad Sci U S A 71(4):1286–1290
20. Zetterberg A, Larsson O, Wiman KG (1995) What is the restriction point? Curr Opin Cell Biol 7(6):835–842
21. Frolov MV, Dyson NJ (2004) Molecular mechanisms of E2F-dependent activation and pRB-mediated repression. J Cell Sci 117 (11):2173–2181. doi:10.1242/jcs.01227
22. Stein GH, Drullinger LF, Soulard A, Dulić V (1999) Differential roles for cyclin-dependent kinase inhibitors p21 and p16 in the mechanisms of senescence and differentiation in human fibroblasts. Mol Cell Biol 19 (3):2109–2117
23. Wang W, Martindale JL, Yang X, Chrest FJ, Gorospe M (2005) Increased stability of the p16 mRNA with replicative senescence. EMBO Rep 6(2):158–164. doi:10.1038/sj.embor.7400346
24. Hitomi M, Stacey DW (1999) Cellular ras and cyclin D1 are required during different cell cycle periods in cycling NIH 3T3 cells. Mol Cell Biol 19(7):4623–4632
25. Chassot A-A, Lossaint G, Turchi L, Meneguzzi G, Fisher D, Ponzio G, Dulic V (2008) Confluence-induced cell cycle exit involves pre-mitotic CDK inhibition by p27 (Kip1) and cyclin D1 downregulation. Cell Cycle Georget Tex 7(13):2038–2046. doi:10.4161/cc.7.13.6233
26. Spencer SL, Cappell SD, Tsai F-C, Overton KW, Wang CL, Meyer T (2013) The proliferation-quiescence decision is controlled by a bifurcation in CDK2 activity at mitotic exit. Cell 155(2):369–383. doi:10.1016/j.cell.2013.08.062
27. Rodgers JT, King KY, Brett JO, Cromie MJ, Charville GW, Maguire KK, Brunson C, Mastey N, Liu L, Tsai C-R, Goodell MA, Rando TA (2014) mTORC1 controls the adaptive transition of quiescent stem cells from G0 to G(Alert). Nature 510(7505):393–396. doi:10.1038/nature13255
28. Bradley TR, Metcalf D (1966) The growth of mouse bone marrow cells in vitro. Aust J Exp Biol Med Sci 44(3):287–299
29. Dexter TM, Allen TD, Lajtha LG (1977) Conditions controlling the proliferation of haemopoietic stem cells in vitro. J Cell Physiol 91(3):335–344. doi:10.1002/jcp.1040910303
30. Scadden DT (2006) The stem-cell niche as an entity of action. Nature 441 (7097):1075–1079. doi:10.1038/nature04957
31. Lord BI, Testa NG, Hendry JH (1975) The relative spatial distributions of CFUs and CFUc in the normal mouse femur. Blood 46 (1):65–72
32. Lambertsen RH, Weiss L (1984) A model of intramedullary hematopoietic microenvironments based on stereologic study of the distribution of endocloned marrow colonies. Blood 63(2):287–297
33. Schofield R (1978) The relationship between the spleen colony-forming cell and the haemopoietic stem cell. Blood Cells 4 (1–2):7–25
34. Kimble JE, White JG (1981) On the control of germ cell development in Caenorhabditis elegans. Dev Biol 81(2):208–219

35. Austin J, Kimble J (1987) glp-1 Is required in the germ line for regulation of the decision between mitosis and meiosis in C. elegans. Cell 51(4):589–599. doi:10.1016/0092-8674(87)90128-0
36. Hsu Y-C, Fuchs E (2012) A family business: stem cell progeny join the niche to regulate homeostasis. Nat Rev Mol Cell Biol 13 (2):103–114. doi:10.1038/nrm3272
37. Scadden DT (2014) Nice neighborhood: emerging concepts of the stem cell niche. Cell 157(1):41–50. doi:10.1016/j.cell.2014.02.013
38. Olson TS, Caselli A, Otsuru S, Hofmann TJ, Williams R, Paolucci P, Dominici M, Horwitz EM (2013) Megakaryocytes promote murine osteoblastic HSC niche expansion and stem cell engraftment after radioablative conditioning. Blood 121(26):5238–5249. doi:10.1182/blood-2012-10-463414
39. Heazlewood SY, Neaves RJ, Williams B, Haylock DN, Adams TE, Nilsson SK (2013) Megakaryocytes co-localise with hemopoietic stem cells and release cytokines that up-regulate stem cell proliferation. Stem Cell Res 11(2):782–792. doi:10.1016/j.scr.2013.05.007
40. Bruns I, Lucas D, Pinho S, Ahmed J, Lambert MP, Kunisaki Y, Scheiermann C, Schiff L, Poncz M, Bergman A, Frenette PS (2014) Megakaryocytes regulate hematopoietic stem cell quiescence through CXCL4 secretion. Nat Med 20(11):1315–1320. doi:10.1038/nm.3707
41. Zhao M, Perry JM, Marshall H, Venkatraman A, Qian P, He XC, Ahamed J, Li L (2014) Megakaryocytes maintain homeostatic quiescence and promote post-injury regeneration of hematopoietic stem cells. Nat Med 20 (11):1321–1326. doi:10.1038/nm.3706
42. Hsu Y-C, Pasolli HA, Fuchs E (2011) Dynamics between stem cells, niche, and progeny in the hair follicle. Cell 144 (1):92–105. doi:10.1016/j.cell.2010.11.049
43. Brownell I, Guevara E, Bai CB, Loomis CA, Joyner AL (2011) Nerve-derived sonic hedgehog defines a niche for hair follicle stem cells capable of becoming epidermal stem cells. Cell Stem Cell 8(5):552–565. doi:10.1016/j.stem.2011.02.021
44. Plikus MV, Mayer JA, de la Cruz D, Baker RE, Maini PK, Maxson R, Chuong C-M (2008) Cyclic dermal BMP signalling regulates stem cell activation during hair regeneration. Nature 451(7176):340–344. doi:10.1038/nature06457
45. Augustine RA, Ladyman SR, Grattan DR (2008) From feeding one to feeding many: hormone-induced changes in bodyweight homeostasis during pregnancy. J Physiol 586 (2):387–397. doi:10.1113/jphysiol.2007.146316
46. Craven AJ, Ormandy CJ, Robertson FG, Wilkins RJ, Kelly PA, Nixon AJ, Pearson AJ (2001) Prolactin signaling influences the timing mechanism of the hair follicle: analysis of hair growth cycles in prolactin receptor knockout mice. Endocrinology 142 (6):2533–2539. doi:10.1210/endo.142.6.8179
47. Craven AJ, Nixon AJ, Ashby MG, Ormandy CJ, Blazek K, Wilkins RJ, Pearson AJ (2006) Prolactin delays hair regrowth in mice. J Endocrinol 191(2):415–425. doi:10.1677/joe.1.06685
48. Goldstein J, Fletcher S, Roth E, Wu C, Chun A, Horsley V (2014) Calcineurin/Nfatc1 signaling links skin stem cell quiescence to hormonal signaling during pregnancy and lactation. Genes Dev 28(9):983–994. doi:10.1101/gad.236554.113
49. Wu X, Rathbone CR (2013) Satellite cell functional alterations following cutaneous burn in rats include an increase in their osteogenic potential. J Surg Res 184(2):e9–16. doi:10.1016/j.jss.2013.03.046
50. Wu X, Walters TJ, Rathbone CR (2013) Skeletal muscle satellite cell activation following cutaneous burn in rats. Burns 39 (4):736–744. doi:10.1016/j.burns.2012.10.016
51. Cheung TH, Rando TA (2013) Molecular regulation of stem cell quiescence. Nat Rev Mol Cell Biol 14(6):329–340. doi:10.1038/nrm3591
52. Cotsarelis G, Sun TT, Lavker RM (1990) Label-retaining cells reside in the bulge area of pilosebaceous unit: implications for follicular stem cells, hair cycle, and skin carcinogenesis. Cell 61(7):1329–1337
53. Blanpain C, Lowry WE, Geoghegan A, Polak L, Fuchs E (2004) Self-renewal, multipotency, and the existence of two cell populations within an epithelial stem cell niche. Cell 118(5):635–648. doi:10.1016/j.cell.2004.08.012
54. Müller-Röver S, Handjiski B, van der Veen C, Eichmüller S, Foitzik K, McKay IA, Stenn KS, Paus R (2001) A comprehensive guide for the accurate classification of murine hair follicles in distinct hair cycle stages. J Invest Dermatol 117(1):3–15. doi:10.1046/j.0022-202x.2001.01377.x
55. Morris RJ, Potten CS (1999) Highly persistent label-retaining cells in the hair follicles of mice and their fate following induction of anagen. J Invest Dermatol 112(4):470–475. doi:10.1046/j.1523-1747.1999.00537.x

56. Greco V, Chen T, Rendl M, Schober M, Pasolli HA, Stokes N, Dela Cruz-Racelis J, Fuchs E (2009) A two-step mechanism for stem cell activation during hair regeneration. Cell Stem Cell 4(2):155–169. doi:10.1016/j.stem.2008.12.009
57. Zhang YV, Cheong J, Ciapurin N, McDermitt DJ, Tumbar T (2009) Distinct self-renewal and differentiation phases in the niche of infrequently dividing hair follicle stem cells. Cell Stem Cell 5(3):267–278. doi:10.1016/j.stem.2009.06.004
58. Botchkarev VA, Botchkareva NV, Roth W, Nakamura M, Chen LH, Herzog W, Lindner G, McMahon JA, Peters C, Lauster R, McMahon AP, Paus R (1999) Noggin is a mesenchymally derived stimulator of hair-follicle induction. Nat Cell Biol 1(3):158–164. doi:10.1038/11078
59. Oshimori N, Fuchs E (2012) Paracrine TGF-β signaling counterbalances BMP-mediated repression in hair follicle stem cell activation. Cell Stem Cell 10(1):63–75. doi:10.1016/j.stem.2011.11.005
60. Horsley V, Aliprantis AO, Polak L, Glimcher LH, Fuchs E (2008) NFATc1 balances quiescence and proliferation of skin stem cells. Cell 132(2):299–310. doi:10.1016/j.cell.2007.11.047
61. Kobielak K, Pasolli HA, Alonso L, Polak L, Fuchs E (2003) Defining BMP functions in the hair follicle by conditional ablation of BMP receptor IA. J Cell Biol 163(3):609–623. doi:10.1083/jcb.200309042
62. Festa E, Fretz J, Berry R, Schmidt B, Rodeheffer M, Horowitz M, Horsley V (2011) Adipocyte lineage cells contribute to the skin stem cell niche to drive hair cycling. Cell 146(5):761–771. doi:10.1016/j.cell.2011.07.019
63. Huelsken J, Vogel R, Erdmann B, Cotsarelis G, Birchmeier W (2001) beta-Catenin controls hair follicle morphogenesis and stem cell differentiation in the skin. Cell 105(4):533–545
64. Morris RJ, Liu Y, Marles L, Yang Z, Trempus C, Li S, Lin JS, Sawicki JA, Cotsarelis G (2004) Capturing and profiling adult hair follicle stem cells. Nat Biotechnol 22(4):411–417. doi:10.1038/nbt950
65. Tumbar T, Guasch G, Greco V, Blanpain C, Lowry WE, Rendl M, Fuchs E (2004) Defining the epithelial stem cell niche in skin. Science 303(5656):359–363. doi:10.1126/science.1092436
66. Van Mater D, Kolligs FT, Dlugosz AA, Fearon ER (2003) Transient activation of beta-catenin signaling in cutaneous keratinocytes is sufficient to trigger the active growth phase of the hair cycle in mice. Genes Dev 17(10):1219–1224. doi:10.1101/gad.1076103
67. Lowry WE, Blanpain C, Nowak JA, Guasch G, Lewis L, Fuchs E (2005) Defining the impact of beta-catenin/Tcf transactivation on epithelial stem cells. Genes Dev 19(13):1596–1611. doi:10.1101/gad.1324905
68. Lien W-H, Polak L, Lin M, Lay K, Zheng D, Fuchs E (2014) In vivo transcriptional governance of hair follicle stem cells by canonical Wnt regulators. Nat Cell Biol 16(2):179–190. doi:10.1038/ncb2903
69. Botchkarev VA, Botchkareva NV, Nakamura M, Huber O, Funa K, Lauster R, Paus R, Gilchrest BA (2001) Noggin is required for induction of the hair follicle growth phase in postnatal skin. FASEB J 15(12):2205–2214. doi:10.1096/fj.01-0207com
70. Kobielak K, Stokes N, de la Cruz J, Polak L, Fuchs E (2007) Loss of a quiescent niche but not follicle stem cells in the absence of bone morphogenetic protein signaling. Proc Natl Acad Sci U S A 104(24):10063–10068. doi:10.1073/pnas.0703004104
71. Lo Celso C, Prowse DM, Watt FM (2004) Transient activation of beta-catenin signalling in adult mouse epidermis is sufficient to induce new hair follicles but continuous activation is required to maintain hair follicle tumours. Dev Camb Engl 131(8):1787–1799. doi:10.1242/dev.01052
72. Tomita Y, Akiyama M, Shimizu H (2006) PDGF isoforms induce and maintain anagen phase of murine hair follicles. J Dermatol Sci 43(2):105–115. doi:10.1016/j.jdermsci.2006.03.012
73. Ema H, Suda T (2012) Two anatomically distinct niches regulate stem cell activity. Blood 120(11):2174–2181. doi:10.1182/blood-2012-04-424507
74. Suda T, Suda J, Ogawa M (1983) Proliferative kinetics and differentiation of murine blast cell colonies in culture: evidence for variable G0 periods and constant doubling rates of early pluripotent hemopoietic progenitors. J Cell Physiol 117(3):308–318. doi:10.1002/jcp.1041170305
75. Cheshier SH, Morrison SJ, Liao X, Weissman IL (1999) In vivo proliferation and cell cycle kinetics of long-term self-renewing hematopoietic stem cells. Proc Natl Acad Sci U S A 96(6):3120–3125
76. Bradford GB, Williams B, Rossi R, Bertoncello I (1997) Quiescence, cycling, and

turnover in the primitive hematopoietic stem cell compartment. Exp Hematol 25 (5):445–453

77. Morrison SJ, Scadden DT (2014) The bone marrow niche for haematopoietic stem cells. Nature 505(7483):327–334. doi:10.1038/nature12984
78. Kunisaki Y, Bruns I, Scheiermann C, Ahmed J, Pinho S, Zhang D, Mizoguchi T, Wei Q, Lucas D, Ito K, Mar JC, Bergman A, Frenette PS (2013) Arteriolar niches maintain haematopoietic stem cell quiescence. Nature 502 (7473):637–643. doi:10.1038/nature12612
79. Lo Celso C, Fleming HE, Wu JW, Zhao CX, Miake-Lye S, Fujisaki J, Côté D, Rowe DW, Lin CP, Scadden DT (2009) Live-animal tracking of individual haematopoietic stem/progenitor cells in their niche. Nature 457 (7225):92–96. doi:10.1038/nature07434
80. Xie Y, Yin T, Wiegraebe W, He XC, Miller D, Stark D, Perko K, Alexander R, Schwartz J, Grindley JC, Park J, Haug JS, Wunderlich JP, Li H, Zhang S, Johnson T, Feldman RA, Li L (2009) Detection of functional haematopoietic stem cell niche using real-time imaging. Nature 457(7225):97–101. doi:10.1038/nature07639
81. Calvi LM, Adams GB, Weibrecht KW, Weber JM, Olson DP, Knight MC, Martin RP, Schipani E, Divieti P, Bringhurst FR, Milner LA, Kronenberg HM, Scadden DT (2003) Osteoblastic cells regulate the haematopoietic stem cell niche. Nature 425(6960):841–846. doi:10.1038/nature02040
82. Zhang J, Niu C, Ye L, Huang H, He X, Tong W-G, Ross J, Haug J, Johnson T, Feng JQ, Harris S, Wiedemann LM, Mishina Y, Li L (2003) Identification of the haematopoietic stem cell niche and control of the niche size. Nature 425(6960):836–841. doi:10.1038/nature02041
83. Arai F, Hirao A, Ohmura M, Sato H, Matsuoka S, Takubo K, Ito K, Koh GY, Suda T (2004) Tie2/angiopoietin-1 signaling regulates hematopoietic stem cell quiescence in the bone marrow niche. Cell 118 (2):149–161. doi:10.1016/j.cell.2004.07.004
84. Yamazaki S, Ema H, Karlsson G, Yamaguchi T, Miyoshi H, Shioda S, Taketo MM, Karlsson S, Iwama A, Nakauchi H (2011) Nonmyelinating Schwann cells maintain hematopoietic stem cell hibernation in the bone marrow niche. Cell 147 (5):1146–1158. doi:10.1016/j.cell.2011.09.053
85. Dirckx N, Van Hul M, Maes C (2013) Osteoblast recruitment to sites of bone formation in skeletal development, homeostasis, and regeneration. Birth Defects Res C Embryo Today Rev 99(3):170–191. doi:10.1002/bdrc.21047
86. Visnjic D, Kalajzic Z, Rowe DW, Katavic V, Lorenzo J, Aguila HL (2004) Hematopoiesis is severely altered in mice with an induced osteoblast deficiency. Blood 103 (9):3258–3264. doi:10.1182/blood-2003-11-4011
87. El-Badri NS, Wang BY, Cherry, Good RA (1998) Osteoblasts promote engraftment of allogeneic hematopoietic stem cells. Exp Hematol 26(2):110–116
88. Stier S, Ko Y, Forkert R, Lutz C, Neuhaus T, Grünewald E, Cheng T, Dombkowski D, Calvi LM, Rittling SR, Scadden DT (2005) Osteopontin is a hematopoietic stem cell niche component that negatively regulates stem cell pool size. J Exp Med 201 (11):1781–1791. doi:10.1084/jem.20041992
89. Nilsson SK, Johnston HM, Whitty GA, Williams B, Webb RJ, Denhardt DT, Bertoncello I, Bendall LJ, Simmons PJ, Haylock DN (2005) Osteopontin, a key component of the hematopoietic stem cell niche and regulator of primitive hematopoietic progenitor cells. Blood 106(4):1232–1239. doi:10.1182/blood-2004-11-4422
90. Yoshihara H, Arai F, Hosokawa K, Hagiwara T, Takubo K, Nakamura Y, Gomei Y, Iwasaki H, Matsuoka S, Miyamoto K, Miyazaki H, Takahashi T, Suda T (2007) Thrombopoietin/MPL signaling regulates hematopoietic stem cell quiescence and interaction with the osteoblastic niche. Cell Stem Cell 1 (6):685–697. doi:10.1016/j.stem.2007.10.020
91. Qian H, Buza-Vidas N, Hyland CD, Jensen CT, Antonchuk J, Månsson R, Thoren LA, Ekblom M, Alexander WS, Jacobsen SEW (2007) Critical role of thrombopoietin in maintaining adult quiescent hematopoietic stem cells. Cell Stem Cell 1(6):671–684. doi:10.1016/j.stem.2007.10.008
92. Grotewold L, Theil T, Rüther U (1999) Expression pattern of Dkk-1 during mouse limb development. Mech Dev 89 (1–2):151–153
93. MacDonald BT, Adamska M, Meisler MH (2004) Hypomorphic expression of Dkk1 in the doubleridge mouse: dose dependence and compensatory interactions with Lrp6. Development 131(11):2543–2552. doi:10.1242/dev.01126
94. Fleming HE, Janzen V, Lo Celso C, Guo J, Leahy KM, Kronenberg HM, Scadden DT

(2008) Wnt signaling in the niche enforces hematopoietic stem cell quiescence and is necessary to preserve self-renewal in vivo. Cell Stem Cell 2(3):274–283. doi:10.1016/j.stem.2008.01.003

95. Cobas M, Wilson A, Ernst B, Mancini SJC, MacDonald HR, Kemler R, Radtke F (2004) Beta-catenin is dispensable for hematopoiesis and lymphopoiesis. J Exp Med 199 (2):221–229. doi:10.1084/jem.20031615
96. Reya T, Duncan AW, Ailles L, Domen J, Scherer DC, Willert K, Hintz L, Nusse R, Weissman IL (2003) A role for Wnt signalling in self-renewal of haematopoietic stem cells. Nature 423(6938):409–414. doi:10.1038/nature01593
97. Kirstetter P, Anderson K, Porse BT, Jacobsen SEW, Nerlov C (2006) Activation of the canonical Wnt pathway leads to loss of hematopoietic stem cell repopulation and multilineage differentiation block. Nat Immunol 7 (10):1048–1056. doi:10.1038/ni1381
98. Scheller M, Huelsken J, Rosenbauer F, Taketo MM, Birchmeier W, Tenen DG, Leutz A (2006) Hematopoietic stem cell and multilineage defects generated by constitutive beta-catenin activation. Nat Immunol 7 (10):1037–1047. doi:10.1038/ni1387
99. Reya T, O'Riordan M, Okamura R, Devaney E, Willert K, Nusse R, Grosschedl R (2000) Wnt signaling regulates B lymphocyte proliferation through a LEF-1 dependent mechanism. Immunity 13(1):15–24
100. Nemeth MJ, Topol L, Anderson SM, Yang Y, Bodine DM (2007) Wnt5a inhibits canonical Wnt signaling in hematopoietic stem cells and enhances repopulation. Proc Natl Acad Sci U S A 104(39):15436–15441. doi:10.1073/pnas.0704747104
101. Murdoch B, Chadwick K, Martin M, Shojaei F, Shah KV, Gallacher L, Moon RT, Bhatia M (2003) Wnt-5A augments repopulating capacity and primitive hematopoietic development of human blood stem cells in vivo. Proc Natl Acad Sci U S A 100(6):3422–3427. doi:10.1073/pnas.0130233100
102. Yamazaki S, Iwama A, Takayanagi S, Eto K, Ema H, Nakauchi H (2009) TGF-β as a candidate bone marrow niche signal to induce hematopoietic stem cell hibernation. Blood 113(6):1250–1256. doi:10.1182/blood-2008-04-146480
103. Scandura JM, Boccuni P, Massagué J, Nimer SD (2004) Transforming growth factor beta-induced cell cycle arrest of human hematopoietic cells requires p57KIP2 up-regulation. Proc Natl Acad Sci U S A 101(42):15231–15236. doi:10.1073/pnas.0406771101
104. Jung Y, Wang J, Schneider A, Sun Y-X, Koh-Paige AJ, Osman NI, McCauley LK, Taichman RS (2006) Regulation of SDF-1 (CXCL12) production by osteoblasts; a possible mechanism for stem cell homing. Bone 38(4):497–508. doi:10.1016/j.bone.2005.10.003
105. Dar A, Goichberg P, Shinder V, Kalinkovich A, Kollet O, Netzer N, Margalit R, Zsak M, Nagler A, Hardan I, Resnick I, Rot A, Lapidot T (2005) Chemokine receptor CXCR4-dependent internalization and resecretion of functional chemokine SDF-1 by bone marrow endothelial and stromal cells. Nat Immunol 6(10):1038–1046. doi:10.1038/ni1251
106. Sugiyama T, Kohara H, Noda M, Nagasawa T (2006) Maintenance of the hematopoietic stem cell pool by CXCL12-CXCR4 chemokine signaling in bone marrow stromal cell niches. Immunity 25(6):977–988. doi:10.1016/j.immuni.2006.10.016
107. Mauro A (1961) Satellite cell of skeletal muscle fibers. J Biophys Biochem Cytol 9 (2):493–495
108. Collins CA, Olsen I, Zammit PS, Heslop L, Petrie A, Partridge TA, Morgan JE (2005) Stem cell function, self-renewal, and behavioral heterogeneity of cells from the adult muscle satellite cell niche. Cell 122 (2):289–301. doi:10.1016/j.cell.2005.05.010
109. Gilbert PM, Havenstrite KL, Magnusson KEG, Sacco A, Leonardi NA, Kraft P, Nguyen NK, Thrun S, Lutolf MP, Blau HM (2010) Substrate elasticity regulates skeletal muscle stem cell self-renewal in culture. Science 329 (5995):1078–1081. doi:10.1126/science.1191035
110. Relaix F, Rocancourt D, Mansouri A, Buckingham M (2005) A Pax3/Pax7-dependent population of skeletal muscle progenitor cells. Nature 435(7044):948–953. doi:10.1038/nature03594
111. Boppart MD, Burkin DJ, Kaufman SJ (2006) α7β1-Integrin regulates mechanotransduction and prevents skeletal muscle injury. Am J Physiol Cell Physiol 290(6):C1660–C1665. doi:10.1152/ajpcell.00317.2005
112. Shea KL, Xiang W, LaPorta VS, Licht JD, Keller C, Basson MA, Brack AS (2010) Sprouty1 regulates reversible quiescence of a self-renewing adult muscle stem cell pool during regeneration. Cell Stem Cell 6(2):117–129. doi:10.1016/j.stem.2009.12.015
113. Jones NC, Tyner KJ, Nibarger L, Stanley HM, Cornelison DDW, Fedorov YV, Olwin BB (2005) The p38alpha/beta MAPK functions as a molecular switch to activate the

quiescent satellite cell. J Cell Biol 169 (1):105–116. doi:10.1083/jcb.200408066

114. Urciuolo A, Quarta M, Morbidoni V, Gattazzo F, Molon S, Grumati P, Montemurro F, Tedesco FS, Blaauw B, Cossu G, Vozzi G, Rando TA, Bonaldo P (2013) Collagen VI regulates satellite cell self-renewal and muscle regeneration. Nat Commun 4:1964. doi:10.1038/ncomms2964
115. Bischoff R (1986) A satellite cell mitogen from crushed adult muscle. Dev Biol 115 (1):140–147
116. Bischoff R (1990) Interaction between satellite cells and skeletal muscle fibers. Dev Camb Engl 109(4):943–952
117. Conboy IM, Conboy MJ, Smythe GM, Rando TA (2003) Notch-mediated restoration of regenerative potential to aged muscle. Science 302(5650):1575–1577. doi:10.1126/science.1087573
118. Dumont NA, Wang YX, Rudnicki MA (2015) Intrinsic and extrinsic mechanisms regulating satellite cell function. Dev Camb Engl 142 (9):1572–1581. doi:10.1242/dev.114223
119. Fukada S, Yamaguchi M, Kokubo H, Ogawa R, Uezumi A, Yoneda T, Matev MM, Motohashi N, Ito T, Zolkiewska A, Johnson RL, Saga Y, Miyagoe-Suzuki Y, Tsujikawa K, Takeda S, Yamamoto H (2011) Hesr1 and Hesr3 are essential to generate undifferentiated quiescent satellite cells and to maintain satellite cell numbers. Development 138 (21):4609–4619. doi:10.1242/dev.067165
120. Bjornson CRR, Cheung TH, Liu L, Tripathi PV, Steeper KM, Rando TA (2012) Notch signaling is necessary to maintain quiescence in adult muscle stem cells. Stem Cells 30 (2):232–242. doi:10.1002/stem.773
121. Mourikis P, Sambasivan R, Castel D, Rocheteau P, Bizzarro V, Tajbakhsh S (2012) A critical requirement for notch signaling in maintenance of the quiescent skeletal muscle stem cell state. Stem Cells 30(2):243–252. doi:10.1002/stem.775
122. Conboy IM, Rando TA (2002) The regulation of Notch signaling controls satellite cell activation and cell fate determination in postnatal myogenesis. Dev Cell 3(3):397–409
123. Kuang S, Kuroda K, Le Grand F, Rudnicki MA (2007) Asymmetric self-renewal and commitment of satellite stem cells in muscle. Cell 129(5):999–1010. doi:10.1016/j.cell.2007.03.044
124. Fukada S, Uezumi A, Ikemoto M, Masuda S, Segawa M, Tanimura N, Yamamoto H, Miyagoe-Suzuki Y, Takeda S (2007) Molecular signature of quiescent satellite cells in adult skeletal muscle. Stem Cells 25 (10):2448–2459. doi:10.1634/stemcells.2007-0019
125. Mourikis P, Gopalakrishnan S, Sambasivan R, Tajbakhsh S (2012) Cell-autonomous Notch activity maintains the temporal specification potential of skeletal muscle stem cells. Dev Camb Engl 139(24):4536–4548. doi:10.1242/dev.084756
126. Kardami E, Murphy LJ, Liu L, Padua RR, Fandrich RR (1990) Characterization of two preparations of antibodies to basic fibroblast growth factor which exhibit distinct patterns of immunolocalization. Growth Factors 4 (1):69–80
127. Kästner S, Elias MC, Rivera AJ, Yablonka-Reuveni Z (2000) Gene expression patterns of the fibroblast growth factors and their receptors during myogenesis of rat satellite cells. J Histochem Cytochem 48 (8):1079–1096
128. Johnson SE, Allen RE (1993) Proliferating cell nuclear antigen (PCNA) is expressed in activated rat skeletal muscle satellite cells. J Cell Physiol 154(1):39–43. doi:10.1002/jcp.1041540106
129. Yablonka-Reuveni Z, Seger R, Rivera AJ (1999) Fibroblast growth factor promotes recruitment of skeletal muscle satellite cells in young and old rats. J Histochem Cytochem 47(1):23–42
130. Cornelison DDW, Filla MS, Stanley HM, Rapraeger AC, Olwin BB (2001) Syndecan-3 and syndecan-4 specifically mark skeletal muscle satellite cells and are implicated in satellite cell maintenance and muscle regeneration. Dev Biol 239(1):79–94. doi:10.1006/dbio.2001.0416
131. Cornelison DDW, Wilcox-Adelman SA, Goetinck PF, Rauvala H, Rapraeger AC, Olwin BB (2004) Essential and separable roles for Syndecan-3 and Syndecan-4 in skeletal muscle development and regeneration. Genes Dev 18 (18):2231–2236. doi:10.1101/gad.1214204
132. Hacohen N, Kramer S, Sutherland D, Hiromi Y, Krasnow MA (1998) sprouty encodes a novel antagonist of FGF signaling that patterns apical branching of the Drosophila airways. Cell 92(2):253–263
133. Miller KJ, Thaloor D, Matteson S, Pavlath GK (2000) Hepatocyte growth factor affects satellite cell activation and differentiation in regenerating skeletal muscle. Am J Physiol Cell Physiol 278(1):C174–C181
134. Tatsumi R, Anderson JE, Nevoret CJ, Halevy O, Allen RE (1998) HGF/SF is present in

normal adult skeletal muscle and is capable of activating satellite cells. Dev Biol 194 (1):114–128. doi:10.1006/dbio.1997.8803

135. Allen RE, Sheehan SM, Taylor RG, Kendall TL, Rice GM (1995) Hepatocyte growth factor activates quiescent skeletal muscle satellite cells in vitro. J Cell Physiol 165(2):307–312. doi:10.1002/jcp.1041650211
136. Yamada M, Tatsumi R, Kikuiri T, Okamoto S, Nonoshita S, Mizunoya W, Ikeuchi Y, Shimokawa H, Sunagawa K, Allen RE (2006) Matrix metalloproteinases are involved in mechanical stretch-induced activation of skeletal muscle satellite cells. Muscle Nerve 34 (3):313–319. doi:10.1002/mus.20601
137. Gal-Levi R, Leshem Y, Aoki S, Nakamura T, Halevy O (1998) Hepatocyte growth factor plays a dual role in regulating skeletal muscle satellite cell proliferation and differentiation. Biochim Biophys Acta 1402(1):39–51. doi:10.1016/S0167-4889(97)00124-9
138. Rando TA (2006) Stem cells, ageing and the quest for immortality. Nature 441 (7097):1080–1086. doi:10.1038/nature04958
139. Rossi DJ, Bryder D, Zahn JM, Ahlenius H, Sonu R, Wagers AJ, Weissman IL (2005) Cell intrinsic alterations underlie hematopoietic stem cell aging. Proc Natl Acad Sci U S A 102(26):9194–9199. doi:10.1073/pnas.0503280102
140. Conboy IM, Rando TA (2012) Heterochronic parabiosis for the study of the effects of aging on stem cells and their niches. Cell Cycle 11(12):2260–2267. doi:10.4161/cc.20437
141. Conboy IM, Conboy MJ, Wagers AJ, Girma ER, Weissman IL, Rando TA (2005) Rejuvenation of aged progenitor cells by exposure to a young systemic environment. Nature 433 (7027):760–764. doi:10.1038/nature03260
142. Brack AS, Conboy MJ, Roy S, Lee M, Kuo CJ, Keller C, Rando TA (2007) Increased Wnt signaling during aging alters muscle stem cell fate and increases fibrosis. Science 317(5839):807–810. doi:10.1126/science.1144090
143. Carlson BM, Faulkner JA (1989) Muscle transplantation between young and old rats: age of host determines recovery. Am J Phys 256(6 Pt 1):C1262–C1266
144. Chen C-C, Murray PJ, Jiang TX, Plikus MV, Chang Y-T, Lee OK, Widelitz RB, Chuong C-M (2014) Regenerative hair waves in aging mice and extra-follicular modulators follistatin, dkk1, and sfrp4. J Invest Dermatol 134 (8):2086–2096. doi:10.1038/jid.2014.139
145. Carlson ME, Conboy MJ, Hsu M, Barchas L, Jeong J, Agrawal A, Mikels AJ, Agrawal S, Schaffer DV, Conboy IM (2009) Relative roles of TGF-β1 and Wnt in the systemic regulation and aging of satellite cell responses. Aging Cell 8(6):676–689. doi:10.1111/j.1474-9726.2009.00517.x
146. Chakkalakal JV, Jones KM, Basson MA, Brack AS (2012) The aged niche disrupts muscle stem cell quiescence. Nature 490 (7420):355–360. doi:10.1038/nature11438
147. Keyes BE, Segal JP, Heller E, Lien W-H, Chang C-Y, Guo X, Oristian DS, Zheng D, Fuchs E (2013) Nfatc1 orchestrates aging in hair follicle stem cells. Proc Natl Acad Sci U S A 110(51):E4950–E4959. doi:10.1073/pnas.1320301110
148. Doles J, Storer M, Cozzuto L, Roma G, Keyes WM (2012) Age-associated inflammation inhibits epidermal stem cell function. Genes Dev 26(19):2144–2153. doi:10.1101/gad.192294.112
149. Adams GB, Martin RP, Alley IR, Chabner KT, Cohen KS, Calvi LM, Kronenberg HM, Scadden DT (2007) Therapeutic targeting of a stem cell niche. Nat Biotechnol 25 (2):238–243. doi:10.1038/nbt1281
150. McCroskery S, Thomas M, Maxwell L, Sharma M, Kambadur R (2003) Myostatin negatively regulates satellite cell activation and self-renewal. J Cell Biol 162(6):1135–1147. doi:10.1083/jcb.200207056
151. Fowler JA, Mundy GR, Lwin ST, Edwards CM (2012) Bone marrow stromal cells create a permissive microenvironment for myeloma development: a new stromal role for Wnt inhibitor Dkk1. Cancer Res 72 (9):2183–2189. doi:10.1158/0008-5472.CAN-11-2067
152. Gómez-Gaviro MV, Scott CE, Sesay AK, Matheu A, Booth S, Galichet C, Lovell-Badge R (2012) Betacellulin promotes cell proliferation in the neural stem cell niche and stimulates neurogenesis. Proc Natl Acad Sci U S A 109(4):1317–1322. doi:10.1073/pnas.1016199109
153. Arai F, Ohneda O, Miyamoto T, Zhang XQ, Suda T (2002) Mesenchymal stem cells in perichondrium express activated leukocyte cell adhesion molecule and participate in bone marrow formation. J Exp Med 195 (12):1549–1563. doi:10.1084/jem.20011700
154. Schepers K, Hsiao EC, Garg T, Scott MJ, Passegué E (2012) Activated Gs signaling in osteoblastic cells alters the hematopoietic stem cell niche in mice. Blood 120 (17):3425–3435. doi:10.1182/blood-2011-11-395418

# Chapter 2

# An In Vitro Model of Cellular Quiescence in Primary Human Dermal Fibroblasts

**Mithun Mitra, Linda D. Ho, and Hilary A. Coller**

## Abstract

Cellular quiescence is a reversible mode of cell cycle exit that allows cells and organisms to withstand unfavorable stress conditions. The factors that underlie the entry, exit, and maintenance of the quiescent state are crucial for understanding normal tissue development and function as well as pathological conditions such as chronic wound healing and cancer. In vitro models of quiescence have been used to understand the factors that contribute to quiescence under well-controlled experimental conditions. Here, we describe an in vitro model of quiescence that is based on neonatal human dermal fibroblasts. The fibroblasts are induced into quiescence by antiproliferative signals, contact inhibition, and serum-starvation (mitogen withdrawal). We describe the isolation of fibroblasts from skin, methods for inducing quiescence in isolated fibroblasts, and approaches to manipulate the fibroblasts in proliferating and quiescent states to determine critical regulators of quiescence.

**Key words** Fibroblasts, Quiescence, Serum starvation, Contact inhibition

## 1 Introduction

### *1.1 Cell Quiescence and Its Role in Human Biology*

Extracellular signals such as the availability of nutrients, the presence of growth factors, or the presence of cytokines can serve as signals that cells should proliferate to generate daughter cells. When pro-proliferative signals are absent or antiproliferative signals are present, some cells have the capacity to reversibly exit the cell cycle and enter into a quiescent state [1–4]. Quiescent cells are defined by their ability to reenter the cell cycle at a future time when conditions are favorable for cell division. Thus, quiescence represents a reversible, non-dividing state. The reversibility of quiescent cells distinguishes them from senescent and apoptotic cells that cannot reenter the cell cycle [3], and from terminally differentiated cells that no longer divide, such as the cells that have undergone squamous maturation.

Quiescent cells in the human body include memory T cells, hepatocytes, fibroblasts, and stem cells. When quiescent cells sense

H. Daniel Lacorazza (ed.), *Cellular Quiescence: Methods and Protocols*, Methods in Molecular Biology, vol. 1686,
DOI 10.1007/978-1-4939-7371-2_2, 

external stimuli to divide, they can be induced to proliferate. Often this occurs in a context in which the quiescent cells are being called on to proliferate and function as early responders in maintaining tissue homeostasis. For example, during wound healing, quiescent fibroblasts distant from the wound area become activated, resulting in their proliferation and migration to the wound site [5, 6]. These activated fibroblasts synthesize extracellular matrix proteins, such as collagen, that help in closing the wound. Cancer is characterized by cells that ought to exit the proliferative cell cycle but continue proliferating despite anti-proliferative signals. Studying the molecular processes that induce quiescence, maintain quiescence, and stimulate cells to reenter the cell cycle may provide important insights into multiple disease states. A better understanding of the relevant factors can be gained by developing in vivo and in vitro models that mimic the biological system faithfully and in a reproducible manner.

### 1.2 Biological Markers of Quiescent Cells

Quiescent cells have entered a state in which the cells have ceased dividing and no new genomic DNA is being synthesized. Recent studies have described the properties of quiescent cells [3, 7–12], including changes in gene expression patterns [13–19], but more research is required to truly understand the molecular basis of quiescence. This leads to the question: What approaches are available to ascertain whether a cell is in a quiescent state using different cell-based techniques? What biological markers are available for this?

Table 1 summarizes some of the markers and reagents that have been used to probe for quiescent cells. The cell cycle of proliferating cells is driven by the expression of cyclins, which are proteins that activate cyclin-dependent kinases (Cdks) [20, 21]. Cdks, in turn, phosphorylate key proteins at different stages of the cell cycle that allow cells to progress through the cell cycle phases [22]. The activity of these Cdks is inhibited by Cdk inhibitors such as p21 and p27 [23]. These Cdk inhibitors are often induced during quiescence [24]. Some of the markers that have been used for quiescence include reduced Cdk activity and elevated levels of cyclin-dependent kinase inhibitors.

Members of retinoblastoma family of proteins (Rb/p105, p107, and Rb2/p130) bind to the activating E2F transcription factors (E2F1, E2F2, and E2F3) [25]. Binding of Rb family members results in a complex that sequesters E2F, thereby suppressing the transcription of E2F-dependent cell cycle genes [26, 27]. Phosphorylation of retinoblastoma proteins by Cdks releases E2F, which allows cell cycle progression. In some models, the complex p130-E2F accumulates in quiescent cells and has been used as a marker for quiescent cells [28]. In other models, Rb itself, and not p130 or p107, is critical for maintaining quiescence [29].

**Table 1**
**Methods to identify quiescent cells**

| Method | Protein or mRNA marker (s) /reagent | Description | Change in levels with quiescence (relative to dividing cells) | Type of cells (Ref.) |
|---|---|---|---|---|
| Western blot | $p27^{Kip1}$ (p27) | Cyclin-dependent kinase (Cdk) inhibitor; nuclear | Up | Fibroblasts [24], HUVEC [66] |
| | p21 | Cdk inhibitor; nuclear | Up | Fibroblasts [67] |
| | Phosphorylated-retinoblastoma (phospo-pRB) | Phosphorylation of pRB in dividing cells activates E2F (*see* Subheading 1.2). | Down | Lymphocytes [68] |
| | Cd82 | Cell surface protein in the tetraspanin superfamily | Up | Hematopoietic stem cells [69] |
| Real time PCR | p53 | Tumor suppressor that controls proliferation, differentiation, and apoptosis | Up | Hematopoietic stem cells [70] |
| Flow cytometry | Pyronin-Y[a] | Preferentially binds to RNA; emits fluorescence | Down | Fibroblasts [7, 32], Hematopoietic stem cells (HSC)[b] [33, 34] |
| | Bromo-uridine (BrdU)[a] | Thymidine analog; incorporates into newly synthesized DNA; detected by antibody | Down | Fibroblasts [15] |
| | 5-ethynyl-2′ –deoxyuridine (EdU) | Thymidine analog; incorporates into newly synthesized DNA; detected by fluorescent dyes that chemically react with EdU | Down | Fibroblasts [32] |
| | mVenus-p27K$^-$ | p27 that lacks binding to Cdk is fused to a fluorescent protein (mVenus) | Up | NIH3T3 [48] |
| | Reactive oxygen species (ROS) | Generated in the cell due to oxidative metabolism and stress conditions; fluorescence detection | Down | MCF7 ([71]), eMSC [72] |
| Immunohistochemistry/ Immunofluorescence (Tissue Staining) | Ki-67 | Proliferation marker (nuclear) | Down | Many types of cells [73] |
| | Fgf18 and Bmp6 | Maintenance of quiescence of hair follicle stem cells (HFSC) | Up | HFSC [74] |

(continued)

**Table 1**
**(continued)**

| Method | Protein or mRNA marker (s) /reagent | Description | Change in levels with quiescence (relative to dividing cells) | Type of cells (Ref.) |
|---|---|---|---|---|
| Immunocytochemistry/ Immunofluorescence (Cell Staining) | E2F5 and LEK1 | Translocate to nucleus in quiescent myoblasts; fluorescence detection | | Myoblasts [75] |
| | Ki67 and BrdU | See text | | |
| Label retention[c] (In vivo labeling) | BrDU | See text; slow-cycling cells retain BrDU | | HSC[b] [38, 40] |
| | Histone 2B-green fluorescent protein (H2B-GFP) | Fluorescent fusion protein that is incorporated into nucleosomes; slow-cycling cells retain H2B-GFP | | Skin stem cells [41], HSC[b] [40, 42] |
| Live cell imaging | Cdk2 sensor | Translocates to the nucleus when active | Inactive, cytoplasmically localized | MCF10a [10] |
| | p21 | Cdk inhibitor; nuclear | Up | MCF10a [10] |
| | Hypophosphorylated Rb | Rb with fewer phosphorylation events sequesters E2F | Less phosphorylated | MCF10a [10] |
| Kinase assay | $p33^{QIK}$, Quiescence Induced Kinase | | Kinase activity goes up | NIH3T3 [76] |

[a]Cells were also stained with Hoechst 33,342 or DAPI. These dyes bind to A-T base pairs and therefore, measure the total DNA content
[b]See Refs. [3, 11] for a review on quiescent HSC markers
[c]Label-retention techniques by themselves are not sufficient to mark quiescent cells in vivo. They should be accompanied by other methods like lineage tracing [3, 77]

Other methods to detect quiescent cells have been developed based on the lack of DNA synthesis in quiescent cells. Cells that are actively dividing incorporate nucleotides into their DNA. Addition of labeled nucleotides like bromodeoxyuridine (BrdU) can be used to detect cells that have recently replicated their DNA [15]. Quiescent cells are low or negative for this marker. Unlike BrdU, which is detected by an antibody, labeled fluorescent nucleotides have been developed with Click chemistry [30] to attach a fluorescent probe to ethinyldU (eDU) to measure DNA synthesis [31, 32]. Another characteristic of many quiescent cells is low levels of total RNA. Pyronin Y stains total RNA and has been used as a quiescence marker based on FACS analysis of individual cells [7, 32–34].

Identifying quiescent cells within an organism has mostly been based on methods that identify cells that have not divided recently. Cells that are quiescent have been identified with label-retaining assays [35–40]. With these assays, a repeated and prolonged administration of a labeled nucleotide such as tritiated thymidine ([$^3$H] TdR) or BrdU will be taken up by the animal (pulse), followed by a chase during which labeled nucleotides are not provided. Cells that divide slowly can be identified as those that retain the label a long time after the pulse period. A similar concept was developed to fluorescently label cells in living organisms that have not divided recently. An inducible histone H2B-GFP protein has been introduced into organisms [41, 42]. Upon activation, H2B-GFP labels every histone green. After the expression of the H2B-GFP is turned off, and endogenous, unlabeled histone H2B is the dominant form expressed, cells that retain the label will be those that have not divided, and the label will be enriched in quiescent cells.

The Fluorescence Ubiquitin Cell Cycle Indicator (FUCCI) cell cycle sensor can be used to monitor cell progression in living organisms, though by itself, does not specifically distinguish quiescence from the G1 phase of the cell cycle [43–47]. The Fucci system utilizes the chromatin licensing and DNA replication factor 1 (Cdt1) protein and its inhibitor geminin. With the Fucci model, Cdt1, which is expressed at high levels in G1 and declines in S phase, is labeled red. Geminin, which is expressed during S, G2, and M cell cycle phases, is labeled green. Fucci zebrafish, flies, and mice have been developed and the system has been used to gain insight into the proliferative patterns of cells in vivo. Recently, the Fucci system has been combined with a method to monitor p27 levels to identify quiescent cells [48]. Levels of p27 are high in quiescent cells and two different degradation methods eliminate p27. The Skp1 (S-phase kinase-associated protein 1)-cullin-F-box (SCF) ubiquitin ligase complex $SCF^{Skp2}$ binds phosphorylated p27 and mediates its degradation in S and G2 cell cycle phases [49]. KPC (Kip1 ubiquitination-promoting complex), consisting of KPC1 and −2, degrades p27 in G1 [50]. The exquisite control of p27 levels achieved by the cell has been exploited to generate a

quiescent cell marker. The fluorescent protein Venus was fused to a version of p27 that does not bind CDKs (mVenus-27 K-). Introducing this protein into cell allows visualization of G0 cells based on their fluorescence. Combining this method with FUCCI mice allowed sensitive detection of quiescent cells in vivo: cells that were positive for both the mVenus-27 K- fluorescence and Cdt1 fluorescence were considered to be in G0, while cells positive only for Cdt1 fluorescence were considered to be in G1.

A recent exciting advance in this field was the advent of real-time cell monitoring to detect quiescent cells. A CDK2 sensor has been used to monitor Cdk activity in cycling epithelial cells over several cell cycles [10]. This sensor contains four CDK consensus phosphorylation sites and the yellow fluorescent protein Venus. The sensor also contains nuclear localization and export signals so that the protein can be imported into the nucleus and exported from the nucleus based on the extent of Cdk activity in the cells. The ratio of nuclear to cytoplasmic fluorescence provides a readout for CDK2 activity. At the end of mitosis, while most cells exhibited an intermediate amount of CDK2 activity, some cells with low CDK2 activity were identified. These low CDK2 cells entered a temporary state of quiescence. Time-lapse imaging followed by fixation and immunofluorescence revealed that p21 levels were an important determinant of which cells exited the cell cycle.

While these approaches have led to important discoveries about quiescence and quiescent cells, new markers, including cell surface markers, that positively identify quiescent cells and distinguish them from cells in G1 that are about to divide and from those that have irreversibly exited the cell cycle due to senescence or differentiation, would be extremely valuable for the field.

### *1.3 Using Primary Cells Isolated from Tissues for Studying Quiescence In Vitro*

Studying the quiescent behavior of cells using in vivo animal models is important for our understanding of quiescence because it provides information about the physiologically relevant tissue microenvironment. In addition, in vitro models of quiescence can be used to complement in vivo systems. With in vitro quiescence models, proliferating cells isolated from tissues can be induced into quiescence under different conditions (e.g., mitogen removal) in tissue culture dishes. These experiments can provide a controlled environment in which cells can be subjected to specific, reproducible, and well-controlled treatments and isolated for downstream analysis. Although in vitro models lack the complexity of in vivo models, they do provide a simple, readily scalable, and reproducible system for analysis of quiescence. With in vitro models, it is possible to control the specific cell types present, and the levels of extracellular matrix proteins, and signaling and growth factors.

The choice of cell type in establishing an in vitro model of quiescence is important. The cells should be amenable to easy isolation from tissues and they should be able to be cultured readily in vitro by following standard tissue culture techniques. A variety of cell types have been used for establishing in vitro models of quiescence, including pancreatic stellate cells [51], HUVECs [52], myoblasts [53], keratinocytes, astrocytes, and fibroblasts described further below.

Fibroblasts are the predominant cell type in connective tissue. They secrete extracellular matrix proteins such as collagen [54]. Fibroblasts isolated from different tissues such as lung and skin have been extensively used to study quiescence in vitro [7, 15, 55–57]. Dermal fibroblasts are easy to culture and the steps to isolate them from skin have been well established [58–61]. Proliferating dermal fibroblasts can be induced into quiescence by contact inhibition or serumstarvation and these quiescent fibroblasts assume distinct morphologies and gene expression signatures compared to proliferating fibroblasts [15, 19].

We present here steps to establish an in vitro model of quiescence using neonatal dermal fibroblasts. We provide protocols for the isolation of neonatal fibroblasts from foreskin, for culturing these fibroblasts in a laboratory tissue culture setting, and for inducing the fibroblasts into quiescence. We also describe methods to regulate the expression level of a specific gene via transfection of short interfering (siRNA). siRNA-based methods permit the investigation of the functional role of an individual factor in quiescence entry or exit.

## 2 Materials

For all of the tissue culture procedures described, fibroblasts are grown in a 10 cm tissueculture treated plate (10 ml culture volume) in an incubator set at 37 °C with 5% $CO_2$ level, unless otherwise indicated. Culture volumes can be adjusted if using tissue culture plates or dishes of different sizes.

### 2.1 Procurement of Skin Tissue for Fibroblast Isolation

To isolate primary human dermal fibroblasts, we obtained human skin from newborns via the National Disease Research Interchange (http://ndriresource.org/) under a protocol approved by the UCLA Institutional Review Panel. Readers should follow all the safety and ethical guidelines as mandated by their local Institutional Review Board. An authorized person who has received appropriate training, following the procedure approved by the Institutional Review Board and wearing the appropriate personal protective equipment, should be responsible for skin collection.

### 2.2 Materials for Isolating Fibroblasts

1. Antibiotic/antimycotic solution: 100 U/ml penicillin G, 100 μg/ml streptomycin, and 2.5 μg/ml amphotericin B dissolved in Dulbecco's modified phosphate-buffered saline (DPBS) without calcium and magnesium. Filter-sterilize and store at −20 °C protected from light.
2. 15 cm plates.
3. 100% ethanol.
4. Two pairs of eye forceps.
5. Surgical scissors.
6. 0.5% dispase solution: Add 500 mg solid dispase per 100 ml PBS. Filter-sterilize and store at −20 °C in 5 or 25 ml aliquots. All the dispase may not dissolve.
7. Scalpel.
8. 15 ml polypropylene tubes.
9. 1000 U/ml collagenase: Add 320 mg solid collagenase (318 U/mg Collagenase Type 1A) per 100 ml PBS. Filter-sterilize and store at −20 °C in 5 or 25 ml aliquots.
10. Ice-cold DMEM with 7.5% Fetal Bovine Serum (FBS).
11. 70 μm nylon mesh strainers.
12. 100× Antibiotic/antimycotic Solution: Dissolve 10,000 units/ml Penicillin G, 10,000 μg/ml Streptomycin, and 25 μg/ml Amphotericin B in PBS. Filter-sterilize and store at −20 °C protected from light.
13. Fortified growth medium: Dulbecco's Modified Eagle Medium (DMEM), 10% FBS, 1× antibiotic solution, 1 mM sodium pyruvate, 10 mM HEPES buffer, 2 mM L-glutamine, 0.1 mM nonessential amino acids in Minimum Essential Medium (MEM) (1:100 of 10 mM stock).
14. Inverted light microscope.
15. Number 22 disposable surgical blades.

### 2.3 Essential Tissue Culture Reagents for Culturing Fibroblasts

1. Vial of frozen fibroblasts.
2. Water bath at 37 °C.
3. 15 ml conical tubes.
4. Complete medium: Dulbecco's Modified Eagle Medium (DMEM), 10% fetal bovine serum (FBS).
5. 10 cm tissue culture-treated plates.
6. Inverted light microscope.
7. Dulbecco's modified phosphate-buffered saline (DPBS) without calcium and magnesium.
8. 0.05% trypsin in DPBS.

9. Trypan blue.
10. Automated cell counter and disposable chamber slide or hematocytometer and hematocytometer slide.
11. Low serum medium: DMEM and 0.1% serum.
12. Eppendorf tubes (1.5 ml).
13. Cell cooling apparatus (e.g., Mr. Frosty™ freezing container).

### 2.4 Preparation of Cell Lysates

1. Cell lysis buffer (such as commercially available mammalian protein extraction reagent (M-PER) from Life Technologies).
2. Protease inhibitors.
3. Bicinchoninic acid assay (BCA assay) kit.
4. Soybean trypsin inhibitor.
5. Eppendorf tubes (1.5 ml).

### 2.5 siRNA Transfection

1. Plates for transfection (type depends upon the experimental design).
2. Transfection reagent for siRNA transfection (commercially available).
3. siRNAs for the genes of interest (commercially available).

## 3 Methods

Pre-warm all the media and other reagents to 37 °C using a water bath or a dry bath for at least 15 min. Disinfect the outside surfaces of media bottles, frozen cell vials, and other reagent tubes by spraying with 70% ethanol. All steps are performed inside a tissue culture laminar flow hood under sterile conditions, unless otherwise indicated. The laboratory performing the fibroblast isolation procedure should have permission to work with biohazardous materials and be equipped with all instruments needed to perform mammalian cell culture in a sterile manner. All personnel involved in performing tissue culture experiments require training in handling biohazardous materials.

### 3.1 Isolation of Primary Dermal Fibroblasts

Before starting the procedure, clean all the surgical tools (number 22 disposable surgical blade, scalpel handles, eye forceps, and surgical scissors) with 70% ethanol and wrap them into a closed packet of aluminum foil before sterilizing them by autoclaving. Note: do not let the skin dry at any stage, as this will negatively affect fibroblast yield.

1. Wash the skins (5 ml of solution/skin sample) by submerging the tissue in 100× antibiotic/antimycotic solution in a conical tube and then removing the solution. Repeat once.

2. Incubate the washed skin in 5 ml of 100% ethanol for 1 min on ice followed by washing in 5 ml 100× antibiotic/antimycotic solution for 10 min.
3. With two pairs of eye forceps and surgical scissors, scrape the dermal side of the tissue to recover the subcutaneous connective tissue (second layer of red tissue on the dermal side). Using either surgical scissors or a surgical scalpel and forceps, mince the tissue into small ~0.5 cm width pieces on a 15 cm plate. Incubate the pieces at 37 °C for 1–4 h in 5 ml (per skin) of 0.5% dispase solution in a 15 ml tube (*see* **Note 1**) until the epidermis detaches from the dermis. Fine mincing enhances fibroblast yield and viability, as fibroblasts will grow out from sharply cut edges.
4. Remove the epidermal sheet with gentle agitation or by two pairs of forceps as follows. Lay the skin sample (epidermis side up) on a 15 cm plate and with the curved edge of one pair of forceps, pin down the skin sample, while using the other pair of forceps to pinch and peel off the epidermis. Removal of the epidermis reduces keratinocyte contamination.
5. Using a number 22 disposable surgical blade, mince the dermal sample into 2–3 mm square pieces on a 15 cm plate. Place the pieces (~10–20) in a 15 ml polypropylene tube with 3 ml of collagenase solution. Incubate at 37 °C for 1–2 h with vigorous stirring until some of the cells are suspended in the solution. At this point, the solution should be a bit turbid with some visible insoluble debris. Stop before all of the cells are dissolved in the solution.
6. Add 3 ml ice-cold DMEM containing 7.5% FBS. Vortex the tube a few times to separate fibroblasts from collagen fibers. Filter the supernatant through a 70 μm nylon mesh strainer to remove debris.
7. Centrifuge the cells for 10 min at 150 × *g* at 4 °C. Aspirate the supernatant. Resuspend the pellet in a fortified growth medium and plate the cells on a 15 cm plate. This is passage 1 for this batch of fibroblasts.
8. Aspirate the medium after 24 h to remove detached cells and add fresh, fortified growth medium. Confirm by light microscopy that the cells have the characteristic fibroblast morphology: spindle-shaped cells in monolayer (Fig. 1).
9. Grow the fibroblasts until they become ~80% confluent. Passage the fibroblasts (passage 2) to 2–3 new 15 cm plates. *See* **steps 2–4** in Subheading 3.2 for passaging fibroblasts; scale the amount of each reagent for a 15 cm plate (20 ml of culture volume). Use fortified growth medium instead of complete medium.

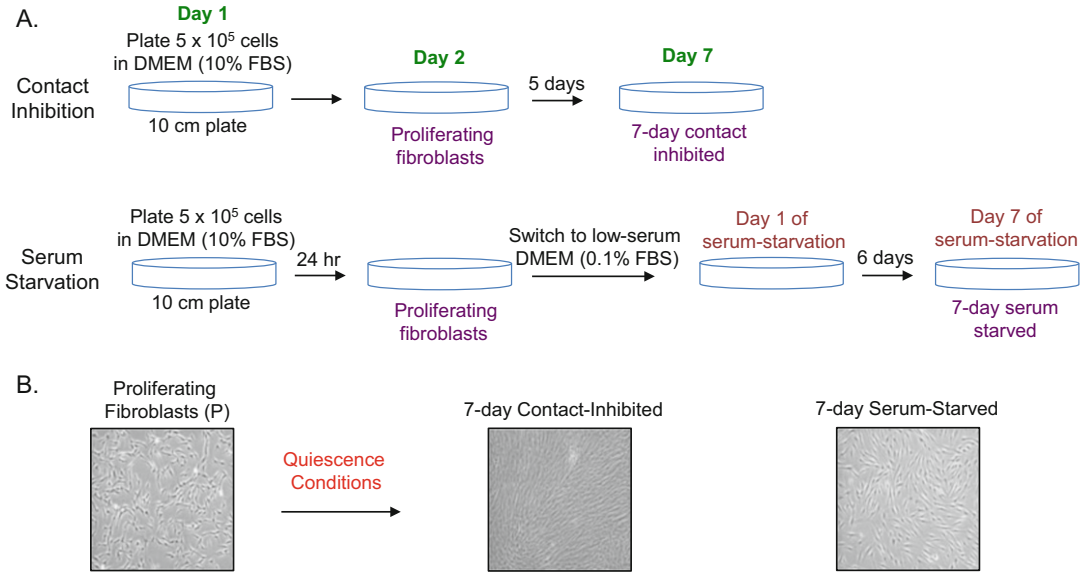


**Fig. 1** Methodology for generating proliferating, contact-inhibited, and serum-starved fibroblasts. (**a**) A schematic showing the protocol for generating proliferating, 7-day contact inhibited and 7 day serum-starved fibroblasts is provided. (**b**) Images of proliferating, serum-starved, and contact-inhibited fibroblasts are provided

10. Freeze cells during passage 3 or 4 (*see* Subheading 3.3 for freezing fibroblasts; scale the reagents for a 15 cm plate and use fortified growth medium instead of complete medium). Make sure the cells are in the exponential growth phase when they are collected for freezing (*see* **Note 2**).

### *3.2 Culturing Proliferating Fibroblasts*

1. Check the 10 cm plate containing fibroblasts under the microscope. Passage the cells if the confluency reaches about 80%. Use complete medium (without antibiotics) for regular culturing of cells (*see* **Note 3**).
2. To passage the cells, remove the medium containing dead and non-adherent cells from the plate by aspiration. Add 5–10 ml DPBS to the plate and gently swirl the plate to wash the cells. This washing step will remove any remaining complete medium that might inhibit the activity of trypsin added in the next step. Aspirate the DPBS from the plate. Add 3 ml of 0.05% trypsin solution to the plate and swirl the plate to coat the cells uniformly with trypsin. Incubate the cells in the incubator for 5 min.
3. After 5 min incubation, check the cells under the microscope to make sure that all the cells have been detached. If the cells are still attached, incubate the cells in the incubator for a few additional minutes. Exposure of the cells to trypsin should be minimized as trypsin affects cell viability. Tap the plate gently

(if needed) to release the cells that are loosely attached to the plate. Add 10 ml of complete medium to neutralize the trypsin. Transfer the cell suspension (13 ml) to a 15 ml conical tube. Spin the tube at 500 × *g* for 5 min to pellet the cells.

4. Aspirate the supernatant containing trypsin from the tube. This removal of trypsin after trypsinization helps in maintaining cell viability. Resuspend the cell pellet in 1 ml of complete medium. A portion of this cell suspension is then added to a fresh tube and mixed with complete medium to achieve a final volume of 10 ml and the desired dilution of the cells. For example, to dilute the cells four times (4× dilution), 250 μl of cells are mixed with 9.75 ml of complete medium and then added to a 10 cm plate.

### 3.3 Freezing and Thawing the Fibroblasts

1. Use proliferating cells of low passage number for freezing (*see* **Note 4**). Pellet the cells as described before (*see* **steps 2** and **3** in Subheading 3.2). Aspirate the supernatant.
2. Add 3 ml of cell freezing medium to the cell pellet and resuspend the pellet by gently pipetting up and down.
3. Add the cell suspension to a cryovial. Using a cryo marker pen or a cryo-label suitable for liquid $N_2$ storage, label the cryovial with the following information: name of investigator, type of cells, cell source, passage number, number of cells in the vial, and date of freezing. An electronic log sheet should be maintained separately containing all the above information and other important information such as type of culture medium and freezing reagent used.
4. Transfer the cryovial to a cooling apparatus for slow cooling and place the apparatus inside a −80 °C freezer overnight. The next day, move the cryovial to a liquid nitrogen freezer for long-term storage.
5. Thaw a vial of frozen fibroblasts by gently swirling the tube in the water bath set at 37 °C. Transfer the cells (1 ml) to a 15 ml conical tube, add 9 ml of complete medium and mix gently by pipetting up and down using a 10 ml serological pipette. Try to avoid generation of air bubbles.
6. Spin the tube at 500 × *g* for 5 min at room temperature to harvest the cells. Remove the supernatant and add 1 ml of complete medium. Suspend the cell pellet by gently pipetting up and down a few times using a 1 ml pipet tip (*see* **Note 5**). Make sure that the cell pellet is completely suspended. Add 9 ml of complete medium and mix. Add the 10 ml of cell suspension to a 10 cm plate. Place the plate inside an incubator. Move the plate forward and backward and sideways to distribute the cells across the surface of the plate. Swirling in a circle may result in cells piling in the middle of the plate.

### 3.4 Induction of Fibroblast Quiescence by Contact Inhibition

1. Grow fibroblasts in a 10 cm plate until the cells are about 80% confluent. Change the medium after every 48 h. Wash the cells, trypsinize, and prepare the cell pellet (*see* **steps 2** and **3** in Subheading 3.2). Resuspend the cell pellet in ~1 ml of complete medium (stock suspension).
2. Take 10 μl of cell suspension in an Eppendorf tube and add 10 μl of trypan blue. Mix well by pipetting up and down. Add 10 μl to the hematocytometer slide or into a disposable chamber slide for automatic counting. Count the cells manually using a hematocytometer or an automated cell counter by following the manufacturer's instructions. For more detailed protocols on cell counting using trypan blue refer to [62]. Note the density (cells/ml) of live cells (*see* **Note 6**). The live cells show bright centers and dark edges upon trypan blue staining. Repeat the counting procedure. Average the two counts to get the final number for live-cell density (Y cells/ml).
3. Calculate the volume of the stock suspension (X ml) needed for plating $5 \times 10^5$ cells per 10 cm plate using the density of live cells (Y cells/ml). Pipet the calculated amount of stock suspension (X ml) to a 15 ml conical tube and then add the appropriate amount of complete medium to make the total volume 10 ml. Mix well and add the suspension to one or many 10 cm plate(s) (Day 1). Incubate the plate(s) in the incubator for about 24 h.
4. Depending upon the strain of fibroblast, the cell confluency can be expected to reach 50–70% after 24 h (Day 2). The cells can be harvested at this stage and the pellet can be prepared as described above (*see* **steps 2** and **3** in Subheading 3.2). At this stage, cell lysates from proliferating cells (P) for western blot can be prepared (*see* Subheading 3.7).
5. Grow the cells until Day 7 changing the medium every 48 h. The cells should cover the bottom of the plate by day 3–4. By day 7, the cells will have ceased to grow due to contact inhibition (Fig. 1). Prepare the cell lysates for 7 day contact inhibited cells (*see* Subheading 3.7).

### 3.5 Induction of Fibroblast Quiescence by Serum Starvation

1. Plate $5 \times 10^5$ cells in a 10 cm plate (*see* **steps 1–3** in Subheading 3.4).
2. After 24 h, wash the cells twice with 5 ml of DPBS to completely remove the medium. Add 10 ml of low serum medium (containing DMEM and 0.01% serum) to the plate. Incubate the plate in the incubator (Day 1 of serum starvation).
3. Change medium (low serum) every 48 h. Continue to grow the cells until Day 7 (Fig. 1). On Day 7, harvest the cells and prepare cell lysate for 7 day serum-starved cells (7dSS) (*see* Subheading 3.8 for modified protocol using trypsin inhibitor).

### 3.6 Restimulation of Quiescent Fibroblasts into a Proliferating State

Cells made quiescent by either contact inhibition or serum starvation can be induced to reenter a proliferative state (restimulation). This is useful for studying the effects of specific proteins and molecular pathways on the transition of cells from a quiescent to a proliferative state.

1. Begin with a 10 cm plate containing fibroblasts in a contact-inhibited state (*see* Subheading 3.4). Detach the cells from the plate by trypsinization and collect the cell pellet (*see* **steps 2** and **3** in Subheading 3.2).
2. Resuspend the cell pellet in 1 ml of complete medium. Take the desired amount of cell suspension (e.g., 200 μl for 5× dilution) in a 15 ml tube and add complete medium so that the final volume is 10 ml. Mix well. Add the cells to a 10 cm plate and culture them under proliferation conditions (cells should be <80% confluent). The proliferating cells can be used for downstream analysis like monitoring protein expression by western blot (*see* Subheading 3.7).
3. For restimulating serum-starved fibroblasts, take a 10 cm plate containing serum-starved cells (*see* Subheading 3.5) and aspirate the low-serum medium. Wash the cells (*see* **step 2** in Subheading 3.2) with 5 ml of DPBS. Detach the cells by trypsinization and neutralize the trypsin with complete medium followed by pelleting the cells by centrifugation (*see* **steps 2** and **3** in Subheading 3.2). Dilute the cells and plate them (*see* **step 4** in Subheading 3.2). This process will restimulate serum-starved cells into a proliferating state. The proliferating cells can be used for downstream analysis (*see* Subheading 3.8).
4. The confluency of serum-starved cells is less than 100%, so depending upon the application, restimulation can be performed with (*see* **step 3** in Subheading 3.5) or without cell dilution (adding complete medium directly to serum-starved cells without any dilution).

### 3.7 Preparation of Cell Lysates for P, 7dCI, and Restimulated Cells

1. Detach the cells from the plate with trypsinization (*see* **Note 7**) and pellet the cells (*see* **steps 2** and **3** in Subheading 3.2). Resuspend the pellet in 0.5–1 ml of DPBS and transfer the cell suspension to a 1.5 ml Eppendorf tube. Keep the cell suspension on ice until the next step. Centrifuge the tube at 2500 × *g* for 10 min to pellet the cells again. Remove the supernatant. This step will remove any residual complete medium and trypsin. If needed, the cell pellet could be flash frozen in dry ice and stored in −80 °C freezer.
2. Add cell lysis buffer containing protease inhibitors to the tube and pipet up and down to suspend the cell pellet completely. Incubate the cell suspension for 10 min at room temperature with gentle shaking. Check the instructions for using the cell

lysis buffer if using a commercially available one. See Ref. 63 for recipes of traditional cell lysis buffers such as NP-40 and RIPA lysis buffers.

3. Centrifuge the tube at 14,000 × *g* for 10 min. Remove the supernatant (cell lysate) and transfer it to a fresh microcentrifuge tube. Measure the concentration of the cell lysate using BCA assay kit by following the manufacturer's instructions. Perform western blot analysis using the collected cell lysates to probe for the proteins of interest.

### 3.8 Preparation of Cell Lysates for 7dSS Cells

1. For a 10 cm plate containing 7dSS cells, aspirate the low-serum medium and trypsinize the cells from the plate (*see* **steps 2** and **3** in Subheading 3.2). Add 3 ml of soybean trypsin inhibitor (instead of complete medium) to quench the activity of trypsin. The use of soybean trypsin inhibitor ensures the cells are not stimulated by serum.
2. Transfer the cell suspension to a 15 ml conical tube. Spin the tube at 500 × *g* for 5 min to pellet the cells. Remove the supernatant. Prepare cell lysates from the cell pellets (*see* **steps 2** and **3** in Subheading 3.7). Perform western blot analysis using these cell lysates to probe for the proteins of interest.

### 3.9 Studying Cell Cycle Exit to a Quiescent State by siRNA Transfection

1. Thaw a vial of frozen fibroblasts and grow a plate of proliferating fibroblasts (*see* **steps 5** and **6** in Subheading 3.3). Count the cells when the confluency reaches ~80% (*see* **steps 1** and **2** in Subheading 3.4). Check the amount of cells to be plated for different plate formats (e.g., 6-well plate or 10 cm plate) by referring to the instruction sheet provided by the manufacturer of the transfection reagent. Plate the desired amount of cells (for the chosen plate format) depending upon the experimental goals and the amount of cells required for downstream analysis.
2. On the next day, check to see if the cells are at the recommended confluency for transfection. Grow the cells for a longer duration or split the cells and replate to achieve the required confluency. Perform the transfection using the desired siRNAs and transfection reagent by following the manufacturer's instructions (*see* **Note 8**). The siRNAs for the genes of interest can be obtained commercially. Usually two or more siRNAs per gene are used. At least one control siRNA should also be used (*see* **Note 9**).
3. Forty-eight hours after transfection (*see* **Note 10**), maintain some cells as proliferating and switch some cells to a low-serum medium (0.1% serum) (*see* **steps 1** and **2** in Subheading 3.5) to induce cell cycle arrest. Cells should be replated at the required confluency before adding the low serum medium.
4. After 24 h, pellet the cells. Prepare cell lysates for western blot analysis, if required (*see* Subheading 3.8).

### 3.10 Studying Cell Cycle Entry from a Quiescent State by siRNA Transfection

1. Take a plate of proliferating cells and switch to a low-serum medium (*see* **steps 1** and **2** in Subheading 3.5).
2. Keep the cells in the low-serum medium (0.1% serum) for 24 h or more depending upon the experimental design. Change the medium every 48 h if serum-starving the cells for more than 48 h.
3. Pellet the cells and suspend the cells in 1 ml of low-serum medium (0.1% serum) (*see* **steps 1** and **2** in Subheading 3.8). Count the serum-starved cells (*see* **step 2** in Subheading 3.2), and plate them according to the instruction sheet for the transfection reagent (*see* **step 1** in Subheading 3.9).
4. On the next day, perform the transfection using the transfection reagent by following the manufacturer's instructions.
5. Forty-eight hours later, switch to a complete medium to induce proliferation.
6. Twenty-four hours after performing **step 5**, harvest the cells for downstream analysis, such as making cell lysates for western blot (*see* Subheading 3.7).

## 4 Notes

1. The incubation time for fibroblast release from tissue will depend upon the freshness of the dispase solution. Freshly prepared solution, same day is ideal, will decrease the incubation time. Also, the powder form of the dispase used to make the solution should be less than a year old. An alternative to dispase treatment is to incubate the skin in 0.3% trypsin solution in DPBS for 10 min. If trypsin is used, agitate the solution every 2–3 min.
2. Fibroblasts are generally passaged or frozen while the cells are still proliferating (i.e., exponential phase). The cells should not be allowed to reach 100% confluency for proliferating samples.
3. Human skin is contaminated with bacteria and other microorganisms, which need to be removed by the addition of antibiotics (penicillin and streptomycin) and antimycotics (amphotericin B). For regular culturing of fibroblasts after they are isolated from skin, the antibiotics can be omitted.
4. Primary cells like fibroblasts can only be passaged for a limited number of times due to a decrease in proliferative potential. The cells will ultimately become senescent upon prolonged passaging. In our laboratory, we culture the fibroblasts to ~12 passages after their isolation. For the same reason, it is also good to freeze the fibroblasts at low passage number (<7). This also allows the investigator to have reserves of fibroblasts

isolated from a specific skin tissue in case an experiment needs to be repeated later. The different strains of fibroblasts isolated from the skin tissue of different infants may be heterogeneous in terms of their proliferation potential and other cellular properties.

5. When resuspending a cell pellet, make sure to gently pipet up and down using a pipet tip a few times (10–12 times) to obtain a uniform cell suspension and to avoid cell clumping. There should not be any visible lumps present in the suspension. A uniform cell suspension will prevent formation of cell clusters when the cells are plated.
6. When counting the cells, use trypan blue to count the number of live cells. Using the counts for live cells, and not total cells, for estimating the cells to be plated ensures that the same number of cells is plated in different experiments. See Ref. 62 for more information on cell counting using trypan blue.
7. Trypsin is used to detach the cells from the plate. If trypsin cannot be used, a cell lysis buffer can be added directly to the plate containing cells [63]. If cell lysis buffer is being used, first aspirate the medium. Wash the cells with PBS and then add the appropriate amount of cell lysis buffer to the plate, maintaining a small volume to ensure proteins will be present in a high concentration. Incubate the plate for 5–10 min with gentle shaking. Collect the lysate (and debris) by tilting the plate and transfer to a 1.5 ml microcentrifuge tube. Centrifuge the tube at 14,000 $\times$ *g* for 10 min. Transfer the supernatant (cell lysate) to a fresh microcentrifuge tube.
8. A forward transfection procedure (plating the cells a day before the transfection) is described here in detail, but transfection can also be performed by following a reverse transfection protocol, i.e., transfection and plating of the cells are performed at the same time. Check the instruction manual of the transfection reagent for more information.
9. siRNAs are double-stranded RNAs (21–28 bp) containing 2-nucleotide overhangs at their 3′ ends. A single RNA strand of the duplex containing a region that is perfectly complementary to a region of target mRNA is incorporated into a silencing complex. This complex is then involved in recognizing and cleaving the target mRNA [64, 65]. Different siRNAs targeting different regions of the same gene may have different knockdown efficiencies, so it is best to use two or more siRNAs for a gene. Follow the manufacturer's protocol for reconstituting and storing siRNAs. Avoid repeated freeze and thaw cycles by aliquoting the reconstituted siRNAs before freezing them.
10. It may take about 48 h for siRNA transfection to affect the targeted gene. Knockdown of the gene of interest should be

monitored 24, 48, and 72 h after transfection using quantitative reverse transcriptase-polymerase chain reaction (RT-PCR) or western blot to find the time for optimal knockdown levels.

## Acknowledgments

H.A.C. was the Milton E. Cassel scholar of the Rita Allen Foundation. This work was funded by grants to H.A.C. from National Institute of General Medical Sciences R01 GM081686, and National Institute of General Medical Sciences R01 GM0866465. H.A.C. acknowledges a Leukemia Lymphoma Society New Idea Award, the Iris Cantor Women's Health Center/UCLA CTSI NIH Grant UL1TR000124, Innovation Awards from the Broad Stem Cell Research Center, and a Career Development Award from the UCLA SPORE in Prostate Cancer. Research reported in this publication was supported by the National Cancer Institute of the National Institutes of Health under Award Number P50CA092131. L.D.H. acknowledges the CARE Fellows and Scholars Program. H.A.C. is a member of the Eli & Edythe Broad Center of Regenerative Medicine & Stem Cell Research, the Jonsson Comprehensive Cancer Center, the UCLA Molecular Biology Institute, and the UCLA Bioinformatics Interdepartmental Program.

### References

1. Coller HA (2011) Cell biology. The essence of quiescence. Science 334(6059):1074–1075. doi:10.1126/science.1216242
2. Daignan-Fornier B, Sagot I (2011) Proliferation/quiescence: When to start? Where to stop? What to stock? Cell Div 6(1):20. doi:10.1186/1747-1028-6-20
3. Cheung TH, Rando TA (2013) Molecular regulation of stem cell quiescence. Nat Rev Mol Cell Biol 14(6):329–340. doi:10.1038/nrm3591
4. Pardee AB (1974) A restriction point for control of normal animal cell proliferation. Proc Natl Acad Sci U S A 71(4):1286–1290
5. Darby IA, Hewitson TD (2007) Fibroblast differentiation in wound healing and fibrosis. Int Rev Cytol 257:143–179. doi:10.1016/S0074-7696(07)57004-X
6. Bainbridge P (2013) Wound healing and the role of fibroblasts. J Wound Care 22 (8):407–408. 410–412. doi:10.12968/jowc.2013.22.8.407
7. Lemons JM, Feng XJ, Bennett BD, Legesse-Miller A, Johnson EL, Raitman I, Pollina EA, Rabitz HA, Rabinowitz JD, Coller HA (2010) Quiescent fibroblasts exhibit high metabolic activity. PLoS Biol 8(10):e1000514. doi:10.1371/journal.pbio.1000514
8. Evertts AG, Manning AL, Wang X, Dyson NJ, Garcia BA, Coller HA (2013) H4K20 methylation regulates quiescence and chromatin compaction. Mol Biol Cell 24(19):3025–3037. doi:10.1091/mbc.E12-07-0529
9. Polioudakis D, Bhinge AA, Killion PJ, Lee BK, Abell NS, Iyer VR (2013) A Myc-microRNA network promotes exit from quiescence by suppressing the interferon response and cell-cycle arrest genes. Nucleic Acids Res 41 (4):2239–2254. doi:10.1093/nar/gks1452
10. Spencer SL, Cappell SD, Tsai FC, Overton KW, Wang CL, Meyer T (2013) The proliferation-quiescence decision is controlled by a bifurcation in CDK2 activity at mitotic exit. Cell 155 (2):369–383. doi:10.1016/j.cell.2013.08.062
11. Nakamura-Ishizu A, Takizawa H, Suda T (2014) The analysis, roles and regulation of quiescence in hematopoietic stem cells. Development 141(24):4656–4666. doi:10.1242/dev.106575

12. Wang L, Siegenthaler JA, Dowell RD, Yi R (2016) Foxc1 reinforces quiescence in self-renewing hair follicle stem cells. Science 351 (6273):613–617. doi:10.1126/science.aad5440
13. Yusuf I, Fruman DA (2003) Regulation of quiescence in lymphocytes. Trends Immunol 24 (7):380–386
14. Blanpain C, Lowry WE, Geoghegan A, Polak L, Fuchs E (2004) Self-renewal, multipotency, and the existence of two cell populations within an epithelial stem cell niche. Cell 118 (5):635–648. doi:10.1016/j.cell.2004.08.012
15. Coller HA, Sang L, Roberts JM (2006) A new description of cellular quiescence. PLoS Biol 4 (3):e83
16. Fukada S, Uezumi A, Ikemoto M, Masuda S, Segawa M, Tanimura N, Yamamoto H, Miyagoe-Suzuki Y, Takeda S (2007) Molecular signature of quiescent satellite cells in adult skeletal muscle. Stem Cells 25 (10):2448–2459. doi:10.1634/stemcells.2007-0019
17. Forsberg EC, Passegue E, Prohaska SS, Wagers AJ, Koeva M, Stuart JM, Weissman IL (2010) Molecular signatures of quiescent, mobilized and leukemia-initiating hematopoietic stem cells. PLoS One 5(1):e8785. doi:10.1371/journal.pone.0008785
18. Elkon R, Drost J, van Haaften G, Jenal M, Schrier M, Oude Vrielink JA, Agami R (2012) E2F mediates enhanced alternative polyadenylation in proliferation. Genome Biol 13(7): R59. doi:10.1186/gb-2012-13-7-r59
19. Suh EJ, Remillard MY, Legesse-Miller A, Johnson EL, Lemons JM, Chapman TR, Forman JJ, Kojima M, Silberman ES, Coller HA (2012) A microRNA network regulates proliferative timing and extracellular matrix synthesis during cellular quiescence in fibroblasts. Genome Biol 13(12):R121. doi:10.1186/gb-2012-13-12-r121
20. Hochegger H, Takeda S, Hunt T (2008) Cyclin-dependent kinases and cell-cycle transitions: does one fit all? Nat Rev Mol Cell Biol 9 (11):910–916. doi:10.1038/nrm2510
21. Lim S, Kaldis P (2013) Cdks, cyclins and CKIs: roles beyond cell cycle regulation. Development 140(15):3079–3093. doi:10.1242/dev.091744
22. Malumbres M (2014) Cyclin-dependent kinases. Genome Biol 15(6):122
23. Sherr CJ, Roberts JM (1999) CDK inhibitors: positive and negative regulators of G1-phase progression. Genes Dev 13:1501–1512
24. Coats S, Flanagan WM, Nourse J, Roberts JM (1996) Requirement of p27Kip1 for restriction point control of the fibroblast cell cycle. Science 272(5263):877–880
25. Giacinti C, Giordano A (2006) RB and cell cycle progression. Oncogene 25 (38):5220–5227. doi:10.1038/sj.onc.1209615
26. Trimarchi JM, Lees JA (2002) Sibling rivalry in the E2F family. Nat Rev Mol Cell Biol 3 (1):11–20. doi:10.1038/nrm714
27. Weinberg RA (1995) The retinoblastoma protein and cell cycle control. Cell 81(3):323–330
28. Smith EJ, Leone G, DeGregori J, Jakoi L, Nevins JR (1996) The accumulation of an E2F-p130 transcriptional repressor distinguishes a G0 cell state from a G1 cell state. Mol Cell Biol 16(12):6965–6976
29. Guo J, Longshore S, Nair R, Warner BW (2009) Retinoblastoma protein (pRb), but not p107 or p130, is required for maintenance of enterocyte quiescence and differentiation in small intestine. J Biol Chem 284(1):134–140. doi:10.1074/jbc.M806133200
30. El-Sagheer AH, Brown T (2010) Click chemistry with DNA. Chem Soc Rev 39 (4):1388–1405. doi:10.1039/b901971p
31. Salic A, Mitchison TJ (2008) A chemical method for fast and sensitive detection of DNA synthesis in vivo. Proc Natl Acad Sci U S A 105(7):2415–2420. doi:10.1073/pnas.0712168105
32. Johnson EL, Suh EJ, Chapman TR, Coller HA (2012) Identifying Functional miRNA Targets Using Overexpression and Knockdown Methods. In: Mallick B, Ghosh Z (eds) Regulatory RNAs: basics, methods and applications. Springer, Berlin, Heidelberg, pp 295–317. doi:10.1007/978-3-642-22517-8_12
33. Gothot A, Pyatt R, McMahel J, Rice S, Srour EF (1997) Functional heterogeneity of human CD34(+) cells isolated in subcompartments of the G0 /G1 phase of the cell cycle. Blood 90 (11):4384–4393
34. Passegue E, Wagers AJ, Giuriato S, Anderson WC, Weissman IL (2005) Global analysis of proliferation and cell cycle gene expression in the regulation of hematopoietic stem and progenitor cell fates. J Exp Med 202 (11):1599–1611
35. Bickenbach JR (1981) Identification and behavior of label-retaining cells in oral mucosa and skin. J Dent Res 60. Spec No C:1611–1620
36. Morris RJ, Fischer SM, Slaga TJ (1985) Evidence that the centrally and peripherally located cells in the murine epidermal proliferative unit are two distinct cell populations. J Invest Dermatol 84(4):277–281

37. Cotsarelis G, Sun TT, Lavker RM (1990) Label-retaining cells reside in the bulge area of pilosebaceous unit: implications for follicular stem cells, hair cycle, and skin carcinogenesis. Cell 61(7):1329–1337
38. Cheshier SH, Morrison SJ, Liao X, Weissman IL (1999) In vivo proliferation and cell cycle kinetics of long-term self-renewing hematopoietic stem cells. Proc Natl Acad Sci U S A 96(6):3120–3125
39. Kiel MJ, He S, Ashkenazi R, Gentry SN, Teta M, Kushner JA, Jackson TL, Morrison SJ (2007) Haematopoietic stem cells do not asymmetrically segregate chromosomes or retain BrdU. Nature 449(7159):238–242. doi:10.1038/nature06115
40. Wilson A, Laurenti E, Oser G, van der Wath RC, Blanco-Bose W, Jaworski M, Offner S, Dunant CF, Eshkind L, Bockamp E, Lio P, Macdonald HR, Trumpp A (2008) Hematopoietic stem cells reversibly switch from dormancy to self-renewal during homeostasis and repair. Cell 135(6):1118–1129. doi:10.1016/j.cell.2008.10.048
41. Tumbar T, Guasch G, Greco V, Blanpain C, Lowry WE, Rendl M, Fuchs E (2004) Defining the epithelial stem cell niche in skin. Science 303(5656):359–363. doi:10.1126/science.1092436
42. Foudi A, Hochedlinger K, Van Buren D, Schindler JW, Jaenisch R, Carey V, Hock H (2009) Analysis of histone 2B-GFP retention reveals slowly cycling hematopoietic stem cells. Nat Biotechnol 27(1):84–90. doi:10.1038/nbt.1517
43. Sakaue-Sawano A, Kurokawa H, Morimura T, Hanyu A, Hama H, Osawa H, Kashiwagi S, Fukami K, Miyata T, Miyoshi H, Imamura T, Ogawa M, Masai H, Miyawaki A (2008) Visualizing spatiotemporal dynamics of multicellular cell-cycle progression. Cell 132(3):487–498. doi:10.1016/j.cell.2007.12.033
44. Sakaue-Sawano A, Ohtawa K, Hama H, Kawano M, Ogawa M, Miyawaki A (2008) Tracing the silhouette of individual cells in S/G2/M phases with fluorescence. Chem Biol 15(12):1243–1248. doi:10.1016/j.chembiol.2008.10.015
45. Sakaue-Sawano A, Hoshida T, Yo M, Takahashi R, Ohtawa K, Arai T, Takahashi E, Noda S, Miyoshi H, Miyawaki A (2013) Visualizing developmentally programmed endoreplication in mammals using ubiquitin oscillators. Development 140(22):4624–4632. doi:10.1242/dev.099226
46. Bouldin CM, Kimelman D (2014) Dual fucci: a new transgenic line for studying the cell cycle from embryos to adults. Zebrafish 11(2):182–183. doi:10.1089/zeb.2014.0986
47. Zielke N, Edgar BA (2015) FUCCI sensors: powerful new tools for analysis of cell proliferation. Wiley Interdiscip Rev Dev Biol 4(5):469–487. doi:10.1002/wdev.189
48. Oki T, Nishimura K, Kitaura J, Togami K, Maehara A, Izawa K, Sakaue-Sawano A, Niida A, Miyano S, Aburatani H, Kiyonari H, Miyawaki A, Kitamura T (2014) A novel cell-cycle-indicator, mVenus-p27K-, identifies quiescent cells and visualizes G0-G1 transition. Sci Rep 4:4012. doi:10.1038/srep04012
49. Carrano AC, Eytan E, Hershko A, Pagano M (1999) SKP2 is required for ubiquitin-mediated degradation of the CDK inhibitor p27. Nat Cell Biol 1(4):193–199
50. Kamura T, Hara T, Matsumoto M, Ishida N, Okumura F, Hatakeyama S, Yoshida M, Nakayama K, Nakayama KI (2004) Cytoplasmic ubiquitin ligase KPC regulates proteolysis of p27(Kip1) at G1 phase. Nat Cell Biol 6(12):1229–1235. doi:10.1038/ncb1194
51. Vonlaufen A, Phillips PA, Yang L, Xu Z, Fiala-Beer E, Zhang X, Pirola RC, Wilson JS, Apte MV (2010) Isolation of quiescent human pancreatic stellate cells: a promising in vitro tool for studies of human pancreatic stellate cell biology. Pancreatology 10(4):434–443. doi:10.1159/000260900
52. Vag T, Schramm T, Kaiser WA, Hilger I (2009) Proliferating and quiescent human umbilical vein endothelial cells (HUVECs): a potential in vitro model to evaluate contrast agents for molecular imaging of angiogenesis. Contrast Media Mol Imaging 4(4):192–198. doi:10.1002/cmmi.280
53. Sellathurai J, Cheedipudi S, Dhawan J, Schroder HD (2013) A novel in vitro model for studying quiescence and activation of primary isolated human myoblasts. PLoS One 8(5):e64067. doi:10.1371/journal.pone.0064067
54. Alberts B et al (2002) Fibroblasts and their transformations: the connective-tissue cell family. In: Alberts B, Johnson A, Lewis J, Raff M, Roberts K, Walter P (eds) Molecular biology of the cell, 4th edn. Garland Science, New York
55. Nishiyama T, Akutsu N, Horii I, Nakayama Y, Ozawa T, Hayashi T (1991) Response to growth factors of human dermal fibroblasts in a quiescent state owing to cell-matrix contact inhibition. Matrix 11(2):71–75
56. Bridger JM, Boyle S, Kill IR, Bickmore WA (2000) Re-modelling of nuclear architecture in quiescent and senescent human fibroblasts. Curr Biol 10(3):149–152

57. Boraldi F, Annovi G, Paolinelli-Devincenzi C, Tiozzo R, Quaglino D (2008) The effect of serum withdrawal on the protein profile of quiescent human dermal fibroblasts in primary cell culture. Proteomics 8(1):66–82. doi:10.1002/pmic.200700833
58. Takashima A (2001) Establishment of fibroblast cultures. Curr Protoc Cell Biol Chapter 2:Unit 2 1. doi:10.1002/0471143030.cb0201s00
59. Rittie L, Fisher GJ (2005) Isolation and culture of skin fibroblasts. Methods Mol Med 117:83–98. doi:10.1385/1-59259-940-0:083
60. Villegas J, McPhaul M (2005) Establishment and culture of human skin fibroblasts. Curr Protoc Mol Biol Chapter 28:Unit 28 23. doi:10.1002/0471142727.mb2803s71
61. Huschtscha LI, Napier CE, Noble JR, Bower K, Au AY, Campbell HG, Braithwaite AW, Reddel RR (2012) Enhanced isolation of fibroblasts from human skin explants. BioTechniques 53(4):239–244. doi:10.2144/0000113939
62. Louis KS, Siegel AC (2011) Cell viability analysis using trypan blue: manual and automated methods. Methods Mol Biol 740:7–12. doi:10.1007/978-1-61779-108-6_2
63. Ji H (2010) Lysis of cultured cells for immunoprecipitation. Cold Spring Harb Protoc 2010(8):pdb prot5466. doi:10.1101/pdb.prot5466
64. Dorsett Y, Tuschl T (2004) siRNAs: applications in functional genomics and potential as therapeutics. Nat Rev Drug Discov 3 (4):318–329. doi:10.1038/nrd1345
65. Wittrup A, Lieberman J (2015) Knocking down disease: a progress report on siRNA therapeutics. Nat Rev Genet 16(9):543–552. doi:10.1038/nrg3978
66. Bryant P, Zheng Q, Pumiglia K (2006) Focal adhesion kinase controls cellular levels of p27/Kip1 and p21/Cip1 through Skp2-dependent and -independent mechanisms. Mol Cell Biol 26(11):4201–4213
67. Perucca P, Cazzalini O, Madine M, Savio M, Laskey RA, Vannini V, Prosperi E, Stivala LA (2009) Loss of p21 CDKN1A impairs entry to quiescence and activates a DNA damage response in normal fibroblasts induced to quiescence. Cell Cycle 8(1):105–114
68. Ezhevsky SA, Ho A, Becker-Hapak M, Davis PK, Dowdy SF (2001) Differential regulation of retinoblastoma tumor suppressor protein by G(1) cyclin-dependent kinase complexes in vivo. Mol Cell Biol 21(14):4773–4784
69. Hur J, Choi JI, Lee H, Nham P, Kim TW, Chae CW, Yun JY, Kang JA, Kang J, Lee SE, Yoon CH, Boo K, Ham S, Roh TY, Jun JK, Lee H, Baek SH, Kim HS (2016) CD82/KAI1 Maintains the dormancy of long-term hematopoietic stem cells through interaction with DARC-expressing macrophages. Cell Stem Cell 18 (4):508–521
70. Liu Y, Elf SE, Asai T, Miyata Y, Liu Y, Sashida G, Huang G, Di Giandomenico S, Koff A, Nimer SD (2009) The p53 tumor suppressor protein is a critical regulator of hematopoietic stem cell behavior. Cell Cycle 8 (19):3120–3124
71. Dey-Guha I, Wolfer A, Yeh AC, G Albeck J, Darp R, Leon E, Wulfkuhle J, Petricoin EF III, Wittner BS, Ramaswamy S (2011) Asymmetric cancer cell division regulated by AKT. Proc Natl Acad Sci U S A 108(31):12845–12850
72. Lyublinskaya OG, Borisov YG, Pugovkina NA, Smirnova IS, Obidina JV, Ivanova JS, Zenin VV, Shatrova AN, Borodkina AV, Aksenov ND, Zemelko VI, Burova EB, Puzanov MV, Nikolsky NN (2015) Reactive oxygen species are required for human mesenchymal stem cells to initiate proliferation after the quiescence exit. Oxid Med Cell Longev 2015:502105
73. Key G, Becker MH, Baron B, Duchrow M, Schluter C, Flad HD, Gerdes J (1993) New Ki-67-equivalent murine monoclonal antibodies (MIB 1-3) generated against bacterially expressed parts of the Ki-67 cDNA containing three 62 base pair repetitive elements encoding for the Ki-67 epitope. Lab Invest 68 (6):629–636
74. Osada S, Minematsu N, Oda F, Akimoto K, Kawana S, Ohno S (2015) Atypical protein kinase C isoform, aPKClambda, is essential for maintaining hair follicle stem cell quiescence. J Invest Dermatol 135(11):2584–2592
75. Reed SA, Ouellette SE, Liu X, Allen RE, Johnson SE (2007) E2F5 and LEK1 translocation to the nucleus is an early event demarcating myoblast quiescence. J Cell Biochem 101 (6):1394–1408
76. Wang HC, Fecteau KA (2000) Detection of a novel quiescence-dependent protein kinase. J Biol Chem 275(33):25850–25857
77. Blanpain C, Simons BD (2013) Unravelling stem cell dynamics by lineage tracing. Nat Rev Mol Cell Biol 14(8):489–502

# Chapter 3

# Flow Cytometric Detection of G0 in Live Cells by Hoechst 33342 and Pyronin Y Staining

**Ayad Eddaoudi, Stephanie Louise Canning, and Itaru Kato**

## Abstract

Hoechst 33342 and Pyronin Y double staining can be used to measure DNA and RNA content in live cells by flow cytometry. Quiescent cells at G0 phase have the same amount of DNA as cells at G1 phase but lower RNA levels compared to proliferating cells. Therefore, resting cells in G0 phase can be distinguished from proliferating cells in G1, S, and G2 M phases. This chapter describes a protocol for double staining of live cells with Hoechst 33342 and Pyronin Y. Combined with immunophenotyping of intact and live cells Hoechst 33342 and Pyronin Y staining is a powerful noninvasive method for the analysis and isolation of quiescent cells from any defined cell population.

**Key words** Cell cycle, G0, Hoechst 33342, Pyronin Y, Multiparametric flow cytometry, Live-cell sorting

## 1 Introduction

G0 is described as the cell cycle phase where cells remain in a state of dormancy characterized by mitotic and metabolic quiescence after exiting the cell cycle in response to environmental stimuli or a cell intrinsic genetic program. For example, conditions such as high cell density or serum starvation can drive cells into a quiescent non-proliferative state, which is defined as G0 phase in the cell cycle. Recent advances in molecular and cellular biology suggest that quiescence (G0) is an actively regulated state controlled by not yet fully elucidated regulatory mechanisms allowing cells to survive for an extended period of time and reenter cell cycle when necessary in response to specific physiological stimuli [1]. Quiescence allows unicellular organisms to avoid exhaustion [2] and is crucial for proper homeostasis and regeneration of stem cells [3]. In addition, cancer stem cells use cellular quiescence to escape chemotherapy and maintain malignancy and to progress into metastasis [4].

Cellular quiescence can be identified and measured by multi-parametric flow cytometry and other methods [5] that take

H. Daniel Lacorazza (ed.), *Cellular Quiescence: Methods and Protocols*, Methods in Molecular Biology, vol. 1686,
DOI 10.1007/978-1-4939-7371-2_3, 

advantage of the status of cellular components in quiescent cells, such as mitochondria, nuclear proteins, and RNA. In this chapter, we focus on the flow cytometric detection of G0 by simultaneous staining of live cells with Hoechst 33342 and Pyronin Y dyes.

This noninvasive method is used for the separation of G0 and G1 cell cycle phases in intact live cells and is based on the measurement of cellular DNA and RNA content using the cell permeant dyes Hoechst 33342 and Pyronin Y and multiparametric flow cytometry as initially described by Howard Shapiro in 1981 [6] and successfully employed by Srour and Jordan in 2001 to sort and culture viable human bone marrow cells [7]. Non-cycling quiescent cells that are arrested in G0 phase have a lower level of RNA compared to active cells that are in G1, S, G2, or M phases [8]. Hoechst 33342 is a cell-membrane permeant dye that reacts exclusively with double-stranded DNA, while Pyronin Y, also a cell-membrane permeant dye, reacts with DNA, RNA, and mitochondrial membranes. In the presence of Hoechst 33342, the Pyronin Y reaction with DNA is blocked and predominantly stains RNA when used at lower concentrations [9, 10]. When cells are stained first with Hoechst 33342 and then with Pyronin Y, it is possible to distinguish DNA from RNA using fluorescence simultaneously emitted by both dyes and detected by flow cytometry. When these dyes are used at lower concentrations stained human cells can survive cell staining and also can be sorted and cultured successfully. However, at these concentrations Pyronin Y is toxic to murine cells [10].

Hoechst 33342 dye is excited at 350 nm and its blue emission can be recorded between 440 and 480 nm. Pyronin Y optimal excitation is at 550 nm and its optimal emission is around 575 nm. Hence, the ideal cell analyzer for this method would be a flow cytometer fitted with yellow-green (561 nm) and UV (350 nm) lasers. However, a standard flow cytometer fitted with a UV laser is also convenient as Pyronin Y/RNA complex is efficiently excited by the standard 488 nm blue laser most flow cytometers have, and generates strong signals. Pyronin Y can be detected through the same emission filters (band pass filters around 575 or 580 nm) normally used for phycoerythrin (PE) on standard flow cytometers.

## 2 Materials

1. Hoechst 33342 (Hoechst) stock solution (10 mg/ml): dissolve 10 mg of Hoechst powder in 1 ml of distilled water or DMSO (Hoechst is not soluble in PBS but diluted solutions of Hoechst can be used with PBS). Filter-sterilize through a 0.22 μm pore size filter. When stored at 4 °C and protected from light the Hoechst stock solution can last for at least 6 months.

2. Pyronin Y (Pyronin) (1 mg/ml): dissolve 1 mg of Pyronin powder in 1 ml of distilled water. Filter-sterilize through a 0.22 μm filter. Store at 4 °C protected from light.
3. Appropriate cell culture medium.
4. Fetal calf serum (FCS).
5. Water bath that can protect incubated samples from light, adjusted to 37 °C.
6. Sterile phosphate-buffered saline (PBS), pH 7.2.
7. 4-(2-hydroxyethyl)-1-piperazineethanesulfonic acid (HEPES) buffer, 10–25 mM.
8. Flow cytometer fitted with 488 nm and 350 nm UV lasers.

## 3 Methods

### 3.1 Staining Procedure

Hoechst/Pyronin staining of live cells requires approximately 2 h. When combining Hoechst/Pyronin staining with immunophenotyping an additional 30 min period is required. This protocol can be performed under aseptic conditions for sterile cell sorting so that sorted cells can be cultured for further study. The concentration and incubation time for Hoechst and Pyronin require prior optimization for each particular cell type.

1. Resuspend live cells (*see* **Note 1**) in their pre-warmed (37 °C) optimal culture medium (*see* **Note 2**) at a concentration of $1 \times 10^6$ cell/ml. The cell density is crucial for better dyes uptake. Higher numbers of cells can be stained as long as the final cell density is kept at one million cells per ml. Include two extra tubes of one million cells each for single positive controls (one for Hoechst only and one for Pyronin only).
2. Add Hoechst dye to a final concentration of 1–10 μg/ml (1.6–16.2 μM). Hoechst concentration requires optimization (*see* **Note 3**).
3. Mix well and incubate in a water bath pre-adjusted to 37 °C for 45 min (*see* **Note 4**) in the dark. Mix every 15 min.
4. Add Pyronin directly to cells at a final concentration of 1–5 μg/ml (3.3–16.5 μM). Pyronin concentration requires optimization (*see* **Note 5**).
5. Mix well and incubate in the water bath at 37 °C for another 45 min in the dark.
6. Transfer cells onto ice and protect samples from direct exposure to light (*see* **Note 6**).
7. For cell analysis only (no cell sorting), cells can be directly analyzed on a flow cytometer (no wash is needed). *See* Subheading 3.2 for instrument setup, data acquisition, and cell sorting.

8. For cell sorting wash cells with cold PBS and resuspend in PBS at higher cell concentration (up to 20 million cells/ml) with 3% FCS. Keep cells at 4 °C and in the dark during cell sorting.
9. When combining with immunophenotyping staining, centrifuge cells at 250 × *g* for 10 min at 4 °C (*see* **Note 7**). Remove the supernatant and wash once with PBS containing Hoechst and Pyronin at the optimized concentration used during the Hoechst/Pyronin staining (*see* **Note 8**). Centrifuge as before and discard the supernatant leaving 50–100 μl of medium depending on total number of cells.
10. Add fluorochrome-conjugated antibodies cocktail to the cells (*see* **Note 9**), mix well, and incubate on ice for at least 30 min in the dark. At this stage extra tubes could be prepared for single positive controls (compensation beads can be used instead of precious cells) and fluorescence minus one (FMO) controls. FMO controls are cell samples; each one contains all antibodies you are testing except one. Obviously, this kind of multiparametric flow cytometry experiments including phenotyping needs to be designed in advance for the type of flow cytometer available.
11. Wash off remaining antibodies by adding ice-cold PBS containing Hoechst and Pyronin as described above.
12. Centrifuge the cells at 250 × *g* for 10 min at 4 °C.
13. Discard the supernatant and resuspend cells in PBS supplemented with HEPS (10–25 mM, *see* **Note 10**) and 2% serum at the desired density, transfer cells onto ice, and store in the dark.
14. Proceed to analysis or cell sorting by flow cytometry.

### 3.2 Instrument Setup, Data Acquisition, and Cell Sorting

#### 3.2.1 Instrument

A dual-laser flow cytometer fitted with a 488 nm blue laser and a 350 nm UV laser is required to acquire data from samples stained with Hoechst and Pyronin (*see* **Note 11**). When combining this staining with immunophenotyping, a multi-laser multi-parameter flow cytometer that can excite and collect signals from all chosen fluorochromes will be needed. If a green (532 nm) or a yellow-green (561 nm) laser is available, it is preferable to use it to excite Pyronin. With the recent advances in flow cytometry technology multi-laser multi-parameter flow cytometers have become available and more affordable.

#### 3.2.2 Instrument Setup

Keep cells on ice protected from light during the data acquisition time.

1. Adjust the flow cytometer using unstained cells and single positive controls. Ensure the linear scale is selected for Hoechst and Pyronin fluorescence as well as area, height, and width parameters for Hoechst fluorescence.

2. When cell surface immunophenotyping is included, a single positive control for each fluorochrome should be added. FMO controls should also be considered for clear gating strategy. Single positive controls can be prepared from compensation beads in case cells are scarce.
3. Use single positive controls to correct spillover between all fluorochromes and FMO controls to draw correct gates that exclude any background contributed by data spread caused by compensation.
4. Run cells at low Pressure Differential (*see* **Note 12**).
5. Use a dot plot showing Hoechst parameters "Area vs. Height" or "Area vs. Width" to exclude doublets and clumps. Draw a gate around single cells. Be as inclusive as possible.
6. Show single cells in a scatter diagram (FSC vs. SSC). Draw a second gate around cells excluding debris (bottom left corner of the scatter diagram). Use these two gates to look at Hoechst and Pyronin fluorescence.
7. A dot plot with Hoechst fluorescence in X-axis and Pyronin fluorescence in Y-axis should show a distribution of DNA content and RNA content with G0 cells having 2n DNA content and the lowest Pyronin Y signal (Fig. 1). G1 cells have the same amount of DNA as G0 but have higher level of RNA. Cells in G0 also have less RNA level than cells in S phase. A good resolution of cell cycle phases is crucial for the success of this assay.

#### 3.2.3 Cell Sorting

Define your gating strategy and target your cell populations of interest. Cells in G0, G1, S, and G2 M phases from any identified cell populations of interest can be purified using a cell sorter and put back to culture for further studies (Fig. 2).

## 4 Notes

1. Fixed cells can also be stained with Hoechst 33342 and Pyronin Y solutions [11–13]. Cells can be fixed with ice-cold 70% ethanol for 30 min on ice, washed and resuspended in Hoechst 33342 (2 μg/ml final concentration) and Pyronin Y (4 μg/ml final concentration) solution on ice for 20 min. In this case 7-Aminoactinomycin D (7-AAD, excitation: 548 nm, emission: 648 nm, which is also reasonably excited by the 488 nm blue laser) can replace Hoechst 33342 [14] and a UV laser is no longer required.
2. Hoechst uptake by live cells is an active process (it requires internalization by ABC transporter activity) that depends on cell type and should be performed under optimal culture

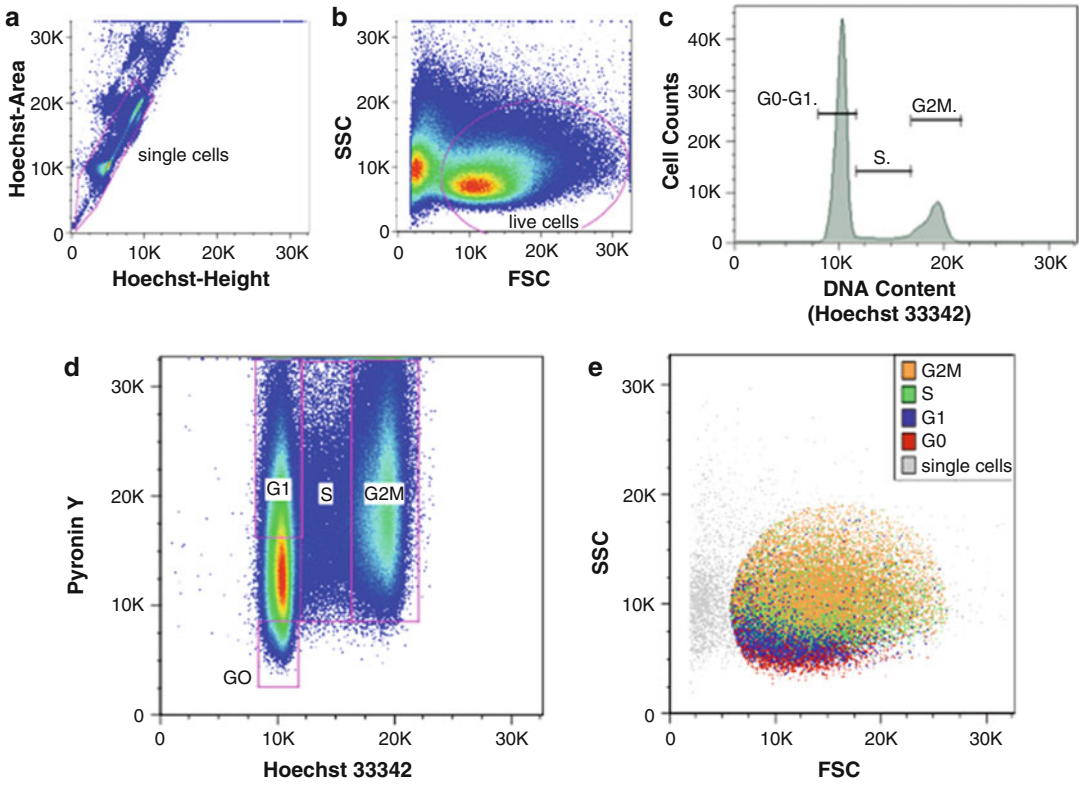


**Fig. 1** Gating strategy. Hoechst 33342 (10 μg/ml, 45 min) and Pyronin Y (3 μg/ml, 15 min) staining in leukemic cells (acute lymphoblastic leukemia, patient sample expanded in mouse): (**a**) Singlet events are gated on Hoechst Area vs. Hoechst Height bivariate. (**b**) Forward scatter (FSC) and side scatter (SSC) characteristics of singlet events. A second gate that excludes debris and dead cells targets live cells. (**c**) DNA content distribution showing cell cycle phases of live cells. Hoechst fluorescence alone cannot discriminate G0 from G1. (**d**) Single cells are analyzed in terms of Hoechst 33342 and Pyronin Y fluorescence with boxes showing G0, G1, S, and G2 M phases as discriminated by the DNA and RNA levels. (**e**) Scatter overlay of cells from each cell cycle phase

conditions. Healthy intact cells of interest (including adherent cells) should be harvested and prepared in single-cell suspension free of clumps prior to staining. Cells should be kept in their own optimal culture medium and under their optimal growing conditions during Hoechst and Pyronin Y staining.

3. Higher concentrations of Hoechst 33342 are toxic to cells while lower concentrations of Hoechst 33342 will lead to less resolved cell cycle phases. The optimal concentration of Hoechst 33342 and incubation time have to be determined empirically in advance for each cell type. In general, dye concentrations between 1 μg/ml and 10 μg/ml and incubation times between 20 min and 90 min lead to well-resolved cell cycle phases. It is advisable to add a viability dye, such as 7-AAD, Propidium Iodide, Topro-3, etc. to monitor cell death during the titration of Hoechst 33342.

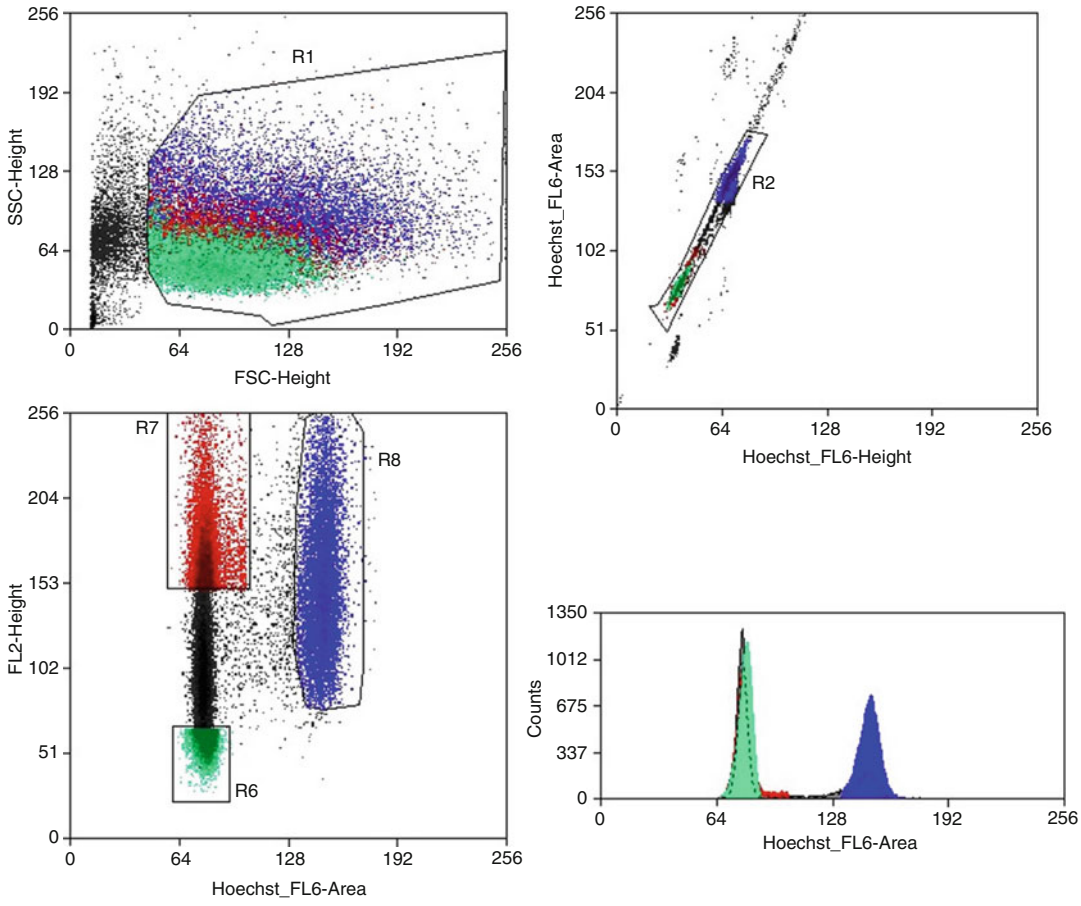


**Fig. 2** A cell-sorting snapshot. MoFlo XDP high-speed cell sorter fitted with 488 nm bleu laser (150 mW) and 350 nm UV laser (100 mW) was used to sort leukemic cells in Go (R6 box), G1 (R7 box), and G2 M (R8 box) phases. We used the same gating strategy as in Fig. 1

4. A cell culture incubator can also be used as long as it could be kept at constant 37 °C for the entire staining procedure. Any drop in temperature will affect the ability of cells to uptake the dyes. When incubating cells in a water bath HEPES should be added to the incubation medium. Cell culture medium with bicarbonate as a buffering system is not suitable to use when cells are kept outside the $CO_2$ cell culture incubator because they are formulated to keep a stable pH under $CO_2$ atmosphere. The cell suspension medium should be buffered properly to avoid cell death during incubation. HEPES buffer maintains a stable pH outside the $CO_2$ incubator.
5. Optimal Pyronin Y concentration is critical. At low concentrations (<1 μg/ml) Pyronin Y does not stain RNA stoichiometrically. At high concentrations, Pyronin Y is toxic to cells and Pyronin Y/RNA complex precipitates, which in turn quenches

PY fluorescence. Optimal Pyronin Y concentration and incubation time have to be determined empirically in advance for each cell type. Depending on cell type, Pyronin Y incubation time can take 15–45 min to achieve stoichiometric staining of RNA.

6. Cells loaded with Hoechst 33342 and Pyronin Y become photosensitive and should be protected from exposure to direct light during staining, cell sorting, and after cell sorting.
7. To keep cells viable and avoid cell loss use low centrifugation force with the brake off and longer centrifugation time. Again, this should be optimized for each cell type beforehand to make sure you are not losing your cells after centrifugation. 250 × *g* for 10 min is a good start for most suspension and blood cells when spun down in small volumes. Cell loss can be avoided by using a centrifuge with the brake set to off.
8. Concentration of both Hoechst 33342 and Pyronin Y should be maintained in all washing and staining solutions during immunophenotyping staining to prevent efflux of the dyes. When working with mouse bone marrow cells, verapamil hydrochloride (50 μM in DMSO or Ethanol), a multidrug-resistant (MDR1) protein inhibitor, could be added to the cells alongside Hoechst 33342 and Pyronin Y to block efflux of the dyes or to check that stem-cell-enriched side population (SP), defined by Hoechst blue and red fluorescence [15] and which has strong dye efflux activity, is not affecting the DNA and RNA profiles [16]. SP cells show a lower intensity of Hoechst 33342 blue and red fluorescence that is below the level emitted by cells in G0/G1.
9. With the introduction of Brilliant Violet and Brilliant Ultra Violet fluorochromes (BD Biosciences and Biolegend) in addition to standard fluorochromes such as FITC, PECy7, APC, and its conjugates, there are a few good choices of non-overlapping fluorochromes to combine with Hoechst 33342 and Pyronin Y staining without major compensation issues. A suitable viability dye could also be added to exclude dead cells.
10. Cells should be kept viable during long cell sorting period. Any change in pH will affect their viability. High-speed cell sorting involves applying high pressure to cell suspensions that decreases pH. Adding HEPES buffer to cell suspension (and collection) medium will maintain the optimal pH 7.2 for the cells during the cell sorting.
11. Because Hoechst 33342 requires an expensive UV laser that most flow cytometers are not equipped with, it may be replaced with a cell membrane permeant DNA dye that is excited with the standard lasers (488 nm blue laser, 633–647 nm red laser, or 405 Violet laser). Vital DNA-specific dyes such as Draq5, Vybrant DyeCycle Green, Vybrant DyeCycle Ruby, or Vybrant DyeCycle Violet are potential candidates.

12. Pressure Differential (difference between sheath and sample pressure) is used in flow cytometry to drive the cell suspension through a hydrodynamically focused sheath fluid. The higher the Pressure Differential the wider the core of the medium—in which cells are suspended—inside the sheath stream. The manufacturer usually sets the low Pressure Differential level that delivers cells one-by-one in a single lane for interrogation by lasers. At low Pressure Differential, an acceptable high event rate can be achieved by concentrating cell suspension without increasing coincidence and aborts. This event rate depends on the type of the flow cytometer. New instruments equipped with the latest flow cytometry technology can accommodate up to 20,000 cells per second without losing precision and accuracy of signal measurement (low coefficient of variation).

## References


1. Cheung TH, Rando TA (2013) Molecular regulation of stem cell quiescence. Nat Rev Mol Cell Biol 14(6):329–340
2. Gray JV, Petsko GA, Johnston GC, Ringe D, Singer RA, Werner-Washburne M (2004) 'Sleeping beauty': quiescence in Saccharomyces cerevisiae. Microbiol Mol Biol Rev 68 (2):187–206
3. Arai F, Suda T (2008) Quiescent stem cells in the niche. In: StemBook, ed. The stem cell research community, StemBook. doi/103824/stembook16.1
4. Moore N, Lyle S (2011) Quiescent, slow-cycling stem cell populations in cancer: a review of the evidence and discussion of significance. J Oncol 2011:1–11. doi:10.1155/2011/396076
5. Nakamura-Ishizu A, Takizawa H, Suda T (2014) The analysis, roles and regulation of quiescence in hematopoietic stem cells. Development 141(24):4656–4666
6. Shapiro HM (1981) Flow cytometric estimation of DNA and RNA content in intact cells stained with Hoechst 33342 and Pyronin Y. Cytometry 2(3):143–150
7. Srour EF, Jordan CT (2011) Isolation and characterization of primitive hematopoietic cells based on their position in cell cycle. In: Klug CA, Jordan CT (eds) Hematopoietic stem cell protocols, Methods in molecular medicine, 63rd edn. Humana, Totowa, NJ
8. Darzynkiewicz Z, Traganos F, Melamed MR (1980) New cell cycle compartments identified by multiparameter flow cytometry. Cytometry 1(2):98–108
9. Darzynkiewicz Z, Kapuscinski J, Traganos F, Crissman HA (1987) Application of pyronin Y(G) in cytochemistry of nucleic acids. Cytometry 8(2):138–145
10. Chitteti BR, Srour EF (2014) Cell cycle measurement of mouse hematopoietic stem/progenitor cells. In: Bunting KD, Qu C-K (eds) Hematopoietic stem cell protocols, Methods in molecular biology, vol 1185. Springer, New York, pp 65–78
11. Crissman HA, Darzynkiewicz Z, Tobey RA, Steinkamp JA (1985) Correlated measurements of DNA, RNA, and protein in individual cells by flow cytometry. Science 228 (4705):1321–1324
12. Crissman HA, Darzynkiewicz Z, Tobey RA, Steinkamp JA (1985) Normal and perturbed Chinese hamster ovary cells: correlation of DNA, RNA, and protein content by flow cytometry. J Cell Biol 101(1):141–147
13. Lemons JM, Feng XJ, Bennett BD, Legesse-Miller A, Johnson EL, Raitman I, Pollina EA, Rabitz HA, Rabinowitz JD, Coller HA (2010) Quiescent fibroblasts exhibit high metabolic activity. PLoS Biol 8(10):e1000514. doi:10.1371/journal.pbio.10005, e1000514
14. Toba K, Winton EF, Koike T, Shibata A (1995) Simultaneous three-color analysis of the surface phenotype and DNA-RNA quantitation using 7-amino-actinomycin D and pyronin Y. J Immunol Methods 182(2):193–207
15. Goodell MA, Brose K, Paradis G, Conner AS, Mulligan RC (1996) Isolation and functional properties of murine hematopoietic stem cells that are replicating in vivo. J Exp Med 183 (4):1797–1806
16. Bhatt RI, Brown MD, Hart CA, Gilmore P, Ramani VA, George NJ, Clarke NW (2003) Novel method for the isolation and characterisation of the putative prostatic stem cell. Cytometry A 54(2):89–99

# Chapter 4

# Using Carboxy Fluorescein Succinimidyl Ester (CFSE) to Identify Quiescent Glioblastoma Stem-Like Cells

**Hassan Azari, Loic P. Deleyrolle, and Brent A. Reynolds**

## Abstract

Tumor resistance to conventional therapies is a major challenge toward the eradication of cancer, a life-threatening disease. This resistance mainly results from tumor heterogeneity and more specifically from the existence of "stem-like" cells that remain in a quiescent state for long periods of time and thus escape commonly used anti-cancer drugs resulting in treatment failure. Therefore, targeting this subpopulation would present a viable strategy to overcome tumor burden. This daunting task requires a deep and thorough understanding of the biology of the quiescent stem-cell population, their interaction with tumor microenvironments, and mechanisms used to sustain themselves despite aggressive therapies. In this chapter, we describe detailed technical procedures for the isolation of quiescent or infrequently dividing stem-like cells in cultured glioblastoma tumor cells using carboxy fluorescein succinimidyl ester (CFSE) staining and flow cytometric analysis. Quiescent glioblastoma cells with stem-like features are characterized and subsequently isolated based on their ability to retain the CFSE labeling.

**Key words** Cancer stem cell, Glioblastoma, Flow cytometry, CFSE, Quiescence

## 1 Introduction

Surgical resection, chemotherapy, and radiotherapy are conventional therapeutic approaches for many malignant tumors including glioblastoma (GBM). However, despite aggressive treatment regimens, the majority of tumors would return causing death of tumor-bearing individuals [1, 2]. It has been shown that subpopulations of tumor cells called tumor stem-like cells contribute to this resistance and subsequent tumor recurrence. It is hypothesized that stem-like cells that are slow cycling or remain in a quiescent state are spared from aggressive conventional therapy, which targets preferentially actively proliferating cells [3–5]. As a result, targeting quiescent stem-like cells appears a promising approach to develop more efficient anticancer strategies. Different methodologies were used to isolate this rare cell population from the bulk of tumor cells. Of these include expression of neural stem cell markers such as CD133

H. Daniel Lacorazza (ed.), *Cellular Quiescence: Methods and Protocols*, Methods in Molecular Biology, vol. 1686,
DOI 10.1007/978-1-4939-7371-2_4, 

[6], and CD15 [7]; aldehyde dehydrogenase activity [8]; and elevated expression of adenosine triphosphate-binding cassette (ABC) transporters (Hoechst 33342 dye exclusion), such as breast cancer resistance protein (ABCG2) [9]. Label retention property was also utilized as a tool to identify tumor-initiating cells from many solid tumors including breast [10], skin [11], pancreatic cancers [12], as well as GBM [4]. The fluorescent dye carboxyfluorescein succinimidyl ester (CFSE) was previously used for tracking frequency of cell division in blood-borne tumors in vitro and in vivo [13]. Using this approach, our group identified for the first time a slow cycling population with stem cell-like properties in human GBM. CFSE is a non-fluorescent pro-drug that can easily permeate inside cells and undergo conversion by intracellular esterases into a fluorescent compound that remains inside the cells by forming stable amide bonds through covalent binding of succinimidyl moiety with amine groups of intracellular proteins [14]. Upon each division, the fluorescent dye is equally distributed between daughter cells leading to halving of fluorescence intensity. This approach enables tracking cell cycle frequency for up to eight to ten rounds of division. Using CFSE retention capacity, we identified and isolated a slow cycling subpopulation (top 5% dye-retaining cells) in human GBM cells enriched in cells with cancer stem cell activity [14, 15].

This chapter describes the procedure for CFSE staining and subsequent isolation of quiescent stem-like cell population within a culture of human GBM-derived cells using flow cytometry.

## 2 Materials

### *2.1 Cell Culture*

#### *2.1.1 Cell Culture Plasticware*

1. Tissue culture flasks: 25 and 75 $cm^2$ with 0.2 μm vented filter cap.
2. Sterile polypropylene conical tubes: 15, 50 ml.
3. 40 μm cell strainer.
4. 0.22 μm bottle-top filter.
5. Media bottles (100, 250, or 500 ml).

#### *2.1.2 Culture Medium, Supplements, and Reagents*

1. Neural Stem Cell (NSC) basal medium. This protocol is based on reagents for culture primary neural stem cells from StemCell Technologies (NeuroCult®).
2. NSC proliferation supplement (NeuroCult®).
3. Complete NSC medium: Mix the neural basal medium and the NSC proliferation supplement at a ratio of 9:1, respectively.
4. Solution of Penicillin–Streptomycin.
5. Heat inactivated fetal calf serum.
6. 0.05% Trypsin–EDTA.

7. Phosphate-buffered saline (PBS).
8. Minimal essential medium (MEM).
9. HEPES-buffered minimum essential medium (HEM): Mix 1 × 10 l pack of MEM powder with 160 ml of 1 M HEPES and bring volume to 8.75 l with distilled water. Set the final pH to 7.4 and store at 4 °C.
10. Trypsin inhibitor solution: Make DNase solution by dissolving 10 mg of DNase in 10 ml of HEM. Then, add 0.14 g of trypsin inhibitor to the DNase solution and bring volume to 1 l using HEM. Keep aliquots at −20 °C freezer.
11. 10 μg/ml stock solution of epidermal growth factor (EGF).
12. CellTrace™ CFSE Cell Proliferation Kit.

### 2.2 Flow Cytometry

1. PBS.
2. Fluorescence-activated Cell Sorter (i.e., BD FACSAria II).
3. Propidium Iodide (PI) solution: Dissolve PI in sterile water to a final concentration of 500 μg/ml.

## 3 Methods

In this section, we describe how to prepare a single-cell suspension from glioblastoma-derived spheres, CFSE staining, and CFSE loading verification.

### 3.1 Preparation of Single-Cell Suspension from Glioma Spheres

1. Isolate and expand glioma cells from resected tumor specimens or established cell lines, as described in separate protocols [16, 17].
2. When glioma spheres reach around 200 μm, collect the medium containing spheres, transfer to an sterile tube, and centrifuge at 110 × *g* for 5 min at room temperature (*see* **Note 1**).
3. Decant the supernatant, resuspend the pellet of spheres with 1 ml of 0.05% trypsin-EDTA, and incubate at 37 °C in a water bath for 3–5 min.
4. Mix the trypsin-digested pellet with an equal volume of soybean trypsin inhibitor to quench the trypsin activity (*see* **Note 2**).
5. Very gently pipette the cell suspension to achieve a homogeneous single-cell suspension without any residual spheres and also to ensure that the trypsin activity is stopped (*see* **Note 3**).
6. Centrifuge mixed cell suspension at 110 × *g* for 5 min. Decant the supernatant and resuspend cell pellet with 1 ml of NeuroCult® NSC Basal Medium.
7. Take 10 μl of the single-cell suspension and mix with 90 μl of trypan blue (0.04% in PBS) to perform a cell count.

### 3.2 Staining Single Cells with the CFSE Dye

1. Prepare CFSE staining solution by adding 1 μl of 5 mM CellTrace™ CFSE dye to 1 ml of NeuroCult® Basal Medium to reach a final concentration of 5 μM.
2. Add the staining solution to the cells (1 ml of staining solution for every one million cell), gently mix to reach homogeneity, and incubate suspension at room temperature for 10 min (*see* **Note 4**).
3. Prepare ice-cold NSC Basal Medium as a quenching solution while incubation is ongoing.
4. Add 5–10 volumes of ice-cold quenching solution to CFSE-stained cells to stop labeling process.
5. Centrifuge the resulting suspension at 110 × *g* for 5 min and decant the supernatant (*see* **Note 5**).
6. Wash the pellet to remove free CFSE dye. To achieve this, resuspend the pellet with 1–2 ml of fresh NSC basal medium, centrifuge at 110 × *g* for 5 min, and decant the supernatant. Repeat this procedure for a total of three washes.
7. After the third wash, resuspend cells with 1 ml of NSC basal medium and count cells.
8. Plate CFSE-stained cells in sterile tissue culture flasks at a density 50,000 cells/mL and incubate flasks at 37 °C in a 5% $CO_2$ humidified incubator.

### 3.3 CFSE Staining Evaluation

1. Monitor cells plated in NSA culture under a fluorescent microscope (Fig. 1) to ensure a homogenous CFSE staining (*see* **Note 6**).
2. Run the sample in a flow cytometer to confirm uniform CFSE labeling. Place suspension of CFSE-labeled cells and non-labeled negative control cells in 1× PBS or NSC basal medium in separate FACS tubes. As many as 1–5 × $10^5$ cells in a total volume of 500 μl are adequate to determine successful CFSE staining.
3. Calibrate the flow cytometer based on its user manual instructions and keep in mind that CFSE has a wavelength excitation maximum of 492 nm and emission maximum of 517 nm.
4. Run first non-labeled cells and record the acquired events in forward and side scatter (FSC vs. SSC) and histogram plots gating on main cell population (Fig. 2).
5. Analyze CFSE-labeled cells using same settings used for control cells (Fig. 2).

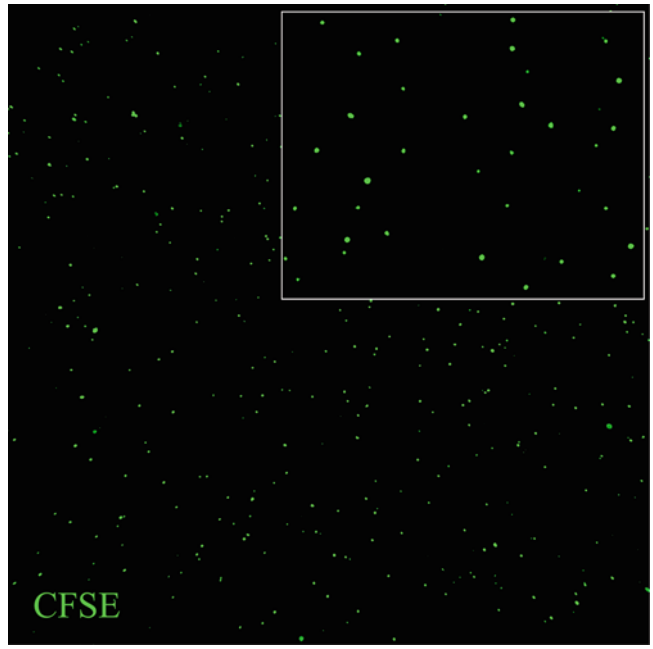


**Fig. 1** Gliomasphere-derived single cells immediately after staining with CFSE dye. The *bright green* color demonstrates successful labeling. Original magnification (5×)

### *3.4 Identification and Isolation of the Quiescent [i.e., CFSE Retaining] Stem-Like Cell Population Using Fluorescent Activated Cell Sorting (FACS)*

As human GBM cells divide to form gliomaspheres, the CFSE intensity decreases and the resulting spheres are composed of cells with different levels of green fluorescence intensity (Fig. 2). The following steps describe procedures required to isolate CFSE retaining cells using FACS.

1. Collect the content of each flask when the spheres have reached an average size of approximately 150–200 μm in diameter (approximately 5–10 days after CFSE labeling depending on growth rate of each cell line), and place them in an appropriate size sterile tissue culture tube.
2. Centrifuge at 110 × *g* for 5 min at room temperature. Decant the supernatant and prepare a single-cell suspension (*see* Subheading 3.1). Resuspend cells in PBS, count cells, and adjust the volume to reach a cell density of $10^7$ cells/ml.
3. Add 1 μl of the solution of propidium iodide (500 μg/ml) for each ml of cell suspension in order to exclude dead cells during flow cytometry analysis or cell sorting.
4. Run non-labeled cells using a flow cytometer and plot forward scatter (FSC) versus side scatter (SSC). Ensure that the majority of the cells are included in the FSC/SSC plot by adjusting voltages for both the FSC and SCC parameters.
5. Plot the events based on SSC versus PI and gate the single live-cell population (PI negative) to exclude dead or damaged cells (PI positive, *see* **Note 7**).

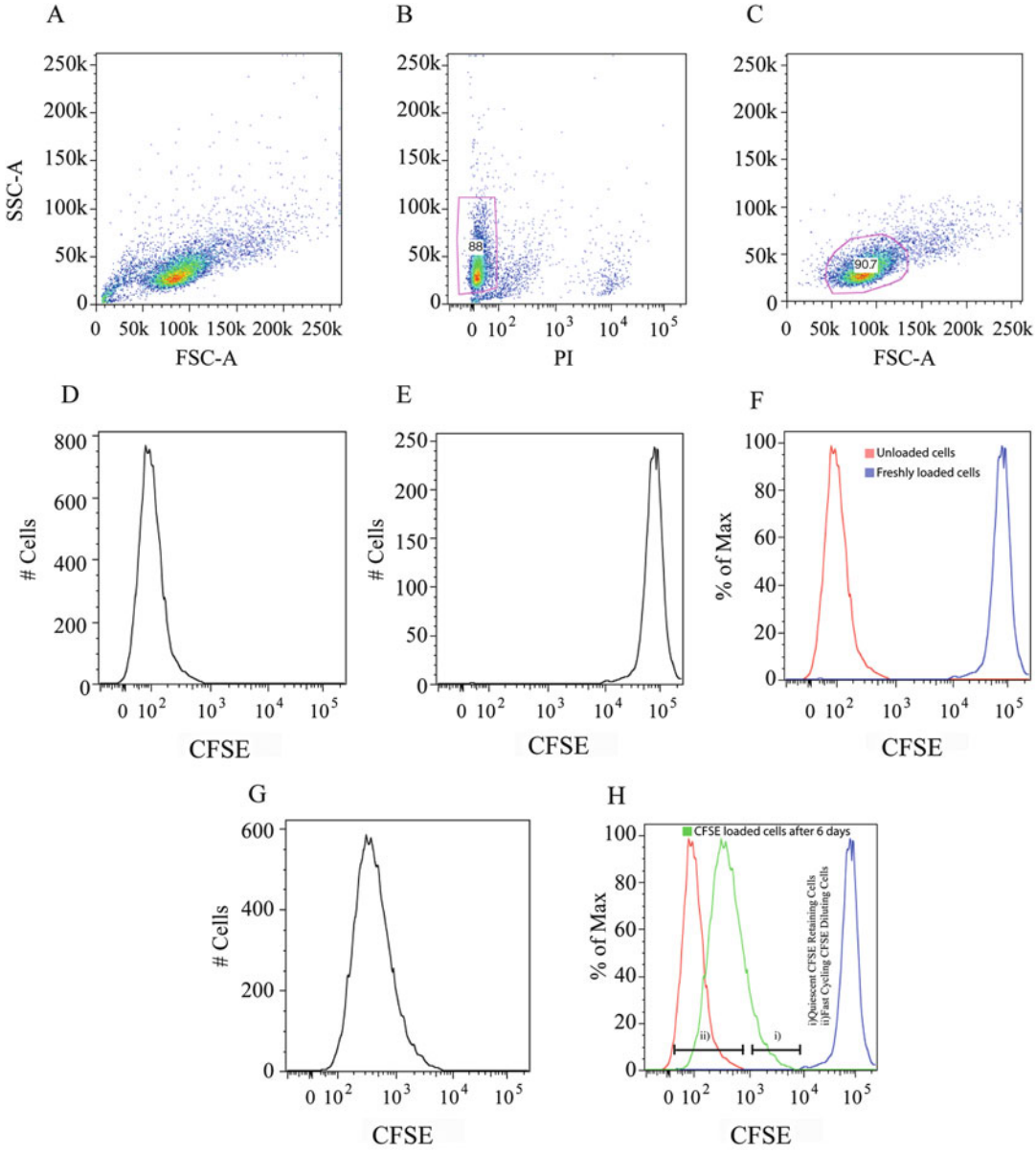


**Fig. 2** CFSE-loading verification and isolation of quiescent stem-like cells 6 days after CFSE labeling using flow cytometry. (**a**) SSC vs. FSC to show the entire cell population, (**b**) SSC vs. PI signal to exclude dead or damaged cells, (**c**) SSC vs. FSC to gate live-cell population, (**d**) Non-labeled gliomasphere-derived cells (CFSE negative), (**e**) Freshly CFSE-labeled gliomasphere-derived cells (CFSE bright), (**f**) Overlap of these two populations shows several orders of magnitude difference in the CFSE fluorescence intensity, (**g**) Gliomasphere-derived cells cultured for 6 days after CFSE labeling, (**h**) Comparing non-labeled cells, freshly labeled cells, and labeled cells after 6 days culture. Although fluorescence intensity decreased over time, it is still much higher in a fraction of cells (quiescent stem-like cells) as compared to the negative control. Histogram displaying the gating strategy to identify CFSE-retaining cells (*i*, top 5%) and CFSE-diluting cells (*ii*, bottom 85%) on day 6 after CFSE labeling

6. Gate live-cell population based on FSC/SSC and then plot live cells in a histogram of CFSE intensity set on a logarithmic scale. Adjust the CFSE laser intensity to place the negative signal between 0 and 100.
7. Run and analyze CFSE-labeled cells in a flow cytometer using the same parameters and gating strategy (Fig. 2).
8. Identify different cell populations based on their ability to retain CFSE ($CFSE^{high}$: top 5% and $CFSE^{low}$: bottom 85%, respectively).
9. Sort and collect the slow-cycling cells ($CFSE^{high}$ cells) and the fast cycling cells ($CFSE^{low}$ cells) in two separate 15 ml sterile tissue culture tubes containing 1 ml of complete NSC basal medium.
10. Centrifuge sorted cells at 110 × *g* for 5 min. Discard the supernatant and resuspend the cell pellet in an appropriate volume of medium and perform a cell count.
11. Use the sorted cells from different populations for downstream experiments such as serial passaging in neurosphere assay, tumor formation experiments, and genetic or molecular analysis.

## 4 Notes

1. The gliomaspheres should not grow beyond 200 μm in diameter. Single cells are difficult to obtain from overgrown spheres and will result in cell death upon dissociation.
2. Do not leave the gliomaspheres in trypsin–EDTA for more than 5 min. Over-trypsinization increases the rate of cell death and subsequently lead to low yield of CFSE-retaining cells.
3. The gliomasphere digested in trypsin–EDTA should not be pipetted before adding trypsin inhibitor. Pipetting at this stage causes membrane rupture and cell death. After the addition of the trypsin inhibitor, gently pipette suspension up and down to ensure a single-cell suspension without damaging cells.
4. Sufficient resuspension of cells in the staining media is required to establish a proper density and ensure homogenous staining.
5. At this point, one should be able to observe a bright-green tinted color in cell pellets at the bottom of the tube, indicating that labeling was successful.
6. At this stage, all cells should have a homogenous bright green color. You can also add a drop of CFSE-labeled cells on a

microscope slide to verify labeling efficiency under the fluorescent microscope.

7. Propidium iodide (PI) is essential for identifying live cells and to be able to remove dead and damaged cells from cells of interest because dead cells might affect downstream applications.

## Acknowledgments

This work was supported by the Florida Center for Brain Tumor Research, the Preston A. Wells Jr. Center for Brain Tumor Therapy, the National Institutes of Health and the American Cancer Society.

### References

1. Veliz I, Loo Y, Castillo O, Karachaliou N, Nigro O, Rosell R (2015) Advances and challenges in the molecular biology and treatment of glioblastoma-is there any hope for the future? Ann Transl Med 3(1):7. doi:10.3978/j.issn.2305-5839.2014.10.06
2. Mrugala MM (2013) Advances and challenges in the treatment of glioblastoma: a clinician's perspective. Discov Med 15(83):221–230
3. Dick JE (2008) Stem cell concepts renew cancer research. Blood 112(13):4793–4807. doi:10.1182/blood-2008-08-077941
4. Deleyrolle LP, Harding A, Cato K, Siebzehnrubl FA, Rahman M, Azari H, Olson S, Gabrielli B, Osborne G, Vescovi A, Reynolds BA (2011) Evidence for label-retaining tumour-initiating cells in human glioblastoma. Brain 134(Pt 5):1331–1343. doi:10.1093/brain/awr081
5. Jackson M, Hassiotou F, Nowak A (2015) Glioblastoma stem-like cells: at the root of tumor recurrence and a therapeutic target. Carcinogenesis 36(2):177–185. doi:10.1093/carcin/bgu243
6. Singh SK, Hawkins C, Clarke ID, Squire JA, Bayani J, Hide T, Henkelman RM, Cusimano MD, Dirks PB (2004) Identification of human brain tumour initiating cells. Nature 432(7015):396–401. doi:10.1038/nature03128
7. Son MJ, Woolard K, Nam DH, Lee J, Fine HA (2009) SSEA-1 is an enrichment marker for tumor-initiating cells in human glioblastoma. Cell Stem Cell 4(5):440–452. doi:10.1016/j.stem.2009.03.003
8. Rasper M, Schafer A, Piontek G, Teufel J, Brockhoff G, Ringel F, Heindl S, Zimmer C, Schlegel J (2010) Aldehyde dehydrogenase 1 positive glioblastoma cells show brain tumor stem cell capacity. Neuro Oncol 12(10):1024–1033. doi:10.1093/neuonc/noq070
9. Bleau AM, Hambardzumyan D, Ozawa T, Fomchenko EI, Huse JT, Brennan CW, Holland EC (2009) PTEN/PI3K/Akt pathway regulates the side population phenotype and ABCG2 activity in glioma tumor stem-like cells. Cell Stem Cell 4(3):226–235. doi:10.1016/j.stem.2009.01.007
10. Krishnamurthy K, Wang G, Rokhfeld D, Bieberich E (2008) Deoxycholate promotes survival of breast cancer cells by reducing the level of pro-apoptotic ceramide. Breast Cancer Res 10(6):R106. doi:10.1186/bcr2211
11. Roesch A, Fukunaga-Kalabis M, Schmidt EC, Zabierowski SE, Brafford PA, Vultur A, Basu D, Gimotty P, Vogt T, Herlyn M (2010) A temporarily distinct subpopulation of slow-cycling melanoma cells is required for continuous tumor growth. Cell 141(4):583–594. doi:10.1016/j.cell.2010.04.020
12. Dembinski JL, Krauss S (2009) Characterization and functional analysis of a slow cycling stem cell-like subpopulation in pancreas adenocarcinoma. Clin Exp Metastasis 26(7):611–623. doi:10.1007/s10585-009-9260-0
13. Graham SM, Jorgensen HG, Allan E, Pearson C, Alcorn MJ, Richmond L, Holyoake TL (2002) Primitive, quiescent, Philadelphia-positive stem cells from patients with chronic myeloid leukemia are insensitive to STI571 in vitro. Blood 99(1):319–325
14. Lyons AB (2000) Analysing cell division in vivo and in vitro using flow cytometric measurement of CFSE dye dilution. J Immunol Methods 243(1–2):147–154

15. Deleyrolle LP, Rohaus MR, Fortin JM, Reynolds BA, Azari H (2012) Identification and isolation of slow-dividing cells in human glioblastoma using carboxy fluorescein succinimidyl ester (CFSE). J Vis Exp 62. doi:10.3791/3918
16. Azari H, Millette S, Ansari S, Rahman M, Deleyrolle LP, Reynolds BA (2011) Isolation and expansion of human glioblastoma multiforme tumor cells using the neurosphere assay. J Vis Exp 56:e3633. doi:10.3791/3633
17. Rahman M, Reyner K, Deleyrolle L, Millette S, Azari H, Day BW, Stringer BW, Boyd AW, Johns TG, Blot V, Duggal R, Reynolds BA (2015) Neurosphere and adherent culture conditions are equivalent for malignant glioma stem cell lines. Anat Cell Biol 48(1):25–35. doi:10.5115/acb.2015.48.1.25

# Chapter 5

# Isolation of Neural Stem and Progenitor Cells from the Adult Brain and Live Imaging of Their Cell Cycle with the FUCCI System

**Alexandra Chicheportiche, Martial Ruat, François D. Boussin, and Mathieu Daynac**

## Abstract

Neural stem cells (NSCs) enter quiescence in early embryonic stages to create a reservoir of dormant NSCs able to enter proliferation and produce neuronal precursors in the adult mammalian brain. Various approaches of fluorescent-activated cell sorting (FACS) have emerged to allow the distinction between quiescent NSCs (qNSCs), their activated counterpart (aNSCs), and the resulting progeny. In this article, we review two FACS techniques that can be used alternatively. We also show that their association with transgenic Fluorescence Ubiquitination Cell Cycle Indicator (FUCCI) mice allows an unprecedented overlook on the cell cycle dynamics of adult NSCs.

**Key words** FUCCI, FACS, Neural stem and progenitor cells, Sub-ventricular zone, Time-lapse video microscopy, Cell cycle

## 1 Introduction

New neurons continue to be produced in the neonatal [1] and the adult rodent brain, emerging from neural stem cells (NSCs) present in two main regions: the sub-ventricular zone (SVZ) along the lateral ventricles [2, 3] and the sub-granular zone (SGZ) of the dentate gyrus in the hippocampus [4, 5]. Adult NSCs are mostly quiescent and only a fraction is actively proliferating [6, 7]. Recent breakthrough studies have identified a slowly dividing population of embryonic NSCs that are the origin of most of the adult NSCs [8–10]. NSCs from the developing ventral hippocampus will migrate from the temporal to septal poles and remain as quiescent NSCs in the SGZ of the adult hippocampus [10], while the vast majority of adult NSCs in the SVZ are produced between E13.5 and E15.5 in the embryonic lateral ganglionic eminences and enter quiescence until their eventual reactivation in the adult [8].

H. Daniel Lacorazza (ed.), *Cellular Quiescence: Methods and Protocols*, Methods in Molecular Biology, vol. 1686,
DOI 10.1007/978-1-4939-7371-2_5, 

The perspective of using endogenous quiescent NSCs (qNSCs) for therapeutic purposes in the adult brain has shed the light on the study of NSCs cell cycle dynamics. However, the rarity of adult quiescent NSCs (qNSCs) and the difficulty to distinguish them from their proliferative counterpart (aNSCs) has kept this study challenging. Here, we review two emerging flow cytometry techniques that have allowed the distinction between qNSCs and aNSCs [11–13] and show how their association with the transgenic FUCCI mice that "color" the cell cycle phases [14] allows a better understanding of the cell cycle dynamics of adult NSCs.

## 2 Materials

### 2.1 Cell Culture and Media

1. Glass-bottom 96-well or 24-well culture plates or micro-plates are coated with poly-D-lysine (PDL 10 μg/ml in distilled H2O) overnight at 37 °C and washed three times after coating with distilled $H_2O$. Allow plates to dry for 2–3 h under a laminar flow (*see* **Note 1**).
2. Culture the medium for activated NSCs and transit-amplifying cells (TACs): NeuroCult NSC Basal Medium (STEMCELL Technologies) mixed with 1:10 of NeuroCult NSC Proliferation Supplement (STEMCELL Technologies) along with 2 μg/ml heparin, 20 ng/ml purified human recombinant epidermal growth factor (EGF), and 10 ng/ml human recombinant fibroblast growth factor 2 (FGF-2).
3. Culture medium for quiescent NSCs [15]: DMEM/F12 supplemented with 0.6% glucose, HEPES buffer (1×), Insulin-Selenium-Transferrin (1×), N-2 and B-27 supplements in the presence of 20 ng/ml EGF or 20 ng/ml EGF and 20 ng/ml bFGF (*see* **Note 2**).

### 2.2 SVZ Dissociation

1. Use PBS with 0.6% Glucose to collect brains and PBS with 0.15% BSA for washing steps and for antibody staining (*see* **Note 3**).
2. Dissociation tools include scissors, dissecting and fine tying forceps (F.S.T), scalpel. Autoclave surgical instruments before use.
3. SVZ dissociation solution (Papain): 1 mg/ml papain in Earl's Balance Salt Solution containing 0.2 mg/ml L-cysteine, 0.2 mg/ml EDTA, and 0.01 mg/ml DNase I in PBS. Sterilize the solution using a 0.22 μm filter. For use warm the solution at 37 °C (*see* **Note 4**).
4. Protease inhibitor solution (Ovomucoid): DMEM/F-12 medium containing 0.7 mg/ml trypsin inhibitor type II.

Sterilize the solution using a 0.22 μm filter. For use warm the solution at 37 °C.

5. 20 μm filters (BD Medimachine Filcon).
6. Percol 22% Plus GE Healthcare in PBS.

### 2.3 DNA Staining, Antibodies, and FACS

1. 5 μg/ml Hoechst 33342 (*see* **Note 5**).
2. Propidium iodine in PBS (final concentration 2 μg/ml).
3. DMEM/F-12 medium supplemented with 2% B27 prior to antibody staining [11].
4. CD15/LeX fluorescein isothiocyanate [FITC] conjugated.
5. GLAST phycoerythrin [PE] (mouse IgG2a).
6. CD24 phycoerythrin [PE]/Cy7 conjugated (rat IgG2b).
7. Alexa647-conjugated EGF ligand.
8. Compensation beads were used as single color controls (*see* **Note 6**).

### 2.4 FUCCI Mice

Two different constructs of FUCCI mice can be used in this protocol [14]: mKO2-hCdt1(30/120) (FUCCI-Red) construct to follow the $G_1$ phase with red fluorescence and mAG-hGem(1/110) (FUCCI-Green) to follow the $S/G_2$ phases with green fluorescence (RIKEN BioResource Center, JAPAN) (*see* **Note 7**).

## 3 Methods

### 3.1 FUCCI Mouse Brain Harvesting and SVZ Dissection

1. Euthanize adult mice following the appropriate institutional guidelines [14]. Choose FUCCI-Red or FUCCI-Green mice depending on the antibody combination used for analysis (*see* **Note 7**).
2. Decapitate dead mice with sharp scissors after spraying the neck with 70% ethanol.
3. Use fine scissors to cut the base of the skull and follow a longitudinal midline until the olfactory bulbs. Remove the skull with fine forceps.
4. Collect the brain in PBS containing 0.6% Glucose, preferably in small cell culture dishes (*see* **Note 3**).
5. Turn the brain to face the ventral side and perform a coronal cut at the level of the optic chiasm using a scalpel.
6. To dissect the SVZ under a microscope, first remove the septum with fine curved forceps and then insert one tip of fine forceps into the adjacent striatum and the other tip into the cortex and gently detach the SVZ. Cut as thin as possible. For additional information watch video describing this procedure [16]. Collect the SVZ in a new small cell culture dish containing PBS 0.6% Glucose.

### 3.2 SVZ Dissociation

1. Mince the SVZ tissue into small pieces using a scalpel or fine forceps and transfer minced tissue to a tube containing SVZ dissociation solution (*see* **item 3** in Subheading 2.2). Use 500 µl–1 ml per mouse.
2. Incubate at 37 °C for 10 min (*see* **Note 8**).
3. Centrifuge at 250 × *g* for 5 min and discard the supernatant.
4. Add 500 µl of pre-warmed protease inhibitor solution (*see* **item 4** in Subheading 2.2) to stop papain activity. The enzymatically dissociated tissue needs to be further dissociated mechanically to reach single-cell suspension by gently pipetting up and down 20–30 times through a p1000 micropipette tip.
5. Filter cell suspension through a 20 µm filter in a new 15 ml tube. Wash the filter with 5 ml of PBS 0.15% BSA.
6. Centrifuge at 250 × *g* for 10 min and discard the supernatant.
7. Add 1 ml of PBS 0.15% BSA, resuspend cells, and then centrifuge in 22% Percoll for 20 min at 4 °C without brakes (*see* **Note 9**).
8. Wash cell suspension with 5 ml PBS 0.15% BSA, centrifuge at 250 × *g* for 10 min, and discard the supernatant.

### 3.3 Live DNA Staining

1. To evaluate the DNA content of each population, cells can be incubated with Hoechst-33342. Warning: the dye Hoechst-33342 can be toxic for cell culture (*see* **Note 5**).
2. Resuspend the cells with 500 µl of DNA content analysis medium (*see* **item 1** in Subheading 2.3) and incubate for 1.5 h at 37 °C.
3. Wash the suspension with 5 ml PBS 0.15% BSA and centrifuge at 250 × *g* for 10 min.

### 3.4 Immunofluorescence Staining for FACS

1. Resuspend cells in 100 µl per mouse of PBS containing 0.15% BSA and the appropriate antibody dilution (*see* **Note 10**). Combination of antibodies depends on FUCCI mice used (Fig. 1a and **Note 7**): (a) For cell cycle analyses using FUCCI-Red mice use CD15/LeX fluorescein isothiocyanate [FITC]-conjugated (1:50; mouse IgM); CD24 phycoerythrin-cyanine7 conjugate [PC7] (1:100; Rat IgG2b; clone M1/69); Alexa647-conjugated EGF ligand (1:150). (b) For cell cycle analyses using FUCCI-Green mice use GLAST phycoerythrin [PE] (mouse IgG2a); CD24 phycoerythrin-cyanine7 conjugate [PC7] (1:100; Rat IgG2b; clone M1/69); Alexa647-conjugated EGF ligand (1:150).
2. Prepare Fluorescence Minus One (FMO) controls. Use Compensation Beads for single-color controls (*see* **Note 11**).
3. Incubate cells and fluorescence-conjugated antibodies for 20 min at 4 °C in the dark.

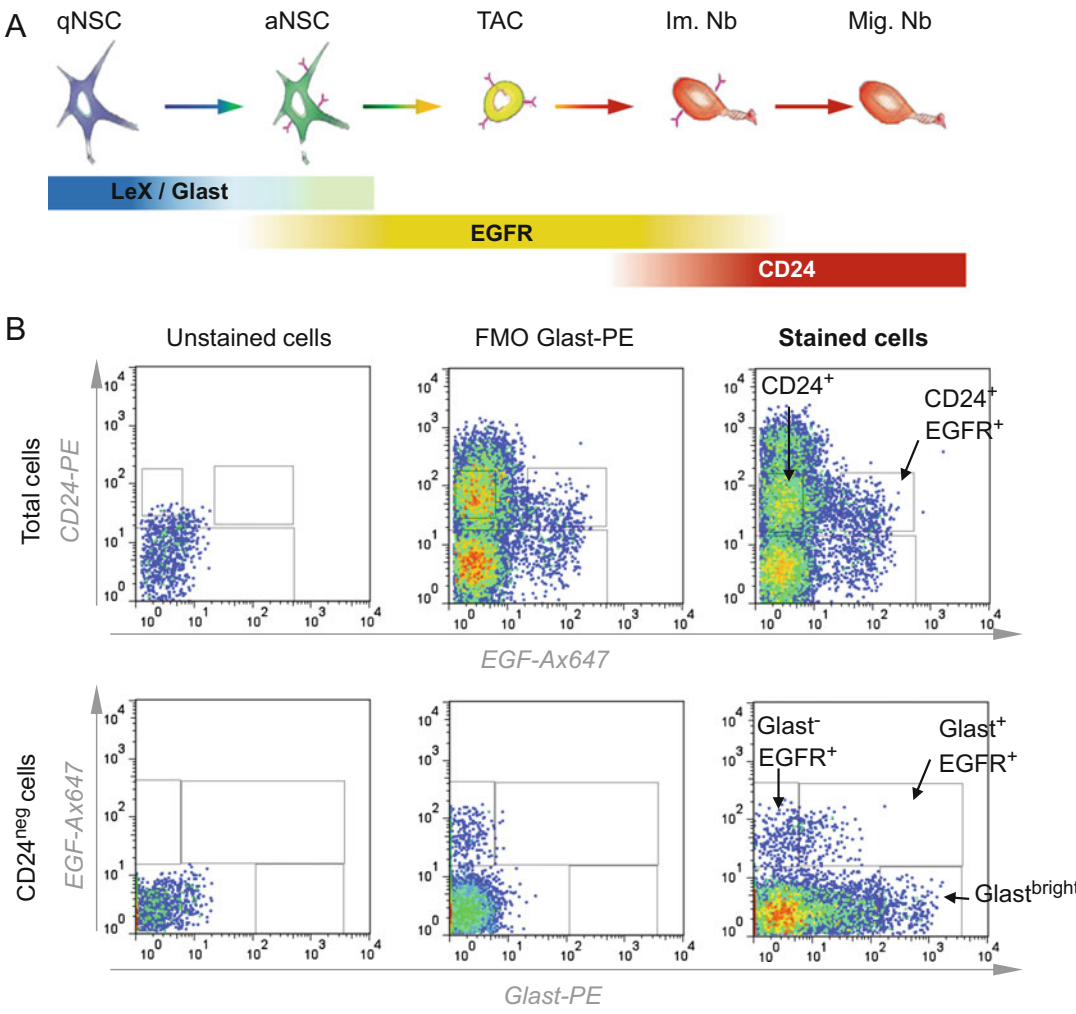


**Fig. 1** FACS strategies to distinguish NSCs from their progeny in the SVZ. (**a**) Two different strategies can be used to distinguish qNSCs, aNSCs, and their progeny. LeX and Glast NSCs markers can be used alternatively with EGFR TACs marker and CD24 neuroblast marker. Diagram was adapted from [13]. qNSC: quiescent Neural Stem Cell; aNSC: activated Neural Stem Cell; TAC: Transit-amplifying cell; Im. Nb: Immature Neuroblast; Mig. Nb: Migrating Neuroblast. (**b**) Example of gate selection with Glast/EGFR/CD24 markers (FUCCI green). Gates are set using the FMO Glast-PE. Glast$^{bright}$ cells represent qNSCs, Glast$^{+}$ EGFR$^{+}$ cells are aNSCs, EGFR$^{+}$ stains for TACs, CD24$^{+}$ EGFR$^{+}$ for immature neuroblasts and CD24$^{+}$ labels migrating neuroblasts. For clarity negative markers are not shown

4. Wash the suspension with 5 ml PBS 0.15% BSA and centrifuge at 250 × *g* for 10 min.
5. Resuspend cells in 200–300 μl of PBS 0.15% BSA per brain. Keep tubes with cells on ice protected from light. Proceed immediately with cell sorting.
6. An example of gating strategy is shown in Fig. 1b for FUCCI red. Glast$^{bright}$ cells are qNSCs, Glast$^{+}$ EGFR$^{+}$ cells are aNSCs.

$EGFR^+$ stains for TACs, $CD24^+$ $EGFR^+$ for immature neuroblasts and $CD24^+$ labels migrating neuroblasts. The gating for FUCCI-green has been previously reported [11, 17].

### 3.5 Cell Sorting with FACS

1. Prior to cell sorting, add Hoechst 33258 or propidium iodine at 2 μg/ml final concentration to discriminate live from dead cells (*see* **Note 12**).
2. In this study cells were sorted using a FACS Aria II (BD Biosciences) at 40 psi with an 85 μm nozzle (*see* **Note 13**). The following filter set was used: 520/35 nm (FITC/FUCCI-Green), 575/26 nm (PE/FUCCI-Red), 670/20 nm (Alexa647) and 740LP (PC7) and 605/40 nm (optional for Hoechst-33342).
3. Adjust voltage of photomultiplier tube (PMT) and compensate with single-color controls. Set the gates with FMO-controls (Fig. 1b).
4. Set the sorting gates with FMO-controls (Fig. 1b).
5. Collect the cells in 100 μl of culture medium.

### 3.6 Time-Lapse Video Microscopy

1. Freshly sorted cells were plated at a density of $\sim 3 \times 10^3$ cells/mL on Poly-D-Lysine-coated 96-well (300μL of culture medium) or 24-well glass-bottom plates (1mL of culture medium).
2. Allow cells to adhere for 1 h in the incubator at 37 °C and 5% $CO_2$.
3. Live imaging can be performed using a Plan Apo VC 20× DIC objective (NA: 0.75) on a Nikon A1R confocal laser scanning microscope system attached to an inverted ECLIPSE Ti. The chamber should be previously warmed at 37 °C under 5% of $CO_2$.
4. Acquire images at a 512 × 512 pixels format with a resolution of 1.26 μm/pixel. A mosaic image can be created to acquire more cells; for better results overlap for the mosaic large image should be set to to 10% (*see* **Note 14**).
5. Capture images every 20 min for 24 h.

### 3.7 Data Analysis

1. Analyze the data using the NIS-Elements AR.4.13.04 64-bit software or ImageJ by tracking cells individually.
2. The use of FUCCI-Red and FUCCI-Green allows calculating $G_1$ and S-$G_2$/M cell cycle phase length independently (Fig. 2a, d, e):
   (a) FUCCI-Green mice: Calculate first S-$G_2$/M phase length by selecting a single non-fluorescent cell and set time 0 ($t = 0$) when green-fluorescence switches "on" until the cell divides (Fig. 2d). The following $G_1$ phase can be

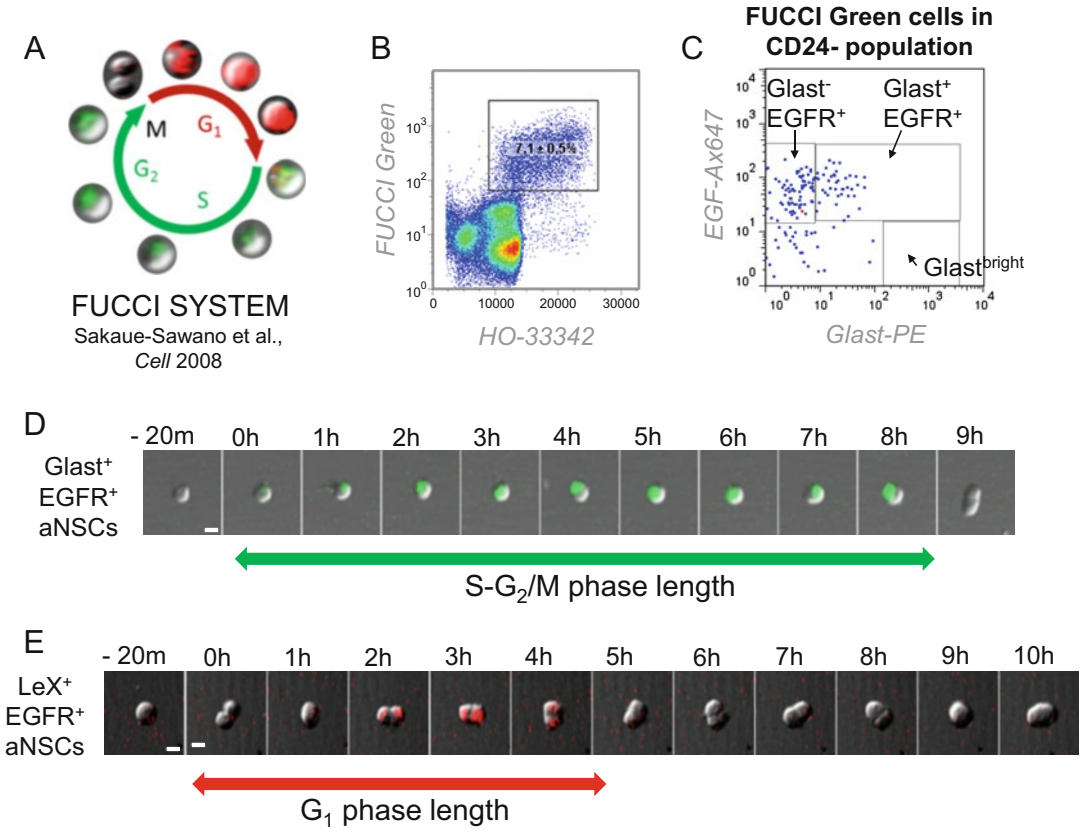


**Fig. 2** Cell cycle tracking using FUCCI mice. (**a**) Schematic of the FUCCI system. Cells acquire red fluorescence during $G_1$ phase driven from the mKO2-hCdt1(30/120) construct and green fluorescence during S-$G_2$/M from the mAG-hGem(1/110) construct [14]. (**b**) The association of Hoechst-33342 (HO-33342) live staining with FUCCI-Green mice allows a precise characterization of proliferating cells. (**c**) Distribution in different populations. (**d**) Example of S-$G_2$/M phase tracking using FUCCI-Green mice (Glast$^+$ EGFR$^+$ aNSCs, FUCCI green). (**e**) Example of $G_1$ phase tracking using FUCCI-Red mice (LeX$^+$ EGFR$^+$ aNSCs, FUCCI red)

measured by calculating the length of time until next green-fluorescence switches back on again. The following S-$G_2$/M and $G_1$ phases can be calculated following the same procedure.

(b) FUCCI-Red mice: Calculate the first S-$G_2$/M phase length (Fig. 2e) by selecting a single red fluorescent cell (in $G_1$) and then set $t = 0$ when red-fluorescence switches "off" to calculate S-$G_2$/M phase length, until the cell divides. The following $G_1$ phase can be calculated by following red-fluorescence until it switches off. The following S-$G_2$/M and $G_1$ phases can be calculated following the same procedure (*see* **Note 15**).

3. For a better distinction of proliferating cells, the combination of FUCCI-Green fluorescence and Hoescht-33342 live

staining can be used as shown in Fig. 2b (*see* **Note 16**). As expected, proliferating FUCCI-Green$^+$ Hoechst-33342 $>$ 2 N cells in the CD24 negative population are mainly activated NSCs (Glast$^+$ EGFR$^+$) and TACs (EGFR$^+$), while very few quiescent NSCs (Glast$^{bright}$) are in proliferation (Fig. 2c).

4. Both flow cytometry strategies give similar results in terms of population selection because the expression of Glast and LeX markers is correlated [13]. For a precise tracking of $G_1$ and its alteration for example in neurodegenerative conditions like aging [18, 19], use FUCCI-Red mice. For a sharp analysis of neural stem and progenitor cells proliferation or cell cycle-entry [13], you should rather track S-$G_2$/M phases with FUCCI-Green fluorescence.

## 4 Notes

1. Better results can be achieved with glass-bottom culture plates notably in terms of image quality at the microscope.
2. We recommend using the minimum cell density ($3 \times 10^3$ cells/mL of medium) to avoid cell aggregation.
3. Small cell culture dishes (e.g., 35 mm $\times$ 10 mm) can be used to collect brains in PBS 0.6% glucose.
4. Because duration of papain treatment is critical to avoid antigen degradation, warm up the papain solution to 37 °C before use.
5. During FACS analysis, dead cells can be excluded using propidium iodide (PI) or Hoechst 33258 added at a final concentration of 2 μg/ml to label dead cells. If the purpose of the experiment is to sort cells for in vitro cultures, we recommend not using live staining with Hoechst-33342 because this dye can be toxic for cells [11]. The use of live DNA staining is recommended for a sharper cell cycle analysis of FACS data.
6. Combination of the antibodies LeX-FITC/CD24PE-Cy7/EGFAx647 [11] and Glast-PE/CD24PE-Cy7/EGFAx647 [12, 13] allows distinguishing NSCs from their progeny.
7. LeX-FITC/CD24PE-Cy7/EGFAx647 antibodies combination needs to be used only with FUCCI-Red mice [17, 18] because mAG-hGem(1/110) (FUCCI-Green) share the same emission wavelength as LeX-FITC. The combination of Glast-PE/CD24PE-Cy7/EGFAx647 [12, 13] needs to be used only with FUCCI-Green mice because mKO2-hCdt1 (30/120) (FUCCI-Red) shares same emission wavelength as Glast-PE.
8. To avoid affecting antibody binding, determine the optimal dissociation time with SVZ dissociation solution time

(10 min in this protocol). Incubations for 15–30 min diminish LeX-FITC antibody binding [11].

9. We recommend using Percoll to remove myelin and ensure cell viability.
10. Avoid pooling more than 2–3 mice to limit the duration of cell sorting because it can affect cell viability and differentiation.
11. Follow the manufacturer's protocol to use compensation beads (Compbead, BD Biosciences). In case of Alexa647-conjugated EGF ligand, use cells for single control.
12. To discriminate live from dead cells, use Hoechst-33258 preferentially because propidium iodine (PI) has a wider emission spectrum that could lead to additional compensation.
13. Any cell sorter can be used but we recommend not exceeding 40 psi to limit cell death.
14. Try to limit exposure to light to ensure cell viability and avoid bleaching of fluorescent dyes conjugated to antibody.
15. If the $G_1$ red fluorescence is too weak at the beginning, choose the onset of the $G_1$ phase on the frame where the cell has divided to avoid approximations.
16. We recommend using HO-33342 + FUCCI-Green for a sharper and precise analysis of proliferating cells (Fig. 2b). However, Hoechst-33342 live staining restricts culture of sorted cells because of dye toxicity (*see* **Note 5**).

## Acknowledgments

We are indebted to members of the LRP, C. Joubert, V. Neuville, V. Barroca, J. Tilliet and all the staff of animal facilities; to J. Baijer and N. Dechamps for cell sorting; O. Etienne for technical assistance, and A. Gouret for her administrative assistance. Flow cytometry and cell sorting were carried out at the iRCM Flow Cytometry Shared Resource, established by equipment grants from DIM-Stem-Pôle, INSERM, Fondation ARC, and CEA. This work was supported by grants of Electricité de France (EDF).

### References

1. Luskin MB (1993) Restricted proliferation and migration of postnatally generated neurons derived from the forebrain subventricular zone. Neuron 11(1):173–189
2. Lois C, Alvarez-Buylla A (1993) Proliferating subventricular zone cells in the adult mammalian forebrain can differentiate into neurons and glia. Proc Natl Acad Sci U S A 90 (5):2074–2077
3. Doetsch F, Caille I, Lim DA, Garcia-Verdugo JM, Alvarez-Buylla A (1999) Subventricular zone astrocytes are neural stem cells in the adult mammalian brain. Cell 97(6):703–716
4. Kaplan MS, Hinds JW (1977) Neurogenesis in the adult rat: electron microscopic analysis of light radioautographs. Science 197 (4308):1092–1094

5. Gage FH, Kempermann G, Palmer TD, Peterson DA, Ray J (1998) Multipotent progenitor cells in the adult dentate gyrus. J Neurobiol 36 (2):249–266
6. Ponti G, Obernier K, Guinto C, Jose L, Bonfanti L, Alvarez-Buylla A (2013) Cell cycle and lineage progression of neural progenitors in the ventricular-subventricular zones of adult mice. Proc Natl Acad Sci U S A 110(11): E1045–E1054. doi:10.1073/pnas.1219563110
7. Furutachi S, Matsumoto A, Nakayama KI, Gotoh Y (2013) p57 controls adult neural stem cell quiescence and modulates the pace of lifelong neurogenesis. EMBO J 32 (7):970–981. doi:10.1038/emboj.2013.50
8. Fuentealba LC, Rompani SB, Parraguez JI, Obernier K, Romero R, Cepko CL, Alvarez-Buylla A (2015) Embryonic origin of postnatal neural stem cells. Cell 161(7):1644–1655. doi:10.1016/j.cell.2015.05.041
9. Furutachi S, Miya H, Watanabe T, Kawai H, Yamasaki N, Harada Y, Imayoshi I, Nelson M, Nakayama KI, Hirabayashi Y, Gotoh Y (2015) Slowly dividing neural progenitors are an embryonic origin of adult neural stem cells. Nat Neurosci 18(5):657–665. doi:10.1038/nn.3989
10. Li G, Fang L, Fernandez G, Pleasure SJ (2013) The ventral hippocampus is the embryonic origin for adult neural stem cells in the dentate gyrus. Neuron 78(4):658–672. doi:10.1016/j.neuron.2013.03.019
11. Daynac M, Chicheportiche A, Pineda JR, Gauthier LR, Boussin FD, Mouthon MA (2013) Quiescent neural stem cells exit dormancy upon alteration of GABAAR signaling following radiation damage. Stem Cell Res 11 (1):516–528. doi:10.1016/j.scr.2013.02.008
12. Mich JK, Signer RA, Nakada D, Pineda A, Burgess RJ, Vue TY, Johnson JE, Morrison SJ (2014) Prospective identification of functionally distinct stem cells and neurosphere-initiating cells in adult mouse forebrain. Elife 3:e02669. doi:10.7554/eLife.02669
13. Daynac M, Tirou L, Faure H, Mouthon MA, Gauthier LR, Hahn H, Boussin FD, Ruat M (2016) Hedgehog controls quiescence and activation of neural stem cells in the adult ventricular-subventricular zone. Stem Cell Reports 7:735–748. doi:10.1016/j.stemcr.2016.08.016
14. Sakaue-Sawano A, Kurokawa H, Morimura T, Hanyu A, Hama H, Osawa H, Kashiwagi S, Fukami K, Miyata T, Miyoshi H, Imamura T, Ogawa M, Masai H, Miyawaki A (2008) Visualizing spatiotemporal dynamics of multicellular cell-cycle progression. Cell 132(3):487–498. doi:10.1016/j.cell.2007.12.033
15. Codega P, Silva-Vargas V, Paul A, Maldonado-Soto AR, Deleo AM, Pastrana E, Doetsch F (2014) Prospective identification and purification of quiescent adult neural stem cells from their in vivo niche. Neuron 82(3):545–559. doi:10.1016/j.neuron.2014.02.039
16. Azari H, Rahman M, Sharififar S, Reynolds BA (2010) Isolation and expansion of the adult mouse neural stem cells using the neurosphere assay. J Vis Exp 45:2393. doi:10.3791/2393
17. Daynac M, Morizur L, Kortulewski T, Gauthier LR, Ruat M, Mouthon MA, Boussin FD (2015) Cell sorting of neural stem and progenitor cells from the adult mouse subventricular zone and live-imaging of their cell cycle dynamics. J Vis Exp 103. doi:10.3791/53247
18. Daynac M, Pineda JR, Chicheportiche A, Gauthier LR, Morizur L, Boussin FD, Mouthon MA (2014) TGFbeta lengthens the G1 phase of stem cells in aged mouse brain. Stem Cells 32(12):3257–3265. doi:10.1002/stem.1815
19. Daynac M, Morizur L, Chicheportiche A, Mouthon MA, Boussin FD (2016) Age-related neurogenesis decline in the subventricular zone is associated with specific cell cycle regulation changes in activated neural stem cells. Sci Rep 6:21505. doi:10.1038/srep21505

# Chapter 6

# Determination of Histone 2B–Green Fluorescent Protein (GFP) Retention in Intestinal Stem Cells

**Kevin R. Hughes and Yashwant R. Mahida**

## Abstract

The epithelium of the gastrointestinal tract represents the interface between the luminal contents of the gut and that of the host tissues and plays a central role not only in regulating absorption of dietary nutrients but also in providing a barrier to prevent the entry of bacteria and other pathogens. Repair and replacement of damaged aging cells within the epithelium is modulated by stem cells, which are located in the intestinal crypts of the small intestine.

Two distinct populations of intestinal stem cells have been described in the literature, one population at the very base of the crypt and a second population of long-lived stem cells located just above the Paneth cell zone. Herein, we describe a method to label this population of long-lived GFP label retaining cells. This method is free from confounding factors of previous methodologies based on radioactive tracers and also enables functional studies not previously possible using the radioactive tracer techniques described in the literature.

**Key words** Intestinal stem cells, Green fluorescent protein, Histone-2B, TetOp H2B–GFP mice, Transgenic mice, Immunohistochemistry

## 1 Introduction

The gastrointestinal tract (GIT) is responsible not only for the digestion of food, but also the transport and absorption of nutrients into the host and the expulsion of waste material. The GIT also represents the interface between the host, luminal gut bacteria (microbiota), and ingested products. It modulates immunological programming and host/microbial mutualism. Most of this regulation occurs via the intestinal epithelial cells, which represent the first host cells that interact with luminal constituents [1, 2].

The GIT can be divided into four main compartments, the oesophagus, stomach, small intestine, and colon. Histologically, the intestine can be subdivided into four compartments, known as the mucosa, submucosa, muscular layer, and serosa. Each region does have a specialized function and consequently, exhibits distinct

H. Daniel Lacorazza (ed.), *Cellular Quiescence: Methods and Protocols*, Methods in Molecular Biology, vol. 1686,
DOI 10.1007/978-1-4939-7371-2_6, 

features with regard to its cellular organization. Specialization is observed, particularly with regard to the intestinal epithelial cell (IEC) subpopulations that line the surface of the intestine [3].

In the small intestine, the intestinal epithelium is folded to form finger-like projections known as intestinal villi, which project out into the intestinal lumen, increasing the effective surface area of the mucosa for improved absorption of nutrients. These villi are separated by invaginations of the epithelial layer known as the crypts of Lieberkühn. These crypts are home to populations of intestinal epithelial stem cells (ISCs), which are important for cellular replacement along the length of the small intestine. Thus, new IECs borne from the ISCs located in the crypts mature and differentiate as they migrate up the tip of the villus into one of five specialized epithelial cell types (*see* Table 1).

Once IECs reach the tip of the intestinal villi, they are lost into the intestinal lumen via a normal homeostatic process known as cell shedding [4]. In this process, dying cells are lost from the intestinal epithelium in a controlled manner via a purse string effect, maintaining epithelial barrier integrity and thus preventing the entry of luminal contents into host tissues.

In the colon, the finger-like villus projections are absent and instead, crypt invaginations into the mucosa are seen at regular intervals. As with the small intestine, new cells formed from ISCs at the crypt base migrate up through the crypt and are lost at the

**Table 1**
**Specialized intestinal epithelial types and their primary functions**

| Epithelial cell type | Shape/organization | Primary function | Lifespan |
|---|---|---|---|
| Enterocytes | Tall columnar cells | Specialized for transport | 5–6 days |
| Goblet cells | Glandular, modified simple columnar epithelial cells, interspersed among other cell types | Secretion of mucus | 5–6 days |
| Paneth cells | Granular cells located in intestinal crypt | Production of antibacterial peptides and lysozyme for defense | Up to 3 months |
| Enteroendocrine cells | Specialized epithelial cell type | Produce gastrointestinal hormones | 5–6 days |
| M-cells | Located near Peyer's patches | Endocytosis of luminal antigens for immune programming | 3–4 days |
| Stem cells | Located at the base of the crypt | Production of new cells | Variable dependent upon population |

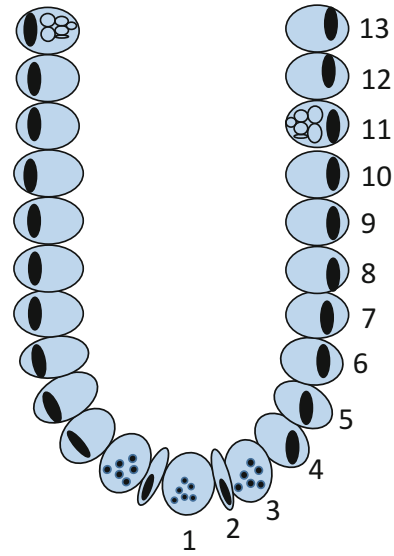


**Fig. 1** Organization of ISCs within the small intestinal crypt. Cells can be identified by their numerical position from the base of the crypt, as indicated. Crypt base columnar (CBC) stem cells sit at the very base of the crypt (cell position 2 in the diagram). Long-lived label-retaining stem cells (LRSCs) sit above the Paneth cell zone, at cell positions 4–6 from the base of the crypt. Paneth cells (cell position 1 and 3) and goblet cells (cell position 11) are also shown

opening of the crypt by similar cell shedding processes as part of the normal everyday replacement of cells.

Positions of cells within the intestinal epithelial cell compartments of the crypt and villus axis can be studied by their cell position relative to crypt base such that cells at cell position 1 reside at the very base of the intestinal crypt and are numbered sequentially from the base of the crypt to the villus tip (Fig. 1) [5]. As shown in Fig. 2, CP4 ISC usually sits above Paneth cells.

Small intestinal stem cells have been studied for more than 40 years and have been identified in two locations in the crypt. One population reside at the crypt base, where they are intercalated with Paneth cells [6]. A second population are located above the Paneth cell zone at cell position 4–6 [7, 8]. Stem cells at the crypt base are marked by Lgr5 and cycle frequently. DNA label-retaining studies have shown that stem cells located above the Paneth cell zone are long lived, with heterogeneity in cycling rates and sensitivity to radiation and may also include those that are dividing asymmetrically [5, 9–11].

Incorporation of bromodeoxyuridine and tritiated thymidine has previously been used to study DNA label-retaining stem cells but disadvantages of this method include the inability to consistently label all quiescent cells (because many may not be dividing at

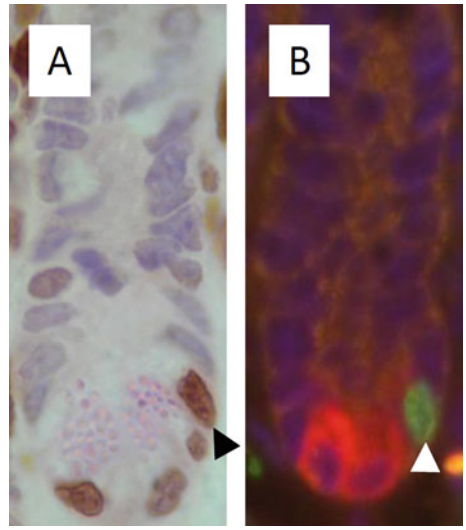


**Fig. 2** Example staining of GFP label-retaining putative ISCs. Panel A shows GFP-labeled ISC (at cell position 4) detected by conventional immuno-histochemical staining (*black arrowhead*). GFP-labeled and unlabeled Paneth cells contain eosinophilic granules. Panel B shows GFP-labeled (*green nucleus*) putative ISC detected by immuno-fluorescence (*white arrowhead*). Paneth cells are identified by cytoplasmic staining for lysozyme (*red*)

the time the label is administered), potential for DNA damage (leading to cell division), and difficulties in their isolation for functional studies. Mice in which transient DNA label can be induced in all epithelial cells have recently been used to identify label-retaining stem cells, following a period when the label is withdrawn (and the DNA label lost from rapidly cycling cells that are subsequently shed into the lumen).

In 2009, studies by the Hock laboratory generated a transgenic mouse in which expression of histone 2B–green fluorescent protein (GFP) fusion protein, which interacts with DNA, was under the dynamic control of the antibiotic doxycycline [12]. These mice are subsequently referred to as Tet-op H2B–GFP mice. In this model, expression of H2B–GFP in the nuclei of cells can be effectively turned "on" or "off" by the administration of doxycycline in the drinking water.

We reasoned that this model would enable labeling of the long lived quiescent population of ISCs in the IEC layer, which was confirmed in our published studies [5]. Below, we outline the optimized methodology for labeling the quiescent ISC population using this mouse model and their identification in histological samples collected from these mice using immuno-histochemical and immuno-fluorescent techniques.

## 2 Materials

### 2.1 In Vivo ISC Labeling Study

1. Tet-op H2BGFP mice.
2. Doxycycline (2 mg/ml) and sucrose (10 mg/ml) in the drinking water.

### 2.2 Tissue Collection

1. Dissection instruments and plasticware.
2. 10% neutral buffered formalin.
3. Whatman filter paper and micropore tape for bundling.
4. 70% Ethanol.

### 2.3 Tissue Processing

1. Ethanol (100%, 90%, 80% and 70%).
2. Xylene.
3. Paraffin wax.
4. Tissue processor (optional).
5. Embedding station.

### 2.4 Immuno-Histochemical Staining

1. Super-frost plus glass slides.
2. Microtome.
3. Water bath.
4. Solvents: Xylene, ethanol, methanol.
5. 0.2% Oxygen peroxide ($H_2O_2$) in methanol.
6. Phosphate-buffered saline (PBS).
7. Antigen retrieval solution (Vector).
8. Wax pen.
9. Rabbit anti-GFP antibody.
10. Peroxidase labeled polymer.
11. Colorimetric peroxidase substrate kit.
12. Mayer's hematoxylin solution.
13. Eosin Y solution.
14. 1% Hydrogen chloride (HCl) and 70% ethanol.
15. 0.1% sodium bicarbonate solution.
16. DPX mounting medium.

### 2.5 Additional Reagents for Immuno-Fluorescent Staining

1. Goat anti-lysozyme antibody.
2. FITC-conjugated anti-rabbit.
3. Rhodamine-conjugated anti-goat.
4. Fluorescent mounting medium.

### 2.6 Cell Count Analysis and Quantification

1. Microscope with fluorescent capability and FITC and TRITC filter channels.
2. Score and WinCrypts analysis software or other counting software.
3. Statistical analysis package.

## 3 Methods

### 3.1 In Vivo ISC Labeling

1. Administer 2 mg/ml Doxycycline (DOX) and 10 mg/ml sucrose in the drinking water to Tet-op H2BGFP transgenic mice from 3 weeks of age and onward (*see* **Note 1**).
2. Fully replenish DOX water at regular intervals thrice weekly (*see* **Note 2**).
3. Continue with DOX administration in drinking water for a period of 23 days to fully label the IEC compartment.
4. Place mice on regular drinking water for 28–162 days (*see* **Note 3**).
5. Collect tissue at defined time points during the chase period.

### 3.2 Tissue Collection

1. Euthanize mice using an approved method and following institutional guidelines.
2. Open the abdominal cavity to expose the peritoneal cavity and locate the intestinal segments of interest.
3. Dissect out the small intestine and flush with 10% neutral buffered formalin to remove luminal contents and prefix the tissue (*see* **Note 4**).
4. Immediately transfer the intestinal tissue to a labeled vial containing 10% neutral buffered formalin.
5. Fix the tissue for 24 h.
6. Following fixation transfer the tissue to 70% ethanol. Samples can be stored short term in 70% ethanol before proceeding to dehydration and embedding steps.
7. Dehydrate the tissue through an ethanol and xylene series either manually, or preferably using an automated device such as a Leica ASP 300S processing station.

At the end of the processing stages, embed tissue samples in paraffin wax ready for sectioning and staining (*see* **Notes 5** and **6**).

### 3.3 Immuno-Histochemical Staining (Single Staining for GFP)

In most cases, single immuno-histochemical staining using hematoxylin and eosin counter-staining is appropriate for discerning GFP-labeled stem cells from GFP-labeled Paneth cells that stain positive for eosinophilic granules (Fig. 2). In cases where staining with two antibodies is required to definitively confirm cellular

identity, serial sections may be double stained as described in Subheading 3.4.

1. Rehydrate the slides through a xylene (×3 solutions) and ethanol series (100, 90, 80, and 70%) by placing slides in each solution for approximately 2 min each.
2. Block endogenous peroxidase activity by incubating in 100% methanol solution containing 0.2% $H_2O_2$ for 30 min at room temperature.
3. Wash slides twice with phosphate-buffered saline (PBS) solution for 5 min each.
4. Perform antigen retrieval using the Vector antigen retrieval solution by diluting according to the manufacturer's instructions and microwaving in a conventional microwave oven in a suitable container for 20 min. Ensure that the slides remain constantly immersed in antigen retrieval buffer.
5. Allow slides to cool at room temperature for 30 min.
6. Wash slides twice in PBS for 5 min.
7. Mark around the edge of the sections using a wax pen.
8. Apply a small volume of Rockland anti-GFP antibody at a concentration 1:200 in PBS (*see* **Note 7**).
9. Incubate for 1 h at room temperature or overnight at 4°C.
10. Wash 3× for 5 min in PBS.
11. Apply peroxidase labeled polymer for 30 min at room temperature (*see* **Note 7**).
12. Wash 3× for 5 min in PBS.
13. Apply colorimetric peroxidase substrate to detect signal. Use an on-slide incubation time of 2 min.
14. Wash slides for 5 min in distilled water.
15. Counterstain slides in Mayer's hematoxylin solution for 10 min.
16. Wash slides briefly in distilled water.
17. Counterstain in eosin Y solution for 2 min (*see* **Note 8**).
18. Wash slides briefly with distilled water.
19. Differentiate slides in 1% HCl and 70% Ethanol for 15 s.
20. Wash slides briefly in distilled water.
21. Differentiate slides in 0.1% sodium bicarbonate solution.
22. Wash slides briefly in distilled water.
23. Dehydrate slides through ethanol (70, 80, 90, and 100%) and Xylene (×3 solutions) series.

24. Apply DPX mounting medium and coverslips to the slides and leave slides to air-dry overnight.
25. Example staining is shown in Fig. 2.

### 3.4 Immuno-Histochemical Staining (Double Staining for GFP and Lysozyme) (See Note 9)

1. Proceed with **steps 1–9** in Subheading 3.3.
2. After the application of anti-GFP antibody, wash slide 3× for 5 min in PBS.
3. Apply anti-lysozyme antibody at a concentration of 1:100 in PBS.
4. Incubate for 1 h at room temperature.
5. Apply rhodamine-conjugated anti-goat and FITC-conjugated anti-rabbit antibodies at a concentration of 1:500 in PBS.
6. Incubate for 30 min at room temperature.
7. Wash 3× for 5 min in PBS.
8. Apply the VECTASHIELD mounting medium and photograph immediately.
9. Example staining is shown in Fig. 2.

### 3.5 Cell Count Analysis and Quantification

1. At least 50 well-oriented, longitudinally sectioned half crypts should be analyzed per mouse (*see* **Note 10**).
2. Assign cells to a cell position relative to the base of the crypt and also to one of four categories: GFP labeled Paneth cell, GFP labeled epithelial cell, unlabeled Paneth cell, or unlabeled epithelial cell.
3. Score and Wincrypts analysis packages can then be used alongside statistical analysis packages to interrogate the data (*see* **Note 11**) and identify the appearance of long-lived GFP labeled stem cells within the stem cell zone.

## 4 Notes

1. Tet-op H2BGFP mice can be used from 6 weeks of age onward, when maturation of the intestinal epithelium is complete and mice exhibit mature intestinal epithelial cell physiology. Labeling of intestinal cells in the preparation for experimental procedures can however be initiated at weaning (3–4 weeks of age) to ensure availability of fully labeled mice at the beginning of adulthood. Transgene expression in all animals is induced by the administration of Doyxcycline hydrochloride in the drinking water. In order to improve palatability, the addition of sucrose in the drinking water is recommended. Sucrose itself does not impact transgene expression and therefore may be excluded in situations where it may affect other aspects of the study design.

2. Doxycycline is an antibiotic normally stored at 4°C. To circumvent issues that may be caused by degradation of the active ingredient once reconstituted, regular replenishment of the drinking water is recommended. In our studies, a thrice-weekly replacement regimen was employed.
3. To achieve complete labeling of intestinal epithelial cells, mice should be administered doxycycline for 23 days. At this point, mice are switched to regular drinking water for the remainder of the study (known as "chase" period). During this chase period, labeled cells are gradually lost as a natural process of cell division and replenishment of old and dying cells within the intestinal epithelial cell compartment. Meanwhile, slow cycling cells of the ISC compartment retain the long-lived H2B–GFP label during chase period. Typically, chase period of 28 days or longer is required to eliminate all but the long-lived subpopulations of cells. The length of the chase period required may need to be optimized by each investigator.
4. Following euthanasia of the animals, immediate fixation of tissue by flushing the intestinal lumen with formalin ensures that cells are fixed in their native state before postmortem cell death processes are initiated. Such preservation may be particularly important in circumstances where susceptibility of label-retaining cells to cell death following irradiation is being investigated and where fixation of cells in their native state, prior to initiation of radiation-independent cell death processes, is paramount. Following the fixation of the tissue, proper orientation of the tissue is essential for subsequent histological analysis and to ensure adequate numbers of well-oriented crypt and villus units for subsequent histological analyses. We recommended using bundling techniques described elsewhere which were successfully employed in our studies [13].
5. Tissue processing and embedding can be achieved in an automated fashion using most standard processors and embedding instrumentation, although these can also be accomplished manually where such equipment is not available. Incubation times as defined in Table 2 should be followed wherever possible, although this may require optimization by the individual experimenter for manual processing techniques.
6. Following embedding, best results for subsequent sectioning and staining are achieved by mounting 3–5 μm sections onto poly-L-lysine-coated slides or superfrost plus positively charged slides to ensure proper adherence of tissue during antigen retrieval steps. Tissue sections should be placed onto histological water bath for around 5–10 min prior to mounting to slides to avoid folding and are then left to dry overnight at room temperature before staining.

**Table 2**
**Typical processing times for preparation of intestinal tissue ready for embedding**

| Step number | Reagent | Incubation time (h) |
|---|---|---|
| 1 | 70% ethanol | 1.5 |
| 2 | 80% ethanol | 1.5 |
| 3 | 90% ethanol | 1.5 |
| 4 | 100% ethanol | 1.5 |
| 5 | 100% ethanol | 1 |
| 6 | 100% ethanol | 1 |
| 7 | Xylene | 1.5 |
| 8 | Xylene | 1 |
| 9 | Xylene | 1 |
| 10 | Paraffin wax | 1.5 |
| 11 | Paraffin wax | 1.5 |

7. Staining with the anti-GFP antibody and secondary reagents that are described provides very robust and reliable staining. Alternative anti-GFP antibodies and secondary reagents are also expected to be suitable, although conditions and dilutions for staining with different reagents will need to be optimized by the individual experimenter, particularly with regard to antigen retrieval, where certain antibody clones may not be suitable for particular retrieval methods.
8. As described, in the majority of cases, standard immunohistochemical techniques are suitable for discerning label-retaining stem cells from residual label-retaining Paneth cells, since the latter can be very easily identified by the presence of eosinophilic granules. Since eosin is water soluble, it is especially important to stick rigidly to the slide-processing schedule described to ensure good staining of eosinophillic granules.
9. As detailed, double immuno-fluorescent staining can also be employed to distinguish labeled Paneth cells from labeled stem cells, but requires more specialized equipment (fluorescent microscope) and can be more challenging for cell count analysis versus assessment with standard bright-field microscopy. If using secondary reagents not detailed in our method, concentration and incubation times may need to be optimized by the individual investigator.
10. Only crypts with a clear intestinal epithelial layer from base to mouth of the crypt should be scored. Any crypts in which a good longitudinal section across the crypt has not been

achieved should be excluded along with crypts where the epithelium is not clearly discernible from the lamina propria. Using the score and Wincrypts analysis package [9], a cell is assigned to a cell position relative to the crypt base and identified as positive or negative for GFP and lysozyme.

11. While our method for cell count analysis employed the Score and Wincrypts programs to quantify and interpret the labeling indices, cell count analysis can be very easily achieved using other software packages such as data logging using EXCEL and subsequent analysis in statistical analysis packages such as PRISM software. To ensure that count analysis is not biased, we recommend blinding all samples prior to counting. Ideally, cell count analysis should be performed by two independent investigators to verify findings.

## References


1. Peterson LW, Artis D (2014) Intestinal epithelial cells: regulators of barrier function and immune homeostasis. Nat Rev Immunol 14 (3):141–153. doi:10.1038/nri3608
2. Thaiss CA, Zmora N, Levy M, Elinav E (2016) The microbiome and innate immunity. Nature 535(7610):65–74. doi:10.1038/nature18847
3. van der Flier LG, Clevers H (2009) Stem cells, self-renewal, and differentiation in the intestinal epithelium. Annu Rev Physiol 71:241–260. doi:10.1146/annurev.physiol.010908.163145
4. Watson AJ, Hughes KR (2012) TNF-alpha-induced intestinal epithelial cell shedding: implications for intestinal barrier function. Ann N Y Acad Sci 1258:1–8. doi:10.1111/j.1749-6632.2012.06523.x
5. Hughes KR, Gandara RM, Javkar T, Sablitzky F, Hock H, Potten CS, Mahida YR (2012) Heterogeneity in histone 2B-green fluorescent protein-retaining putative small intestinal stem cells at cell position 4 and their absence in the colon. Am J Physiol Gastrointest Liver Physiol 303(11):G1188–G1201. doi:10.1152/ajpgi.00080.2012
6. Barker N, van Es JH, Kuipers J, Kujala P, van den Born M, Cozijnsen M, Haegebarth A, Korving J, Begthel H, Peters PJ, Clevers H (2007) Identification of stem cells in small intestine and colon by marker gene Lgr5. Nature 449(7165):1003–1007. doi:10.1038/nature06196
7. Potten CS, Gandara R, Mahida YR, Loeffler M, Wright NA (2009) The stem cells of small intestinal crypts: where are they? Cell Prolif 42(6):731–750. doi:10.1111/j.1365-2184.2009.00642.x
8. Henning SJ, von Furstenberg RJ (2016) GI stem cells - new insights into roles in physiology and pathophysiology. J Physiol 594 (17):4769–4779. doi:10.1113/JP271663
9. Potten CS, Owen G, Booth D (2002) Intestinal stem cells protect their genome by selective segregation of template DNA strands. J Cell Sci 115(Pt 11):2381–2388
10. Potten CS (1977) Extreme sensitivity of some intestinal crypt cells to X and gamma irradiation. Nature 269(5628):518–521
11. Cheng H, Merzel J, Leblond CP (1969) Renewal of Paneth cells in the small intestine of the mouse. Am J Anat 126(4):507–525. doi:10.1002/aja.1001260409
12. Foudi A, Hochedlinger K, Van Buren D, Schindler JW, Jaenisch R, Carey V, Hock H (2009) Analysis of histone 2B-GFP retention reveals slowly cycling hematopoietic stem cells. Nat Biotechnol 27(1):84–90. doi:10.1038/nbt.1517
13. Williams JM, Duckworth CA, Vowell K, Burkitt MD, Pritchard DM (2016) Intestinal preparation techniques for histological analysis in the mouse. Curr Protoc Mouse Biol 6 (2):148–168. doi:10.1002/cpmo.2

# Chapter 7

# Detecting Hematopoietic Stem Cell Proliferation Using BrdU Incorporation

**Katie A. Matatall, Claudine S. Kadmon, and Katherine Y. King**

## Abstract

Cellular quiescence is a key component of hematopoietic stem cell (HSC) homeostasis; therefore, a reliable method to measure HSC cell division is critical in many studies. However, measuring the proliferation rate of largely quiescent and rare populations of cells can be challenging. Bromo-deoxyuridine (BrdU) incorporation into replicating DNA is a commonly used and highly reproducible method to detect cell division history. Here, we describe a protocol for BrdU incorporation analysis in hematopoietic stem and progenitor cells that can provide a sensitive measure of cell division even in rare cell populations. In combination with flow cytometry, this method can be generalized to analyze other cell populations and other tissues as identified by cell surface markers.

**Key words** BrdU, Flow cytometry, Proliferation, Hematopoietic stem cells, Cell cycle

## 1 Introduction

Many methods are available to study the proliferative status of cells, including measuring DNA synthesis, metabolic activity, cell division, or the presence of proteins associated with proliferation, such as Ki67. Each of these techniques has inherent advantages and disadvantages, and investigators should carefully consider which is most appropriate to answer a particular scientific question [1–3].

As stem cells are relatively few in number and mostly quiescent, many commonly used methods of detection may not be sensitive enough to accurately identify their proliferation. Also, since stem cells are not easy to maintain in vitro and behave differently in culture, it is beneficial to assess them in an in vivo setting. Methods to detect the presence of proteins associated with proliferation, such as Ki67, PCNA, or MCM-2, provide a snapshot of a given cell population at the time of assay [4–7]. However, these proteins are expressed in the S, G1, and G2/M phases of the cell cycle and so mark loss of quiescence as opposed to proliferation per se. In addition, quantifying the results of staining for markers such as

H. Daniel Lacorazza (ed.), *Cellular Quiescence: Methods and Protocols*, Methods in Molecular Biology, vol. 1686,
DOI 10.1007/978-1-4939-7371-2_7, 

Ki67 can often be subjective because protein levels are expressed on a continuum, rather than as a bimodal distribution [8]. Another approach is to measure the metabolic activity of cells with the use of tetrazolium salts, such as MTT, XTT, or WST-1 [9–12]. These assays can be read using a spectrophotometer and are easily quantifiable, but they may be less accurate, can be toxic, and require in vitro culture of the cells. A third common method to assess proliferation is tracking cell division with a dye such as CFSE (carboxyfluorescein diacetate succinimidyl ester), which readily diffuses into cells and covalently binds to intracellular amines [13–16]. The dye is split evenly between daughter cells upon division which allows for the tracking of subsequent cell divisions. This method has the advantage of allowing cell tracking over long periods of time, but is subject to staining efficiency and dependent on following stained cells that have been isolated, stained, and transplanted back into an animal model.

Unlike the above methods, DNA intercalating agents can be injected directly into animals to allow for direct tracking of cells over time in their native in vivo state. Synthetic thymidine analogs, such as BrdU and EdU, which incorporate into newly synthesized DNA during the S phase of the cell cycle, are a common method for directly tracking DNA replication [17–19]. In order to identify incorporated BrdU, DNA must first be denatured so that antibodies can gain access [20]. EdU, however, uses Click-iT technology, which allows EdU analogs to be fluorescently tagged with the addition of a small dye-labeled azide that is able to access DNA without denaturation [21]. Therefore, if DNA structure is important for other assays, it could be advantageous to use EdU staining over BrdU despite its higher cost. One potential disadvantage of both the methods is that the analogs themselves can damage cells and cause mutations, making downstream, long-term experiments problematic [22, 23]. Despite this caveat, these techniques are especially useful for cell types that are not highly proliferative because incorporation can be tracked in vivo over the course of several days. In addition, BrdU and EdU incorporation assays can be used in conjunction with other techniques such as flow cytometry or immunohistochemistry [24–27], making it feasible to analyze a large number of cells and cell types.

Here, we describe a protocol to identify proliferating hematopoietic stem cells (HSCs) using BrdU incorporation and subsequent analysis using flow cytometry. Briefly, whole bone marrow is isolated from mice following BrdU injection. Bone marrow cells are then stained for HSC surface markers, after which they are fixed and permeabilized. DNA is then denatured to allow BrdU antibodies access to the incorporated analogs. Finally, flow cytometry is used to identify BrdU positive HSCs. In addition to this protocol, we provide a method by which rare cell populations can be sorted prior to fixation in order to allow for co-staining

protocols that may be disrupted by fixation, such as the use of Hoechst dye for the identification of HSC side population cells [28, 33]. While we focus on a method to identify proliferation in HSCs, this technique is applicable to many other rare cell populations and largely quiescent cell types.

## 2 Materials

* These items are optional; see associated notes for details.

### 2.1 BrdU Administration

1. Insulin syringes: 29G × ½ inch.
2. BrdU solution: 10 mg/ml BrdU solution diluted in 1× Dulbecco's phosphate-buffered saline (DPBS).

### 2.2 Bone Marrow Isolation

1. HBSS+: 500 ml Hank's balanced salt solution without calcium or magnesium (HBSS), 10 ml of fetal bovine serum (FBS), 5 ml of 1 M HEPES (N-2-hydroxyethylpiperazine-N-2-ethane sulfonic acid).
2. Needles: 27G × ½ inch and 18G × 1½ inch.
3. Luer-Lok Syringes: 5 and 10 ml.
4. 15 cm tissue culture dish.
5. 40 μm cell strainers.
6. * RBC lysis buffer: 9 ml 0.16 M amonium chloride ($NH_4Cl$), 1 ml 0.17 M Tris–HCl pH 7.65 (*see* **Note 7**).
7. * Mortar and pestle (*see* **Note 5**).

### 2.3 Enrichment of Hematopoietic Progenitors

1. CD117 (c-Kit) MicroBeads, mouse (Miltenyi-Biotec).
2. AutoMACS Pro Separator (Miltenyi-Biotec) (*see* **Note 9**).
3. * Running buffer: 1× DPBS, 0.5% BSA (bovine serum albumin), 2 mM EDTA; filter sterilized (*see* **Note 9**).
4. * MACS Columns (Miltenyi-Biotec) (*see* **Note 9**).
5. * MACS Separators (Miltenyi-Biotec) (*see* **Note 9**).

### 2.4 Hematopoietic Stem Cell Staining

1. * Antibodies for lineage markers (Gr1, B220, Mac1, CD4, CD8, Ter119), c-Kit, Sca1, CD150, CD48, and CD34 (*see* **Note 10**).

### 2.5 Carrier Cell Isolation

1. Murine splenocytes.
2. Anti-mouse B220-Biotin.
3. Anti-Biotin MicroBeads (Miltenyi-Biotec).

### 2.6 Cell Sorting

1. FBS (fetal bovine serum).
2. 1.5 ml tubes.
3. FACS tubes.

### 2.7 BrdU Staining

We use FITC BrdU Flow Kit (BD Biosciences); however, components of this kit can be purchased separately from other sources:

1. Fluorochrome-conjugated anti-BrdU Antibody.
2. Cytofix/Cytoperm Buffer.
3. Perm/Wash™ Buffer (10×).
4. Cytoperm Permeabilization Buffer Plus, 7-AAD, BrdU (10 mg/ml).
5. DNase solution.

## 3 Methods

All centrifugation steps should be carried out at 4 °C.

### 3.1 BrdU Administration

1. Weigh mice to be injected with BrdU.
2. Prepare 0.5 ml insulin syringes with BrdU solution at 1 mg BrdU per 6 g of body weight. Stock BrdU solution is 10 mg/ml so 100 μl per 6 g of body weight is required (*see* **Note 1**).
3. Inject the prepared BrdU solution i.p. (intraperitonal) 24–72 h before time of euthanasia. As an adjunctive to i.p. injection, BrdU may also be administered in the drinking water (*see* **Note 2**). The time of BrdU exposure must be tailored to the cell population being studied. The more quiescent the population, the more time is required to gain measurable incorporation (*see* **Note 3**).

### 3.2 Bone Marrow Isolation

1. Euthanize mice using an approved procedure and following institutional guidelines.
2. Remove 6 bones per mouse. Collect two tibiae, two femurs, and two pelvic bones. Six bones may not be required if cells are not being purified by cell sorting (*see* **Note 4**).
3. Flush bone marrow from bones using HBSS+ solution. Use a 5 ml syringe with a 27G needle to flush each bone with 5 ml of HBSS+ into a 15 cm culture dish. Pool bone marrow from all six bones. If several mice will be combined into a single group for analysis then crushing the bones may be more advantageous (*see* **Note 5**).
4. Disassociate bone marrow clumps. Use a 10 ml syringe with an 18G needle to draw up HBSS+ containing bone marrow from the previous step. Repeatedly draw up and expel bone marrow with the bevel against the bottom of the culture plate until no visible clumps remain, avoiding aeration of the solution. Approximately 5–6 repetitions are sufficient for normal bone marrow (*see* **Note 6**).

5. Filter the bone marrow. Use a 40 μm cell stainer to filter the bone marrow to remove any clumps that may remain.
6. Remove red blood cells from the bone marrow using RBC lysis buffer. This lysis step is optional (*see* **Note 7**). Centrifuge filtered bone marrow at 400 × *g* for 6 min. Remove the supernatant and resuspend cell pellet in 2 ml of RBC lysis buffer. Incubate at room temperature for 20 min.
7. Wash cells to remove RBC lysis buffer. Add 10 ml of HBSS+ to cells in RBC lysis buffer and centrifuge at 400 × *g* for 6 min. Remove the supernatant.

### 3.3 Enrichment of Hematopoietic Progenitors

1. Incubate with c-Kit beads. Resuspend the cell pellet in 800 μl of HBSS+ and add 200 μl of c-Kit beads. The amount of c-Kit beads used should be adjusted for the total cell number (*see* **Note 8**). Mix well and incubate at 4 °C for 30 min. Add 10 ml of HBSS+ to cells and centrifuge at 400 × *g* for 6 min. Remove the supernatant.
2. Resuspend cell pellet in 5 ml of HBSS+ and filter cells through a 40 μm cell strainer into a new tube.
3. Magnetic bead enrichment to isolate c-Kit positive cells. Use a positive selection program (poseld2) on an AutoMACS machine to enrich for c-Kit-tagged cells. The negative fraction after enrichment can be discarded or kept for other experiments. Manual isolation columns can also be used here in place of an AutoMACS machine (*see* **Note 9**).
4. Centrifuge the positive fraction (c-Kit$^+$ cells) at 400 × *g* for 6 min and discard the supernatant.

### 3.4 Hematopoietic Stem Cell Staining

1. Stain bone marrow for HSCs. For staining of long-term HSCs (LT-HSCs) the antibody cocktail should contain lineage markers (Gr1, B220, Mac1, CD4, CD8, Ter119), c-Kit, Sca1, CD150, CD48, and CD34 (*see* **Note 10**). Make an antibody cocktail with antibodies at a 1:100 dilution in HBSS+, with the exception of CD34 which should be used at a 1:50 dilution. Resuspend cell pellets in 100 μl of antibody cocktail. Incubate in the dark at 4 °C for 15 min (*see* **Note 11**).
2. Wash cells with 2 ml of HBSS+. Centrifuge at 400 × *g* for 6 min and discard the supernatant.
3. If analysis of LT-HSCs using cell surface markers (Lineage$^-$ cKit$^+$ Sca1$^+$ CD150$^+$ CD48$^-$ CD34$^-$) is sufficient, skip directly to Subheading 3.7 for fixation and BrdU staining.
4. If the staining method used will be disrupted by fixation, then sorting of HSCs before fixation may be required (such as using Hoechst staining for side population identification [28]). For sorting proceed to Subheadings 3.5 and 3.6.

### 3.5 Carrier Cell Isolation

Due to the low number of HSCs after sorting, it is recommended to use carrier cells during the subsequent fixation and staining steps to minimize loss of HSCs and enable flow cytometric analysis.

1. Isolate spleen cells. Remove spleen from a control mouse and gently crush in HBBS+ to release cells from the capsule. Use a 5 ml syringe with an 18G needle to draw up HBSS+ containing splenocytes. Repeatedly draw up and expel cells until no more visible clumps are remaining.
2. Filter the splenocytes. Use a 40 μm cell stainer to filter the cells to remove any clumps that may remain. Centrifuge splenocytes at 400 × *g* for 6 min and discard the supernatant.
3. Stain $B220^+$ splenocytes (B cells). Resuspend cell pellet in 100 μl of HBSS+ with 1 μl of B220-biotin antibody. Incubate in the dark for 15 min at 4 °C. Wash with 1 ml HBSS+. Centrifuge at 400 × *g* for 6 min and discard the supernatant.
4. Incubate splenocytes with biotin beads. Resuspend the cell pellet in 800 μl of HBSS+ and add 200 μl of biotin beads. Mix well and incubate at 4 °C for 30 min. Add 10 ml of HBSS+ to cells and centrifuge at 400 × *g* for 6 min. Remove the supernatant.
5. Resuspend cell pellet in 5 ml of HBSS+ and filter cells through a 40-μm cell strainer into a new tube.
6. Magnetic bead enrichment to isolate $B220^+$ splenocytes. For AutoMACS use a positive selection program (poseld2) to enrich for B220-tagged cells. The negative fraction after enrichment can be discarded or kept for other experiments. Manual isolation columns can also be used here in place of an AutoMACS machine (*see* **Note 9**).
7. Centrifuge the positive fraction ($B220^+$ splenocytes) at 400 × *g* for 6 min and discard the supernatant.
8. Stain $B220^+$ splenocytes. Resuspend cell pellet in 100 μl of HBSS+ with 1 μl of streptavidin antibody (*see* **Note 12**). Incubate in the dark for 15 min at 4 °C. Wash with 1 ml HBSS+. Centrifuge at 400 × *g* for 6 min and discard the supernatant.

### 3.6 Cell Sorting

1. Prepare collection tubes. Add approximately 1 ml of 100% FBS to a 1.5 ml eppendorf tube (*see* **Note 13**). Invert the tube ten times to ensure complete coating of the inside walls of the tube. Transfer FBS to a new tube and repeat until all collection tubes are coated. Use a vacuum to remove trace amounts of FBS remaining in tubes. Fill tubes with 1 ml of HBSS+.
2. Sort $B220^+$ splenocytes. Sort the $B220^+$ splenocytes using FSC/SSC, singlet and live discrimination. Sort enough cells to allow for approximately $1 \times 10^5$ $B220^+$ splenocytes per sample of sorted HSCs.

3. Sort HSCs. Sort Lineage$^-$ cKit$^+$ Sca1$^+$ CD150$^+$ CD48$^-$ CD34$^-$ HSCs using FSC/SSC, singlet and live discrimination. Each mouse should yield on average about 2000 HSCs.
4. Re-stain B220+ splenocytes (*see* **Note 14**). Centrifuge cells at 400 × *g* for 6 min and discard the supernatant. Resuspend cell pellet in 100 μl of HBSS+ with 1 μl of anti-B220 antibody. Incubate in the dark for 15 min at 4 °C. Wash with 1 ml HBSS+. Centrifuge at 400 × *g* for 6 min and discard the supernatant.
5. Mix sorted HSCs and B220$^+$ splenocytes. Add approximately $1 \times 10^5$ re-stained B220$^+$ splenocytes per sorted HSC sample. Mix well and centrifuge at 400 × *g* for 6 min. Discard the supernatant and proceed with fixation and BrdU staining (*see* Subheading 3.7).

### 3.7 BrdU Staining

1. Fix cells. Resuspend the cell pellet in 100 μl of Cytofix/Cytoperm Buffer. Incubate in the dark for 15 min at room temperature. Wash the cells with 1 ml of 1× Perm/Wash Buffer (*see* **Note 15**). Centrifuge at 300 × *g* for 6 min and discard the supernatant (*see* **Note 16**). The protocol can be stopped here and stored overnight (*see* **Note 17**).
2. Permeabilize cells. Resuspend the cell pellet in 100 μl of Cytoperm Permeabilization Buffer Plus. Incubate in the dark for 10 min on ice. Wash cells with 1 ml of 1× Perm/Wash Buffer. Centrifuge at 300 × *g* for 6 min and discard the supernatant.
3. Re-fix cells. Resuspend the cell pellet in 100 μl of Cytofix/Cytoperm Buffer. Incubate in the dark for 5 min at room temperature. Wash the cells with 1 ml of 1× Perm/Wash Buffer. Centrifuge at 300 × *g* for 6 min and discard the supernatant.
4. DNase treatment. Resuspend the cell pellet in 100 μl of 300 μg/ml DNase (*see* **Note 18**). Incubate cells in the dark for 1 h at 37 °C. Wash the cells with 1 ml of 1× Perm/Wash Buffer. Centrifuge at 300 × *g* for 6 min and discard the supernatant.
5. BrdU staining. Resuspend the cell pellet in 50 μl of BrdU antibody mix, which contains 1 μl of BrdU antibody per 50 μl of 1× Perm/Wash Buffer. If staining for other intracellular markers is desired, they can be included here in the BrdU antibody mix. Incubate cells in the dark for 20 min at room temperature. Wash the cells with 1 ml of 1× Perm/Wash Buffer. Centrifuge at 300 × *g* for 6 min and discard the supernatant.
6. Resuspend the cells in 500 μl of HBSS+. Optional: To stain for total DNA content 20 μl of 7-AAD can be added to the cell pellet before addition of HBSS+.

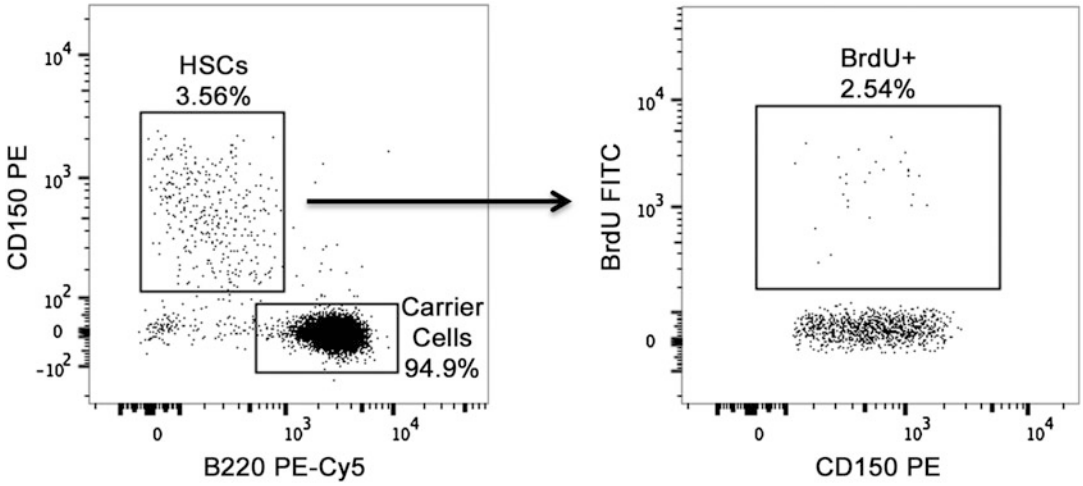


**Fig. 1** Example flow plots of sorted HSCs after BrdU staining. The panel on the left depicts the separation of carrier cells (B220+ splenocytes) from sorted HSCs. In this example, CD150 is used as a representative marker of the HSC population. The sorted HSC gate (shown in the *right panel*) is then gated for BrdU positive cells. The following markers are used in this example: B220 PE Cy5, CD150 PE, and BrdU FITC

### 3.8 Flow Cytometry

1. Single-color controls should be prepared for each fluorophore used to allow for correct voltage and compensation setup (*see* **Note 19**).
2. Gating strategies for flow cytometry will depend on whether c-Kit$^+$ hematopoietic progenitors or sorted HSCs were used for BrdU staining:
   (a) *c-Kit$^+$ progenitors*. Cells should first be gated through FSC/SSC and singlet discriminations. As the number of BrdU positive LT-HSCs will be low, it is helpful to set the gate for BrdU positive cells before gating for HSCs. This BrdU$^+$ gate can then be applied to the final HSC gate (*see* **Note 20**).
   (b) *Sorted LT-HSCs*. Cells should first be gated through FSC/SSC and singlet discriminations. As the cells here are a mixture of HSCs and B220$^+$ splenocytes, the splenocytes must be removed from further analysis. Since the B220 splenocytes were re-stained after cell sorting, they should still retain strong signal and can easily be separated from the remaining HSCs. After removing the B220$^+$ cells, the remaining HSCs can then be gated for BrdU positivity (Fig. 1) (*see* **Note 21**).

## 4 Notes

1. For an average mouse weight of 25 g, 416.7 μl of BrdU solution would be needed (100 μl/6 g of body weight).

2. For longer labeling studies BrdU can also be administered in the drinking water either as an alternative to IP injections or in conjunction. BrdU drinking water (1 mg/ml) should be protected from light and replaced daily. 1% glucose can also be added to improve palatability. Care should be taken if periods of longer than 1 week of administration are used as BrdU can become toxic to animals and may adversely affect results [29, 30].
3. The length of BrdU treatment before time of euthanasia should be varied depending on the cell population under investigation. For rapidly dividing cells, a shorter period of BrdU incorporation should be used to achieve data in dynamic range of the assay. 24 h of BrdU incorporation will result in approximately 2–5% of LT-HSCs ($Lineage^-$ $cKit^+$ $Sca1^+$ $CD150^+$ $CD48^-$ $CD34^-$) being labeled. If having a higher percentage of HSCs labeled is desirable, the length of time can be extended from 24 to 48 or 72 h, resulting in approximately 7–15% of LT-HSCs being labeled at baseline.
4. The collection of six bones per mouse is recommended if the enriched progenitor cells will be sorted for a more rare HSC population. If, however, the c-Kit-enriched progenitor population will be directly analyzed by flow cytometry without prior sorting, collecting four bones should provide adequate cell numbers. An estimate of the number of bones required can be determined assuming that each bone will yield between 10 and 20 million whole marrow cells (this number can be further increased with proficient crushing). LT-HSCs are approximately 0.01% of the bone marrow, thus one bone would give about 1000–2000 HSCs on average, although the achieved number will be lower than this due to loss at each staining step.
5. If multiple mice will be combined to form a single group for analysis, then crushing bones may be preferred over flushing to extract whole bone marrow from the bones. If many bones are pooled, crushing can generate a higher bone marrow yield and is often quicker than flushing. However, it is important to note that over-crushing can result in cell shearing and produce small fragments of bone, both of which can decrease the overall yield. For crushing, bones should be cleaned of extraneous muscle and fat. This can be accomplished using a scalpel or razor blade to scrape the tissue from the outside of the bones. Cleaned bones are then crushed in approximately 5–10 ml of cold HBSS+ using a mortar and pestle. Bones should only be crushed until large bone fragments are removed. After a minimal amount of crushing, the HBSS+ should be pipetted up and down to break up bone marrow clumps and filtered through a 40 μm cell strainer. This process is then repeated one or two more times until the majority of the bone marrow is released from the bones. After crushing for a maximum of three times, the bones should

then be repeatedly washed with additional HBSS+ to release the last of the bone marrow. After bone marrow has been filtered, continue with **step 6** in Subheading 3.2.

6. Be careful not to draw up the bone marrow with the syringe too many times as this will shear the cells.
7. Strictly speaking, RBC lysis is not required. Whole bone marrow will be enriched for c-Kit$^+$ cells in the next step and so red blood cells will be removed at this point. However, removal of RBCs before enrichment greatly reduces the number of total cells, thus allowing for the use of fewer c-Kit beads for enrichment.
8. The volume of c-Kit beads used will vary depending on the total cell number. 200 μl of beads should be used for every $1 \times 10^8$ cells. The appropriate volume of beads should be diluted 1:5 in HBSS+.
9. As an alternative to an automated separation machine, manual columns can also be used for enrichment. Miltenyi Biotec MACS Columns used with MACS Separators work well for this. The specific column used will depend on the number of labeled cells. Briefly, cells are resuspended in running buffer and applied to a pre-washed column housed in a magnetic separator. The column is washed repeatedly, removed from the magnet, and then cells are eluted with the addition of running buffer. The resulting enriched cells are then ready for staining.
10. There are many potential staining schemes for hematopoietic stem and progenitor cell staining, for more detailed information *see* [31, 32].
11. Make sure cells are kept covered from this point forward to avoid bleaching of the fluorophores.
12. Stain the splenocytes using an anti-B220 antibody with a unique fluorophore that was not used for HSC staining. If an additional fluorophore is not available, use the same fluorophore as was used for the lineage markers in the HSC stain on bone marrow. Only lineage negative cells will be sorted from the bone marrow, so the resulting cells should not contain this fluorophore.
13. Precoating the collection tubes with FBS can significantly increase the survival of sorted cells, as they are much less likely to stick to the walls of the tubes.
14. The intensity of the B220 fluorophore will have diminished during the sorting process. It will be critical to have strong signal from the B220 cells in order to separate them from the HSCs during later flow analysis after BrdU staining.

15. If using the Perm/Wash Buffer from the BD Biosciences BrdU Flow Kit, it is supplied at 10× and should be diluted 1:10 with deionized water prior to use. Unused diluted buffer can be stored at 4 °C for future use.
16. After fixation the cells will be fragile. In addition to the slower centrifugation speed (400 × *g* reduced to 300 × *g*), care should also be taken when resuspending cell pellets. Flick the tubes to resuspend instead of vortexing.
17. The protocol can be stopped here following the initial fixation (**step 1** in Subheading 3.7). After centrifugation, resuspend the cell pellet in HBSS+ and store overnight in the dark at 4 °C.
18. If using the DNase solution from the BD Biosciences BrdU Flow Kit, it is supplied at 1 mg/ml and should be diluted with 1× DPBS immediately prior to use to make a working stock of 300 μg/ml.
19. As the cells being analyzed for flow cytometry have been fixed they will have very different FSC and SSC properties than live cells. For this reason if cells will be used for single-color controls, it may be helpful to fix them as well in order to more accurately set these parameters.
20. For long-term HSCs, cells should first be gated for Lineage$^-$ cells, then for c-Kit$^+$ Sca1$^+$. This double positive gate should then be gated for CD150$^+$ CD48$^-$ cells. The final LT-HSC gate is CD34$^-$ cells. There will not be many cells left at this point, so it may be helpful to bring forward the CD48$^+$ population from the previous window as a reference point for determining where the CD34 gate should be placed. Of note, the CD48$^+$ cells should not be included in the gating strategy here, just used to help set the appropriate gate. Once the final Lin$^-$ cKit$^+$ Sca1$^+$ CD150$^+$ CD48$^-$ CD34$^-$ gate is set, the BrdU$^+$ gate that was set on the total cells can then be applied.
21. After removing B220$^+$ splenocytes, the remaining HSCs may not be easily identified by surface HSC markers as the signal intensity will have decreased during sorting. It may be helpful here to pick one positive HSC marker that has retained signal to separate the remaining cells from any contaminating debris or unstained cells. This entire population can then be gated for BrdU positive cells (Fig. 1).

## Acknowledgments

The work summarized here was supported by grants from the NIDDK DK060445 (KAM) and the NHLBI K08HL098898, the Department of Defense IDEA award in bone marrow failure

research (10505346), the Caroline Wiess Law Foundation for Molecular Medicine, the Aplastic Anemia and MDS International Foundation Liviya Anderson Award, and a March of Dimes Basil O'Connor Starter Scholar Award (KYK).

## References


1. Wiepz GJ, Edwin F, Patel T, Bertics PJ (2006) Methods for determining the proliferation of cells in response to EGFR ligands. Methods Mol Biol 327:179–187. doi:10.1385/1-59745-012-X:179
2. Hall PA, Levison DA (1990) Review: assessment of cell proliferation in histological material. J Clin Pathol 43(3):184–192
3. Yu CC, Woods AL, Levison DA (1992) The assessment of cellular proliferation by immunohistochemistry: a review of currently available methods and their applications. Histochem J 24(3):121–131
4. Oka S, Uramoto H, Shimokawa H, Iwanami T, Tanaka F (2011) The expression of Ki-67, but not proliferating cell nuclear antigen, predicts poor disease free survival in patients with adenocarcinoma of the lung. Anticancer Res 31 (12):4277–4282
5. Li LT, Jiang G, Chen Q, Zheng JN (2015) Ki67 is a promising molecular target in the diagnosis of cancer (review). Mol Med Rep 11 (3):1566–1572. doi:10.3892/mmr.2014.2914
6. Bologna-Molina R, Mosqueda-Taylor A, Molina-Frechero N, Mori-Estevez AD, Sánchez-Acuña G (2013) Comparison of the value of PCNA and Ki-67 as markers of cell proliferation in ameloblastic tumors. Med Oral Patol Oral Cir Bucal 18(2):e174–e179
7. Szelachowska J, Dziegiel P, Jelen-Krzeszewska J, Jelen M, Matkowski R, Pomiecko A, Spytkowska B, Jagas M, Gisterek I, Kornafel J (2006) Mcm-2 protein expression predicts prognosis better than Ki-67 antigen in oral cavity squamocellular carcinoma. Anticancer Res 26(3B):2473–2478
8. Reid MD, Bagci P, Ohike N, Saka B, Erbarut Seven I, Dursun N, Balci S, Gucer H, Jang KT, Tajiri T, Basturk O, Kong SY, Goodman M, Akkas G, Adsay V (2015) Calculation of the Ki67 index in pancreatic neuroendocrine tumors: a comparative analysis of four counting methodologies. Mod Pathol 28(5):686–694. doi:10.1038/modpathol.2014.156
9. Vega-Avila E, Pugsley MK (2011) An overview of colorimetric assay methods used to assess survival or proliferation of mammalian cells. Proc West Pharmacol Soc 54:10–14
10. Mosmann T (1983) Rapid colorimetric assay for cellular growth and survival: application to proliferation and cytotoxicity assays. J Immunol Methods 65(1–2):55–63
11. Roehm NW, Rodgers GH, Hatfield SM, Glasebrook AL (1991) An improved colorimetric assay for cell proliferation and viability utilizing the tetrazolium salt XTT. J Immunol Methods 142(2):257–265
12. Riss TL, Moravec RA, Niles AL, Duellman S, Benink HA, Worzella TJ, Minor L (2016) Cell viability assays. doi:https://www.ncbi.nlm.nih.gov/books/NBK144065/
13. Quah BJ, Parish CR (2012) New and improved methods for measuring lymphocyte proliferation in vitro and in vivo using CFSE-like fluorescent dyes. J Immunol Methods 379 (1–2):1–14. doi:10.1016/j.jim.2012.02.012
14. Quah BJ, Parish CR (2010) The use of carboxyfluorescein diacetate succinimidyl ester (CFSE) to monitor lymphocyte proliferation. J Vis Exp 44:2259. doi:10.3791/2259
15. Lyons AB (2000) Analysing cell division in vivo and in vitro using flow cytometric measurement of CFSE dye dilution. J Immunol Methods 243(1–2):147–154
16. Lyons AB, Parish CR (1994) Determination of lymphocyte division by flow cytometry. J Immunol Methods 171(1):131–137
17. Miltenburger HG, Sachse G, Schliermann M (1987) S-phase cell detection with a monoclonal antibody. Dev Biol Stand 66:91–99
18. Cavanagh BL, Walker T, Norazit A, Meedeniya AC (2011) Thymidine analogues for tracking DNA synthesis. Molecules 16(9):7980–7993. doi:10.3390/molecules16097980
19. Zeng C, Pan F, Jones LA, Lim MM, Griffin EA, Sheline YI, Mintun MA, Holtzman DM, Mach RH (2010) Evaluation of 5-ethynyl-2′-deoxyuridine staining as a sensitive and reliable method for studying cell proliferation in the adult nervous system. Brain Res 1319:21–32. doi:10.1016/j.brainres.2009.12.092
20. Moran R, Darzynkiewicz Z, Staiano-Coico L, Melamed MR (1985) Detection of 5-bromodeoxyuridine (BrdUrd) incorporation by monoclonal antibodies: role of the DNA denaturation step. J Histochem Cytochem 33 (8):821–827

21. Cappella P, Gasparri F, Pulici M, Moll J (2015) Cell proliferation method: click chemistry based on BrdU coupling for multiplex antibody staining. Curr Protoc Cytom 72:7.34.31–7.34.17. doi:10.1002/0471142956.cy0734s72
22. Breunig JJ, Arellano JI, Macklis JD, Rakic P (2007) Everything that glitters isn't gold: a critical review of postnatal neural precursor analyses. Cell Stem Cell 1(6):612–627. doi:10.1016/j.stem.2007.11.008
23. Anda S, Boye E, Grallert B (2014) Cell-cycle analyses using thymidine analogues in fission yeast. PLoS One 9(2):e88629. doi:10.1371/journal.pone.0088629
24. Gratzner HG, Leif RC (1981) An immunofluorescence method for monitoring DNA synthesis by flow cytometry. Cytometry 1 (6):385–393. doi:10.1002/cyto.990010606
25. Lacombe F, Belloc F, Bernard P, Boisseau MR (1988) Evaluation of four methods of DNA distribution data analysis based on bromodeoxyuridine/DNA bivariate data. Cytometry 9 (3):245–253. doi:10.1002/cyto.990090310
26. Houck DW, Loken MR (1985) Simultaneous analysis of cell surface antigens, bromodeoxyuridine incorporation and DNA content. Cytometry 6(6):531–538. doi:10.1002/cyto.990060607
27. Holm M, Thomsen M, Høyer M, Hokland P (1998) Optimization of a flow cytometric method for the simultaneous measurement of cell surface antigen, DNA content, and in vitro BrdUrd incorporation into normal and malignant hematopoietic cells. Cytometry 32 (1):28–36
28. Ergen AV, Jeong M, Lin KK, Challen GA, Goodell MA (2013) Isolation and characterization of mouse side population cells. Methods Mol Biol 946:151–162. doi:10.1007/978-1-62703-128-8_10
29. Reome JB, Johnston DS, Helmich BK, Morgan TM, Dutton-Swain N, Dutton RW (2000) The effects of prolonged administration of 5-bromodeoxyuridine on cells of the immune system. J Immunol 165(8):4226–4230
30. Rocha B, Penit C, Baron C, Vasseur F, Dautigny N, Freitas AA (1990) Accumulation of bromodeoxyuridine-labeled cells in central and peripheral lymphoid organs: minimal estimates of production and turnover rates of mature lymphocytes. Eur J Immunol 20 (8):1697–1708. doi:10.1002/eji.1830200812
31. Kent DG, Dykstra BJ, Eaves CJ (2016) Isolation and assessment of single long-term reconstituting hematopoietic stem cells from adult mouse bone marrow. Curr Protoc Stem Cell Biol 38:2A.4.1–2A.4.24. doi:10.1002/cpsc.10
32. Rossi L, Challen GA, Sirin O, Lin KK, Goodell MA (2011) Hematopoietic stem cell characterization and isolation. Methods Mol Biol 750:47–59. doi:10.1007/978-1-61779-145-1_3
33. Katie A. Matatall, Ching-Chieh Shen, Grant A. Challen, Katherine Y. King, (2014) Type II Interferon Promotes Differentiation of Myeloid-Biased Hematopoietic Stem Cells. STEM CELLS 32(11):3023–3030

# Chapter 8

# Cell Cycle Analysis by Mass Cytometry

Gregory K. Behbehani

## Abstract

The regulated progression of cells through the cell cycle during proliferation is a critical factor in tumor progression, anti-neoplastic therapy response, immune system regulation, and developmental biology. While flow cytometric measurement of cell cycle progression is well established, mass cytometry assays allow the cell cycle to be measured along with up to 39 other antigens enabling characterization of the complex interactions between the cell cycle and a wide variety of cellular processes. This method describes the use of mass cytometry for the analysis of cell cycle state for cells from three different sources: in vitro cultured cell lines, ex vivo human blood or bone marrow, and in vivo labeling and ex vivo analysis of murine tissues. The method utilizes incorporation of 5-Iodo-2′-deoxyuridine (IdU), combined with measurement of phosphorylated retinoblastoma protein (pRb), cyclin B1, and phosphorylated histone H3 (p-HH3). These measurements can be integrated into a gating strategy that allows for clear separation of all five phases of the cell cycle.

**Key words** Cell cycle, Mass cytometry, CyTOF, Iodo-deoxyuridine, Cyclin, Retinoblastoma protein, Phosphorylated histone H3, Ki-67

## 1 Introduction

Alterations in the cell cycle are a critical aspect of normal development and the regulation of almost every tissue in complex organisms. The cell cycle is also critical for understanding diseases of abnormal cell proliferation such as malignancies, and the therapies used to treat them. Fluorescent flow cytometry has long been used for the characterization of DNA and RNA content at the single-cell level and these measurements were the first to enable the determination of DNA ploidy and cell cycle phase [1]. The combination of these DNA and RNA stains with the antibody-mediated measurement of the incorporation of halogenated nucleoside analogs (e.g., BrdU) enables a relatively precise characterization of cell cycle phase [2]. Such studies have been used for the characterization of malignant cell proliferation, immune cell activation, and developmental regulation of cell proliferation. While very useful, these assays rely on bright fluorescent dyes that can significantly hamper

H. Daniel Lacorazza (ed.), *Cellular Quiescence: Methods and Protocols*, Methods in Molecular Biology, vol. 1686,
DOI 10.1007/978-1-4939-7371-2_8, 

measurement of other surface or intracellular markers. The measurement of BrdU incorporation can also further complicate the assessment of other antigens as this requires partial DNA degradation using acid or DNase, and these steps can potentially damage antigens of interest.

Mass cytometry is a cytometric technique similar to fluorescent flow cytometry in which antibody binding to cellular antigens is detected through the use of mass spectrometry rather than fluorescent detection [3, 4]. The technology utilizes the same antigen-specific antibodies used in conventional flow cytometry, but measures their binding by attaching isotopically purified heavy metal atoms to the antibodies instead of fluorophores. The presence of the bound metal-conjugated antibodies is then detected through the use of inductively coupled plasma ionization and time-of-flight mass spectrometry analysis of the cells. The use of mass spectrometry-based detection enables mass cytometers to measure many more channels (currently up to 50) than fluorescence-based machines. This technology has both advantages and disadvantages with respect to cell cycle analysis. The major disadvantage is that there are no comparable DNA or RNA stains with the same level of resolution as those used in fluorescent flow cytometry (e.g., DAPI, Hoechst, Pyronin Y, etc.). The high resolution of these dyes stems in part from changes in their fluorescent properties that occur upon interaction with nucleotide bases, and this property cannot be replicated in mass spectrometry detection. Mass cytometry measurement of the cell cycle state thus requires a different approach based on measurement of IdU incorporation, Cyclin B1 levels, and phosphorylation of the Retinoblastoma protein (Rb) and histone H3 [5]. While slightly more complicated, this approach has two major advantages: first, cell cycle measurements can be combined with detection of up to 35 or more additional antigens; second, 5-Iodo-2′-deoxyuridine (IdU) incorporation can be measured directly without the need for an antibody or for the degradation of DNA with acid or DNase.

Mass cytometric cell cycle analysis is well suited for the analysis of cell cycle state in highly complex cell mixtures, or for the correlation of cell cycle state with a large number of other functional variables within less complex cell populations. We have previously utilized this approach for the measurement of cell cycle state during normal hematopoiesis in human bone marrow [5], and transgenic murine models of telomerase deficiency [6]. We also utilized this method to demonstrate that subtype-specific differences in leukemia stem cell S-phase fractions in patients with acute myeloid leukemia [7]. Such high parameter studies would be extremely difficult or impossible with current fluorescent cell cycle analysis methods. Other researchers have utilized this methodology to characterize differences in proliferation rates across different immune cell subsets [8] and proliferation and chemotherapy

response of tumors xenografted into mice [9]. The protocol described here is heavily based on the standard phospho-flow cytometry methods originally developed by Krutzik and Nolan [10] and additional background for some of the methods can be found in their original protocol. Finally, it is worth noting that this analysis approach also works well for performing cell cycle analysis by fluorescent flow cytometry, allowing avoidance of bright DNA or RNA dyes [5].

## 2 Materials

All solutions for mass cytometry should be prepared with ultrapure water and all reagent solutions should be tested for heavy metal contamination. (Do not inject any concentrated solution that may contain heavy metal directly into the mass cytometer without first testing a 1/10th or 1/100th dilution of the solution.) Note that IdU, paraformaldehyde, and the Smart Tube buffer are all toxic and potentially mutagenic. They should be handled with appropriate protection (gloves, eye, and respiratory protection as appropriate). It is also worth noting that standard laboratory dishwashers, autoclaves, and dishwashing detergents are frequently contaminated with heavy metals (particularly Barium), which can disrupt experiments or damage the mass cytometer. We use either disposable plastic or glassware that we wash by hand for the production and storage of all solutions and reagents.

### 2.1 IdU

1. Dry 5-Iodo-2′-deoxyuridine powder can be purchased from various suppliers. We typically store the dry powder at 4 °C and use it to periodically prepare concentrated stock solutions.
2. IdU is not soluble at high concentrations in water. We typically make 50 mM stock solutions in DMSO (5000× final concentration). 88.5 mg of IdU will make 5 ml of stock solution at 50 mM, which can be aliquoted into small volumes of 20–50 μl and frozen at −80 °C (though it is likely stable at −20 °C). Sterilize this solution using a syringe filter prior to making aliquots. Stocks of up to 250 mM in DMSO can also be made for the purposes of creating IdU solutions for injection (*see* **Note 1**).
3. Before adding IdU stock solution to cells, it is advisable to dilute the stock solution to 100× final concentration in a pre-warmed aqueous solution so that the IdU will readily mix with the cells without the requirement for vigorous pipetting or mixing that might disrupt the cell cycle state of the cells being studied.

### 2.2 Fixatives, Buffers, and Tubes

1. Paraformaldehyde (PFA), 16% solution: This must be methanol-free (i.e., not formalin). We purchase this in 10 ml

ampules (Electron Microscopy Sciences) and transfer it to foil-wrapped tubes, as it will lose activity over several weeks upon exposure to air and light. We will throw out any PFA that has been open for more than 1 month.

2. Smart Tube proteomic stabilizer (STPS; alternate fixative): This can be purchased from Smart Tube incorporated (San Carlos, CA). This comes as a working solution that can be added directly to cell samples at a sample:buffer ratio of 1:1.4.
3. Pure Methanol: This should be kept cold (−20 °C to 4 °C) in a sealed bottle. This should not have any drying agents added as these may contain heavy metals.
4. Culture medium: Typically, the standard culture medium used for routine cell culture will work well; however, barium contamination can occasionally be present in the cell culture medium.
5. Cell staining medium: Standard phosphate-buffered saline (PBS), plus 0.5% bovine serum albumin (BSA), and 0.02% sodium azide, pH 7.4. This is typically made in 4 l batches by adding 20 g of BSA and 800 mg of sodium azide. Start with 3 l of sterile PBS and mix in the dry ingredients until dissolved. Then add additional PBS to a total volume of 4 l. Sterile filter this using a 0.2 μm bottle-top filter into rinsed, 500 ml glass bottles. Rinse and hand-wash these bottles as necessary, but do not place into standard laboratory dishwashers.
6. An intercalator solution is made by the addition of the Iridium-based intercalator solution (Fluidigm, 201192A or 201192B) to PBS at a final concentration of approximately 125 nM. To this add 1/10th volume of 16% PFA to achieve a final concentration of 1.5% PFA. This solution should be made fresh just before the addition to the cells.
7. This protocol is written for use with standard 5 ml polystyrene FACS tubes, but a variety of other tubes can be used. We have successfully performed the protocol in 1.5 ml Eppendorf-style micro-centrifuge tubes, and 1.1 ml polypropylene "cluster" microcentrifuge tubes, though additional washes may be required if the tube size is small relative to the staining volume.

### 2.3 Antibodies

1. A wide variety of antibodies can be utilized for mass cytometry analysis of cell cycle state; however, we routinely use four antibodies: phosphorylated retinoblastoma protein (S807/811), Cyclin B1, phospho-Histone H3 (S28), and Ki-67 that allow for the determination of all five cell cycle phases when combined with measurement of IdU incorporation (*see* **Note 2**). These are detailed in Table 1. Additionally, several other antibodies can be used to subset cell cycle phases or provide additional confirmation of cell cycle state or checkpoint activation, the most useful are summarized in Table 1. All antibodies

**Table 1**
**Common antibodies used for mass cytometry cell cycle assessment**

| Antibody | Clone | Manufacturer | Purpose | Notes |
|---|---|---|---|---|
| *Essential antibodies* | | | | |
| p-Rb (S807/811) | J112-906 | BD biosciences | G0/G1 resolution | (*see* **Note 3**) |
| Cyclin B1 | GNS-1 | BD biosciences | G2 resolution | (*see* **Note 4**) |
| p-HH3 (S28) | HTA28 | Biolegend | M-phase resolution | (*see* **Note 5**) |
| *Optional antibodies* | | | | |
| Ki-67 | SolA15 | eBiosciences | Confirmation of G0/G1 | (*see* **Note 6**) |
| Cleaved-Caspase3 (D175) | C92-605 D3E9 | BD biosciences CST | Identification of apoptotic cells | (*see* **Note 7**) |
| Cleaved-PARP (D214) | F21-852 | BD biosciences | Identification of apoptotic cells | (*see* **Note 8**) |
| PCNA | PC10 | BD biosciences | Confirmation of G0/G1 | (*see* **Note 9**) |
| p-RP-S6 (S236/236) | N7-548 | BD biosciences | Confirmation of M phase Sample quality | (*see* **Note 10**) |
| p-H2AX (S139) | JBW301 | Millipore | Detection of DNA damage | (*see* **Note 11**) |
| Cyclin A | BF683 | BD biosciences | Confirmation of G0/G1, G2 resolution | (*see* **Note 12**) |
| Cyclin E | HE12 | Invitrogen | Confirmation of G0/G1, G2 resolution | (*see* **Note 13**) |
| pCDK1 (Y15) | 10A11 | CST | Confirmation of M phase, G2 resolution | (*see* **Note 14**) |

should be titrated to determine the optimal staining concentration for the cells of interest, as the staining properties of these antibodies are dependent on the cell type being stained as well as the approximate cell cycle distribution of the cells (this is particularly true for p-Histone H3 which must be used at concentrations below antigen saturation).

2. All intracellular antibodies described in this protocol have previously been tested following PFA or STPS fixation and methanol cell permeabilization. We have not extensively tested staining under other fixation permeabilization conditions (e.g., saponin), though other permeabilization methods would likely be compatible with this method as these same antigens have been successfully analyzed with other protocols [9, 11].

## 3 Methods

Sample collection and processing is described in Subheadings 3.1–3.4.

### 3.1 IdU Incubation and Processing of Cultured Cells In Vitro

1. Quickly and carefully place the desired number of cells for analysis into a separate culture container at least several hours before analysis. Each mass cytometry sample typically requires at least 500,000 cells (we typically collect a minimum of 2 million cells to allow for 1 million cells to be stained and analyzed twice if necessary; *see* **Note 15**).
2. At the desired time-point, add IdU to the cell culture medium while cells are still growing under normal culture conditions. Try to minimize the time required to add IdU to the cells so that the cell cycle is not disrupted. We typically add IdU to a final concentration of 10 μM for 10–15 min incubations, but higher or lower concentrations can be used (particularly if longer IdU incubations will be performed). If starting with the 50 mM IdU stock solution, add 0.2 μl of IdU for each 1 ml of cell culture medium (2 μl total for a 10 ml culture dish). Be sure to gently swirl or pipette the cells to ensure that the IdU is evenly distributed (the DMSO stock solution will sink to the bottom of an aqueous solution). Alternatively, it is preferable to pre-dilute the IdU (to 50–500×) in a pre-warmed medium so that a larger volume of an aqueous solution can be added to the cells enabling much more rapid mixing of the IdU solution with the culture medium.
3. Once IdU is added, the cells should be returned to the incubator for approximately 10 min. The duration of the incubation is not critical, but each sample of an experiment should be treated consistently (IdU incorporation works well with incubations in the 10–30 min range). Longer incubations will lead to higher intensity of IdU labeling in S-phase cells but reduced resolution of G2 and M cells, which may exhibit IdU that was incorporated at the end of S-phase before these cells progressed to G2 or M when IdU incubations are prolonged (*see* **Note 16**).
4. Optional: If you plan to perform viability staining with cisplatin [12], it should be performed at the completion of the IdU incubation and before cell fixation (as this could lead to partial permeabilization of the cell membrane reducing the accuracy of the viability stain).
5. At the completion of the incubation, add 1/10th volume of 16% paraformaldehyde to achieve a final concentration of 1.5% PFA. The medium should turn yellow. Leave the cells at room temperature for 10 min. During this time, cells can be transferred from the culture tube to a centrifuge tube.

6. At the end of the 10 min incubation, centrifuge the cells to pellet them (this is typically done at 300 × *g* for 5 min but this may be cell-type specific; *see* **Note 17**).
7. Aspirate the medium from the cells, removing as much as possible, preferably to a pellet of 50 μl or less. This will enable enough methanol to be added to achieve a final concentration of 90–95%.
8. Optional: If cells will require assessment of surface antigens that are disrupted by methanol exposure or if an alternative permeabilization method will be employed, cells can be washed twice with CSM and then snap frozen (using a dry ice methanol bath or liquid nitrogen) in CSM with DMSO added to a final concentration of 10% (*see* **Notes 18** and **19**).
9. Thoroughly vortex the cell pellet to resuspend the residual cells into a single-cell suspension.
10. While gently vortexing the cell pellet, rapidly add 1–2 ml of ice-cold methanol (this volume depends on the cell number and desired storage tube; final concentration of methanol should be 90–95%). It is very important to add the methanol to a completely resuspended cell pellet while vortexing. If the cells are not maintained in an even single-cell suspension, the cells will clump and be useless for cytometry analysis. Once the methanol has been added, transfer the cells onto ice for at least 10 min.
11. Cells can then be transferred into one or more storage tubes and stored at −80 °C (in methanol) until analysis. We routinely store the cells at 5–10 million cells per ml in methanol, so up to 15 million cells will fit into a 1.5 ml Eppendorf microcentrifuge tube or a cryogenic freezing tube.

### 3.2 IdU Incorporation and Processing of Ex Vivo Human Cell Suspensions

For the analysis of fresh primary human cell suspensions (typically, human peripheral blood or bone marrow aspirate), we will typically utilize Smart Tube proteomic stabilizer (STPS) solution. This solution utilizes a fixative cocktail, but is sufficiently gentle to allow subsequent lysis of red blood cells as well as detection of antigens known to be disrupted by standard PFA fixation. An alternative fixation procedure developed by Chow et al. [13] utilizing PFA fixation followed by Triton X-100 can also work well for ex vivo sample fixation; however, this method tends to be slightly more disruptive to fixation-sensitive antigens in our experience.

1. Human blood or bone marrow is typically collected in green top (sodium heparin) blood tubes. Samples should be obtained as fresh as practically possible. For cell cycle analysis of human leukemia cells, we will typically collect bone marrow aspirates at the bedside and begin IdU incubation within 1-2 min of collection. We have not determined a maximum time from

collection; however, we have seen intracellular signaling and cell cycle changes occur in as a little as an hour after sample collection.

2. As soon as possible after sample collection, cells are placed in a 37 °C incubator and a 100× (1 mM) solution of IdU in PBS is added to achieve a final concentration of 10 μM IdU. The 100× solution is made by dilution of the 50 mM DMSO stock into sterile PBS. This solution can be added to the empty green top tube prior to sample collection, or added after the sample has already been placed into the tube. Invert the sample several times after IdU addition to ensure adequate mixing (*see* **Note 20**).
3. Incubate the green top blood collection tube containing the sample with IdU added for 10–15 min at 37 °C.
4. Following the 37 °C incubation, the STPS solution should be added at a ratio of 1 part sample to 1.4 parts STPS. Following the addition of the STPS, invert the sample several times and then incubate this at room temperature for 10 min.
5. Following the 10 min incubation with STPS, the sample can be frozen at −80 °C and stored for up to 2 years (or more).
6. At the desired time of sample analysis, the fixed cells should be thawed at 4 °C (this can be done rapidly in a circulating 4 °C water bath). Once thawed, red cells in the sample can be lysed with incubation with 10 volumes of Smart Tube lysis solution (per the manufacturer's protocol).

### *3.3 Sample Processing In Vivo IdU Incorporation in Mice*

1. Mice should be maintained under desired experimental condition up to and during IdU incorporation. Twenty minutes prior to euthanasia, each mouse should be given an intraperitoneal injection of 1 ml of IdU solution in PBS with 0.5% DMSO. This solution can be prepared by diluting 250 mM IdU (in DMSO) into sterile saline.
2. To minimize any effects from hypoxia, we typically euthanize mice by deeply sedating them with using isofluorane (mixed with oxygen) and then perform cervical dislocation according to institutional guidelines.
3. The desired mouse tissues can then be harvested, using any desired application-specific protocol. We have found that the tissue harvesting is best done on ice (to prevent blood clotting). We have harvested the spleen, lymph nodes, and long bones (for preparation of bone marrow cells), although this protocol should work for most other tissues as well.
4. It is important to harvest the tissues as quickly as possible to preserve the intracellular signaling and cell cycle state. If the tissues are harvested on ice, we will fix them with PFA while

simultaneously warming them (in our experience, this prevents the cells from adversely responding to cooling process).

5. Fixation is performed by adding PFA to a final concentration of 1.5%. If the cell samples are at room temperature, fixation can be performed for 10 min. If the samples are on ice when PFA is added, the PFA should be added directly to the cold samples (to a final concentration of 1.5%) and the cold samples should be placed on a mixer at room temperature. As the fixation is temperature-dependent, fixation should be performed for 20 min if the starting temperature is 0 °C and the samples warm to 20 °C.
6. Centrifuge the fixed cells at 500 × *g* (5 min at 4 °C) and aspirate the supernate. Wash the fixed cells two times in CSM (500 × *g* for 5 min at 4 °C). After these washes the cells are resuspended in CSM plus 10% DMSO, aliquoted (if desired) and then snap frozen (using liquid nitrogen or a dry ice alcohol bath). The cells can be stored at −80 °C for up to 2 years (or potentially longer; *see* **Note 19**).

### 3.4 Antibody Staining

All cell cycle antibody staining should be performed after cell permeabilization. If the planned permeabilization will disrupt surface antigens required for the experiment, a two-step stain can be utilized by first staining cells with antibodies directed against surface markers of interest, then permeabilizing the cells and staining for intracellular antibodies. This protocol is compatible with cellular barcoding either before or after cell permeabilization [14, 15]. With either type of barcoding, the barcoding should be performed after cell fixation and freezing (if done) but before antibody staining. If cell surface staining will be performed before permeabilization, we will typically perform a second fixation step and methanol permeabilization after the completion of the surface stain and two washes with CSM (*see* **steps 5–10** in Subheading 3.1).

1. Add the desired number of cells in methanol to a tube half-filled with PBS. Fill the remaining volume of the tube with CSM. Pellet cells by centrifugation for 5 min at 600 × *g* and aspirate the supernatant (*see* **Note 21**).
2. Wash cells once with CSM. If the volume of methanol added in **step 1** was more than 10% of the volume of the tube being used, then a second wash with CSM should also be performed so that the final methanol concentration of the residual buffer and cell pellet is less than 0.5%.
3. Add a staining cocktail containing the desired antibodies for cell cycle analysis (*see* Table 1) and any additional antibodies needed for the experiment. We typically stain 1–2 million cells in 100 µl staining reaction for 40–50 min at room temperature, but other staining volumes, incubation times, or incubation temperatures

can be used provided the antibodies are titrated for optimal staining under the same conditions.

4. After the completion of staining, wash cells at least twice with CSM.
5. Add at least 100–200 μl of intercalator solution for each million cells in the cell pellet. This can also be titrated for the specific cell types being stained. Mix or vortex cells gently to resuspend them evenly in the intercalator solution. Place the cells at 4 °C for at least 20 min. The cells will be stable in the intercalator solution at 4 °C for at least a week.
6. Analyze cells on CyTOF mass cytometer. Exact acquisition settings are dependent on which CyTOF version is being used and the cell types being studied.
   Data analysis is described in Subheadings 3.5–3.9.

### 3.5 S-Phase Gating

1. The S-phase gate is typically the easiest to determine, but is also the most important, as almost all other cell cycle gates are made on the basis of a biaxial gate of IdU incorporation versus a second cell cycle parameter. Several ways of making the standard S-phase gate are shown in Fig. 1a. This gate can be created in a biaxial plot of IdU (I127) versus either Ki-67, pRb, or Cyclin B1. For healthy cells under normal growth conditions, any of these plots should result in the same S-phase fraction (plotting IdU incorporation versus Iridium intercalator signal will also

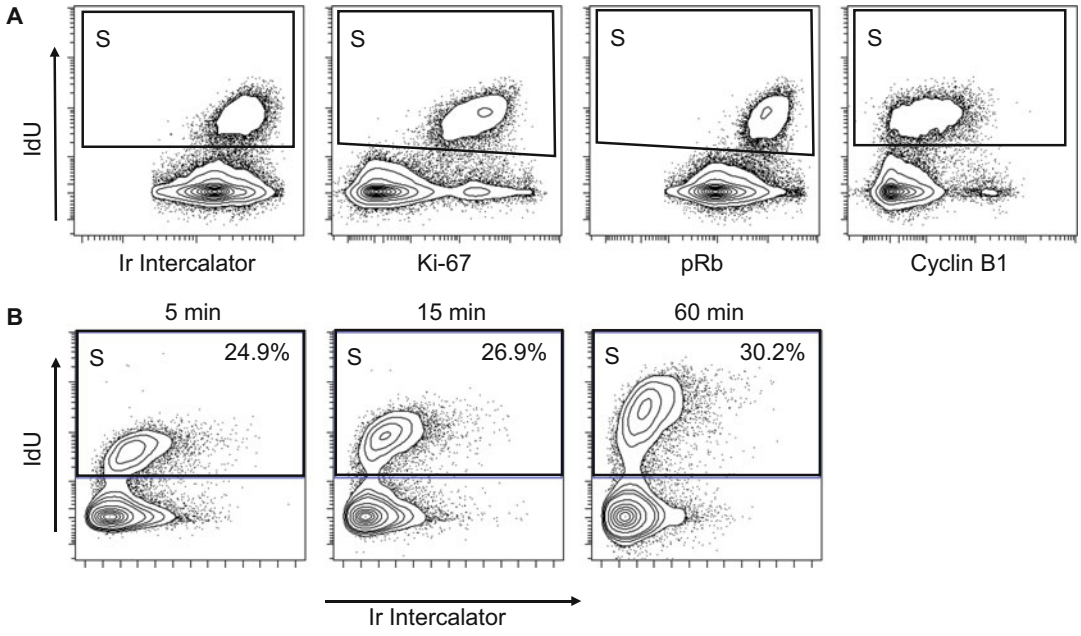


**Fig. 1** S-phase gating based on IdU incorporation. (**a**) The S-phase cell population can be gated using a variety of biaxial plots. (**b**) The effect of increased IdU incubation time

work well in this setting); however, disruption of the cell cycle or S-phase can reduce the resolution of the IdU gate, and under these conditions, a plot of IdU versus Ki-67 or pRb may be most useful.

2. The incorporation of IdU into S-phase cells is dependent on the time of IdU incubation, the IdU concentration, and the rate of nucleotide synthesis of the cells being studied. As shown in Fig. 1b, as the time of incubation increases, both the IdU signal and the fraction of IdU positive events will increase. The increase in signal intensity is due to more IdU being incorporated as the constant rate of IdU incorporation continues over a longer time period. The increase in S-phase fraction occurs due to the entry of additional cells into S-phase during the course of the incubation. For most cell types, the fraction of G1 cells that enter S-phase or progress to G2 during the incubation is quite small during a typical 10–30 min IdU incubation; however, incubations longer than 1–2 h can result in a significant fraction of the cells in G2 at the time of fixation having IdU incorporated into their DNA from the cell's previous S-phase.

### 3.6 G1 and G2-M Gating

1. The discrimination of cells in G1 from cells in G2-M is based on the level of Cyclin B1; however, Cyclin B1 levels increase continuously from G1 to M phase making it impossible to determine the exact phase boundaries of Cyclin B1 expression unless the S-phase cells can be clearly separated. Thus, this distinction is made based on a plot of IdU incorporation versus Cyclin B1. This biaxial plot has 3 distinct populations: CyclinB1$^{low}$ IdUl$^{-}$, correlating to G0-G1 phase cells; Cyclin B1$^{mid}$ IdU$^{+}$, correlating to S-phase cells; and CyclinB1$^{high}$ IdU$^{-}$, correlating to cells in the G2-M phase (Fig. 2).
2. This gate can be difficult to draw for two reasons. First, normal (i.e., healthy, untransformed) cells have a very low fraction of cells in G2 compared to commonly used cancer cell lines, thus the small size of the G2-M phase cell fraction (~2–4%) can make identification of this distinct cell group difficult. Second, the amount of cyclin B1 antigen in the G2 cells appears to be sensitive to inadequate fixation, with relatively low levels of cyclin B1 observed in cells that have not been completely fixed. It is thus important to ensure good sample processing and that the cyclin B1 antibody is labeled well with metal and that this antibody is conjugated to a relatively sensitive metal channel.
3. If G2-M phase gating is difficult, back gating with the M-phase population may help to identify the boundaries of this population. Cyclin B1 levels are high early in M phase and drop during M phase progression, thus, if a significant number of M phase cells are present in the cell population of interest, displaying these cells in the plot of IdU versus cyclin B1 will show a large

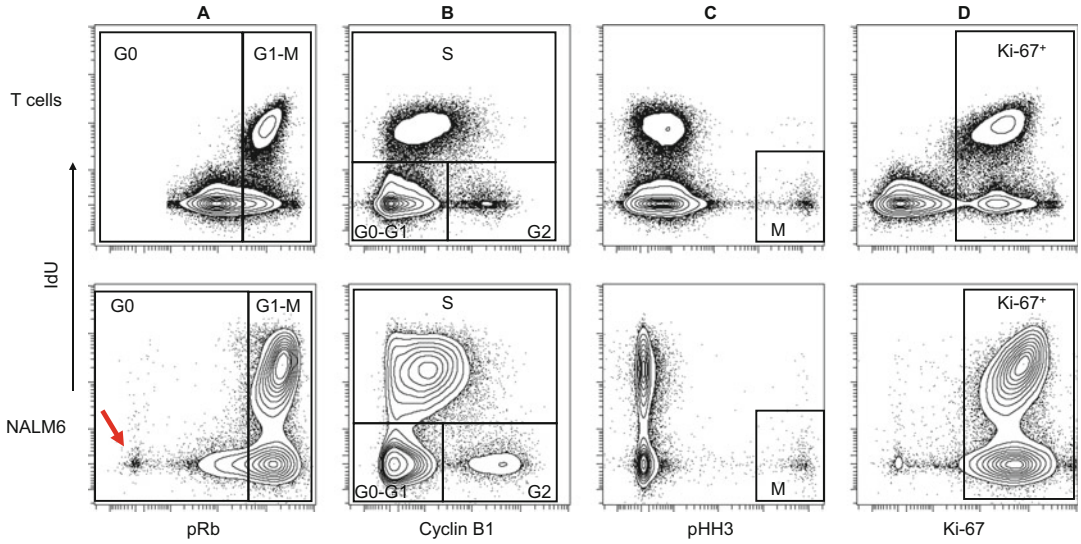


**Fig. 2** Major cell cycle phase gates are shown for stimulated human T cells and the NALM6 leukemia cell line. (**a**) G0 cells are identified as having pRb levels of less than 95–99% of S-phase cells. A pRb-negative population is also commonly observed (*red arrow*); this appears to be composed primarily of apoptotic and necrotic cells, though senescent cells may also be present. (**b**) A biaxial plot of IdU incorporation versus cyclin B1 allows for gating of G0-G1 cells, S phase cells, and G2-M cells. (**c**) M-phase cells can be identified based on high levels of p-HH3. (**d**) Ki-67 positive cells are defined based on the level of Ki-67 in 95–99% of S-phase cells, and this cutoff varies across cell types

fraction of cells with G2 cyclin B1 expression and a smaller fraction with very low (G0/G1) Cyclin B1 levels.

### 3.7 G0/G1 Gating

1. The discrimination of G0 cells from those in G1 is based on previous work demonstrating that Rb becomes phosphorylated at serine 807 and 811 by a Cyclin C-CDK3 complex during the transition from G0 to G1 [16]. Importantly, in many cell types there is not a clear separation of the level of pRb between G0 and G1 cells, making it essential that this gate is determined from a plot of pRb versus IdU incorporation (Fig. 2). We typically draw a $pRb^+$ gate that includes 95–99% of S-phase cells, though this rule may require modification in circumstances where cell cycle checkpoint activation is anticipated. For instance, cells with IdU staining and high levels of DNA damage (e.g., following genotoxin exposure) may exhibit reduced pRb staining, presumably due to the activation of an S-phase cell cycle checkpoint.
2. We have also noted that the absolute level of pRb in S-phase cells varies in different cell types, and can vary with cellular differentiation. The G0/G1 gate should thus be examined for each distinct cell type being studied, and the biaxial gate of IdU versus pRb should be adjusted as needed if the level of pRb in the S-phase cells is found to be different between cell types or stages of differentiation (Figs. 2 and 3a).

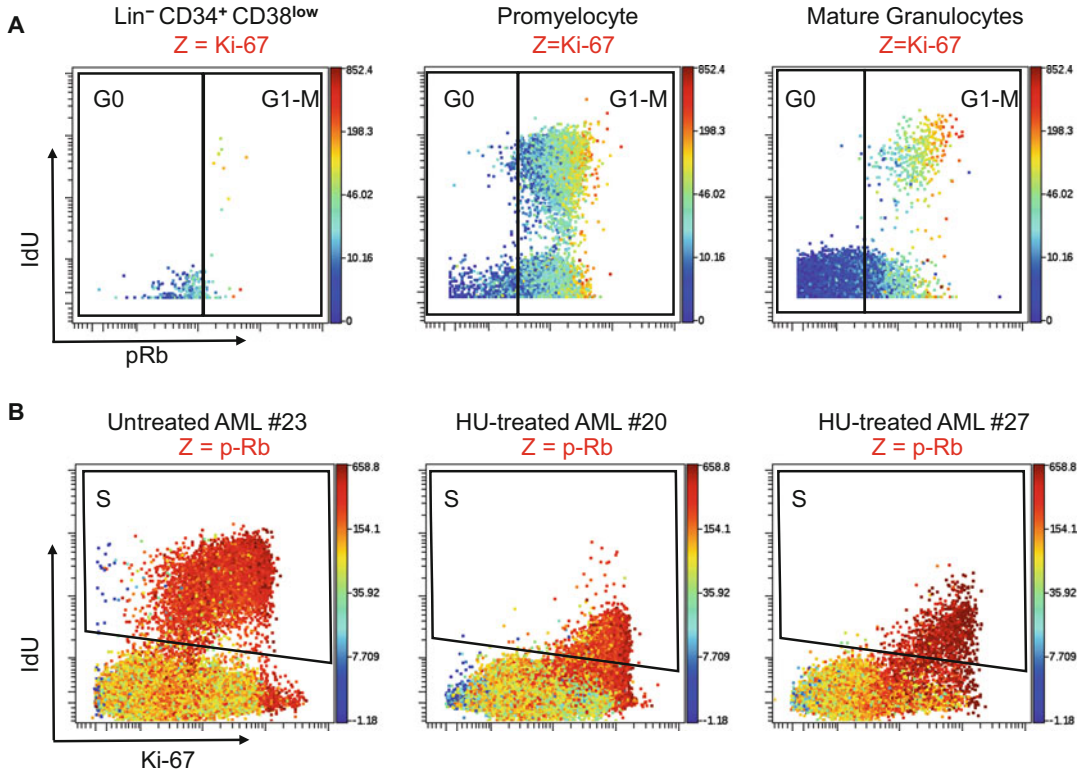


**Fig. 3** Special situations in cell cycle gating. (**a**) When the pRb gate position is based on the pRb levels in S-phase cells, the exact gate position changes throughout cellular differentiation from stem and early progenitor cells (Lin$^-$ CD34$^+$ CD38$^{low}$) to mature granulocytes. Cells events are colored according to Ki-67 expression level from low expression in *blue* to high expression in *red*. (**b**) Samples of CD34$^+$ leukemia cells from patients with AML prior to treatment or during treatment with hydroxyurea (HU). HU treatment leads to a decrease in IdU incorporation and an increase in Ki-67 levels. Cells events are colored according to p-Rb expression level from low expression in *blue* to high expression in *red*

3. The IdU versus pRb gate is typically drawn on the total cell population, and then applied to the population of G0-G1 cells gated from the IdU versus cyclin B1 plot (as described in Subheading 3.6) to arrive at the population of G0 cells (*see* Table 2). This approach closely correlates with G0 estimation using Pyronin Y staining of total RNA [5].
4. In most cell types, an Rb negative population is also observed that is significantly dimmer than the majority of cells with levels of pRb below that of the S-phase cells (*see* Fig. 2; *red arrow*). This cell population typically represents apoptotic or necrotic cells (though senescent cells may also be present in this population). The addition of antibodies against Ki-67, PCNA, cleaved-

**Table 2**
**Assignment of cell cycle phase based on gated cell populations**

| Cell cycle Phase | IdU gate | Cyclin B1 gate | pRb | p-HH3 |
|---|---|---|---|---|
| G0 | Negative | Low | Low-mid | Negative |
| G1 | Negative | Low | High | Negative |
| S | Positive | | High | Negative |
| G2 | Negative | High | High | Negative |
| M | Negative | | | Positive |

caspase3, and cleaved-PARP can all help further delineate the exact state of these cells (*see* **Notes 6–9**).

### 3.8 M-Phase Gating

1. Gating of M phase cells on the basis of histone H3 phosphorylation at serine 10 and 28 are both well-established markers of M phase [17, 18]. This assay utilizes antibodies against the S28 phosphorylation on the basis of its slightly higher specificity for M phase cells. M phase cells typically exhibit very high levels of p-HH3, so this population is usually easily identifiable; however, these cells are normally quite rare (<1%). This gate is typically drawn around the $IdU^{-}$ $pHH3^{+}$ cells in a plot of IdU incorporation versus p-HH3 (Fig. 2). In healthy untransformed cells, however, progression from S-phase to M-phase can occur quite rapidly. Thus, if IdU incubations are prolonged, cells in M phase at the time of cell fixation my exhibit IdU that was incorporated during the previous S-phase.
2. The pHH3 antibody requires careful titration and thoughtful selection of its position in the design of the antibody panel, since this antibody cannot be used at saturating concentrations (due to the extremely large amount of this antigen in M-phase cells; *see* **Note 5**).
3. M-phase cells also typically exhibit high levels of phosphorylated ribosomal protein S6 (S236/235), Ki-67, and phosphorylated MAMKAPK2 (T334). These markers can be used for confirmation of cell cycle phase assignment or as a control for appropriate cell processing and viability.

### 3.9 Final Assignment of Cell Cycle States

1. Final cell cycle phase assignment is typically done on the basis of the gate combinations (Table 2). Careful attention should be paid to ensure that the boundaries of positive and negative gates for each marker are immediately adjacent to one another, such that all cells fall within either the positive or the negative gate for each marker. If this is done, the sum of the percentage of cells in each cell cycle phase will be very close to 100%.

2. We have previously validated this methodology in head-to-head comparisons with a fluorescent flow cytometer method utilizing IdU incorporation, Hoechst DNA staining, and Pyronin Y RNA staining [5]. However, it is likely that this methodology will yield different results from methods utilizing total DNA or RNA staining when cells are arrested in cell cycle checkpoints. For instance, a cell that has completely arrested DNA synthesis after entering an S-phase checkpoint will not actively incorporate IdU (appearing to be in G0 or G1 by mass cytometry), but may have a total DNA content between 2n and 4n (indicative of S-phase by fluorescent total DNA staining). Researchers should understand these differences when interpreting data generated by this assay. Fortunately, mass cytometry allows for multiple other antibodies to be incorporated into staining panels that enable assessment of other aspects of any expected checkpoint response (e.g., p-H2AX, p-ATM, etc.). Other analysis strategies can also be used to derive cell cycle phase information from the measurement of these same markers (*see* **Note 22**).
3. The assay described in this protocol has been designed for measuring a "snapshot" of the cell cycle at the time of fixation. Assessment of the total cell cycle time or of precise cell cycle kinetics typically requires labeling with two different halogenated uridine analogs (e.g., CldU and IdU) [2]. This method is compatible with these protocols; however, assessment of uridine analogs that incorporate halogen atoms of less than 75 Daltons (FdU, CldU) cannot be measured directly by mass cytometry. While BrdU should theoretically be measureable, its low mass, higher ionization energy, isotopic distribution (51% $^{79}$Br; 49% $^{81}$Br), and the presence of a strong argon dimer signal at 80 Daltons, all complicate direct measurement of this reagent. It is however possible to utilize metal-conjugated antibodies directed against any of these uridine analogs to perform double-labeling experiments (provided the antibody chosen does not crossreact with IdU).

## 4 Notes

1. We have noted the IdU solution will turn brown if left at room temperature, so we typically make aliquots for single use.
2. Ki-67 is not essential for identification of cell-cycle phases; however, it is quite useful given its broad use in cell biology and pathology. This marker also provides additional resolution of G0 and G1 cell cycle phases.
3. p-Rb (S807/811) increases during the transition from G0 to G1 [16] and is used for the separation of G0 and G1 cells. This phosphorylation site is different from the classical Rb

phosphorylation site (S780) associated with G1-S phase progression. pRb (S807/811) staining typically identifies 3 populations: negative cells that are apoptotic or senescent, pRb-mid cells that are G0 cells, and pRb bright that are cells in G1-M phase of the cell cycle. pRb requires a relatively bright metal channel that does not have significant isotopic contamination or high level of oxidation (as the signal can become quite bright). Best metal channels are Tb159, Ho165, Tm169, or La175.

4. Cyclin B1 is used to define G2/M cells (Cyclin B1 high, IdU negative). This antibody does not label well with metals, so it needs to be used on a relatively bright channel, but most channels above Eu151 should work well. Clear resolution of G2 cells with Cyclin B1 requires good cell fixation, and tends to be slightly better if cells are permeabilized with methanol immediately after fixation. Note that normal cells (i.e., not transformed) tend to have much lower frequencies of G2 cells than cancer cell lines.
5. p-Histone H3 staining is extremely bright on M-phase cells. This metal needs to be used on a channel without significant isotopic contamination and any antibody used on the mass channel 1 Dalton above may receive spillover from bright p-Histone H3 signal on M-phase cells. Good metals to use for this antibody are La175, or Lu176. Because of the very large amount of antigen present on M-phase cells, it is difficult to saturate this antigen, as a result, staining reactions will be sensitive to the number of M-phase cells present (higher cell numbers will result in dimmer staining, lower cell numbers in brighter staining).
6. Ki-67 is used as a second measure of proliferation. It is generally quite consistent with pRb, but we have observed subtle differences between the two markers. Measuring both gives additional confidence to the assignment of G0 cells (i.e., cells negative for both Ki-67 and pRb). We typically use clone SolA15 which is actually raised against mouse Ki-67, but has good cross reactivity with human Ki-67 allowing this reagent to be used for both murine and human cells (unlike many other human-specific anti-Ki-67 antibody clones).
7. Cleaved-Caspase 3 is used to identify apoptotic cells. In our experience, cleaved-Caspase 3 is slightly more specific for apoptotic cells than cleaved-PARP, however, cleaved-Caspase 3 typically gives slightly dimmer staining. For experiments where identification of all apoptotic cells is extremely important, we will use both cleaved-Caspase 3 and cleaved-PARP.
8. Cleaved-PARP is used to identify apoptotic cells. In our experience, cleaved-PARP gives slightly higher staining intensities

than cleaved-Caspase 3; however, we have rarely observed small cell subsets with cleaved PARP staining that do not appear to be apoptotic by cleaved-Caspase 3 and other cell cycle measures. For experiments where identification of all apoptotic cells is extremely important, we will use both cleaved-Caspase 3 and cleaved-PARP.

9. Like Ki-67, PCNA is used as a second measure of proliferation to identify the G0 to G1 transition. All three makers (pRb, Ki-67, and PCNA) can be used simultaneously if identification of G0 cells is essential; however, we have only rarely observed significant discrepancies between Ki-67 and PCNA.
10. p-RP-S6 signal is strongly positive on M-phase cells. We use this antibody to provide confirmation of M-phase assignment. This marker is also useful for quality control, as we have observed cells that were not fixed immediately after collection of loose p-RP-S6 signal on M-phase cells, suggesting that other cell cycle or intracellular signaling measures may also be disrupted.
11. pH2AX staining helps to identify cells with DNA damage, which may indicate that these cells have entered a cell cycle checkpoint. Knowing which cells have DNA damage can help to explain alterations of expected correlations in cell cycle response (e.g., unexpected observation of low levels of pRb in IdU positive cells), and it may be helpful to ignore p-H2AX positive cells when determining some gate boundaries (e.g., G0/G1 gates).
12. Cyclin A staining can be used to help identify G0 cells (negative for Cyclin A) and to assist with G2 gating (G2 cells should be slightly lower for Cyclin A relative to Cyclin B1) [5, 11]. However, the resolution of this marker is not as good as Cyclin B1 or p-Rb making it less useful for cell cycle assignment than these other markers.
13. Cyclin E staining can also help with resolution of G0 versus G1 (G0 cells should be negative) and is useful for resolution of G2 phase cells (which should be negative for Cyclin E) [5, 11]. Like Cyclin A, however, the lower staining intensity of this antigen by mass cytometry limits its utility.
14. p-CDK1 staining should peak in G2 phase and be lost upon transition to M phase, it can thus be helpful as a confirmatory marker of these cell cycle phases. The resolution of this marker is also not very good, making it less useful than the other markers of these cell cycle phases.
15. The minimum number of cells required for mass cytometry analysis varies based on the exact number of centrifugation steps, the type of centrifuge tubes employed, and the number of washes performed. For the protocol described here

(utilizing standard 5 ml polystyrene FACS tubes), 500,000 cells is a good minimum number as the mass cytometer generates data from 30 to 50% of the cells that are injected, requiring a proportional increase in the number of starting cells (as compared to fluorescent flow cytometry). Utilizing smaller, polypropylene tubes, and reducing the number of staining and wash steps can allow for the analysis to be performed with lower starting cell numbers (as low as 100,000). Cells fixed according to this protocol will be stable for at least several months, and we have successfully analyzed cells 2–3 years after fixation.

16. While we have not observed any evidence of DNA damage or cell death with short IdU incubations, we have observed poor cell proliferation and toxicity with prolonged IdU incubations. We suspect that toxicity may occur during the replication of DNA strands containing IdU that had been incorporated during the previous S-phase.
17. All the centrifugation steps prior to methanol permeabilization can be performed at 300–600 × *g* (or whatever centrifugal force is known to be optimal for the cells of interest) for 5 min. After methanol permeabilization, centrifugation should be performed at least 600 × *g*. We recommend use of a refrigerated swinging bucket centrifuge (e.g., Sorvall Legend XTR [Thermo/Fisher], or similar) set to 4 °C.
18. Throughout this protocol, a "wash" refers to resuspending the cell pellet in 10–20 volumes (typically about 5 ml) of cell staining medium followed by a centrifugation to pellet the cells (typically 300–600 × *g* for 5 min at 4 °C) and aspiration of the supernatant. If the volume of the tube being used is not large enough to allow for 10 volumes of CSM to be added, perform additional washes until the total dilution is greater than 200-fold. Note that washing is much more important in mass cytometry than fluorescent flow cytometry, since residual antibody in a solution can create significant background, measurement errors, and may increase wear of the mass cytometer's detector.
19. It is not required to freeze samples after fixation, however, given the time required to perform mass cytometry experiments, and the frequent need to collect multiple time-points for cell cycle studies, freezing is typically required for practical purposes. If freezing is not desired, samples can be taken strait onto the staining steps after fixation and two CSM washes.
20. The Smart Tube proteomic stabilizer can also be purchased as part of Smart Tubes that are designed to work with an automated processing machine, the Smart Tube base station. These tubes have the fixative solution contained in a glass vial that is

broken open by the base station at a user-specified time to start fixation. The user can also program the base station to perform incubations at any desired temperature or duration allowing these tubes to be used to perform the incubations for IdU incorporation (*see* **steps 3–4** in Subheading 3.2) prior to fixation. Following the 10 min fixation, the Smart Tube base station will cool the sample to 4 °C slowing the fixation reaction and allow the user several hours to move the sample to −80 °C.

21. The BSA in the CSM will precipitate if added to a solution with a high concentration of methanol, so it is important to reduce the methanol concentration before adding the CSM to the cell suspension.
22. Alternate gating approaches, in addition to the biaxial plots described above, can be used. Measurement of these same markers enables cell cycle state assignment through the use of clustering methods such as SPADE [19] or viSNE [20]. When the core markers cell cycle markers (shown in Table 1) are used as the basis for clustering in these analysis algorithms, clear populations that correlate with each cell cycle state are readily identifiable.

## References


1. Darzynkiewicz Z, Juan G, Srour EF (2004) Differential staining of DNA and RNA. Curr Protoc Cytom Chapter 7(Unit 7):3. doi:10.1002/0471142956.cy0703s30
2. Pozarowski P, Darzynkiewicz Z (2004) Analysis of cell cycle by flow cytometry. Methods Mol Biol 281:301–311. doi:10.1385/1-59259-811-0:301
3. Tanner SD, Baranov VI, Ornatsky OI, Bandura DR, George TC (2013) An introduction to mass cytometry: fundamentals and applications. Cancer Immun, Immunother 62 (5):955–965. doi:10.1007/s00262-013-1416-8
4. Ornatsky OI, Lou X, Nitz M, Schafer S, Sheldrick WS, Baranov VI, Bandura DR, Tanner SD (2008) Study of cell antigens and intracellular DNA by identification of element-containing labels and metallointercalators using inductively coupled plasma mass spectrometry. Anal Chem 80(7):2539–2547. doi:10.1021/ac702128m
5. Behbehani GK, Bendall SC, Clutter MR, Fantl WJ, Nolan GP (2012) Single-cell mass cytometry adapted to measurements of the cell cycle. Cytometry A 81(7):552–566. doi:10.1002/cyto.a.22075
6. Raval A, Behbehani GK, Nguyen le XT, Thomas D, Kusler B, Garbuzov A, Ramunas J, Holbrook C, Park CY, Blau H, Nolan GP, Artandi SE, Mitchell BS (2015) Reversibility of defective Hematopoiesis caused by telomere shortening in telomerase knockout mice. PLoS One 10(7):e0131722. doi:10.1371/journal.pone.0131722
7. Behbehani GK, Samusik N, Bjornson ZB, Fantl WJ, Medeiros BC, Nolan GP (2015) Mass cytometric functional profiling of acute myeloid Leukemia defines cell-cycle and Immunophenotypic properties that correlate with known responses to therapy. Cancer Discov 5(9):988–1003. doi:10.1158/2159-8290.cd-15-0298
8. Strauss-Albee DM, Fukuyama J, Liang EC, Yao Y, Jarrell JA, Drake AL, Kinuthia J, Montgomery RR, John-Stewart G, Holmes S, Blish CA (2015) Human NK cell repertoire diversity reflects immune experience and correlates with viral susceptibility. Sci Transl Med 7 (297):297ra115. doi:10.1126/scitranslmed.aac5722
9. Chang Q, Ornatsky OI, Koch CJ, Chaudary N, Marie-Egyptienne DT, Hill RP, Tanner SD, Hedley DW (2015) Single-cell measurement of the uptake, intratumoral distribution and

cell cycle effects of cisplatin using mass cytometry. Int J Cancer 136(5):1202–1209. doi:10.1002/ijc.29074

10. Krutzik PO, Nolan GP (2003) Intracellular phospho-protein staining techniques for flow cytometry: monitoring single cell signaling events. Cytometry A 55(2):61–70. doi:10.1002/cyto.a.10072
11. Darzynkiewicz Z, Gong J, Juan G, Ardelt B, Traganos F (1996) Cytometry of cyclin proteins. Cytometry 25(1):1–13. doi:10.1002/(sici)1097-0320(19960901)25:1<1::aid-cyto1>3.0.co;2-n
12. Fienberg HG, Simonds EF, Fantl WJ, Nolan GP, Bodenmiller B (2012) A platinum-based covalent viability reagent for single-cell mass cytometry. Cytometry A 81(6):467–475. doi:10.1002/cyto.a.22067
13. Chow S, Hedley D, Grom P, Magari R, Jacobberger JW, Shankey TV (2005) Whole blood fixation and permeabilization protocol with red blood cell lysis for flow cytometry of intracellular phosphorylated epitopes in leukocyte subpopulations. Cytometry A 67(1):4–17. doi:10.1002/cyto.a.20167
14. Behbehani GK, Thom C, Zunder ER, Finck R, Gaudilliere B, Fragiadakis GK, Fantl WJ, Nolan GP (2014) Transient partial permeabilization with saponin enables cellular barcoding prior to surface marker staining. Cytometry A 85(12):1011–1019. doi:10.1002/cyto.a.22573
15. Zunder ER, Finck R, Behbehani GK, Amir E-aD, Krishnaswamy S, Gonzalez VD, Lorang CG, Bjornson Z, Spitzer MH, Bodenmiller B, Fantl WJ, Pe'er D, Nolan GP (2015) Palladium-based mass tag cell barcoding with a doublet-filtering scheme and single-cell deconvolution algorithm. Nat Prot 10(2):316–333. doi:10.1038/nprot.2015.020. http://www.nature.com/nprot/journal/v10/n2/abs/nprot.2015.020.html-supplementary-information
16. Ren S, Rollins BJ (2004) Cyclin C/Cdk3 promotes Rb-dependent G0 exit. Cell 117(2):239–251. doi:10.1016/s0092-8674(04)00300-9
17. Goto H, Yasui Y, Nigg EA, Inagaki M (2002) Aurora-B phosphorylates histone H3 at serine28 with regard to the mitotic chromosome condensation. Genes Cells 7(1):11–17. doi:10.1046/j.1356-9597.2001.00498.x
18. Hirata A, Inada K, Tsukamoto T, Sakai H, Mizoshita T, Yanai T, Masegi T, Goto H, Inagaki M, Tatematsu M (2004) Characterization of a monoclonal antibody, HTA28, recognizing a histone H3 phosphorylation site as a useful marker of M-phase cells. J Histochem Cytochem 52(11):1503–1509. doi:10.1369/jhc.4A6285.2004
19. Qiu P, Simonds EF, Bendall SC, Gibbs KD, Bruggner RV, Linderman MD, Sachs K, Nolan GP, Plevritis SK (2011) Extracting a cellular hierarchy from high-dimensional cytometry data with SPADE. Nat Biotechnol 29(10):886–891. http://www.nature.com/nbt/journal/v29/n10/abs/nbt.1991.html-supplementary-information
20. Amir el AD, Davis KL, Tadmor MD, Simonds EF, Levine JH, Bendall SC, Shenfeld DK, Krishnaswamy S, Nolan GP, Pe'er D (2013) viSNE enables visualization of high dimensional single-cell data and reveals phenotypic heterogeneity of leukemia. Nat Biotechnol 31(6):545–552. doi:10.1038/nbt.2594

# Chapter 9

# Preparation and Analysis of *Saccharomyces cerevisiae* Quiescent Cells

**Marla M. Spain, Sarah G. Swygert, and Toshio Tsukiyama**

## Abstract

*Saccharomyces cerevisiae* enter quiescence during extended growth in culture (greater than 7 days). Here, we describe a method to separate quiescent from non-quiescent cells by density gradient. We also describe approaches for DAPI staining the chromatin of quiescent cells, measuring quiescent cell viability, and extracting RNA from quiescent cells for use in genomics experiments.

**Key words** Quiescence, Quiescent cells, *Saccharomyces cerevisiae*, DAPI, RNA, DNA, Protein, Viability

## 1 Introduction

Quiescence is a reversible cellular state during which cells exit the cell cycle and arrest in an extended $G_1$-like state often referred to as $G_0$. Although quiescence is the most common cellular state in organisms from yeast to human and the regulation of quiescence plays essential roles in such diverse processes as stem cell maintenance, oncogenesis, wound-healing, and microbial pathogenesis, the factors governing quiescence entry, maintenance, and exit remain largely unknown. A significant barrier to the study of quiescence has been the difficulty of obtaining sufficient quantities of pure quiescent (Q) cells, as cells do not uniformly enter quiescence and thus generally exist in a mixed population. The recent development of a method to separate quiescent from non-quiescent (NQ) cells in *S. cerevisiae* has made budding yeast a key model in the field.

Yeast in stationary phase culture (greater than 7 days) exist in two populations—an asynchronous population of replicatively older, NQ cells, and a uniform population of younger, unbudded Q cells [1]. These two populations can be separated by density gradient. Due to their thickened cell walls and increased amounts of storage carbohydrates such as glycogen and trehalose, which

H. Daniel Lacorazza (ed.), *Cellular Quiescence: Methods and Protocols*, Methods in Molecular Biology, vol. 1686,
DOI 10.1007/978-1-4939-7371-2_9, 

causes them to be significantly denser than NQ cells, Q cells sediment at the bottom of the density gradient [1]. Studies using this method of purifying Q from NQ cells have revealed much of what is currently understood about quiescence [1–5]. During the process of quiescence entry, Q cells build up their cell walls, increase their thermotolerance, suspend the majority of transcription and translation, condense their chromatin, and arrest with $G_1$ DNA content [1–8]. Whereas the majority of NQ cells lose the ability to re-enter the cell cycle upon the reintroduction of nutrients after 7 days, quiescent cells retain the ability to re-enter the cell cycle for as long as they are viable [2, 9]. While progress has been made into the elucidation of the factors that control quiescence, future investigations into the mechanisms of quiescence are needed.

In this chapter, we describe a method to grow and isolate pure populations of Q and NQ cells. We also provide information for how to quantify Q cell viability, which is useful for characterizing mutants that affect quiescence, and strategies for staining Q cell chromatin with DAPI and purifying RNA from Q cells. A major consideration when implementing experimental methods to study Q cells is that the cell wall fortification that helps to confer increased thermotolerance and resistance to various types of stress also results in reduced cell wall permeability [4]. As such, dyes that stain DNA such as Sytox green or DAPI are unable to enter Q cells to the same extent that they enter log phase cells [4]. This likely holds true for various chemicals and antibodies commonly used in immunostaining as well.

The thickened cell walls of Q cells further render them resistant to breakage. Although standard methods of preparing DNA, chromatin, and protein lysates are sufficient for Q cells, the initial breakage of Q cells requires additional effort. When using a bead beating approach to open cells, we find that Q cells require twice as long as log phase cells. When using zymolyase to digest cell walls, we scale up both the concentration of enzyme and the incubation time, using up to five times the concentration of zymolyase and often incubating for several hours [7, 10]. Both bead beating and zymolyase treatment require careful monitoring of lysis by microscopy, and must be scaled to each strain and condition. For these reasons, we have not further described these methods here.

Finally, while standard methods of RNA purification may be used successfully in Q cells, overall transcription decreases drastically as yeast cells enter stationary phase [7], leaving less mRNA available per quiescent cell. In addition, more than 2000 transcripts are sequestered in protein-RNA complexes in p-bodies in stationary phase cells [11]. Nearly all of these transcripts are sequestered in Q rather than NQ cells [11]. The sequestered RNAs are not released by traditional hot phenol extraction methods [11], resulting in

much lower total RNA levels in Q cells versus log phase cells. To prepare RNA that includes sequestered mRNAs, protease treatment, such as Proteinase K [12], may be more complete [2, 11].

## 2 Materials

### 2.1 Quiescent Cell Purification

1. Yeast W303 (prototrophic).
2. YPD medium: 1% Yeast Extract, 2% Bacto Peptone, 2% glucose.
3. Percoll™.
4. 1.5 M NaCl.
5. Parafilm.
6. Shaking platform or incubator.
7. Centrifuge with fixed angle and swinging bucket rotors.
8. 30 ml glass round-bottom centrifuge tubes with appropriate adapters.
9. Glass slides and coverslips.
10. Light microscope with at least 20× magnification.
11. Glucose strips.

### 2.2 DAPI Staining Quiescent Cells

1. Purified quiescent yeast cells.
2. 10% paraformaldehyde: Pre-warm 1 ml of water in a 1.5 ml microfuge tube to 65 °C. Weigh 100 mg of paraformaldehyde in a hood or while wearing a mask for protection. Add it to the pre-warmed water. Add 1 µl of 1 M NaOH and shake or invert the tube to mix. Place at 4 °C once the solution becomes clear and use when cool. Store at 4 °C for up to 2 weeks.
3. 1× PBS.
4. 100% ethanol.
5. DAPI (4′,6-Diamidino-2-Phenylindole, Dihydrochloride) 1 mg/ml in 1× PBS.
6. Mounting Medium: 1.4% low melting agarose, 1 M Sorbitol in 1× PBS.

### 2.3 Viability Assay for Quiescent Cells

1. Purified quiescent yeast cells.
2. Sterile water.
3. YPD plates: 1% Yeast Extract, 2% Bacto Peptone, 2% Bacto Agar, 2% glucose.

### 2.4 Preparing RNA from Quiescent Cells: Hot Acid-Phenol Method

1. Purified quiescent yeast cells.
2. Liquid Nitrogen.
3. Acid washed glass beads (~0.1 mm in size).
4. Mortar and pestle.
5. TES buffer: 10 mM Tris pH 7.5, 10 mM EDTA, 0.5% SDS.
6. Acid phenol.
7. 100% ethanol.
8. 80% ethanol.
9. Chloroform.
10. 3 M sodium acetate, pH 5.2.
11. Glycogen 20 mg/ml.
12. Nanodrop or RiboGreen Assay

### 2.5 Preparing RNA from Quiescent Cells: Proteinase K Method

1. Purified quiescent yeast cells.
2. Proteinase K buffer: 10 mM Tris pH 8.0, 5 mM EDTA pH 8.0, 150 mM NaCl, 1% SDS, add Proteinase K to 0.4 mg/ml before use.
3. Potassium acetate Buffer: 3 M potassium acetate, 11.5% glacial acetic acid (v/v) in water.
4. 65 °C water bath or heat block.
5. Bead beater (e.g., Biospec Products MiniBeadBeater or similar).
6. 100% ethanol.
7. RNeasy Clean-up Kit (Qiagen).
8. Nanodrop or RiboGreen Assay.

## 3 Methods

### 3.1 Quiescent Cell Purification (Based on Ref. [1])

1. Inoculate 3 ml of YPD with a single colony of yeast (*see* **Note 1**). Allow the cells to grow overnight at 30 °C on a shaker at 180–200 rpm.
2. On the second day, inoculate 25 ml of YPD in a 125 ml Erlenmeyer flask at a density $O.D_{600}$ 0.02 (*see* **Note 2**), and let the cells grow for 7 days at 30 °C on a shaker at 180–200 rpm (*see* **Note 3**).
3. After 7 days, remove 7 μl of cells from each culture and place them on a glass slide. Cover with a coverslip and examine the cells under a standard light microscope with 20× or 40× magnification. Q cells should appear small, round, shiny, and unbudded. Confirm that there is no bacterial contamination in

the culture. If bacteria are detected, discard the cultures and repeat **steps 1** and **2**.

4. Pipette 11.25 ml of Percoll™ Plus into a 30 ml glass round-bottom centrifuge tube. Pipette 1.25 ml of 1.5 M NaCl on the top of the Percoll.
5. Place a strip of parafilm over the opening of the glass tube and secure it. Mix by vortexing for 10 s (*see* **Note 4**).
6. Spin the gradients in a fixed angle rotor (Beckman JA17 or equivalent) for 15 min at 10,000 × *g* at room temperature.
7. While the gradients are being centrifuged, pour each 25 ml yeast culture into a 50 ml falcon tube and spin at 2100 × *g* in a swing bucket rotor centrifuge (Beckman JS4.2A or equivalent), in a Beckman J6B or equivalent centrifuge, for 5–10 min to pellet the cells.
8. Discard the medium and resuspend cells in 1 ml of sterile deionized $H_2O$ by vortexing.
9. Carefully pipette the cell slurry onto each gradient by placing the pipette at the side of the glass tube just above the meniscus of the gradient and slowly and gently overlaying the cells onto the gradient.
10. Spin the cells through the gradients in a swinging bucket rotor at 296 × *g* for 1 h at room temperature.
11. Carefully remove the gradients from the centrifuge. The cells should be separated into two distinct layers with NQ cells at the top and Q cells at the bottom (Fig. 1).

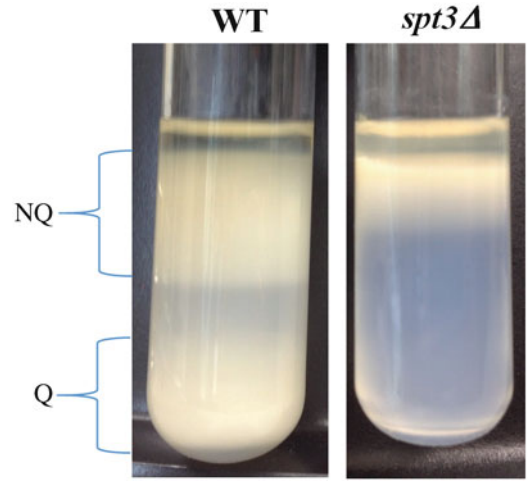


**Fig. 1** Density gradient purification of WT and *spt3Δ* stationary phase cells. NQ cells remain at the top of the gradient, while Q cells sediment at the bottom. No cells sediment in *spt3Δ,* because this strain is incapable of forming Q cells

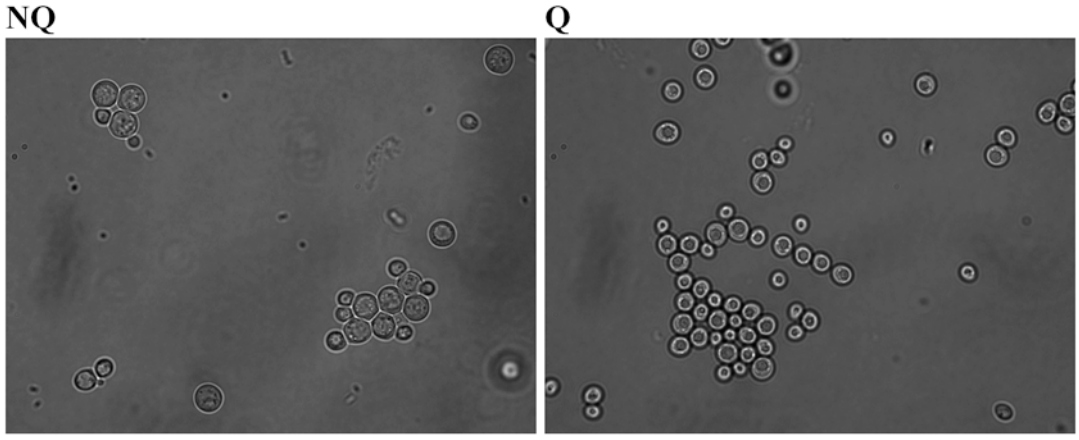


**Fig. 2** DIC images of wild-type non-quiescent (NQ, left) and quiescent (Q, right) cells. NQ cells are generally larger and budded. Q cells are smaller and predominantly unbudded

12. Carefully pipette the top layer of cells (NQ cells) into a clean 15 ml falcon tube.
13. Discard the Percoll in between the cell layers.
14. Carefully pipette the bottom cell layer (Q cells) into a clean 15 ml falcon tube.
15. Add sterile deionized $H_2O$ to fill the remaining space in each of the 15 ml tubes with cells.
16. Spin at 2100 × *g* for 10 min to pellet the cells.
17. If the pellets are not tight, carefully remove as much of the supernatant as possible and repeat **steps 16** and **17**. Repeat **step 18** until pellets are tight.
18. Remove the supernatant from the pellets. Place 10 μl of cells into 10 ml sterile deionized $H_2O$ in a 15 ml falcon tube and determine the $O.D_{600}$ of each sample using a spectrophotometer (*see* **Note 5**).
19. Examine the NQ and Q cells under a light microscope at 20× or 40× magnification to confirm the efficiency of the purification. Q cells should all be small, round and shiny, whereas the NQ fraction will contain larger cells and many budded cells (Fig. 2).

### *3.2 Viability Assay for Quiescent Cells*

1. Resuspend cells in 5 ml sterile water to $O.D._{600} = 0.1$.
2. Add cells to culture tubes, using a marker to mark the meniscus.
3. Incubate cells with rotation at 30 °C.
4. Every few days, check that the volume of water has not fallen below the initial mark. Replenish water as necessary.
5. At time 0, take 10 μl of cells and dilute in 10 ml sterile water (*see* **Note 6**).

6. Plate 100 µl of this dilution onto a YPD plate.
7. Grow the plate at 30 °C for 2 days, or until colonies are fully visible.
8. Count the number of colonies.
9. Each week, repeat **steps 5–8** until the desired duration has been reached (*see* **Note 7**).
10. Set the viability at time 0 to 100%. At each subsequent time point, calculate the percentage of colonies as compared to time 0.

### 3.3 DAPI Staining Quiescent Cells (Based on Ref. [13])

1. Resuspend 1 $O.D_{600}$ unit of purified Q cells (~$3 \times 10^7$) in 500 µl sterile deionized $H_2O$ in a 1.5 ml microfuge tube.
2. Fix cells by adding 100 µl of 10% paraformaldehyde to the tube and letting sit on the bench at room temperature for 20 min mixing two to three times by inversion over the course of the incubation.
3. Add 50 µl of 100% ethanol and centrifuge at 3500 × *g* for 1 min at room temperature using a microcentrifuge.
4. Remove the supernatant and resuspend cells in 100 µl of 1× PBS and 350 µl of 100% ethanol. Leave the cells at room temperature on a rotator or rocking platform for 2 h or overnight. Freeze cells at −20 °C or continue with the next step.
5. Spin the cells at 3500 × *g* for 1 min at room temperature using a microcentrifuge.
6. Resuspend the pellet in 100 µl of 0.5 µg/ml DAPI in 1× PBS.
7. Allow the cells to incubate for 10–30 min in the dark by placing them in a drawer or cupboard.
8. Spin the cells at 3500 × *g* for 1 min at room temperature using a microcentrifuge.
9. Resuspend cells in 40 µl of 1× PBS.
10. Pre-warm the mounting medium in a 95 °C heat block.
11. Add 2 µl of cells and 2 µl of mounting medium to a glass slide.
12. Immediately place a glass coverslip over the cell/mounting medium suspension by gently but firmly pressing on two opposing corners of the glass coverslip.
13. View slides on a fluorescent microscope using the DAPI filter (Fig. 3).

### 3.4 Preparing RNA from Quiescent Cells: Hot Acid-Phenol Method (Based on Refs. [10, 14])

1. Fill a mortar partially with liquid nitrogen. Add acid-washed glass beads to lightly coat the bottom. Grind 100 $O.D_{600}$ units of purified Q cells, together with glass beads, with a chilled mortar until the cells and beads have turned to a fine white powder.
2. Resuspend the cells in 300 µl of TES buffer.

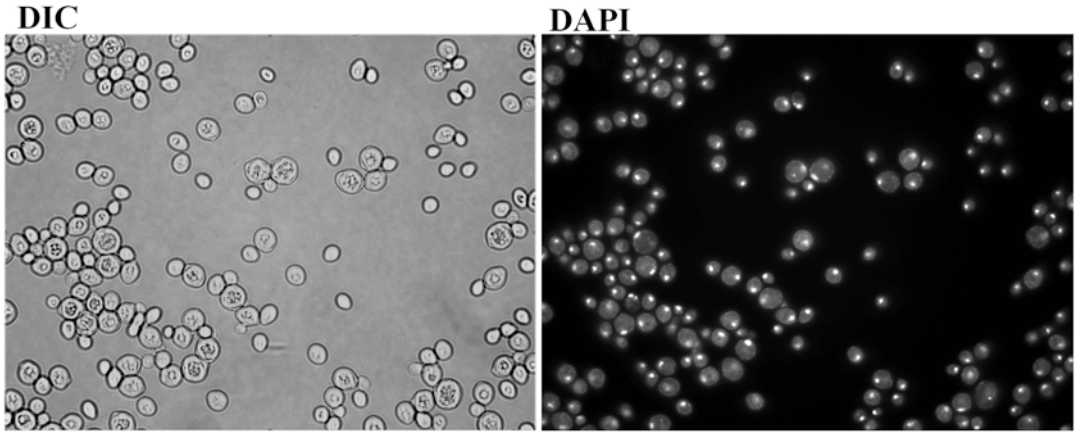


**Fig. 3** DAPI staining of an unpurified WT 7-day stationary phase culture. The nuclei of both the NQ and Q cells are stained with DAPI, indicating that the cells have been sufficiently permeabilized

3. Add 300 μl of acid phenol pre-warmed to 65 °C.
4. Incubate at 65 °C for 30 min. Vortex for 10 s every 10 min.
5. Centrifuge samples at 16,000 × *g* for 10 min at 4 °C.
6. Carefully remove the aqueous layer and place it in a clean 1.5 ml microfuge tube.
7. Add 300 μl of pre-warmed acid phenol and vortex for 20 s.
8. Repeat **steps 5** and **6**.
9. Add 300 μl of chloroform and vortex for 20 s.
10. Repeat **steps 5** and **6**.
11. Add 0.1 volumes of 3 M sodium acetate, pH 5.2, and 1 μl of glycogen (20 mg/ml) to the aqueous layer.
12. Add 2.5 volumes of 100% ethanol and vortex for 20 s.
13. Incubate at −20 °C for 1 h to overnight.
14. Spin the samples at maximum speed in a microcentrifuge for 20 min at 4 °C to pellet the RNA.
15. Remove ethanol without disturbing the pellet.
16. Add 1 ml of 80% ethanol.
17. Repeat **steps 14** and **15**.
18. Spin at maximum speed for 1 min and carefully remove remaining ethanol with a pipette.
19. Dry the pellets to eliminate any residual ethanol.
20. Resuspend the pellets in 100 μl nuclease-free $H_2O$.
21. Quantify the RNA concentration using a nanodrop or fluorescent assay such as RiboGreen (*see* **Note 8**).

22. For downstream sequencing or other sensitive assays, utilize the Qiagen RNeasy Clean Up Kit with on-column DNase treatment per the manufacturer's instructions.

### 3.5 Preparing RNA from Quiescent Cells: Proteinase-K Method (Based on Ref. [12])

1. Pre-warm 300 μl of Proteinase K buffer to 65 °C in a nuclease-free 1.5 ml microfuge tube for each sample of RNA to be extracted.
2. Add 50–100 μl of nuclease-free acid washed beads to each tube and incubate for 5 min at 65 °C.
3. Add 1 $O.D_{600}$ unit of purified Q cells (~$3 \times 10^7$) to the pre-warmed buffer and incubate at 65 °C for 10 min (*see* **Note 9**).
4. Bead beat the samples for 5 min.
5. Incubate the samples at 65 °C for 10 min.
6. Place cells on ice for 20 min.
7. Add 175 μl of potassium acetate buffer and vortex for 20 s.
8. Spin in a microcentrifuge at 1650 × *g* for 20 min at room temperature.
9. Transfer the supernatant to a clean nuclease-free 1.5 ml microfuge tube.
10. Add 600 μl of 100% ethanol and mix thoroughly by pipetting up and down.
11. Transfer the mixture, 700 μl at a time, to a Qiagen RNeasy Clean Up column, spinning in a microcentrifuge at maximum speed each time until all RNA has been bound to the column.
12. Continue following the manufacturer's instructions (*see* **Note 10**).
13. Quantify the RNA concentration by nanodrop or RiboGreen assay.

## 4 Notes

1. The protocols in this chapter are based on the growth of prototrophic W303 yeast cells grown in rich medium (YPD).
2. Q cell growth can be scaled up (e.g., 50 ml of YPD in a 250 ml Erlenmeyer flask, 100 ml in a 1 l or 200 ml in a 2 l). The ratio of medium in the flask to total flask volume is important for aeration and proper Q cell formation. When scaling up growth conditions, for subsequent gradient purification, it is best to split the cells into 25 ml aliquots and to use multiple 12.5 ml gradients per sample (e.g., 2 gradients for 50 ml, 4 for 100 ml, etc.).
3. When inoculated at $O.D_{600}$ 0.02 in 25 ml of YPD in a 125 ml Erlenmeyer flask, WT prototrophic W303 yeast reach the

diauxic shift (DS), the time point at which all glucose has been exhausted from the medium, in about 12 h from inoculation. The time that it takes for cells to reach the DS can vary depending on the starting dilution, the volume of medium and size of the flask, as well as the ratio of medium volume to flask size. The level of glucose in the medium is most easily measured using glucose test strips. Although Q cells can be distinguished by around 10 h after the DS, the culture is not fully in stationary phase at this time. Q cells are commonly purified at 7 days because the $O.D_{600}$ and cell number are stable, and the cells that sediment are most likely to be viable Q cells.

4. If making multiple gradients, the Percoll and NaCl for all of the gradients can be mixed first and aliquoted in 12.5 ml aliquots to each tube (e.g., 5 ml 1.5 M NaCl +45 ml Percoll across four centrifuge tubes).
5. WT prototrophic W303 yeast should produce nearly equal numbers of NQ and Q cells.
6. This dilution is designed to plate approximately 100 cells, and may need to be adjusted based on variations between spectrophotometers and strains. The number is less important than maintaining consistency across time points, and ensuring that cells are plated at a density that permits accurate colony counting.
7. The duration of the experiment will depend on the variable to be studied. We have found that wild-type Q cells retain over 50% viability after 9 weeks, whereas mutants that severely affect Q cell viability show significant reductions by Week 4.
8. The 260/280 and 260/230 ratios on the nanodrop should be over 2.0 for excellent quality RNA. Q cells often yield lower quality RNA, particularly when extracting RNA from smaller numbers of cells. If the 260/280 and 260/230 ratios are lower, the RNA can be cleaned up using either the Qiagen RNeasy Clean-up Kit or by additional chloroform extractions.
9. This protocol works with amounts as low as 50,000 cells and as high as $1 \times 10^8$ cells.
10. If DNA contamination is an issue, follow the manufacturer's instructions for on-column DNase treatment while using the RNeasy Clean Up kit.

## References

1. Allen C, Büttner S, Aragon AD, Thomas JA, Meirelles O, Jaetao JE, Benn D, Ruby SW, Veenhuis M, Madeo F, Werner-Washburne M (2006) Isolation of quiescent and nonquiescent cells from yeast stationary-phase cultures. J Cell Biol 174(1):89–100. doi:10.1083/jcb.200604072
2. Aragon AD, Rodriguez AL, Meirelles O, Roy S, Davidson GS, Tapia PH, Allen C, Joe R, Benn D, Werner-Washburne M (2008)

Characterization of differentiated quiescent and nonquiescent cells in yeast stationary-phase cultures. Mol Biol Cell 19 (3):1271–1280. doi:10.1091/mbc.E07-07-0666

3. Li L, Lu Y, Qin LX, Bar-Joseph Z, Werner-Washburne M, Breeden LL (2009) Budding yeast SSD1-V regulates transcript levels of many longevity genes and extends chronological life span in purified quiescent cells. Mol Biol Cell 20(17):3851–3864. doi:10.1091/mbc.E09-04-0347
4. Li L, Miles S, Melville Z, Prasad A, Bradley G, Breeden LL (2013) Key events during the transition from rapid growth to quiescence in budding yeast require posttranscriptional regulators. Mol Biol Cell 24(23):3697–3709. doi:10.1091/mbc.E13-05-0241
5. Miles S, Li L, Davison J, Breeden LL (2013) Xbp1 directs global repression of budding yeast transcription during the transition to quiescence and is important for the longevity and reversibility of the quiescent state. PLoS Genet 9(10):e1003854. doi:10.1371/journal.pgen.1003854
6. Li L, Miles S, Breeden LL (2015) A genetic screen for *Saccharomyces cerevisiae* mutants that fail to enter quiescence. G3 (Bethesda) 5 (8):1783–1795. doi:10.1534/g3.115.019091
7. McKnight JN, Boerma JW, Breeden LL, Tsukiyama T (2015) Global promoter targeting of a conserved lysine deacetylase for transcriptional shutoff during quiescence entry. Mol Cell 59(5):732–743. doi:10.1016/j.molcel.2015.07.014
8. Rutledge MT, Russo M, Belton JM, Dekker J, Broach JR (2015) The yeast genome undergoes significant topological reorganization in quiescence. Nucleic Acids Res 43 (17):8299–8313. doi:10.1093/nar/gkv723
9. Miles S, Breeden L (2016) A common strategy for initiating the transition from proliferation to quiescence. Curr Genet. doi:10.1007/s00294-016-0640-0
10. McKnight JN, Tsukiyama T (2015) The conserved HDAC Rpd3 drives transcriptional quiescence in *S. cerevisiae*. Genom Data 6:245–248. doi:10.1016/j.gdata.2015.10.008
11. Aragon AD, Quiñones GA, Thomas EV, Roy S, Werner-Washburne M (2006) Release of extraction-resistant mRNA in stationary phase *Saccharomyces cerevisiae* produces a massive increase in transcript abundance in response to stress. Genome Biol 7(2):R9. doi:10.1186/gb-2006-7-2-r9
12. Dye BT, Hao L, Ahlquist P (2005) High-throughput isolation of *Saccharomyces cerevisiae* RNA. Biotechniques 38(6):868. 870
13. Talarek N, Petit J, Gueydon E, Schwob E (2015) EdU incorporation for FACS and microscopy analysis of DNA replication in budding yeast. Methods Mol Biol 1300:105–112. doi:10.1007/978-1-4939-2596-4_7
14. Uppuluri P, Perumal P, Chaffin WL (2007) Analysis of RNA species of various sizes from stationary-phase planktonic yeast cells of *Candida albicans*. FEMS Yeast Res 7(1):110–117. doi:10.1111/j.1567-1364.2006.00143.x

# Chapter 10

# Identifying Quiescent Stem Cells in Hair Follicles

**Christine N. Rodriguez and Hoang Nguyen**

## Abstract

Hair follicle stem cells (HFSCs) are noted for their relative quiescence and therefore can be distinguished from other cells by their differential history of cell division. Replicating cells can be labeled by pulsing the animals repeatedly with 5-bromo-2′-deoxyuridine (BrdU) or tritiated thymidine ([$^3$H]TdR), thymidine analogs that get incorporated into DNA during DNA synthesis. Because dividing cells dilute the label after each cell division, frequently dividing cells will lose the label over time while slow cycling cells will retain the label and thus are termed label retaining cells (LRCs). [$^3$H]TdR can be visualized by autoradiography and BrdU can be detected by immunofluorescence with anti-BrdU antibodies. Alternatively, a well-established tet-regulatable transgenic mouse model can be used to express histone H2B-GFP in epithelial proliferative cells and their dilution and retention of the GFP signal can be followed. In this chapter, we detail the steps to perform BrdU pulse-chase and H2B-GFP pulse-chase experiments to identify quiescent cells in the hair follicle.

**Key words** Skin, Hair follicle epithelial stem cells, Epidermis, Quiescence, Pulse-chase, Label retaining cells, Hair cycle

## 1 Introduction

The skin is a self-renewing tissue made up of the stratified epidermis and its appendages: the hair follicle (HF) and sebaceous gland [1]. Each compartment contains designated stem cell populations that contribute to their homeostasis [2, 3]. Throughout life, HFs undergo cyclical stages of regression (catagen), rest (telogen), and growth (anagen) [4, 5] as illustrated in Fig. 1a. During catagen, cells in the lower two-third portion of the HF degenerate, leaving intact the upper region, the permanent structure of the HF. This region contains a specialized structure called the bulge, where hair follicle stem cells (HFSCs) are localized [6–11]. Through interaction with adjacent cells including the dermal papilla, a cluster of specialized mesenchymal cells at the base of the HF, HFSCs in the bulge transition from being quiescent in telogen to being activated in anagen. In anagen, progeny of HFSCs rapidly amplify before differentiating into mature progeny that occupy distinct layers

H. Daniel Lacorazza (ed.), *Cellular Quiescence: Methods and Protocols*, Methods in Molecular Biology, vol. 1686,
DOI 10.1007/978-1-4939-7371-2_10, 

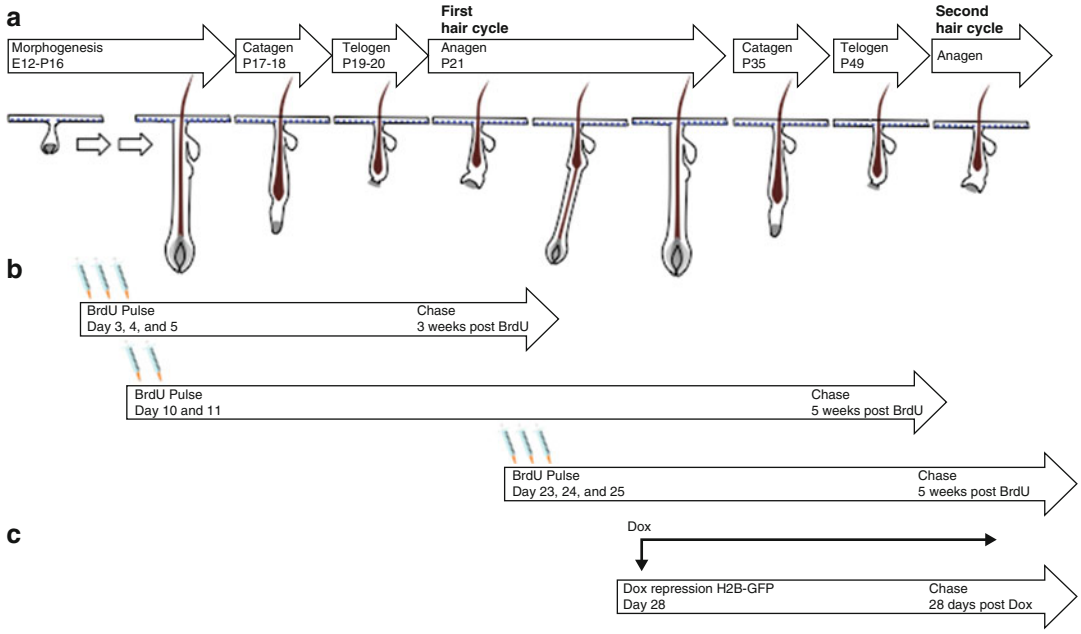


**Fig. 1** Mouse hair cycle in relation to pulse-chase schemes. (**a**) After completion of hair morphogenesis, hair follicles enter the destructive phase (catagen) on postnatal day 16–19. During catagen cells in the lower portion of the hair follicle degenerate, leaving intact the upper part, which contains the bulge region. HFSCs in the bulge enter a quiescent state (telogen) on postnatal day 19 lasting 2–3 days. Hair follicles enter the growth phase (anagen) of the first hair cycle when HFSCs in the bulge are activated and a new hair follicle downgrowth begins. Subsequently the hair follicles enter catagen at day 35 and then telogen at day 49 before reentering anagen of the second hair cycle weeks later. (**b**) BrdU pulse-chase scheme. Multiple injections of BrdU are delivered to mice from postnatal day 3–5, 10–11, or 23–25. After a chase period for an indicated amount of time post-BrdU injection, frequently dividing cells will dilute the amount of incorporated BrdU while the infrequently dividing cells retain BrdU. (**c**) Pulse-chase scheme for using the tet-off system to label and chase K5 positive cells with H2B-GFP. *K5-tTA;TRE-H2B-GFP* mice are placed on a diet containing doxycycline at postnatal day 28 to turn off transcription of H2B-GFP. After 4 weeks, H2B-GFP expression is diluted in frequently dividing cells and is retained in infrequently cycling cells

within the hair follicle [12]. Since murine HFs enter specific phases of the hair cycle quite synchronously within an expected timeframe in the first two hair cycles [5, 13], the HF is an excellent model system to study the regulation of SCs, in particular the signals that govern their quiescence and activation. The HFSCs can be distinguished from other cells based on their high level of quiescence [6, 11, 14–17].

The BrdU pulse-chase method is most commonly used to label dividing cells and to follow their cell division history based on their differential dilution of label [17, 18]. Because BrdU, a pyrimidine analog of thymidine, is incorporated into DNA during DNA synthesis, multiple injections of BrdU into mice in the pulse period will label all cells that replicate within the pulse period. Subsequently in the "chase" period, proliferative cells will lose half of their

incorporated BrdU after each division, while slow-cycling cells retain BrdU label. BrdU can then be detected by immunostaining skin sections with an antibody against BrdU. Depending on the end point of interest (either the first or second hair cycle), BrdU can be pulsed during morphogenesis from postnatal day 3–5 or day 10–11, or in early anagen from day 23–25 (Fig. 1b). When pulsed at day 3–5, LRCs can be visualized in the bulge at the first hair cycle when chased for a period of a minimum of 3 weeks. Pulsing in early anagen of the first hair cycle requires a chase period of a minimum of 5 weeks to localize the LRCs in the second hair cycle.

Alternatively, the well-established tet-regulatable transgenic mice expressing GFP-tagged histone H2B can be used to label and chase epithelial cells. This transgenic mouse model carries two transgenes: one expressing a tetracycline repressor fused to a transactivator VP16 under the control of a keratin 5 promoter (K5-tTA) [19], and another expressing histone H2B fused to green fluorescent protein under the control of tetracycline response element (TRE-H2B-GFP) [11]. These double transgenic mice constitutively express H2B-GFP in K5 positive cells throughout the epithelium, but the transcription of H2B-GFP will cease when the mice are placed on a diet containing a tetracycline analog, doxycycline. As with the BrdU pulse chase procedure, proliferative cells will dilute the H2B-GFP signal after each round of division, while cells that divide less frequently will retain GFP signal. After a 4-week period on doxycycline, H2B-GFP signal will be diluted in frequently dividing cells but will still be substantial in quiescent cells. One caveat of the BrdU pulse chase approach is that the labeling of quiescent cells may be incomplete, since the quiescent cells that are not proliferating during the 2-day period of BrdU pulse will not incorporate BrdU and hence cannot be labeled and chased. The advantage of the tet-regulatable histone H2B-GFP transgenic mouse model is that it allows more complete labeling of quiescent cells, due to the earlier initiation of induced expression of H2B-GFP and a longer duration of pulse. Because of the GFP signal retained in LRCs, this mouse model can also be used to isolate LRCs from the hair follicle bulge through fluorescence activated cell sorting.

## 2 Materials

### 2.1 BrdU Pulse-Chase

1. Postnatal day 3, 10, or 22 mice (*see* **Note 1**). Mice can be wild type or a genetically engineered mouse model of interest.
2. BrdU (Sigma, B5002) at 10 mg/mL in phosphate buffered saline (PBS).
3. 1 mL insulin syringe (or 1 mL syringe and 26G needle).

### 2.2 H2B-GFP Labeling and Chase

1. *K5-tTA* transgenic mice [19] expressing tetracycline repressor fused to transactivator VP16 under the control of the Keratin 5 promoter.
2. *TRE-H2B-GFP* transgenic mice [11] expressing H2B-GFP under the control of tetracycline response element-driven (TRE), which are currently available from Jackson Laboratories (stock number 005104).
3. Doxycycline containing mouse feed 1 mg/g (Bioserv).

### 2.3 Backskin Harvesting and Embedding in O.C.T.

1. Electric shavers or clippers.
2. 4-in. fine point dissection scissors.
3. 4-in. dissection forceps.
4. Razor blade.
5. PBS.
6. Brown paper towel.
7. Cryomold 25 × 20 mm.
8. O.C.T. compound.
9. Dry ice block.

### 2.4 Tissue Sectioning

1. Cryostat.
2. Microscope slides.
3. Hematoxylin 2.
4. Staining jar.
5. Light microscope.

### 2.5 Immunostaining

1. Humidified chamber (*see* **Note 2**).
2. Glass staining jar.
3. 37 °C water bath.
4. PAP pen.
5. PBS.
6. 1 N Hydrochloric acid.
7. 4% Paraformaldehyde in PBS.
8. 10% Triton X-100 solution.
9. 20% Bovine serum albumin (BSA).
10. Cold water fish skin gelatin (Sigma).
11. Normal Donkey Serum (NDS).
12. Normal Goat Serum (NGS).
13. PBS-GT: 2% fish gelatin, 0.2% Triton X-100, in PBS.
14. Blocking buffer: 10% NDS and 2% BSA in PBS-GT.
15. Staining buffer: 1% BSA and 5% NDS in PBS-GT.

16. BrdU gelatin blocking buffer: 2.5% NDS, 2.5% NGS, 1% BSA, 2% fish skin gelatin, 0.1% Triton X-100 in PBS.
17. Hoechst 33342 (Sigma).
18. ProLong Diamond antifade mounting solution (LifeTech, P36961).
19. Microscope slide glass coverslips.
20. Fluorescent microscope.

### 2.6 Primary and Secondary Antibodies

1. Chicken $\alpha$ mouse K5 (BioLegend, Sig-3475-100, dilution 1:1000).
2. Rat $\alpha$ mouse CD34 (eBioscience, dilution 1:50).
3. Rat $\alpha$ BrdU clone BU1/75 (Abcam, ab6326, dilution 1:200).
4. Alexa Fluor 488-conjugated donkey $\alpha$ chicken (Jackson Lab, dilution 1:100).
5. RRX-conjugated donkey $\alpha$ rat (Jackson Lab, dilution 1:150).

## 3 Methods

We describe here two methods for in vivo labeling dividing cells and identifying the quiescent cells in the hair follicles using pulse-chase techniques. We detail the steps to harvest and embed skin sections to best obtain intact hair follicles. We also include a co-immunostaining protocol to visualize BrdU or H2B-GFP with other epithelial/hair follicle markers.

### 3.1 BrdU Pulse-Chase

1. Administer injections of BrdU (50 mg/kg) every 12 h for a total of six injections subcutaneously into 3-day-old mice, or intraperitoneally into 23-day-old mice. Alternatively, administer BrdU every 12 h for a total of four injections subcutaneously into 10-day-old mice (*see* **Note 1**).
2. Allow a chase period of a minimum of 21 days (pulse at day 3–5) or 5 weeks (pulse at day 10–13 or day 23–25) to detect LRCs before continuing to Subheading 3.3.

### 3.2 H2B-GFP Labeling and Chase in Skin Epithelial Cells

1. Mice are maintained as single transgenic parental lines *K5-tTA* and *TRE-H2B-GFP*. Generate double transgenic mice by crossing *K5-tTA* single transgenic and *TRE-H2B-GFP* single transgenic lines.
2. Keep double transgenic pups on a normal diet until 4 weeks of age to allow H2B-GFP expression in all K5 positive cells. To turn off transcription of H2B-GFP, feed the double transgenic mice doxycycline containing chow and maintain them on this dox diet for a minimum of 4 weeks. Continue to Subheading 3.3 at the desired time point after chase.

### 3.3 Harvesting and Embedding Back Skin

1. Euthanize mice according to institution approved protocols and guidelines (*see* **Note 3**).
2. Shave off dorsal hair closely with an electric shaver.
3. Mark the midline of the mouse by drawing a line from head to tail with a marker.
4. As illustrated in Fig. 2a, use fine forceps to lift the skin at the anterior end and generate an incision perpendicularly to the midline (**step 1**). Generate two more incisions that run down both lateral sides of the mouse (**steps 2** and **3**). Finally, generate an incision at the posterior end that runs perpendicular to the midline to create a rectangle (**step 4**).

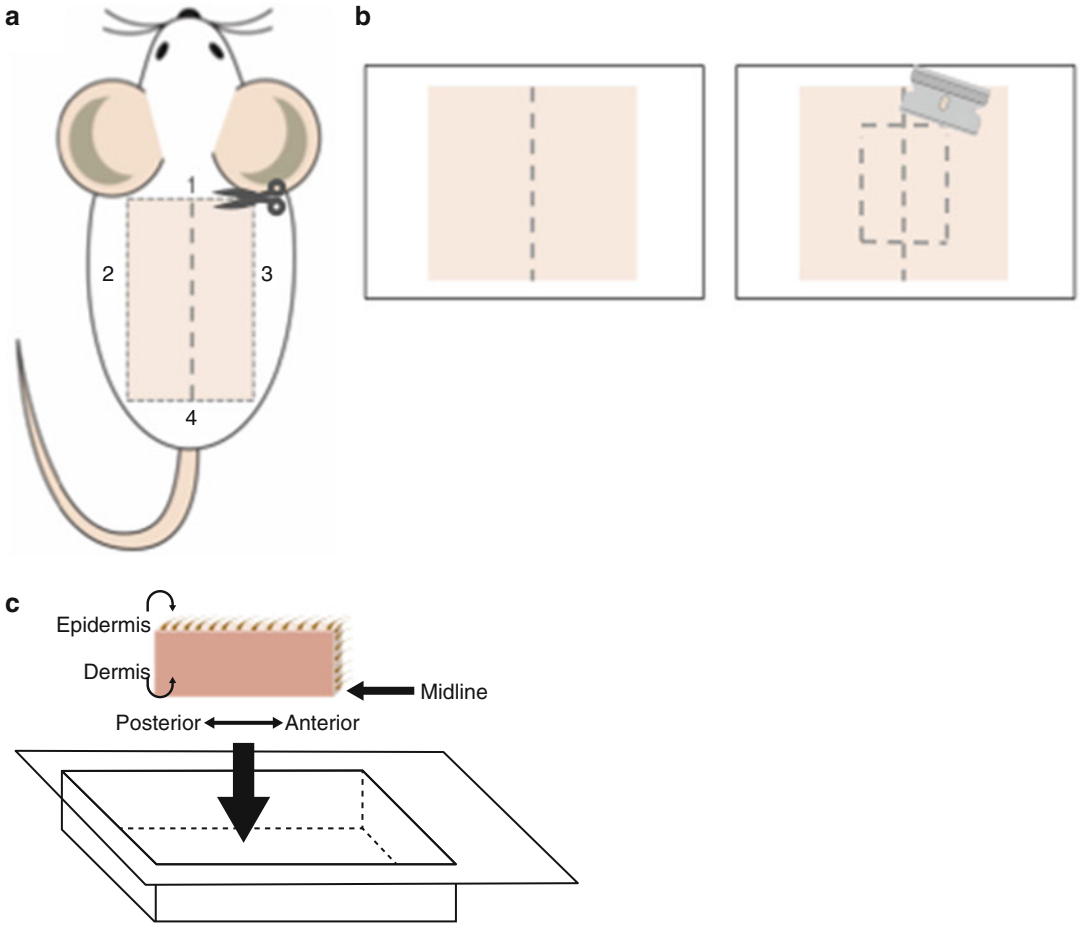


**Fig. 2** Illustration of back skin harvesting and embedding. (**a**) After removing hair from the back skin, draw a midline from neck to tail. Create an incision at the anterior portion of the back skin (**step 1**) and two incisions parallel to the midline (**steps 2–3**). Pull the skin from the anterior end then cut across at the posterior side to remove the skin from the animal (**step 4**). (**b**) Place the skin on a PBS dampened paper towel with the dermis face down. Use a razor blade to create 0.5 cm × 2.5 cm strips. (**c**) Embed the skin in O.C.T. filled Cryomold, with the midline against the bottom of the Cryomold

5. Dampen a paper towel with PBS and flatten skin on paper towel with the dermis facing down on the paper towel (*see* **Note 4**) (Fig. 2b).
6. With a new razor blade cut the skin along the midline. Then generate two parallel cuts about 0.5 cm away from either side of the midline. Lastly, create two cuts perpendicular to the midline to generate two 0.5 cm × 2.5 cm strips (Fig. 2b).
7. Fill the Cryomold with O.C.T.
8. Use forceps to submerge 0.5 cm × 2.5 cm skin strips in O.C.T. (*see* **Note 5**), keeping the skin straight and its midline flush with the bottom of the Cryomold. Place the Cryomold on dry ice (*see* **Note 6**) and allow the O.C.T. to completely freeze (Fig. 2c).
9. Move the O.C.T. tissue blocks to a prechilled cryostat for sectioning or store at −80 °C.

### 3.4 Cryosectioning

1. Set up the cryostat for skin sectioning according to manufacturer instructions (*see* **Note 7**). We typically section skin at 8 μm thickness (6–12 μm) and include two sections per slide.
2. Cut a few sections and air-dry them for a few minutes, then counterstain with hematoxylin for 1–2 min before rinsing briefly in tap water. View slide under light microscope to determine if multiple intact hair follicles can be seen in the skin section (*see* **Note 8**). Adjust the angle of the block accordingly, and recut sections until full hair follicles can be visualized.
3. Collect sections and allow slides to dry for approximately 20 min (*see* **Note 9**). Slides can be used immediately for staining or can be kept at −80 °C for long-term storage.

### 3.5 Immunostaining

#### 3.5.1 Co-immunostaining for Skin Epithelial Markers (or Other Proteins of Interest) in Chased Skin

1. If slides were previously frozen, allow slides to thaw and dry for 10–15 min at room temperature.
2. Use a PAP pen to draw a circle around the skin section on the slide. The hydrophobic PAP pen mark surrounding the skin will retain blocking/staining solution inside the marked area and prevent drying out of the skin section.
3. Fix slides in 4% PFA/PBS at room temperature for 10 min.
4. Wash slides with PBS in a staining jar three times for 5 min for each wash. Aspirate excess liquid from the slides after the final wash, add 200 μL of blocking buffer directly on the skin section encircled by the PAP pen mark, and incubate for 1 h at room temperature.
5. Prepare primary antibody solution by diluting primary antibody of interest in staining solution. Use primary antibody anti-K5 (diluted 1:1000) to mark the basal layer of the stratified epidermis and the outer root sheath of the hair follicle or anti-CD34 to mark bulge cells (*see* **Note 10**).

6. Aspirate the blocking buffer and add 150 μL of primary antibody solution. Incubate overnight in a humidified chamber at 4 °C or 1 h at room temperature.
7. Wash the slides in PBS three times, 5 min for each wash.
8. Prepare secondary antibody solution by diluting the relevant fluorophore-conjugated secondary antibody in staining buffer at the dilution specified in material section.
9. Aspirate excess liquid after the last wash, then apply 150 μL of secondary antibody solution onto the washed skin sections. Incubate for 1 h at room temperature. Slides should be protected from light in all subsequent steps to minimize photobleaching.
10. Wash the slides in PBS three times, 5 min for each wash.
11. For H2B-GFP chased skin sections, proceed to Subheading 3.5.2. Continue to Subheading 3.5.3 for BrdU staining.

### *3.5.2 Visualizing H2B-GFP in Hair Follicle Cells*

1. Dilute Hoechst 33342 in PBS (1:2000) and apply 150–200 μL to each tissue section. Incubate at room temperature for 2 min.
2. Wash the slides in PBS three times for a total of 10 min.
3. Aspirate to remove residual PBS, then mount a coverslip using ProLong Diamond antifade. Allow the slides to cure, protected from light, overnight to 24 h at room temperature.
4. After the slides have cured, seal the edges with nail polish. Allow the nail polish to air-dry for approximately 30 min prior to imaging.
5. Visualize and image with a fluorescent microscope with appropriate filters.
6. Slides can be stored at −20 °C for several months.

### *3.5.3 Detection of BrdU in Hair Follicle Cells*

1. Incubate the slides in a glass Coplin jar that contains prewarmed 1 N HCl in a 37 °C water bath for 40 min to denature DNA and unmask BrdU.
2. Wash in PBS once briefly, then four times for 5 min for each wash.
3. Aspirate any excess liquid after the last wash, then apply 200 μL of BrdU gelatin blocking buffer. Incubate for 1 h at room temperature.
4. Aspirate the blocking buffer then apply 150 μL of anti-BrdU antibody diluted (1:200) in gelatin blocking buffer. Incubate at room temperature for 1 h.
5. Wash the slides in PBS three times, 5 min for each wash.

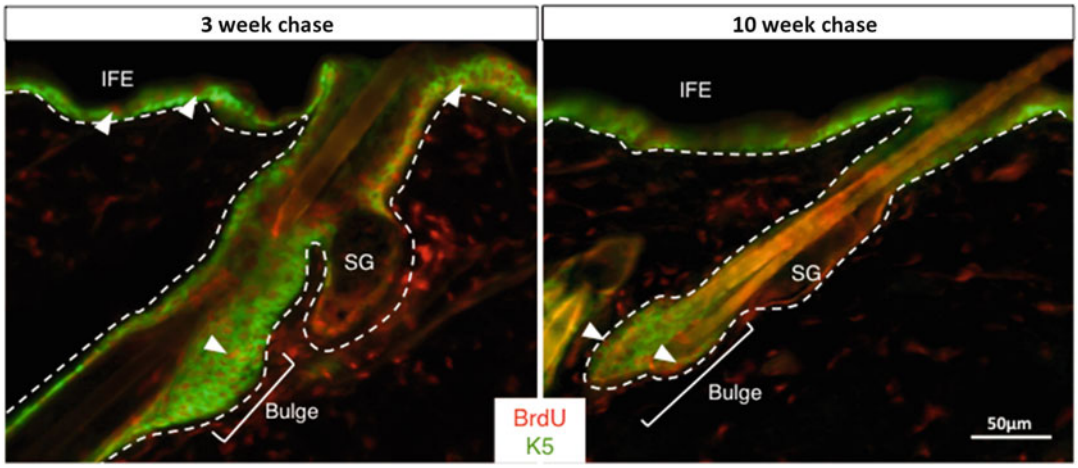


**Fig. 3** BrdU label retaining cells in hair follicle. Immunofluorescence images of BrdU in skin of wild-type mice pulsed at day 10–11 and chased for 3 weeks (*left panel*) or 10 weeks (*right panel*) after BrdU labeling. BrdU positive cells (*red*) are found throughout the skin 3 weeks after labeling and only in the bulge region of the hair follicle after 10 weeks. K5 (*green*) marks outer root sheath. (Scale bar = 50 μm)

6. Prepare secondary antibody (diluted as specified in material section) and Hoechst solution (1:2000) in gelatin blocking buffer.
7. Aspirate excess liquid after the last wash, then apply 150 μL of secondary antibody/Hoechst solution to each tissue section. Incubate at room temperature for 1 h (*see* **Notes 11** and **12**).
8. Wash the slides in PBS three times, 5 min for each wash.
9. Aspirate the residual PBS, then mount a coverslip using ProLong Diamond antifade. Allow the slides to cure, protected from light, overnight-24 h at room temperature.
10. After the slides have cured, seal the edges with nail polish. Allow the nail polish to air-dry for approximately 30 min prior to imaging.
11. Visualize and image with a fluorescent microscope with appropriate filters (Fig. 3).
12. Slides can be stored at −20 °C for several months.

## 4 Notes

1. The choice of the timing of BrdU pulse depends on the end point of interest. Pulsing at day 3–5 allows identification of LRCs at an earlier time point.
2. To create a humidified chamber, use an empty slide box where slides can lay on top of the slide storage slots during staining. Place dampened paper towels underneath to maintain moisture

in the chamber and reduce evaporation during the incubation steps.

3. American Veterinary Medical Association (AVMA) guidelines require $CO_2$ delivery that does not exceed 10–30% of the chamber volume per min to reduce distress. Deliver $CO_2$ for 3 min at the appropriate flow rate for your chamber. Turn off $CO_2$ delivery allowing mice to remain in the chamber for 2 min.
4. When embedding skins, we recommend working in batches of five mice maximum. If working with multiple mice, be sure to keep skins moist with PBS.
5. Multiple skin strips can be embedded in one block, but should be limited to no more than three strips per O.C.T. block. When embedding more than one skin strips, cover each strip with a thin layer of O.C.T then stack the pieces on top of one another. All pieces should be oriented epidermis face up with all midlines facing the same direction.
6. The dry ice block should be flat and level to ensure even freezing.
7. For skin sectioning, the chamber temperature (CT) is set to −24 °C while the object temperature (OT) is set to −27 °C.
8. In addition to proper embedding technique, proper set up of the tissue block on the cryostat is required to ensure that the sectioned skin contain intact hair follicles throughout the section. Hair follicles are considered intact when the entire hair follicle is seen contiguous to the interfollicular epidermis and is also in contact with the dermal papilla at its base.
9. Slides that are left to dry longer than 30 min will have increased background staining.
10. Alternative structural markers such as integrin α-6 (CD49f) or integrin β-4 (CD104) can be used to demark the boundary between epithelial cells and the dermis. Note that antibodies against CD34 and BrdU are both from rat and therefore cannot be used for co-immunostaining.
11. For BrdU staining, we find that acid treatment of the tissue can diminish the signal of some fluorophores. In our experience we find that Alexa Fluor 488 gives superior results and withstands the harsh acid treatment compared to FITC and RRX. (Ranked: AF488 > FITC> > RRX)
12. Acid treatment for BrdU staining tends to reduce Hoechst 33342 signal. We find it is beneficial to integrate Hoechst staining during the secondary antibody incubation.

## References


1. Fuchs E, Raghavan S (2002) Getting under the skin of epidermal morphogenesis. Nat Rev Genet 3(3):199–209
2. Schepeler T, Page ME, Jensen KB (2014) Heterogeneity and plasticity of epidermal stem cells. Development 141(13):2559–2567
3. Goodell MA, Nguyen H, Shroyer N (2015) Somatic stem cell heterogeneity: diversity in the blood, skin and intestinal stem cell compartments. Nat Rev Mol Cell Biol 16 (5):299–309
4. Hardy MH (1992) The secret life of the hair follicle. Trends Genet 8(2):55–61
5. Stenn KS, Paus R (2001) controls of hair follicle cycling. Physiol Rev 81(1):449–494
6. Cotsarelis G, Sun TT, Lavker RM (1990) Label-retaining cells reside in the bulge area of pilosebaceous unit: implications for follicular stem cells, hair cycle, and skin carcinogenesis. Cell 61(7):1329–1337
7. Rochat A, Kobayashi K, Barrandon Y (1994) Location of stem cells of human hair follicles by clonal analysis. Cell 76(6):1063–1073
8. Oshima H et al (2001) Morphogenesis and renewal of hair follicles from adult multipotent stem cells. Cell 104(2):233–245
9. Morris RJ et al (2004) Capturing and profiling adult hair follicle stem cells. Nat Biotechnol 22 (4):411–417
10. Blanpain C et al (2004) Self-renewal, multipotency, and the existence of two cell populations within an epithelial stem cell niche. Cell 118 (5):635–648
11. Tumbar T et al (2004) Defining the epithelial stem cell niche in skin. Science 303 (5656):359–363
12. Schneider MR, Schmidt-Ullrich R, Paus R (2009) The hair follicle as a dynamic miniorgan. Curr Biol 19(3):R132–R142
13. Muller-Rover S et al (2001) A comprehensive guide for the accurate classification of murine hair follicles in distinct hair cycle stages. J Invest Dermatol 117(1):3–15
14. Morris RJ, Potten CS (1994) Slowly cycling (label-retaining) epidermal cells behave like clonogenic stem cells in vitro. Cell Prolif 27 (5):279–289
15. Morris RJ, Potten CS (1999) Highly persistent label-retaining cells in the hair follicles of mice and their fate following induction of anagen. J Invest Dermatol 112(4):470–475
16. Taylor G et al (2000) Involvement of follicular stem cells in forming not only the follicle but also the epidermis. Cell 102(4):451–461
17. Braun KM et al (2003) Manipulation of stem cell proliferation and lineage commitment: visualisation of label-retaining cells in whole-mounts of mouse epidermis. Development 130(21):5241–5255
18. Bickenbach JR, Chism E (1998) Selection and extended growth of murine epidermal stem cells in culture. Exp Cell Res 244(1):184–195
19. Diamond I et al (2000) Conditional gene expression in the epidermis of transgenic mice using the tetracycline-regulated transactivators tTA and rTA linked to the keratin 5 promoter. J Invest Dermatol 115(5):788–794

# Chapter 11

# Single EDL Myofiber Isolation for Analyses of Quiescent and Activated Muscle Stem Cells

**Caroline E. Brun, Yu Xin Wang, and Michael A. Rudnicki**

## Abstract

Adult satellite cells are quiescent, but are poised for activation in response to exercise, injury, or disease allowing adult muscle growth or repair. Once activated, satellite cells proliferate extensively to produce enough myogenic progenitors in order to regenerate the muscles. In order to self-renew, a subset of activated satellite cells can resist the myogenic differentiation and return to quiescence to replenish the satellite cell pool. These cellular processes that normally occur during skeletal muscle regeneration can be recapitulated ex vivo using isolated and cultured myofibers. Here, we describe a protocol to isolate single myofibers from the *extensor digitorum longus* muscle. Moreover, we detail experimental conditions for analyzing satellite cells in quiescence and progression through the myogenic lineage.

**Key words** Skeletal muscle, Extensor digitorum longus, Satellite cells, Muscle stem cells, Myofiber isolation, Quiescence, Proliferation, Differentiation, Cell culture, Immunostaining, Pax7, Myod

## 1 Introduction

Adult skeletal muscles have an outstanding capacity to regenerate that relies on a population of muscle stem cells also called satellite cells [1]. In a resting muscle, satellite cells are intimately associated with the sarcolemma and beneath the basal lamina [2]. They express Pax7 and remain quiescent; however, they are primed for activation [3, 4]. Indeed, following a muscle injury, satellite cells re-enter cell cycle and progress through the myogenic lineage in order to repair or replace the damaged myofibers. Activated satellite cells can quickly upregulate the myogenic transcription factor MyoD and produce large numbers of myogenic progenitors through multiple rounds of cell division [4–6]. Subsequently, myogenic progenitors upregulate the differentiation factor myogenin, exit the cell cycle to become myocytes that either fuse to damaged myofibers or fuse together to form new myofibers [7].

Satellite cell activation, proliferation, and differentiation occurring during skeletal muscle regeneration can be recapitulated

H. Daniel Lacorazza (ed.), *Cellular Quiescence: Methods and Protocols*, Methods in Molecular Biology, vol. 1686,
DOI 10.1007/978-1-4939-7371-2_11, 

ex vivo using isolated single myofibers cultured in floating conditions [8, 9]. Myofiber isolation and culture allows for the visualization and quantification of muscle stem cells in their physiological niche [10, 11]. The protocol detailed below is a quick and efficient method of capturing snapshots of muscle stem cells as they exit the quiescent state, re-enter the cell cycle, and progress through the myogenic program. Fixing the samples at various time points yields insight into the deterministic steps of the adult muscle repair program, which can be utilized for mechanistic and genetic studies regarding the regulation of muscle stem cell behavior. The visualization of muscle stem cells on myofibers presents several advantages over single cell isolation by fluorescence-activated cell sorting (FACS) and on cryosectioned muscle tissues. Isolated single myofibers allow for the visualization of the muscle stem cells within immediate time points, 1–4 h, that are simply unobservable due to the lengthy process required to isolate cells by FACS or in vivo through muscle injuries models. Moreover, muscle fibers provide cell-cell signals to muscle stem cells that are not easily reproduced in a culture dish. Therefore, the culture of isolated single myofibers provides a unique culture system that is currently unmatched for the study of muscle stem cells at a single-cell level.

## 2 Materials

Prepare all solutions fresh prior to muscle dissection.

### 2.1 Dissection Materials

1. Iris scissors.
2. Cohan-Vannas spring scissors.
3. Half-curved Iris forceps.
4. Half-curved micro forceps.
5. $25G^{5}/_{8}$ syringe needle.
6. Stereo dissecting microscope.

### 2.2 Myofiber Isolation and Culture Materials

1. 37 °C water bath.
2. Humidified 37 °C, 5% $CO_2$ incubator.
3. Sterile 100 × 25 mm tissue culture dish.
4. Sterile 60 × 15 mm tissue culture dishes
5. Glass Pasteur pipets.
6. Sterile fetal bovine serum (FBS).
7. Sterile horse serum (HS).
8. Collagenase solution: 2 mg/ml of Collagenase type I in DMEM (Dulbecco's modified Eagle's medium; 1 g/l glucose, L-glutamine with 110 mg/l sodium pyruvate) supplemented with 1% Penicillin/Streptomycin (P/S), filtered through a 0.22 μm filter (*see* **Note 1**).

9. Washing medium: DMEM supplemented with 1% P/S, filtered through a 0.22 μm filter.
10. Myofiber culture medium: DMEM complemented with 20% FBS, 1% P/S and 1% Chicken Embryo Extract (CEE), filtered through a 0.22 μm filter (*see* **Notes 2** and **3**).

### 2.3 Immunostaining Materials

1. Sterile phosphate-buffered saline (PBS), pH 7.4.
2. Paraformaldehyde 4% in PBS, filtered, pH 7.4.
3. Glass Pasteur pipets.
4. Permeabilization solution: 0.1% Triton X-100, 0.1 M Glycine in PBS.
5. Blocking buffer: 5% horse serum or goat serum, 2% BSA, 0.1% Triton X-100 in PBS (*see* **Note 4**).
6. Primary antibodies: anti-Pax7 (1:2, DSHB, culture supernatant), anti-MyoD (1:500, Santa Cruz), or anti-myogenin (1:500, Santa Cruz).
7. Secondary antibodies: goat anti-mouse IgG1 Alexa Fluor 488 conjugate and goat anti-rabbit IgG Alexa Fluor 546, both at 1:1000.
8. DAPI solution: DAPI diluted 1:50,000 in PBS.
9. Permafluor fluorescence mounting medium (*see* **Note 5**).
10. Optional: Transparent quick drying nail polish.

## 3 Methods

### 3.1 Before Starting EDL Dissection

1. For EDL myofiber isolation from one mouse, coat 1 sterile 100 mm tissue culture dish and 3 sterile 60 mm tissue culture dishes with enough volume of sterile HS to cover the surface. Incubate at room temperature for 5 min. Remove the serum and let dishes dry for approximately 15 min. Finally, add 10 and 4 ml of washing medium in the 100 mm and 60 mm dishes respectively and keep the dishes in a humidified 37 °C, 5% $CO_2$ incubator (*see* **Note 6**).
2. For EDL muscle trituration, prepare one wide-bore Pasteur pipette using a diamond pen to cut the glass to obtain an opening size of 4–5 mm diameter. Flame polish to smooth pipette edges. Coat the pipette with HS before use.
3. For EDL myofiber transfer and manipulation, flame polish the opening of a normal Pasteur pipette and curve the tip. This will help in handling the single myofibers. Coat the pipette with FBS or HS before use (*see* **Note 7**).
4. Pre-warm the collagenase solution to 37 °C in a water bath.

### 3.2 EDL Muscle Dissection and Digestion

1. Euthanize the mouse. For the purpose of this experiment, 8-week old C57BL/6 mouse was used.
2. Disinfect the hind limbs with 70% Ethanol and place the mouse (face up) on a support board.
3. Use the Iris scissors to cut the skin all-the-way around the ankle and then, carefully cut the skin proximally along leg until the knee in order to expose the underlying muscles (Fig. 1a). Using a half-curved Iris forceps, lift and remove the skin.
4. Using a half-curved micro forceps, remove the fascia surrounding the *tibialis anterior* (TA), going along the tibia bone from the ankle to the knee.
5. Visually locate the distal tendons of the *extensor digitorum longus* (EDL) and TA muscles. In order to remove the TA muscle, insert a needle between the two distal tendons, under the TA tendon, and glide it toward the ankle (Fig. 1b). Cut the TA distal tendon attaching to the ankle with a Cohan-Vannas spring scissors.
6. Using a half-curved Iris forceps, grab the cut TA tendon and slowly pull the TA muscle away and cut it at the knee, as close as you can to the patella (Fig. 1b). Now, the EDL muscle is entirely visible.
7. In order to identify the proximal tendon of the EDL, cut the *biceps femoris posterior* (BFP) close to the patella (Fig. 1c) (*see* **Note 8**).
8. Insert a needle under the proximal EDL tendon and cut the tendon using a Cohan-Vannas spring scissors, freeing the EDL from the knee (Fig. 1d).
9. Optional: Insert a needle under the distal EDL tendon and gently slide it from the ankle to the knee, freeing the EDL muscle from the knee and the tissue around (*see* **Note 9**).
10. Grab the proximal EDL tendon with a half-curved Iris forceps, pull out the EDL muscle and cut the distal EDL tendon with a Cohan-Vannas spring scissors.
11. Repeat the **steps 3–10** to isolate the EDL muscle of the contralateral hind limb.
12. Place both EDL muscles into a 15 ml Falcon tube containing 2 ml of Collagenase solution and incubate in a water bath at 37 °C for 45 min to 1 h, gently stir the Falcon tube every 15 min, until muscles appear to begin dissociated, hairy in appearance with free fibers coming loose (*see* **Note 10**).

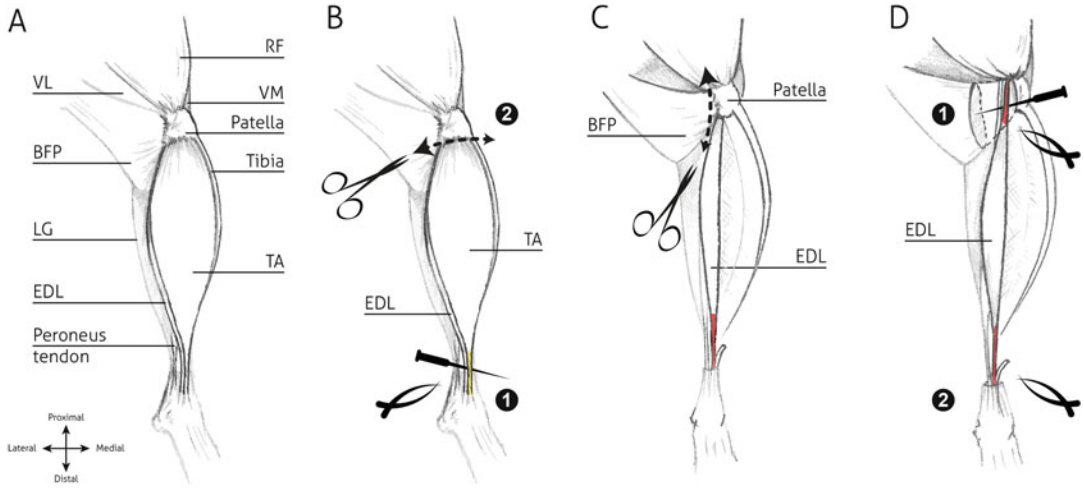


**Fig. 1** Schematic representing the different steps to isolate the EDL muscle. (**a**) Once the skin has been removed, the underlying muscles are visible. The fascia surrounding the *tibialis anterior* (TA) muscle should be removed. (**b**) In order to remove the TA muscle, a needle is inserted under the TA tendon (in *yellow*). Using a Cohan-Vannas spring scissors, the TA distal tendon attaching to the ankle can be cut (1), grabbed it with a half-curved Iris forceps, and slowly pull away the TA muscle. It can be now cut at the knee (2). (**c**) In order to identify the proximal tendon of the *extensor digitorum longus* (EDL) muscle, the *biceps femoris posterior* (BFP) muscle and the connective tissue around the knee is cut close to the patella. (**d**) In order to free the EDL muscle from the knee, a needle is inserted into the proximal EDL tendon (in *red*, *1*). This tendon can now be cut using Cohan-Vannas spring scissors and grabbed with a half-curved Iris forceps to pull out the EDL muscle. Finally, the distal EDL tendon can be cut with Cohan-Vannas spring scissors (2). *BFP, biceps femoris posterior; EDL, extensor digitorum longus; LG, lateral gastrocnemius; RF, rectus femoris; TA, tibialis anterior; VL, vastus lateralis; VM, vastus medialis*

### *3.3 EDL Myofiber Isolation and Culture in Floating Condition*

1. Stop the digestion by transferring the digested muscles into the HS-coated 100 mm tissue culture dish containing 10 ml of washing medium. At this point, the following steps are performed under a stereo dissecting microscope using transmitted bright field illumination.
2. Triturate the muscle using the wide-bore pipette in order to loosen and release the myofibers by gently pipetting up and down against the edge of the dish (*see* **Note 11**).
3. Once the desired number of myofibers has been released from the muscle proper, use a small size bore pipette to transfer live single myofibers into the pre-warmed, coated 60 mm tissue culture dish containing 4 ml of washing medium. Live myofibers look straight and translucent, without any shears or obvious bends.
4. Repeat **step 3** two more times in order to remove all debris and dead, short and hyper-contracted myofibers. Alternatively, if analysis of truly quiescent satellite cells is warranted (Fig. 2a, b), wash the myofibers in PBS and fix them in 2% PFA for 10 min (*see* procedures detailed below).

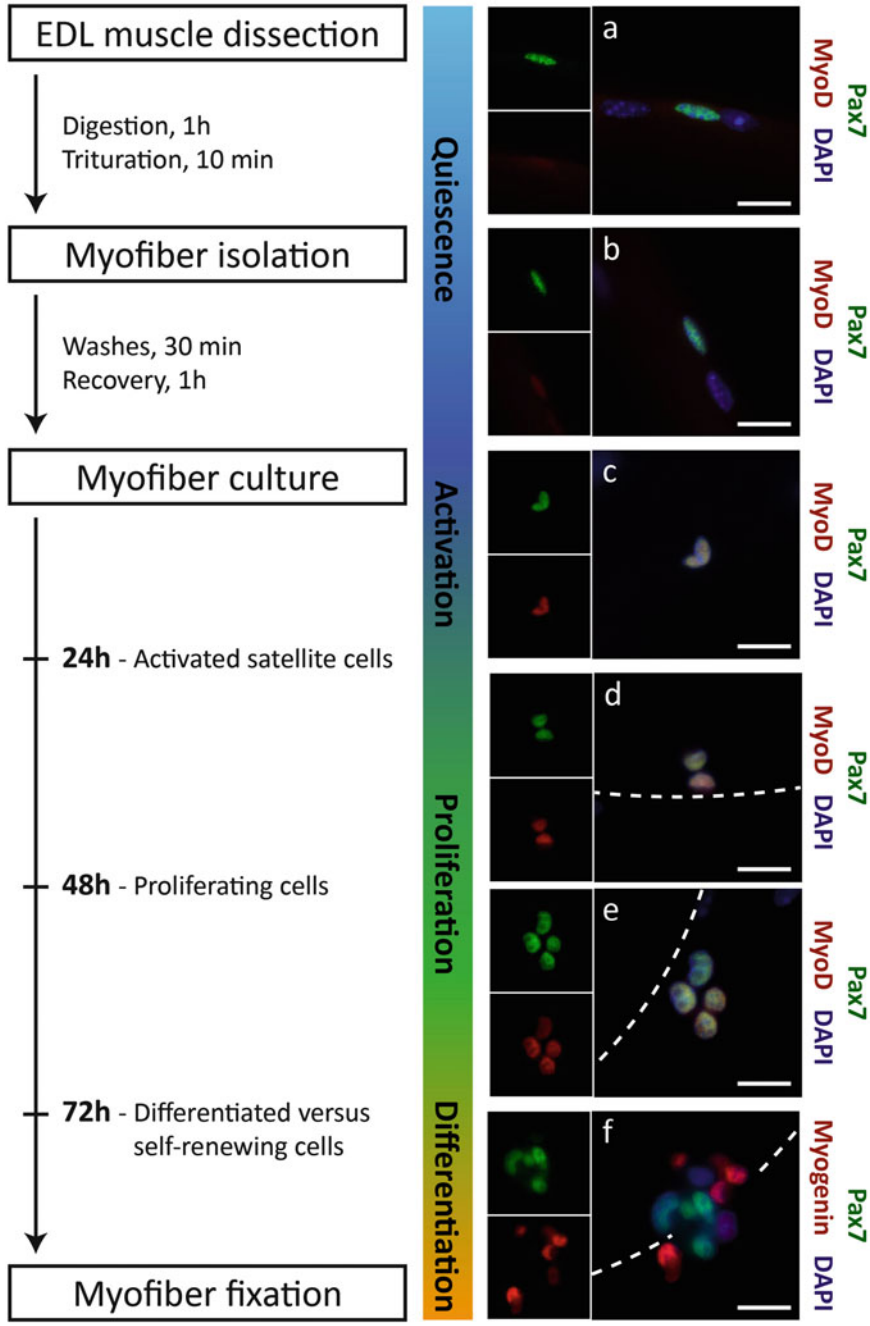


**Fig. 2** Overview of the myofiber isolation protocol. Once dissected, the EDL muscles are put into the collagenase solution for 1 h and triturated for 10 min in order to dissociate each myofiber individually. Then, myofibers are washed and incubated for 1 h into the serum-free recovery medium. At this step, EDL myofibers can be fixed in order to analyze satellite cells in quiescence. As shown on the immunostaining for Pax7 (*green*) and MyoD (*red*) (**a**, **b**), Pax7-expressing satellite cells remain mostly MyoD-negative. Alternatively, myofibers can be transferred into myofiber culture medium and cultured for 24, 48, or 72 h in order to follow their activation, proliferation, or differentiation respectively. Immunostaining for Pax7 (*green*) and MyoD (*red*) allows for identifying the activated (**c**) and proliferating (**d**, **e**) satellite cells. At 72 h, immunostaining for Pax7 (*green*) and myogenin (*red*) (**f**) allows distinguishing the self-renewing satellite cells expressing Pax7 only from the committed myogenic progenitors expressing myogenin. *Scale bars; 25 $\mu m$*

5. Incubate the single myofibers at 37 °C, 5% $CO_2$ in the last 60 mm tissue culture dish containing 4 ml of washing medium for 30 min–1 h. It allows the myofibers to recover from the muscle trituration and the myofiber isolation, prior to switching them to the myofiber culture medium.
6. Transfer live myofibers into wells of a HS-coated 6-well plate each containing 1 ml of a pre-warmed washing medium.
7. Remove the washing medium and replace it with the myofiber culture medium (*see* **Note 12**).
8. To observe satellite cell activation, upregulation of MyoD, and cell cycle re-entry, culture myofibers in a 37 °C incubator for 4–24 h (Fig. 2c). To observe the first divisions of satellite cells, culture myofibers in a 37 °C incubator for 36–48 h (Fig. 2d, e). To monitor the transition into myogenin-expressing differentiating myocytes, culture myofibers in a 37 °C incubator for 72 h (Fig. 2f) (*see* **Notes 13** and **14**).

### 3.4 EDL Myofiber Immunostaining

1. With a small size bore pipette, remove the myofiber culture medium leaving remaining a small amount of medium and wash the myofibers with 2 ml of pre-warmed PBS (*see* **Note 12**).
2. Remove 1 ml of PBS and fix the myofibers in 2% PFA by adding 1 ml of pre-warmed 4% PFA for 10 min at room temperature (RT).
3. Remove the PFA solution and wash the myofibers three times in PBS for 2 min.
4. Incubate the myofibers in the permeabilization solution for 10 min at RT to permeabilize the myofibers and quench the fixative.
5. Incubate then the myofibers in blocking buffer for at least 1 h at RT.
6. Incubate with the appropriate primary antibodies diluted in blocking buffer overnight at 4 °C. Optimized primary antibodies could be incubated at RT for 2 h. For the purpose of this experiment, we used the following primary antibodies: anti-Pax7 (1:2), anti-MyoD (1:500), or anti-myogenin (1:500) (Fig. 2).
7. Wash three times in PBS for 2 min.
8. Incubate with the appropriate secondary antibody diluted in blocking solution for 1 h at RT (keep in the dark). For the purpose of this experiment, we used the following secondary antibodies: goat anti-mouse IgG1 Alexa Fluor 488 conjugate and goat anti-rabbit IgG Alexa Fluor 546, both at 1:1000.

9. Wash two times in PBS for 2 min.
10. Stain nuclei with DAPI solution for 5 min (keep in the dark).
11. Wash two times in PBS for 2 min.
12. Transfer each myofiber onto a glass slide suitable for microscopy. Remove any excess of PBS. Apply mounting medium and add coverslip. Let the slides dry overnight prior to visualizing.
13. Optional: seal the coverslip with clear nail polish.

## 4 Notes

1. All the procedure should be performed with DMEM containing 110 mg/l sodium pyruvate. The sodium pyruvate-free medium would affect myofiber survival. The addition of penicillin and streptomycin prevents contamination while working under the dissection microscope, however, is optional if sterile techniques are maintained.
2. Various commercial sources have different methods in preparing CEE. CEE contains various growth factors that facilitate the activation and proliferation of muscle stem cells. Make sure that the CEE has not been ultrafiltrated because this results in the removal of various growth factors, such as bFGF, and can lead to reduced proliferation of muscle stem cells in culture. If the CEE has been ultrafiltrated, bFGF should be supplemented to the myofiber culture medium.
3. Altered growth factor and serum concentrations will lead to subtle changes in muscle stem cell behavior, cell cycle kinetics, and expression of myogenic factors. FBS and CEE are uncharacterized culture supplements with complex components that can affect cellular signaling; therefore, it is important to eliminate the possibility of batch effects with proper experimental design.
4. The choice of horse or goat serum in your blocking buffer should be optimized with specific combinations of primary and secondary antibodies.
5. Permaflour is a fluorescence mounting medium for general applications; however, it may not be suitable for super resolution imaging using localization microscopy. Suitable alternatives can be used for these specific techniques.
6. The 100 mm HS-coated culture dish will be used for triturating myofibers from the collagenase digested EDL muscles. The remaining 60 mm HS-coated dishes will be used to wash the isolated fibers and remove debris and damaged myofibers. If HS is kept in sterile conditions, it can be re-used several times.

7. To serum coat plastic ware or glass pipettes, either FBS or HS could be used depending on cost and availability.
8. If necessary, cut off the connective tissue around the knee to expose the proximal tendon of the EDL.
9. Using a needle here helps to remove the connective tissue attaching the EDL to other muscle groups. However, if this is not done carefully, the needle could tear the EDL muscle apart and damage the myofibers. It is important to insert the needle between the tendon and the bone and then gently slide it under the EDL muscle.
10. Collagenase solutions can have varying activity. It is important to qualitatively monitor the digestion process. Observe the digestion process by stirring the tubes every 15 min. The ideal point to proceed is when loosened myofibers begin coming away from the muscle. Under-digestion will require additional force to triturate the muscle apart and result in few viable myofibers or bundles of capillaries still being attached to the myofibers. However, over-digesting the muscle could cause damage to the basal lamina structures, create micro tears to the sarcolemma and also result in few viable myofibers.
11. Too much force during the trituration step can cause damage to the myofibers and result in hypercontraction. Hypercontracted myofibers have fewer muscle stem cells, are not reliable for staining, and could skew quantifications if included in the analysis.
12. Washing the myofibers should be done gently. Vigorous forces can cause myofibers to hypercontract or muscle stem cells to detach. A proper count of muscle stem cells before and after the wash steps should be performed as a quality control step (Fig. 3a, b).
13. As previously described, quiescent muscle stem cells are poised for activation and the simple process of isolation can initiate this process. By monitoring the activation of the myogenic determination factor MyoD as a marker of lineage progression and cellular activation, we observe that muscle stem cells quickly transition out of their quiescent state and accumulate MyoD protein (Fig. 3c). Therefore, in order to obtain an accurate representation of quiescence, we recommend that fibers are fixed immediately after trituration.
14. The culture time should be determined according to the biological process that is being studied. Phenotypes can be easily missed by observing the wrong time point.

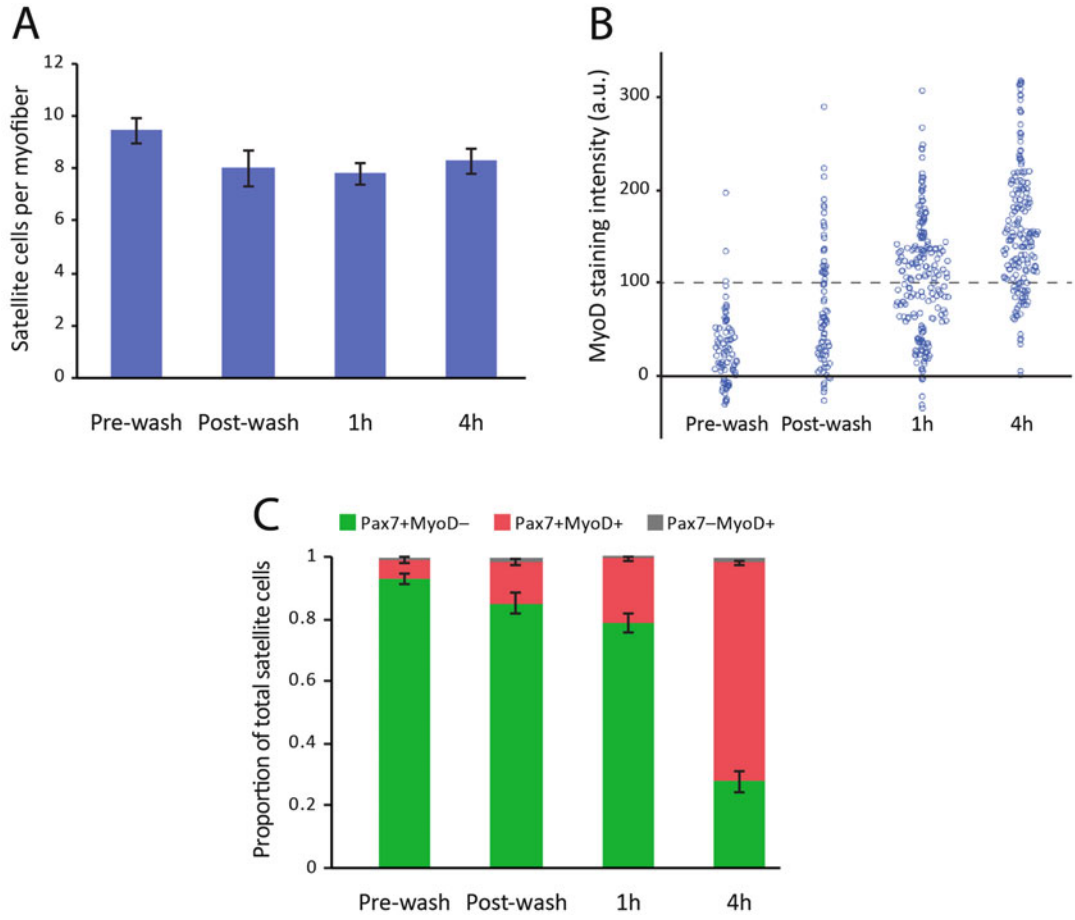


**Fig. 3** Rapid activation response of muscle stem cells after isolation. Muscle stem cell activation can be carefully monitored by expression of molecular markers such as MyoD and by counting cell numbers. (**a**) Quantification of satellite cells (Pax7+ and/or MyoD+ cells) per myofiber after fixation at various steps of the isolation protocol. (**b**) Proportions of total cells expressing only Pax7 (*green*), Pax7 and MyoD (red), or only MyoD (*gray*) after fixation at various steps of the isolation protocol. (**c**) Fluorescence intensity of MyoD immunostaining in single satellite cells after fixation at various steps of the isolation protocol. >50 cells were quantified per condition, dashed line represents a general threshold of MyoD signal that can be confirmed visually. $n = 4$ biological replicates, error bars indicate standard error of the mean (S.E.M.)

## Acknowledgments

C.E.B. is supported by a Postdoctoral Fellowship from the Ontario Institute for Regenerative Medicine. Y.X.W. is supported by fellowships from the Queen Elizabeth II Graduate Scholarships in Science and Technology and the CIHR. M.A.R. holds a Canada Research Chair in Molecular Genetics. These studies were carried out with support of grants to M.A.R. from the US National Institutes for Health [R01AR044031], the Canadian Institutes for Health

Research [MOP-12080, MOP-81288, FDN-148387], E-Rare-2: Canadian Institutes of Health Research/Muscular Dystrophy Canada [ERA-132935], the Muscular Dystrophy Association, and the Stem Cell Network.

## References

1. Dumont NA, Bentzinger CF, Sincennes MC, Rudnicki MA (2015) Satellite cells and skeletal muscle regeneration. Compr Physiol 5 (3):1027–1059. doi:10.1002/cphy.c140068
2. Mauro A (1961) Satellite cell of skeletal muscle fibers. J Biophys Biochem Cytol 9:493–495
3. Seale P, Sabourin LA, Girgis-Gabardo A, Mansouri A, Gruss P, Rudnicki MA (2000) Pax7 is required for the specification of myogenic satellite cells. Cell 102(6):777–786
4. Chang NC, Rudnicki MA (2014) Satellite cells: the architects of skeletal muscle. Curr Top Dev Biol 107:161–181. doi:10.1016/B978-0-12-416022-4.00006-8
5. Zammit PS, Golding JP, Nagata Y, Hudon V, Partridge TA, Beauchamp JR (2004) Muscle satellite cells adopt divergent fates: a mechanism for self-renewal? J Cell Biol 166(3):347–357. doi:10.1083/jcb.200312007
6. Cornelison DD, Wold BJ (1997) Single-cell analysis of regulatory gene expression in quiescent and activated mouse skeletal muscle satellite cells. Dev Biol 191(2):270–283. doi:10.1006/dbio.1997.8721
7. Rudnicki MA, Le Grand F, McKinnell I, Kuang S (2008) The molecular regulation of muscle stem cell function. Cold Spring Harb Symp Quant Biol 73:323–331. doi:10.1101/sqb.2008.73.064
8. Rosenblatt JD, Lunt AI, Parry DJ, Partridge TA (1995) Culturing satellite cells from living single muscle fiber explants. In Vitro Cell Dev Biol Anim 31(10):773–779. doi:10.1007/BF02634119
9. Bischoff R (1986) Proliferation of muscle satellite cells on intact myofibers in culture. Dev Biol 115(1):129–139
10. Kuang S, Gillespie MA, Rudnicki MA (2008) Niche regulation of muscle satellite cell self-renewal and differentiation. Cell Stem Cell 2 (1):22–31. doi:10.1016/j.stem.2007.12.012
11. Pasut A, Jones AE, Rudnicki MA (2013) Isolation and culture of individual myofibers and their satellite cells from adult skeletal muscle. J Vis Exp 73:e50074. doi:10.3791/50074

# Chapter 12

# Investigating Cellular Quiescence of T Lymphocytes and Antigen-Induced Exit from Quiescence

**Kai Yang and Hongbo Chi**

## Abstract

Naïve T cells are in a quiescent state under homeostasis but respond to antigen stimulation by exiting from quiescence and entering the cell cycle. Appropriate regulation of quiescence is crucial for maintaining T cell homeostasis at steady state and initiating proper T cell responses to antigen stimulation. Emerging evidence indicates that signaling by mechanistic target of rapamycin (mTOR) plays a central role in the control of T cell quiescence and antigen-induced exit from quiescence through coordinating immune signals, cellular metabolic programs, and cell cycle machinery. The mTOR-dependent regulation of quiescence has also been implicated in the differentiation and function of memory T cells. In this chapter, we describe techniques to assess quiescent state of naïve T cells under steady state and exit from quiescence upon TCR stimulation.

**Key words** T cell, Quiescence, Metabolism, mTOR, Seahorse, Glycolysis, Oxidative phosphorylation, Fatty acid oxidation

## 1 Introduction

T lymphocytes are pivotal in adaptive immunity. Mature naïve T lymphocytes circulate through the blood and peripheral lymphoid organs in a quiescent state characterized by small cell size, low metabolic activity, and maintaining at G0 phase of the cell cycle [1]. Quiescent state is actively regulated, which is crucial for T cell homeostasis and proper T cell immunity [2, 3]. T cells adopt distinct metabolic programs associated with different requirements for regulating quiescence. To maintain quiescence under steady state, naïve T cells rely on the tricarboxylic acid (TCA) cycle and oxidative phosphorylation (OXPHOS) to generate ATP for cell survival through breakdown of glucose, fatty acids, and amino acids. Upon engagement of antigen and costimulation, naïve T cells initiate metabolic reprogramming and activation of cell growth and cell cycle machinery for quiescence exit. A hallmark of metabolic rewiring during quiescence exit is substantial enhancement of

H. Daniel Lacorazza (ed.), *Cellular Quiescence: Methods and Protocols*, Methods in Molecular Biology, vol. 1686,
DOI 10.1007/978-1-4939-7371-2_12, 

aerobic glycolysis and OXPHOS that fulfill bioenergetic and biosynthetic needs for robust clonal expansion [4–6]. Accumulating evidence indicates the connection between aberrant cellular metabolism and dysregulated quiescent state in T cells. For example, loss of quiescence in T cells is associated with uncontrolled cell growth and hyperactivation of glycolysis and OXPHOS [7, 8], while impaired antigen-induced quiescence exit has been ascribed to defective cell growth and metabolic reprogramming [9, 10]. Therefore, proper metabolic programs are a fundamental mechanism in the regulation of quiescent state.

mTOR is a conserved serine/threonine kinase that controls cell growth and metabolism. It forms two distinct complexes (mTORC1 and mTORC2) through interaction with adaptor proteins Raptor and Rictor, respectively. mTORC1 directly phosphorylates the ribosomal S6 kinase 1 (S6K1) and eukaryotic translation initiation factor 4E-binding protein 1 (4E–BP1) to promote protein translation [9]. In contrast, mTORC2 phosphorylates the kinase AKT on the site of serine 473 and regulates cytoskeletal organization. In T cells, mTOR signaling integrates diverse immune signals and metabolic cues to orchestrate T cell homeostasis and immunity [11]. mTORC1 and mTORC2 have been implicated in dictating the fate and function of diverse T cell subsets [9, 12–16]. In the context of regulating T cell quiescence, mTORC1 functions as a pivotal regulator that coordinates cell growth, metabolic reprogramming, and cell cycle machinery. Antigen-induced activation of mTORC1 orchestrates multiple anabolic pathways to promote the exit of naïve T cells from the quiescence and entry into active cycling [9]. However, aberrant activation of mTORC1, for example, upon deletion of the upstream negative regulator TSC1, results in loss of quiescence of naïve T cells and predisposes them to apoptotic cell death, thereby disrupting T cell-mediated immune responses [7, 8]. Therefore, understanding the regulation and function of mTOR and metabolic pathways provides insights into quiescent state of naïve T cells at steady state and antigen-induced quiescence exit upon immune stimulation.

Here, we describe methods used to examine quiescent state of T cells ex vivo and in vitro. Flow cytometry-based methods are used to assess cell growth, expression of nutrient receptors, activity of mTOR signaling, and cell cycle machinery. Seahorse analyzer-based methods are used to measure glycolysis and OXPHOS. Radiolabeled palmitic acid is used to measure fatty acid oxidation (FAO) in T cells.

## 2 Materials

### 2.1 Preparation of Naïve T Lymphocytes from the Spleen

1. ACK lysing buffer.
2. Nylon mesh.
3. 3 ml syringes.
4. 10 cm petri dish.
5. MACS CD4 (L3T4) MicroBeads, mouse (Miltenyi Biotec).
6. MS columns (Miltenyi Biotec).
7. OctoMACS™ Separator (Miltenyi Biotec).
8. Hank's balance salt solution (HBSS) buffer.
9. Isolation buffer: HBSS supplemented with 2% FBS.
10. Dulbecco's phosphate-buffered saline (DPBS) buffer, pH 7.4.
11. Sorting buffer: DPBS supplemented with 2 mM EDTA and 0.5% BSA.
12. Antibody cocktails for sorting naïve CD4 T cells: Pac-blue-conjugated anti-CD4 (RM4–5), PE-cy7-conjugated anti-CD62L (MEL-14), APC-conjugated anti-CD44 (1M7), FITC-conjugated anti-CD25 (PC61.5).

### 2.2 Flow Cytometry of Cell Size and Expression of Nutrient Receptors

1. DPBS buffer, pH 7.4.
2. Surface staining buffer (FACS buffer): DPBS supplemented with 2% BSA and 0.2% sodium azide.
3. Coat buffer: DPBS supplemented with anti-CD3 (10 μg/ml, clone 2C11) and anti-CD28 (10 μg/ml, clone 37.51).
4. Pac-blue-conjugated anti-CD4 (clone RM4–5).
5. APC-cy7-conjugated anti-TCRβ (clone H57–597).
6. Brilliant Violet 605-conjugated anti-CD8 (clone 53–6.7).
7. PE-cy7-conjugated anti-CD62L (clone MEL-14).
8. Brilliant Violet 650-conjugated anti-CD44 (clone 1M7).
9. PE-conjugated anti-CD98 (clone RL388).
10. FITC-conjugated anti-CD71 (clone R17217).
11. 7-Aminoactinomycin D (7-AAD).

### 2.3 Analysis of mTOR Activity by Phosflow

1. DPBS buffer, pH 7.4.
2. Surface staining buffer (FACS buffer): DPBS supplemented with 2% BSA and 0.2% sodium azide.
3. Phosflow™ Lyse/Fix buffer 5× (BD Biosciences): dilute with deionized or distilled water (1:5), and pre-warm the solution to 37 °C.
4. Phosflow™ Perm buffer III (BD Biosciences).

5. Surface staining buffer: DPBS supplemented with 2% BSA and 0.2% sodium azide.
6. PE-conjugated anti-phospho-4E-BP1 (Thr37/46).
7. APC-conjugated anti-phospho-AKT (S473).
8. FITC-conjugated anti-phospho-S6 (Ser235/236).

### 2.4 5-Bromo-2-Deoxyuridine (BrdU) Incorporation In Vivo and In Vitro

Reagents used for this procedure are from BD Biosciences.

1. BrdU (10 mg/ml).
2. BD Cytofix/Cytoperm™ buffer.
3. BD Cytoperm™ Permeabilization buffer plus.
4. BD Perm/Wash™ buffer (10×).
5. APC-conjugated anti-BrdU antibody.
6. 7-AAD.
7. DNase.

### 2.5 Analysis of Glycolysis and OXPHOS Using a Seahorse Analyzer

1. XF24 Extracellular Flux Analyzer (Agilent Technologies).
2. Seahorse assay media (Agilent Technologies).
3. XF24 FluxPak including cell plates, calibrant, and cartridges (Agilent Technologies).
4. Sodium pyruvate, glutamine, and glucose.
5. Cell-Tak (BD Biosciences).
6. Oligomycin.
7. Carbonyl cyanide-p-trifluromethoxyphenylhydrazone (FCCP).
8. Rotenone.

### 2.6 Fatty Acid $\beta$-Oxidation Flux

1. 5 N HCl.
2. [9, 10-$^3$H]-palmitic acid.
3. Scintillation liquid: ScintiSafe™ 30% cocktail.
4. Etomoxir.
5. Liquid Scintillation Counter.

## 3 Methods

### 3.1 Preparation of Naïve T Lymphocytes from the Spleen

1. Under the hood, add 1 ml of cold isolation buffer to a 10 cm petri dish and place organ within the medium. Lay nylon mesh over the spleen and gently grind it using the flat end of a 3 ml syringe (*see* **Note 1**).
2. Wash the mesh with 10 ml of isolation buffer and collect cells into a 15 ml tube, followed by centrifugation at 600 × *g* for 5 min.

3. Remove the supernatant and resuspend the cell pellet with 1 ml of ACK lysing buffer and incubate the cells for 1–2 min at room temperature (RT) (*see* **Note 2**).
4. Wash cells with 10 ml of isolation buffer, spin down (600 × *g* for 5 min), and thoroughly remove the supernatant.
5. Resuspend the cells in 90 μl of sorting buffer per $10^7$ total cells.
6. Add 10 μl of CD4 (L3T4) MicroBeads per $10^7$ total cells. Mix well and incubate for 15 min at 4 °C.
7. Wash the cells with 10 ml of sorting buffer and spin down (600 × *g* for 5 min).
8. Equilibrate a MS MACS column with 500 μl of sorting buffer.
9. Resuspend the cells in 500 μl of sorting buffer and load cell suspension onto the column through 40 μm nylon container by gravity flow.
10. Wash the column with 3 × 500 μl of sorting buffer.
11. Remove column from the separator and place it on a 15 ml collection tube.
12. Flush out the fraction of magnetically labeled cells with 1 ml sorting buffer using the plunger supplied with the column, and spin down (600 × *g* for 5 min).
13. Resuspend the cells in 200 μl of sorting buffer supplemented with specific antibodies: Pac-blue-CD4, PE-cy7-CD62L, FITC-CD44, and APC-CD25, and incubate for 15 min at 4 °C.
14. Sort naïve $CD4^+$ T cells ($CD4^+CD25^-CD62L^+CD44^-$).

### 3.2 Analysis of Cell Size and Expression of Nutrient Receptors

#### 3.2.1 Freshly Isolated Naïve T Lymphocytes

1. Prepare single-cell suspension from the spleen (*see* **steps 1–5** in Subheading 3.1).
2. Stain 5 × $10^5$ splenocytes with antibodies against surface molecules CD4, CD8α, TCRβ, CD62L, CD44, CD25, CD98, and CD71 in 20 μl of surface staining buffer (*see* **Note 3**).
3. Incubate the cells for 15 min at 4 °C.
4. Wash the cells with 200 μl of surface staining buffer and spin down (600 × *g* for 5 min).
5. Resuspend the cells in 100 μl of surface staining buffer and run samples on a flow cytometer. Forward scatter (FSC) is acquired as a measurement of cell size.

#### 3.2.2 Activation of $CD4^+$ T Cells upon TCR Stimulation

1. Add 100 μl of coat buffer to desired wells in a 96-well plate and incubate for 2 h at 37 °C.
2. Wash the wells with 200 μl of DPBS buffer twice and aspirate completely.

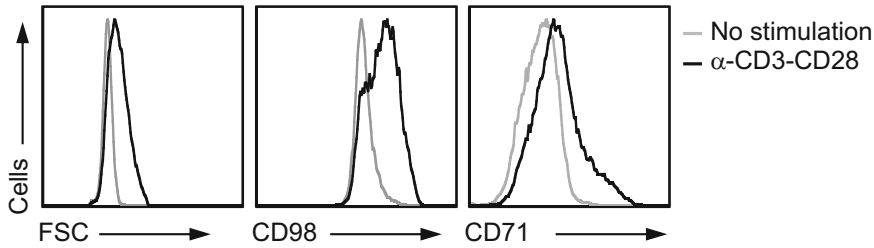


**Fig. 1** Cell size and expression of CD98 and CD71 on naïve and activated $CD4^+$ T cells. Naïve $CD4^+$ T cells ($2 \times 10^5$) were stimulated with or without plate-bound anti-CD3 plus anti-CD28 (10 μg/ml) for 24 h, followed by flow cytometry analysis of cell size and expression of CD98 and CD71 on naïve and activated $CD4^+$ T cells. Histogram plots are gated on live (negative for 7-AAD) cells

3. Plate $2 \times 10^5$ naïve $CD4^+$ T cells purified by cell sorting (*see* Subheading 3.1) per well and incubate for 24 h.
4. Harvest the cells and stain with 20 μl of surface staining buffer supplemented with antibodies CD98 (amino acid transporter) and CD71 (transferrin receptor); their expression is closely associated with T cell metabolic activity. In addition, T cell activation markers such as CD69 and CD25 can be stained as positive controls for T cell activation.
5. Incubate the cells for 15 min at 4 °C.
6. Wash the cells with 200 μl of surface staining buffer and spin down (600 × *g* for 5 min).
7. Resuspend the cells in 100 μl of surface staining buffer and run samples on a flow cytometer. FSC is acquired as a measurement of cell size (Fig. 1).

### *3.3 Analysis of mTOR Activity by Phosflow*

1. Stimulate naïve $CD4^+$ T cells ($2 \times 10^5$/well) with or without plate-bound anti-CD3 plus anti-CD28 (96-well plate) for 24 h or desired time points.
2. Transfer the cells to FACS tubes (size 5 ml) and wash the cells with 2 ml of FACS buffer and spin down (600 × *g* for 5 min).
3. Resuspend the cells with 1 ml of pre-warmed 1× Phosflow™ Lyse/Fix buffer and incubate for 10 min at 37 °C.
4. Add 2 ml of cold FACS buffer to the tube and spin down (600 × *g* for 5 min).
5. Resuspend the cells in 1 ml of ice-cold Phosflow™ Perm buffer III and incubate the tube on ice for 30 min.
6. Add 2 ml of cold FACS buffer to the tube, spin down (600 × *g* for 5 min), and remove the supernatant (*see* **Note 4**).
7. Wash the cells with 3 ml of cold FACS buffer and spin down (600 × *g* for 5 min).
8. Repeat **step 6**.

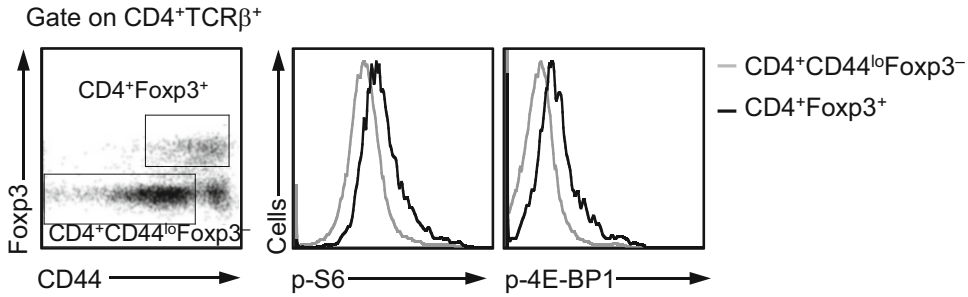


**Fig. 2** Phosphorylation of S6 and 4E-BP1 in $CD4^+Foxp3^+$ (Treg cells) and $CD4^+CD44^{lo}Foxp3^-$ (naïve T cells) from the spleen. Freshly isolated splenocytes were immediately fixed and stained with related surface and phospho-antibodies. Flow cytometry of phospho-S6 and phospho-4E-BP1 in different subsets of CD4 T cells are indicated

9. Resuspend the cells with 200 μl of FACS buffer and transfer the cells to 1.5-ml Eppendorf tube. After spin down (600 × *g* for 5 min), thoroughly remove all supernatant.
10. Resuspend the cells in 20 μl of FACS buffer containing antibodies: FITC-phospho-S6 (Ser235/236) (1:200), PE-phospho-4E-BP1 (Thr37/46) (1:200), APC-phospho-AKT (Ser473) (1:200), and Pac-blue-CD4 (1:400).
11. Transfer cell suspension to a 96-well U-bottom plate and incubate in the dark for 1 h at RT.
12. Wash the cells with 200 μl of FACS buffer per well and spin down (600 × *g* for 5 min).
13. Resuspend the cells with 100 μl of FACS buffer, and run on a flow cytometer.
14. This protocol can also be used to examine activity of mTOR signaling in different subsets of freshly isolated lymphocytes under steady state (Fig. 2; *see* **Note 5**).

### *3.4 BrdU Incorporation In Vivo and In Vitro*

1. Intraperitoneally inject 100 μl (1 mg) of BrdU solution per mouse.
2. After 20 h of BrdU injection, prepare single-cell suspension from the thymus, spleen, and peripheral lymph nodes (PLNs). Incubate $1 \times 10^6$ filtered cells in 20 μl of FACS buffer containing specific antibodies Pac-blue-CD4 (1:400), APC-cy7-TCRβ (1:200), Brilliant Violet 605-CD8 (1:400), PE-cy7-CD62L (1:400), and FITC-CD44 (1:400), for 15 min on ice (*see* **Note 6**).
3. Wash the cells with 1 ml of FACS buffer and spin down (600 × *g* for 5 min).
4. Resuspend the cells in 100 μl of BD Cytofix/Cytoperm buffer per sample.

5. Incubate the cells for 30 min at RT.
6. Wash the cells with 1 ml of 1× BD Perm/Wash buffer and spin down (600 × *g* for 5 min).
7. Resuspend the cells in 100 μl of BD Cytoperm Permeabilization Buffer Plus per sample.
8. Incubate the cells on ice for 10 min.
9. Wash the cells with 1 ml of 1× BD Perm/Wash buffer and spin down (600 × *g* for 5 min).
10. Resuspend the cells in 100 μl of BD Cytofix/Cytoperm Buffer per sample, and incubate the cells for 5 min at RT.
11. Wash the cells with 1 ml of 1× BD Perm/Wash buffer, spin down (600 × *g* for 5 min), and thoroughly remove the supernatant.
12. Resuspend the cells in 100 μl of DNase solution (300 μg/ml in DPBS), and incubate the cells for 1 h at 37 °C.
13. Wash the cells with 1 ml 1× BD Perm/Wash buffer and spin down (600 × *g* for 5 min), and thoroughly remove the supernatant.
14. Resuspend the cells in 20 μl of BD Perm/Wash buffer containing the APC-conjugated anti-BrdU antibody (1:50). Incubate the cells for 20 min at RT.
15. Wash the cells with 1 ml of 1× BD Perm/Wash buffer and spin down (600 × *g* for 5 min).
16. Resuspend the cells in 20 μl of 7-AAD solution for cell cycle analysis.
17. Wash the cells with 1 ml of 1× BD Perm/Wash buffer and spin down (600 × *g* for 5 min).
18. Resuspend the cells in 200 μl of FACS buffer, and run on a flow cytometer.
19. For the examination of in vitro BrdU incorporation, $2 \times 10^5$ naïve T cells are stimulated with or without plate-bound anti-CD3 plus anti-CD28 (96-well plate) for 22 h. Add 10 μM BrdU (final concentration) into the media for additional 2 h.
20. Harvest the cells and spin down (600 × *g* for 5 min). Follow the steps from 4 to 18 to stain BrdU incorporation of T cells (Fig. 3).

### 3.5 Analysis of Glycolysis and OXPHOS Using a Seahorse Analyzer

1. Naïve $CD4^+$ T cells ($1 \times 10^6$ cells/well in a 48-well plate) are stimulated with or without plate-bound anti-CD3 plus anti-CD28 (10 μg/ml) for 24 h.
2. Add 1 ml of XP calibrant to Assay plate of cartridge and incubate the plate overnight at 37 °C in a dry incubator.

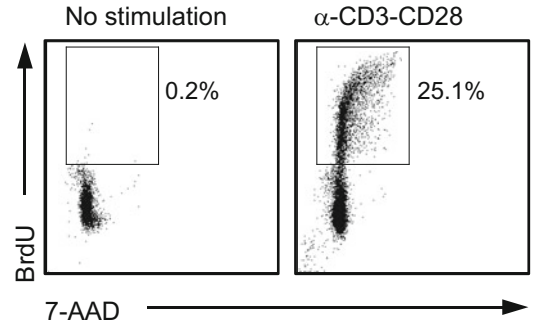


**Fig. 3** BrdU incorporation in naïve and activated T cells. Naïve $CD4^+$ T cells ($2 \times 10^5$/well in a 96-well plate) were stimulated with or without plate-bound anti-CD3 plus anti-CD28 (10 μg/ml) for 22 h. BrdU was added into the media (final concentration 10 μM) for additional 2 h, followed by BrdU staining and flow cytometry of BrdU incorporation and 7-AAD in naïve and activated $CD4^+$ T cells

3. Warm up 50 ml of unbuffered media (Seahorse media) supplemented with 10 mM glucose, 1 mM pyruvate, and 2 mM L-glutamine at 37 °C before use.
4. Adjust pH of Seahorse media to 7.4 (*see* **Note 7**).
5. Precoat cell culture plate (Seahorse) with 50 μl of Cell-Tak solution (22.6 mg/ml) per well for 30 min at RT.
6. Harvest the cultured cells and wash the cells with 5 ml of HBSS supplemented with 2% FBS once. After thoroughly removing the supernatant, resuspend the cells in 200 μl of Seahorse media and count cell number. Adjust cell concentration to 0.5–1 million cells per 100 μl.
7. Remove Cell-Tak solution and wash the wells with 500 μl of DPBS twice.
8. Add 100 μl of cell suspension at desired concentration to each well.
9. Spin the plate for 30 s at 600 × *g* and incubate for 20 min at 37 °C.
10. Add 500 μl of Seahorse media to each well and incubate for additional 30 min at 37 °C.
11. Prepare drugs to test OXPHOS in the mitochondria. Final concentration of drugs: 1 μM of Oligomycin, 2 μM of FCCP, and 0.5 μM of Rotenone (*see* **Note 8**).
12. Add diluted compounds to wells in the cartridge.
13. Set up program and run the plate for glycolysis and OXPHOS in XF24 Extracellular Flux Analyzer 3 according to the manufacturer's manual (Fig. 4).

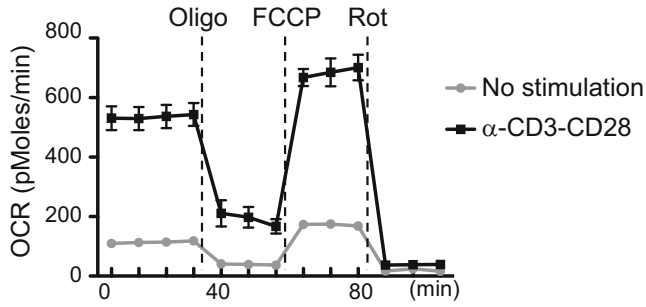


**Fig. 4** OCR in naïve and activated $CD4^+$ T cells. Naïve $CD4^+$ T cells were stimulated with or without plate-bound anti-CD3 plus anti-CD28 (10 μg/ml) for 24 h. $5 \times 10^5$ naïve or activated $CD4^+$ T cells were used for the Seahorse assay. OCR in naïve or activated $CD4^+$ T cells under basal condition or in response to the indicated mitochondrial inhibitors (Oligo, Oligomycin; FCCP, carbonyl cyanide p-trifluoromethoxyphenylhydrazone; and Rot, Rotenone)

### *3.6 Fatty Acid β-Oxidation Flux*

1. Naïve $CD4^+$ T cells ($1 \times 10^6$ cells/well in a 48-well plate) are stimulated with or without plate-bound anti-CD3 plus anti-CD28 (10 μg/ml) for 24 h.
2. Harvest the cells and spin down (600 × *g* for 5 min). Resuspend $1 \times 10^6$ resting and activated cells in 0.5 ml of T cell media supplemented with IL-7 (5 ng/ml) and IL-2 (100 U/ml). In parallel, $1 \times 10^6$ resting and activated cells are treated with 100 μM Etomoxir, an inhibitor of carnitine palmitoyltransferase 1 (CPT1), for 1 h.
3. Add 3 μCi [9,10-$^3$H]-palmitic acid complexed to 5% BSA (lipids free) into the media for 2 h.
4. Transfer each sample including cells and media to a 1.5 ml Eppendorf tube containing 50 μl of 5 N HCl.
5. Place each Eppendorf tube to a scintillation vial (20 ml) containing 0.5 ml water and cap the vials for 24 h at RT (*see* **Note 9**).
6. Remove the Eppendorf tubes from the vials and add 10 ml of scintillation liquid to dissolve $^3H_2O$ for quantification by beta-scintillation counting (*see* **Note 10**).

## 4 Notes

1. Grinding tissues gently can reduce mechanical damage to lymphocytes and maintain their viability. It is important to keep tissues and cells on ice during the sample preparation process.
2. The solution will turn slightly pink when lysis of red blood cells is complete. Over-incubation of ACK lysing buffer can damage lymphocytes.
3. The 96-well U-bottom plate is used for cell staining. It will promote staining quality by thoroughly removing the

supernatant from cell pellets before the addition of the antibody cocktail.

4. Direct addition of FACS buffer into Phosflow™ Perm buffer III can improve recovery of permeabilized cells from the spin down in the next step.
5. It is important to immediately fix freshly isolated cells to reduce alterations of mTOR signaling during sample preparation. We usually stain fixed cells with the antibody cocktail including antibodies against cell surface markers and phosphorylated proteins.
6. Thymocytes are used as control for BrdU incorporation in vivo. Among distinct thymocyte subsets, immature single positive cells (ISP cells; $CD4^{-}CD8^{+}TCR\beta^{+}$) exhibit robust BrdU incorporation compared with double positive cells (DP cells; $CD4^{+}CD8^{+}$) that show low BrdU incorporation.
7. In the Seahorse assay, glycolysis is determined by the measurement of extracellular acidification rate in the media. Non-buffered Seahorse media is sensitive to changes in pH. Thus, it is important to check and adjust pH value of Seahorse media to 7.4 before each assay.
8. Optimization of drug doses is required for different types of lymphocytes.
9. Since $^{3}H_2O$ separates from non-metabolized [9, 10-$^{3}$H]-palmitic acid by evaporation diffusion, it is important to seal the vials properly.
10. Transfer of $^{3}H_2O$ water to smaller size of vials with less requirement of scintillation liquid can enhance the quantification by liquid scintillation counter.

## Acknowledgments

The authors acknowledge H. Zeng and Y. Wang for scientific inputs and editing. This work was supported by NIH AI105887, AI101407, CA176624 and NS064599, and American Asthma Foundation.

### References

1. Takada K, Jameson SC (2009) Naive T cell homeostasis: from awareness of space to a sense of place. Nat Rev Immunol 9 (12):823–832. doi:10.1038/nri2657
2. Yang K, Chi H (2012) mTOR and metabolic pathways in T cell quiescence and functional activation. Semin Immunol 24(6):421–428. doi:10.1016/j.smim.2012.12.004
3. Hamilton SE, Jameson SC (2012) CD8 T cell quiescence revisited. Trends Immunol 33 (5):224–230. doi:10.1016/j.it.2012.01.007
4. MacIver NJ, Michalek RD, Rathmell JC (2013) Metabolic regulation of T lymphocytes. Annu Rev Immunol 31:259–283. doi:10.1146/annurev-immunol-032712-095956

5. Sena LA, Li S, Jairaman A, Prakriya M, Ezponda T, Hildeman DA, Wang CR, Schumacker PT, Licht JD, Perlman H, Bryce PJ, Chandel NS (2013) Mitochondria are required for antigen-specific T cell activation through reactive oxygen species signaling. Immunity 38(2):225–236. doi:10.1016/j.immuni.2012.10.020
6. Buck MD, O'Sullivan D, Pearce EL (2015) T cell metabolism drives immunity. J Exp Med 212(9):1345–1360. doi:10.1084/jem.20151159
7. Yang K, Neale G, Green DR, He W, Chi H (2011) The tumor suppressor Tsc1 enforces quiescence of naive T cells to promote immune homeostasis and function. Nat Immunol 12(9):888–897. doi:10.1038/ni.2068
8. Wu Q, Liu Y, Chen C, Ikenoue T, Qiao Y, Li CS, Li W, Guan KL, Liu Y, Zheng P (2011) The tuberous sclerosis complex-mammalian target of rapamycin pathway maintains the quiescence and survival of naive T cells. J Immunol 187(3):1106–1112. doi:10.4049/jimmunol.1003968
9. Yang K, Shrestha S, Zeng H, Karmaus PW, Neale G, Vogel P, Guertin DA, Lamb RF, Chi H (2013) T cell exit from quiescence and differentiation into Th2 cells depend on raptor-mTORC1-mediated metabolic reprogramming. Immunity 39(6):1043–1056. doi:10.1016/j.immuni.2013.09.015
10. Kidani Y, Elsaesser H, Hock MB, Vergnes L, Williams KJ, Argus JP, Marbois BN, Komisopoulou E, Wilson EB, Osborne TF, Graeber TG, Reue K, Brooks DG, Bensinger SJ (2013) Sterol regulatory element-binding proteins are essential for the metabolic programming of effector T cells and adaptive immunity. Nat Immunol 14(5):489–499. doi:10.1038/ni.2570
11. Chi H (2012) Regulation and function of mTOR signalling in T cell fate decisions. Nat Rev Immunol 12(5):325–338. doi:10.1038/nri3198
12. Zeng H, Yang K, Cloer C, Neale G, Vogel P, Chi H (2013) mTORC1 couples immune signals and metabolic programming to establish T (reg)-cell function. Nature 499(7459):485–490. doi:10.1038/nature12297
13. Delgoffe GM, Pollizzi KN, Waickman AT, Heikamp E, Meyers DJ, Horton MR, Xiao B, Worley PF, Powell JD (2011) The kinase mTOR regulates the differentiation of helper T cells through the selective activation of signaling by mTORC1 and mTORC2. Nat Immunol 12(4):295–303. doi:10.1038/ni.2005
14. Lee K, Nam KT, Cho SH, Gudapati P, Hwang Y, Park DS, Potter R, Chen J, Volanakis E, Boothby M (2012) Vital roles of mTOR complex 2 in notch-driven thymocyte differentiation and leukemia. J Exp Med 209(4):713–728. doi:10.1084/jem.20111470
15. Zeng H, Cohen S, Guy C, Shrestha S, Neale G, Brown SA, Cloer C, Kishton RJ, Gao X, Youngblood B, Do M, Li MO, Locasale JW, Rathmell JC, Chi H (2016) mTORC1 and mTORC2 kinase signaling and glucose metabolism drive follicular helper T cell differentiation. Immunity 45(3):540–554. doi:10.1016/j.immuni.2016.08.017
16. Kurebayashi Y, Nagai S, Ikejiri A, Ohtani M, Ichiyama K, Baba Y, Yamada T, Egami S, Hoshii T, Hirao A, Matsuda S, Koyasu S (2012) PI3K-Akt-mTORC1-S6K1/2 axis controls Th17 differentiation by regulating Gfi1 expression and nuclear translocation of RORgamma. Cell Rep 1(4):360–373. doi:10.1016/j.celrep.2012.02.007

# Chapter 13

# Retroviral Transduction of Quiescent Murine Hematopoietic Stem Cells

**Chun Shik Park and H. Daniel Lacorazza**

## Abstract

Hematopoietic stem cells (HSCs) represent an important target cell population in bone marrow transplantation, cell and gene therapy applications, and the development of leukemia models for research. Because the hematopoietic progeny carries the genetic information of HSCs and replenishes the blood and immune system, corrective gene transfer into HSCs provides an ideal therapeutic approach for many monogenic hematological diseases and a useful tool for studies of HSC function and blood formation in normal and malignant hematopoiesis. However, the efficiency of gene transfer into HSCs has been limited by several features of viral vectors, viral titer, methods of viral transduction, and the property of stem cell quiescence. In this chapter, we describe the production of retrovirus using murine stem cell virus (MSCV)-based retroviral vectors and purification and transduction of murine HSCs.

**Key words** HSC, Retrovirus, Transduction, MSCV vector, RetroNectin

## 1 Introduction

Hematopoietic stem cells (HSCs) have the unique capacity to restore the entire hematopoietic system because of their property of self-renewal and pluripotency; therefore, HSCs represent an important target for the treatment of various blood and immune disorders [1, 2]. The first challenge faced toward transducing stem cells was the selection of viral vectors. Moloney murine leukemia virus (MoMLV)-derived retroviral vectors were used initially as vehicles for gene transfer into hematopoietic cells [3]. However, gene inactivation by transcriptional silencing, frequent downregulation of target genes during HSC differentiation, and the low transduction efficiency of HSCs with the MoMLV retrovirus has been a major obstacle [4–6]. To improve gene transfer into HSCs, the MSCV-based retroviral vector was developed and optimized for the expression of a gene-of-interest driven by the long-terminal repeat (LTR) in both murine and human hematopoietic and embryonic stem cells [7–11]. Co-expression of reporter genes

H. Daniel Lacorazza (ed.), *Cellular Quiescence: Methods and Protocols*, Methods in Molecular Biology, vol. 1686,
DOI 10.1007/978-1-4939-7371-2_13, 

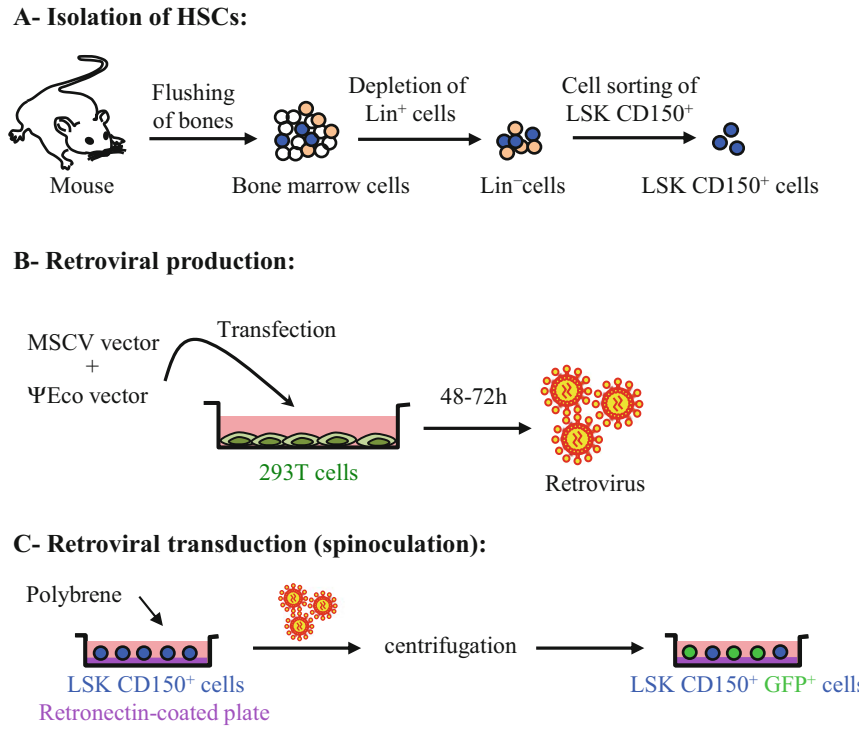


**Fig. 1** Diagram depicting the procedure of retroviral transduction of murine HSCs. (**a**) Bone marrow cells isolated from femur and tibias and lineage-negative ($Lin^-$) cells were prepared by depletion of mature blood lineages using a hematopoietic progenitor (stem) cell kit. $Lin^-$ cells are stained with antibodies against HSC markers (Sca-1, c-Kit, and CD150) for the purification of HSCs by cell sorting. (**b**) Retroviruses are produced by co-transfection of 293 T cells with a retroviral vector and ecotropic viral envelope. (**c**) HSCs are transduced with retrovirus on RetroNectin-coated plates in the presence of polybrene

(e.g., fluorescent markers) along with the gene-of-interest greatly facilitated monitoring of donor-derived cells after transplantation of transduced HSCs [12, 13]. Therefore, the enhanced green fluorescent protein (EGFP) was cloned downstream of an internal-ribosomal entry site (IRES) in bicistronic MSCV-vectors to allow co-expression of the gene-of-interest and EGFP.

A basic protocol of lentiviral and retroviral transduction of HSCs involves the isolation of bone marrow enriched in HSCs, packaging of retroviral particles, and viral transduction by centrifugation, also known as spinoculation (Fig. 1). In this chapter, we describe the use of purified quiescent HSCs for retroviral transduction as an alternative to a widely used approach of a heterogeneous mixture of bone marrow cells collected after the treatment of donor mice with 5-fluorouracil. Although 5-fluorouracil administration induces activation of HSCs to augment retroviral transduction, the isolation of HSCs from this mixture is prevented by changes induced in cell surface markers [14, 15], and this treatment induces myeloid-biased HSCs [16]. Retroviral transduction is achieved by

centrifuging HSCs, viral particles, and polybrene on RetroNectin-coated plates (Fig. 1). RetroNectin (CH-296) is a recombinant fibronectin fragment containing domains for binding target cells (VLA ligands in the CS-1 sequence and C-domain) and viral particles (heparin domain) that was developed to increase transduction efficiency by enabling the colocalization of target cells and virus [17–19]. Viral particles can be preloaded on RetroNectin-coated plates by low-speed centrifugation to achieve active adsorption [20–22]. In addition to RetroNectin, a cationic polymer hexadimethrine bromide (Polybrene) is used to augment transduction efficiency by neutralizing electrostatic repulsions between negatively charged cells and the retroviral envelope [23–25].

## 2 Materials

### 2.1 Production of Retrovirus

1. 293T cells (ATCC CRL-3216).
2. 6-well tissue culture-treated plates.
3. Cell medium: Dulbecco's modified Eagle's medium (DMEM), supplemented with 10% fetal bovine serum (FBS), 2 mM L-glutamine, 100 units/ml penicillin and 100 μg/ml streptomycin.
4. MSCV-derived vector (e.g., MSCV/IRES-EGFP).
5. Expression vector of viral envelope (ψ-ecotropic for murine cells).
6. Calcium phosphate transfection kit: 2 M $CaCl_2$, 2× HEPES-Buffered Saline (2× HBS), and nuclease-free water.
7. Individually wrapped 5 ml polystyrene tubes.
8. 3 ml syringes.
9. Sterile syringe filters, 0.45 μm pore size.

### 2.2 Isolation of Bone Marrow Cells

1. Euthanize adult C57BL/6 mice following the appropriate institutional guidelines.
2. Sterile cell strainers (40 μm), individually wrapped.
3. Straight serrated forceps.
4. Fine point dissection scissors.
5. Tissue wipes.
6. 50 ml conical tubes.
7. Disposable 1 cc Syringe 28G × ½.
8. 3% FBS-PBS: PBS containing 3% fetal bovine serum.

### 2.3 Purification of HSCs

1. Mouse hematopoietic progenitor (stem) cell enrichment kit for lineage depletion. The kit contains a cocktail of biotinylated antibodies against blood lineages (anti-CD3ε, anti-CD45R/

B220, anti-Ter-119, anti-CD11, and anti-Gr-1) and streptavidin beads.

2. PBS supplemented with 3% FBS (3% FBS-PBS).
3. Antibodies for flow cytometric analysis: APC-anti-CD150, PE-anti-Sca-1, and PE-Cy7-anti-c-kit.

### 2.4 Retroviral Transduction of HSCs

1. 96-well flat-bottom, high protein-binding, polystyrene plate.
2. 96-well U bottom, nontreated surfaces, polystyrene plate.
3. RetroNectin: prepare a RetroNectin solution (25 μg/ml) by diluting concentrated stock with sterile PBS (*see* **Note 1**).
4. 2% bovine serum albumin (BSA, Fraction V) in PBS.
5. Polybrene (Hexadimethrine Bromide) solution: suspend 8 mg polybrene into 1 ml water for a 1000× stock solution (8 mg/ml). Filter solution through a 0.2 μm syringe filter.
6. HSC culture medium: X-VIVO 15 serum-free medium with gentamicin supplemented with 100 ng/ml murine stem cell factor (SCF), 6 ng/ml murine interleukin-3 (IL3), and 10 ng/ml human interleukin-6 (IL6) (*see* **Note 2**).

## 3 Methods

### 3.1 Production of Retrovirus

1. Seed $1 \times 10^6$ 293 T cells into a 6-well tissue culture plate with a 2 ml cell culture medium per well and incubate for 24 h (*see* **Note 3**).
2. Calcium phosphate transfection. Prepare DNA and 2× HBS solutions in separate sterile tubes. In tube #1, mix DNA constructs (5 μg of MSCV vector +5 μg of ΨEco envelope vector) and 37 μl of $CaCl_2$ in 300 μl of water (final volume); in tube #2, 300 μl of 2× HBS (*see* **Note 4**).
3. Add the $CaCl_2$-DNA solution (Tube #1) dropwise to the 2× HBS solution (Tube #2) while making bubbles using a Pasteur pipette. Incubate the solution at room temperature for 30 min for the development of calcium phosphate crystals (*see* **Note 5**).
4. Gently vortex the solution containing the DNA-calcium crystals (solution should appear opalescent) and add the solution dropwise throughout each plate containing the 293 T cells. Move plates gently side to side to distribute the precipitate evenly over the cells (*see* **Note 6**).
5. Return the plates to a 37 °C $CO_2$ incubator and incubate for 24 h.

6. Replace the medium with the pre-warmed cell culture medium (2 ml per well) and continue incubation of packaging cells for an additional 48 h (*see* **Note 7**).
7. Take medium containing retrovirus from packaging cells using a 3 ml syringe without a needle. Carefully place a 0.45 μm syringe filter (Acrodisc) on a syringe tip and filter the medium with viruses to remove packaging cells in suspension. The filtered retroviral supernatant can be used immediately or stored at −80 °C. Add 2 ml of the fresh pre-warmed medium (10% FBS in DMEM) to the 293 T cells and incubate for 24 h for additional viral production. This second retroviral supernatant can also be used or stored at −80 °C (*see* **Note 8**).

### 3.2 Isolation of Bone Marrow Cells

1. Euthanize mice (C57BL/6) following recommendations of the institution's animal care committee-approved protocol.
2. Clean the animal surface with 70% ethanol and make an incision in each hind leg using fine point dissection scissors. Remove skin by pulling downward with straight serrated forceps and exposing the muscles.
3. Cut off the hip joint using the fine point dissection scissors, ensuring that the femur head remains intact. Transfer bones in sterile PBS to the laboratory.
4. To separate the femur and tibia, bend the femur and tibia at the knee joint, and then hyperextend the bones in the direction exactly opposite to that of the natural bending motion.
5. Push the tibia through the muscle.
6. Remove the muscle from tibia and femur using dissecting scissors and tissue wipes.
7. Hold the femur with a pair of forceps and snap the tops of both ends with scissors to allow insertion of the needle.
8. Fill the syringe with 3% FBS-PBS and insert the needle into the femur. Flush bone marrow out of the bone onto a 0.45 μm strainer on the top of a 50 ml tube. Wash bone until it is clear with 3% FBS-PBS.
9. Proceed in the same way with the tibiae.
10. Once both the femur and tibia are flushed, remove the plunger from the syringe and use it to dissociate any cell clump remaining on the filter by gently pressing against the filter. Wash the cell strainer with 3% FBS-PBS.
11. Centrifuge the bone marrow cells in the 50 ml tube at 450 × *g* for 5 min at 4 °C.
12. Resuspend the cell pellet in 5 ml of 3% FBS-PBS.
13. Count the viable mononuclear cells using a hemocytometer.

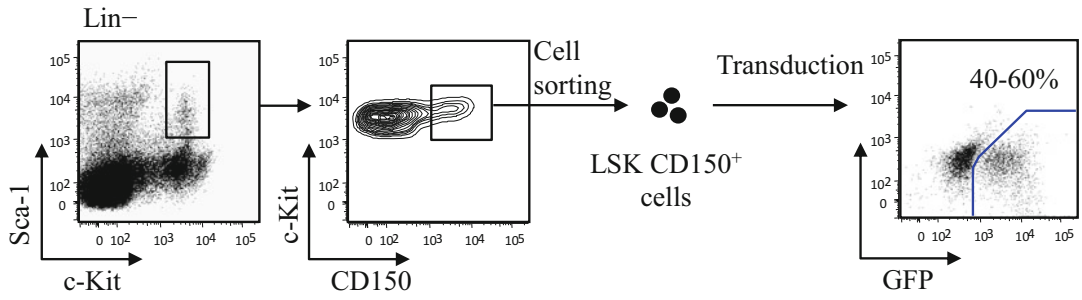


**Fig. 2** Flow cytometric profiles show purification of HSCs (LSK CD150$^+$) by cell sorting and expression of GFP after retroviral transduction

### *3.3 Purification of Murine HSCs*

1. Lineage-negative (Lin$^-$) cells can be prepared from whole bone marrow using a commercially available lineage depletion kit that has been developed for the efficient depletion of mature hematopoietic cells and their committed precursors (T cells, B cells, monocytes/macrophages, granulocytes, erythrocytes).
2. Stain the Lin$^-$ cells with directly conjugated antibodies against the stem cell markers: APC-anti-CD150, PE-anti-Sca-1, and PE-Cy7-anti-c-Kit for identification of Lin$^-$ Sca-1$^+$ c-Kit$^+$ CD150$^+$ (LSK CD150$^+$). Incubate the cells with antibodies for 20 min on ice.
3. Wash cells with 3% FBS-PBS and resuspend the cells in 3% FBS-PBS.
4. Purify LSK CD150$^+$ cells by fluorescence-activated cell sorting (Fig. 2).
5. Culture purified LSK CD150$^+$ cells for 24 h or overnight in 96-well U bottom polystyrene plates, with nontreated surfaces, in 200 μl of HSC culture medium containing cytokines (20,000 cells per well).

### *3.4 Preparation of RetroNectin-Coated Plates*

1. Prepare a RetroNectin solution (25 μg/ml) by resuspending the lyophilized powder with sterile PBS.
2. Dispense 100 μl of sterile RetroNectin (25 μg/ml) solution into 96-well flat-bottom, high binding, polystyrene plates, and allow coating for 2 h at room temperature or overnight at 4 °C.
3. Remove the RetroNectin solution and block the plate with 200 μl of 2% BSA (Fraction V) in PBS.
4. Allow the plate to stand at room temperature for 30 min.
5. Remove the BSA solution and wash the plate once with a 200 μl of PBS. After removing the wash solution, the plate is ready for use.
6. The RetroNectin-coated plate can be sealed with Parafilm and stored at 4 °C for up to 1 week.

### 3.5 Transduction of HSCs

1. Add the retrovirus supernatant (300 μl per well) into RetroNectin-coated plates and centrifuge at 2000 × *g* for 60 min at room temperature for preadsorption of the virus. Carefully remove the supernatant.
2. Transfer cytokine-stimulated LSK CD150$^+$ cells (*see* **step 5** in Subheading 3.3) to virus-bound RetroNectin-coated plates and centrifuge at 450 × *g* for 10 min at room temperature to promote settling of LSK CD150$^+$ cells on RetroNectin. For the centrifuge settings, use slow acceleration and no deceleration to avoid cell detachment.
3. Remove the medium after centrifugation and immediately add the filtered retroviral supernatant supplemented with polybrene (8 μg/ml) (300 μl per well) onto the LSK CD150$^+$ cells bound to the RetroNectin-coated plates. Centrifuge at 450 × *g* for 60 min at room temperature (spinoculation). Transfer the plates to the $CO_2$ incubator and incubate for 2 h in the $CO_2$ incubator.
4. Centrifuge plates at 450 × *g* for 10 min at room temperature. Carefully remove the viral supernatants from the plates and add 200 μl of fresh HSC culture medium (X-VIVO 15 supplemented with SCF/IL-3/IL-6) to promote cell proliferation. Incubate plates for 24 h or overnight.
5. Centrifuge plates at 450 × *g* for 10 min at room temperature and remove the medium. Immediately add the viral supernatant supplemented with polybrene (8 μg/ml) onto the cell-bound plate. Centrifuge at 450 × *g* for 60 min at room temperature for a second spinoculation. Transfer the plates to the $CO_2$ incubator and incubate for 2 h.
6. Centrifuge the plates at 450 × *g* for 10 min at room temperature and remove the medium. Immediately add 200 μl of fresh HSC culture medium and resuspend the cells by pipetting up and down.
7. Transfer the cells into 96-well U bottom polystyrene plates with nontreated surfaces.
8. Incubate the cells in the $CO_2$ incubator for 1–2 days. Check the percentage of GFP-positive cells using a flow cytometer (Fig. 2). The typical yield for transduction is 40–60% of GFP-positive HSCs.

## 4 Notes

1. Prepare RetroNectin in aseptic conditions and sterile PBS. Do not filter the RetroNectin solution to avoid loss of RetroNectin fragments.

2. Preparation of cytokine stock: For the murine SCF stock (100 ng/μl; 1000×), add 100 μl of water to 10 μg of murine SCF. For the murine IL3 stock (6 ng/μl; 1000×), add 1.66 ml of water to 10 μg of murine IL3. For the human IL6 stock (10 ng/μl; 1000×), add 0.5 ml of 10 mM acetic acid to 5 μg of human IL6. IL6 cross reacts between species. Therefore, human IL6 can be used for murine cultures because of its lower cost.
3. When seeding 293 T cells into 6-well tissue-treated plates, the cells should be distributed evenly to achieve a high transfection efficiency.
4. Make sure that the 293 T cells are 50–70% confluent. Thaw the components of the calcium phosphate transfection kit system and let them reach room temperature. Mix each component thoroughly by vortexing.
5. The solution should appear slightly opaque, particularly when the tube is placed in front of a dark background, after addition of DNA because of the formation of a fine calcium phosphate-DNA precipitate.
6. Addition of the DNA-calcium precipitate throughout the well allows an even distribution of the precipitate and avoids localized acidification of cells. Avoid swirling the plate because crystals will concentrate in the center.
7. Handle the plate gently because the 293 T cell monolayer tends to detach. Some protocols call for precoating of plate with poly-lysine before seeding the 293 T cells.
8. Medium can turn "yellow" after 48 h of viral production. To yield high-titer virus, more than 90% of the cells should be positive for GFP when examined under a fluorescence microscope.

## Acknowledgments

The authors thank members of the laboratory for helpful discussions. Support for this work was provided in part by the Cancer Prevention Research Institute of Texas to H.D.L. (RP140179) and the National Cancer Institute to H.D.L. (RO1 CA207086-01A1).

### References

1. Weissman IL (2000) Translating stem and progenitor cell biology to the clinic: barriers and opportunities. Science 287(5457):1442–1446
2. Karlsson S (1991) Treatment of genetic defects in hematopoietic cell function by gene transfer. Blood 78(10):2481–2492
3. Chu P, Lutzko C, Stewart AK, Dube ID (1998) Retrovirus-mediated gene transfer into human hematopoietic stem cells. J Mol Med (Berl) 76(3–4):184–192
4. Kohn DB, Hershfield MS, Carbonaro D, Shigeoka A, Brooks J, Smogorzewska EM, Barsky

LW, Chan R, Burotto F, Annett G, Nolta JA, Crooks G, Kapoor N, Elder M, Wara D, Bowen T, Madsen E, Snyder FF, Bastian J, Muul L, Blaese RM, Weinberg K, Parkman R (1998) T lymphocytes with a normal ADA gene accumulate after transplantation of transduced autologous umbilical cord blood CD34+ cells in ADA-deficient SCID neonates. Nat Med 4 (7):775–780

5. Miller DG, Adam MA, Miller AD (1990) Gene transfer by retrovirus vectors occurs only in cells that are actively replicating at the time of infection. Mol Cell Biol 10(8):4239–4242
6. Orlic D, Girard LJ, Jordan CT, Anderson SM, Cline AP, Bodine DM (1996) The level of mRNA encoding the amphotropic retrovirus receptor in mouse and human hematopoietic stem cells is low and correlates with the efficiency of retrovirus transduction. Proc Natl Acad Sci U S A 93(20):11097–11102
7. Miller AD, Rosman GJ (1989) Improved retroviral vectors for gene transfer and expression. Biotechniques 7(9):980–982. 984-986, 989-990
8. Grez M, Akgun E, Hilberg F, Ostertag W (1990) Embryonic stem cell virus, a recombinant murine retrovirus with expression in embryonic stem cells. Proc Natl Acad Sci U S A 87(23):9202–9206
9. Laker C, Meyer J, Schopen A, Friel J, Heberlein C, Ostertag W, Stocking C (1998) Host cis-mediated extinction of a retrovirus permissive for expression in embryonal stem cells during differentiation. J Virol 72(1):339–348
10. Hawley RG, Lieu FH, Fong AZ, Hawley TS (1994) Versatile retroviral vectors for potential use in gene therapy. Gene Ther 1(2):136–138
11. Hawley RG, Hawley TS, Fong AZ, Quinto C, Collins M, Leonard JP, Goldman SJ (1996) Thrombopoietic potential and serial repopulating ability of murine hematopoietic stem cells constitutively expressing interleukin 11. Proc Natl Acad Sci U S A 93(19):10297–10302
12. Cherry SR, Biniszkiewicz D, van Parijs L, Baltimore D, Jaenisch R (2000) Retroviral expression in embryonic stem cells and hematopoietic stem cells. Mol Cell Biol 20(20):7419–7426
13. Kume A, Xu R, Ueda Y, Urabe M, Ozawa K (2000) Long-term tracking of murine hematopoietic cells transduced with a bicistronic retrovirus containing CD24 and EGFP genes. Gene Ther 7(14):1193–1199. doi:10.1038/sj.gt.3301225
14. Sato T, Laver JH, Ogawa M (1999) Reversible expression of CD34 by murine hematopoietic stem cells. Blood 94(8):2548–2554
15. Randall TD, Weissman IL (1997) Phenotypic and functional changes induced at the clonal level in hematopoietic stem cells after 5-fluorouracil treatment. Blood 89 (10):3596–3606
16. Busch K, Klapproth K, Barile M, Flossdorf M, Holland-Letz T, Schlenner SM, Reth M, Hofer T, Rodewald HR (2015) Fundamental properties of unperturbed haematopoiesis from stem cells in vivo. Nature 518(7540):542–546. doi:10.1038/nature14242
17. Hanenberg H, Xiao XL, Dilloo D, Hashino K, Kato I, Williams DA (1996) Colocalization of retrovirus and target cells on specific fibronectin fragments increases genetic transduction of mammalian cells. Nat Med 2(8):876–882
18. Chono H, Yoshioka H, Ueno M, Kato I (2001) Removal of inhibitory substances with recombinant fibronectin-CH-296 plates enhances the retroviral transduction efficiency of CD34 (+)CD38(−) bone marrow cells. J Biochem 130(3):331–334
19. Hanenberg H, Hashino K, Konishi H, Hock RA, Kato I, Williams DA (1997) Optimization of fibronectin-assisted retroviral gene transfer into human CD34+ hematopoietic cells. Hum Gene Ther 8(18):2193–2206. doi:10.1089/hum.1997.8.18-2193
20. Tonks A, Tonks AJ, Pearn L, Mohamad Z, Burnett AK, Darley RL (2005) Optimized retroviral transduction protocol which preserves the primitive subpopulation of human hematopoietic cells. Biotechnol Prog 21(3):953–958. doi:10.1021/bp0500314
21. Zhou P, Lee J, Moore P, Brasky KM (2001) High-efficiency gene transfer into rhesus macaque primary T lymphocytes by combining 32 degrees C centrifugation and CH-296-coated plates: effect of gene transfer protocol on T cell homing receptor expression. Hum Gene Ther 12(15):1843–1855. doi:10.1089/104303401753153901
22. Quintas-Cardama A, Yeh RK, Hollyman D, Stefanski J, Taylor C, Nikhamin Y, Imperato G, Sadelain M, Riviere I, Brentjens RJ (2007) Multifactorial optimization of gammaretroviral gene transfer into human T lymphocytes for clinical application. Hum Gene Ther 18 (12):1253–1260. doi:10.1089/hum.2007.088

23. Jensen TW, Chen Y, Miller WM (2003) Small increases in pH enhance retroviral vector transduction efficiency of NIH-3T3 cells. Biotechnol Prog 19(1):216–223. doi:10.1021/bp025604g
24. Swaney WP, Sorgi FL, Bahnson AB, Barranger JA (1997) The effect of cationic liposome pretreatment and centrifugation on retrovirus-mediated gene transfer. Gene Ther 4 (12):1379–1386. doi:10.1038/sj.gt.3300529
25. Davis HE, Morgan JR, Yarmush ML (2002) Polybrene increases retrovirus gene transfer efficiency by enhancing receptor-independent virus adsorption on target cell membranes. Biophys Chem 97(2–3):159–172

# Chapter 14

# Analysis of Murine Hematopoietic Stem Cell Proliferation During Inflammation

**Emilie Jalbert and Eric M. Pietras**

## Abstract

Normally, quiescent hematopoietic stem cells (HSC) rapidly enter the cell cycle following exposure to inflammatory stimuli. The analysis of HSC cell cycle activity in murine bone marrow during inflammation is often complicated by the relative rarity of HSCs and shifts in Sca-1, a key cell surface marker used to identify HSCs. Here, we report a method to analyze HSC proliferation and cell cycle distribution under inflammatory conditions. Our approach uses EdU incorporation and Ki67 staining coupled with DNA content quantification by DAPI. We also incorporate the surface marker ESAM to help minimize the potential for contaminating events that may confound analysis in the HSC compartment.

**Key words** Hematopoietic stem cell, Cell cycle, Inflammation, Bone marrow, Flow cytometry

## 1 Introduction

Hematopoietic stem cells (HSC) are a rare population of self-renewing bone marrow (BM) cells that give rise to all lineages of the blood system [1], including erythrocytes, platelets, lymphoid, and myeloid cell types. While actively cycling during fetal life as a means of building the hematopoietic system, in adult vertebrates, HSCs are maintained in a largely quiescent, or dormant, state via a complex array of cell-intrinsic regulators and cell-extrinsic signals from the bone marrow niche [2, 3].

Due to the degree of conservation between human and murine hematopoiesis and the availability of genetic models, the mouse has been a powerful tool in the study of HSC biology [4]. Numerous schemes are used to identify phenotypic HSCs in murine bone marrow, with the SLAM code and Flk2 ($Lin^-$ $cKit^+$ $Sca\text{-}1^+$ $Flk2^-$ $CD48^-$ $CD150^+$) as a commonly used standard for isolating HSCs to a functional purity of about 1:2 cells [5]. Cells within this gate exhibit low cell cycle activity [6]. Moreover, markers such as CD34 have been used in conjunction with the SLAM code to identify a highly quiescent subset of HSCs [6, 7]. Indeed, tracing

H. Daniel Lacorazza (ed.), *Cellular Quiescence: Methods and Protocols*, Methods in Molecular Biology, vol. 1686,
DOI 10.1007/978-1-4939-7371-2_14, 

experiments in mice using long-term pulse-chase experiments employing BrdU or H2B-GFP transgenes indicate that in mice most HSCs cycle only once every 100 days [6, 8, 9]. In contrast, non-self-renewing populations downstream of the HSC, such as multipotent progenitors (MPP) and lineage-committed progenitors such as granulocyte macrophage progenitors (GMP), have a more active cell cycle profile and contribute to blood formation, whereas HSCs appear to function largely, though not exclusively, as a homeostatic reserve that may not actively participate in day-to-day maintenance of the hematopoietic system [10–13].

Notably, in response to physiological stressors, HSCs can rapidly exit quiescence and enter the cell cycle in order to replenish lost blood cells [2, 6], particularly in response to significant regenerative challenges such as transplantation. Notably, many of these stressors are associated with the production of an array of pro-inflammatory cytokines including interleukin (IL)-1, IL-6, TNF and type I and II interferons (IFNs) [14–16], some of which have been demonstrated to activate proliferative responses in HSCs based on BrdU incorporation and Ki67/DAPI staining [17–20]. Some work suggests that specific subsets of cells within the phenotypic HSC gate can be triggered to proliferate in response to inflammatory stimuli such as IFNs [21, 22]. These data support a model in which the HSC compartment is functionally heterogeneous. Importantly, the presence of certain inflammatory factors, particularly IFNs, directly induces the expression of Sca-1 in ordinarily Sca-1$^-$ progenitor populations such as granulocyte/macrophage progenitors (GMPs) and the heterogeneous common lymphoid progenitor (CMP) compartment, causing a phenotypic shift that can significantly complicate analysis of some hematopoietic populations and requires careful validation and interpretation of results [20]. While the SLAM gate is largely free of such contamination, addition of further surface markers such as ESAM [23] which is not expressed in the majority of Sca-1$^-$ progenitors reduces the likelihood of such progenitors confounding HSC analysis [20].

Here, we describe approaches to assess cell cycle activity of HSCs during inflammation in unfractionated bone marrow based on 5-ethenyl-2′-deoxyuridine (EdU) incorporation as well as Ki67 coupled with DNA content quantification by DAPI. EdU is a nucleoside thymidine analog that is incorporated into DNA by cells in S-phase; the use of commercially available kits in which the EdU contains an alkyne group allows for the conjugation of an AlexaFluor-containing azide to the EdU via a "click" reaction that does not require DNA denaturation or the use of an anti-nucleoside analog antibody [24]. When combined with a DNA stain such as DAPI, this approach allows for the specific identification of cells in S-phase. On the other hand, Ki67 is a nuclear antigen that is expressed in cells that have entered $G_1$ and/or are

progressing through the S, $G_2$ and M phases of the cell cycle; its absence in the nuclei of dormant cells such as HSCs allows for discrimination of a $G_0$ population, and in combination with DAPI constitutes a well-established approach for assessing cell cycle status in multiple cell types, including HSCs [25]. Both approaches are well suited to flow cytometry, and here we specifically apply this technique in the context of type I interferon-driven inflammation induced by the double-stranded RNA analog polyinosinic:polycytidylic acid (Poly I:C). Using this method, we can identify and analyze cell cycle activity in phenotypic HSCs from individual mice, with minimal pre-enrichment steps and/or contamination related to surface marker shifts.

## 2 Materials

Biological buffers such as PBS, Dulbecco's PBS (D-PBS), and HBSS are purchased as 0.2 μm filtered sterile solutions from commercial sources.

### 2.1 In Vivo Induction of Inflammation with Poly I:C

1. Adult C57BL/6J (Ly5.2) mice, between 6 and 8 weeks of age (*see* **Notes 1** and **2**).
2. Poly I:C (GE Healthcare), 1 mg/ml stock solution in sterile PBS, stored at −20 °C (*see* **Note 3**). Due to limited solubility of the lyophilized product, after adding PBS Poly I:C should be heated in a 65 °C water bath with frequent mixing to denature and solubilize the RNA oligonucleotides. Once in solution, Poly I:C should be allowed to cool at room temperature prior to aliquoting and storage.
3. Tuberculin syringe (0.3 $cm^3$) with 28.5-gauge needle for intraperitoneal injection.
4. Scale for determining mouse masses.

### 2.2 In Vivo EdU Labeling

1. 5-ethynyl-2-deoxyuridine (EdU), 10 mg/ml stock solution in 5% DMSO and sterile D-PBS, stored at −20 °C protected from light.
2. Tuberculin syringe (0.3 $cm^3$) with 28.5-gauge needle for intraperitoneal injection.

### 2.3 Bone Marrow and Splenocyte Isolation

1. Dissecting scissors with tungsten carbide blades and dissecting forceps.
2. Ice bucket with lid or aluminum foil to cover samples.
3. 3 cm culture dish, or 6- or 12-well culture plate.
4. Staining medium (hereafter SM): Sterile Hank's Buffered Saline Solution (HBSS; without phenol red, $Ca^{2+}$ and $Mg^{2+}$) supplemented with 2% fetal bovine serum (FBS). FBS is heat-

inactivated in a 55 °C water bath for 20 min, allowed to cool at room temperature, aliquoted into 50 ml conical tubes, and stored at −20 °C prior to use.

5. Falcon 5 ml polystyrene round-bottom tubes.
6. 3 ml syringes with 22 or 21-gauge needle.
7. ACK lysis buffer (150 mM $NH_4Cl$, 10 mM $KHCO_3$, 0.1 mM $Na_2EDTA$) prepared using MilliQ-grade $H_2O$.
8. 70 μm filter mesh, cut into small squares.
9. Hemocytometer and microscope equipped with phase contrast for cell counts, or automated cell counter (e.g., Beckman-Coulter ViCell).
10. Benchtop centrifuge equipped with buckets and adapters for 5 ml tubes and carriers for 96-well plates (e.g., Beckman-Coulter Allegra 6).

### 2.4 Cell Surface Staining

1. Antibodies against cell surface antigens (*see* Tables 1 and 2 and **Notes 4** and **5**). We use different staining panels depending on whether we combine Ki67 and EdU stainings.
2. Rat IgG prepared as a 1 mg/ml stock solution in sterile Dulbecco's PBS (D-PBS).
3. 96-well U-bottom polystyrene plates (*see* **Note 6**).
4. Multi-well aspiration manifold. This allows for rapid aspiration of staining wells. We use a manifold from V&P Scientific (catalog number VP-187D).
5. 8- or 12-channel 200 μl capacity multichannel pipette.
6. 50 ml reagent reservoirs for use with multichannel pipette.

### 2.5 Intracellular EdU Staining

1. For EdU staining we use the Click-iT Plus EdU Flow Cytometry Assay Kit containing the Alexa Fluor 488 (individual staining) or the Alexa Fluor 647 (combined staining) picolyl azide (Thermo Fisher Scientific). Preparation of the kit components follows the manufacturer's instructions and is described below.
2. Diluent/wash buffer consisting of D-PBS containing 1% BSA.
3. Permeabilization/wash solution: dilute kit Component E 1:10 in D-PBS containing 1% BSA. Store at 4 °C.
4. 10× stock solution of the EdU buffer additive (Component G), prepared for use by diluting in 2 ml of MilliQ-grade $H_2O$. Store at −20 °C. The required amount of 1× stock for each assay is prepared directly prior to use by diluting the 10× solution in MilliQ-grade $H_2O$.
5. 1 mg/ml DAPI stock prepared in D-PBS, store at −20 °C protected from light (*see* **Note 7**).

### 2.6 Intracellular Ki67 Staining

1. Fixative: We use BD Cytofix/Cytoperm buffer. Equivalent buffers containing 4% paraformaldehyde can also be used.
2. Wash buffer: We use BD PermWash buffer, diluted to 1× using MilliQ-grade $H_2O$.
3. Nuclear permeabilization reagent: We use BD Permeabilization Buffer Plus. Equivalent buffers containing 1% BSA and a low concentration of Triton-X100 detergent (e.g., 0.01%) can be used.
4. Antibody against Ki67 (*see* Tables 1 and 2 and **Note 8**).
5. 1 mg/ml DAPI stock prepared in D-PBS, store at −20 °C protected from light (*see* **Note 7**).

**Table 1**
**Antibody panel and flow cytometer optical setup for individual Ki67 or EdU stainings**

| Marker | Fluorochrome | Clone | Laser line | Filter (LP/BP) |
|---|---|---|---|---|
| DNA | DAPI | – | 405 | 450/40 BP |
| Flk2 | Biotin | A2F10 | – | |
| Streptavidin | BV-605 | – | 405 | 610/20 BP/595 LP |
| Ki67 | FITC | SolA15 or 16A8 | 405 | 530/30 BP/505 LP |
| EdU | AlexaFluor 488 | – | 488 | 530/30 BP/505 LP |
| CD150 | PE | TC15-12F12.2 | 488 | 575/25 BP/550 LP |
| Mac-1 | PE/Cy5 | M1/70 | 488 | 670/30 BP/655 LP |
| Gr1 | PE/Cy5 | RB6-8C5 | 488 | 670/30 BP/655 LP |
| Ter119 | PE/Cy5 | TER-119 | 488 | 670/30 BP/655 LP |
| B220 | PE/Cy5 | RA3-6B2 | 488 | 670/30 BP/655 LP |
| CD3 | PE/Cy5 | 145-2C11 | 488 | 670/30 BP/655 LP |
| CD4 | PE/Cy5 | GK1.5 | 488 | 670/30 BP/655 LP |
| CD5 | PE/Cy5 | 53-7.3 | 488 | 670/30 BP/655 LP |
| CD8 | PE/Cy5 | 53-6.7 | 488 | 670/30 BP/655 LP |
| Sca-1 (Ly6A/E) | PE/Cy7 | D7 | 488 | 780/60 BP/750 LP |
| ESAM | APC | IG8/ESAM | 633 | 670/30 BP |
| CD48 | AlexaFluor 700 | HM48-1 | 633 | 730/45 BP/690 LP |
| CD117 (c-Kit) | APC/Cy7 | 2B8 | 633 | 780/60 BP/750 LP |

Complete listing of antibodies and fluorochromes used for individual Ki67 or EdU staining protocol, as well as antibody clone information. Also included are the laser lines (in nanometer) and corresponding optical filters for each marker based on our BD FACSCelesta flow cytometer. *LP* longpass, *BP* bandpass

**Table 2**
**Antibody panel and flow cytometer optical setup for combined Ki67 and EdU staining**

| Marker | Fluorochrome | Clone | Laser line | Filter (LP/BP) |
|---|---|---|---|---|
| DNA | DAPI | – | 405 | 450/40 BP |
| Flk2 | Biotin | A2F10 | – | |
| Streptavidin | BV-605 | – | 405 | 610/20 BP/595 LP |
| CD150 | BV-785 | TC15-12F12.2 | 405 | 780/60 BP/750 LP |
| Ki67 | FITC | SolA15 or 16A8 | 405 | 530/30 BP/505 LP |
| ESAM | PE | 1G8/ESAM | 488 | 575/25 BP/550 LP |
| Mac-1 | PE/Cy5 | M1/70 | 488 | 670/30 BP/655 LP |
| Gr1 | PE/Cy5 | RB6-8C5 | 488 | 670/30 BP/655 LP |
| Ter119 | PE/Cy5 | TER-119 | 488 | 670/30 BP/655 LP |
| B220 | PE/Cy5 | RA3-6B2 | 488 | 670/30 BP/655 LP |
| CD3 | PE/Cy5 | 145-2C11 | 488 | 670/30 BP/655 LP |
| CD4 | PE/Cy5 | GK1.5 | 488 | 670/30 BP/655 LP |
| CD5 | PE/Cy5 | 53-7.3 | 488 | 670/30 BP/655 LP |
| CD8 | PE/Cy5 | 53-6.7 | 488 | 670/30 BP/655 LP |
| Sca-1 (Ly6A/E) | PE/Cy7 | D7 | 488 | 780/60 BP/750 LP |
| EdU | AlexaFluor 647 | – | 633 | 670/30 BP |
| CD48 | AlexaFluor 700 | HM48-1 | 633 | 730/45 BP/690 LP |
| CD117 (c-Kit) | APC/Cy7 | 2B8 | 633 | 780/60 BP/750 LP |

Complete listing of antibodies and fluorochromes used for the combined staining protocol, as well as antibody clone information. Also included are the laser lines (in nanometer) and corresponding optical filters for each marker based on our BD FACSCelesta flow cytometer. *LP* longpass, *BP* bandpass

### *2.7 Flow Cytometry Analysis*

1. Flow cytometer with 355 nm (UV) (optional), 405 nm (violet), 488 nm (blue), and 633 nm (red) lasers with appropriate PMTs and LP/BP optical filter setups (*see* Tables 1 and 2 for our optical setup).
2. Compensation controls: Splenocytes from PBS-treated control mice and eBioscience UltraComp beads (*see* **Note 9**).
3. Analytical software: We use FlowJo versions 9 and 10 (FlowJo, LLC) on a Mac platform for flow analysis.

## 3 Methods

Ensure all institutional standard operating procedures (SOPs) are followed while performing procedures involving animals and potentially hazardous materials.

### 3.1 In Vivo Induction of Inflammation with Poly I:C

1. Thaw 1 mg/ml poly I:C stock solution at room temperature. Mix thoroughly by inverting the tube and ensure that poly I:C is fully in the solution. No crystals or flakes should be present in the solution.
2. Weigh mice and calculate volume of poly I:C to inject for 10 mg/kg dose.
3. Inject poly I:C intraperitoneally (i.p.) into experimental mice. Inject dose-equivalent volumes of sterile PBS into control animals.
4. Poly I:C treatment can be extended by performing additional injections every other day for the length of the experiment (*see* **Note 10**).

### 3.2 In Vivo EdU Labeling

1. Three hours prior to euthanasia, thaw 10 mg/ml EdU stock solution and mix thoroughly by inverting the tube and ensure that EdU is fully in the solution. No white crystals or flakes should be present in the solution.
2. Inject mice intraperitoneally (i.p) with 200 μl of EdU solution to label cycling cells.
3. Euthanize animals according to approved IACUC protocols, typically $CO_2$ inhalation followed by a physical secondary method such as cervical dislocation or bilateral thoracotomy.

### 3.3 Bone Marrow and Splenocyte Isolation

1. Dissect out and thoroughly clean four long bones of the leg (two femurs, two tibiae). Bones from individual mice can be kept in 3 cm dishes, or in wells of a 6- or 12-well plate containing SM and set on ice. We treat each mouse as an individual biological replicate for our analyses.
2. Remove epiphysis of bones with dissecting scissors and using a 3 ml syringe containing SM, flush thoroughly the central marrow of the bones into a 5 ml round-bottom tube. Flushing can be repeated to clear the marrow from the bones.
3. Remove a spleen from a control (non-inflamed) mouse. Homogenize spleen by crushing into a 3 cm disc containing SM by placing in a 70 μm filter basket and mincing with the blunt end of a syringe plunger. Transfer into a separate 5 ml tube.
4. Spin bone marrow and spleen cells at 500 × *g* for 5 min and decant or aspirate the supernatant.
5. Resuspend bone marrow and spleen cells in 500 μl ACK lysis buffer and incubate on ice for 3 min to deplete erythrocytes. Following the incubation, fill tube with SM and spin cells at 500 × *g* for 5 min to wash.
6. Decant or aspirate the supernatant and resuspend bone marrow and spleen cells in 1 ml of SM. Filter cells through 70 μm nylon mesh into a new 5 ml round-bottom tube and perform a cell count.

7. Prepare a 96-well plate for EdU or Ki67 staining. To combine EdU and Ki67 stainings in a single assay *see* **Note 11** for protocol details and Table 2 for combined staining panel.
8. Pipet $1 \times 10^7$ cells into the 96-well U-bottom plate, 2 wells per mouse. This allows for a total of $2 \times 10^7$ cells to be stained for each data point (*see* **Notes 12** and **13**). For splenocytes, pipet $1 \times 10^7$ cells into 2 wells of the 96-well U-bottom plate to be used for setting baseline PMT values and DAPI channel compensation. Carry splenocytes forward to fixation and permeabilization procedures (Subheadings 3.5 and/or 3.6). One well will remain unstained, the second will be stained with DAPI following fixation/permeabilization in order to adjust the DAPI PMT voltages.
9. Compensation beads are added to the 96-well U-bottom plate for generating single-color compensation controls (*see* Subheading 3.7, **step 1** for additional information).
10. Spin down cells at $900 \times g$ for 3 min.

### 3.4 Cell Surface Staining

1. Aspirate supernatant from both plates using the aspiration manifold and resuspend cells in both plates in 50 μl SM containing a pre-titrated cocktail of antibodies to exclude lineage-positive cells and identify HSC (*see* **Note 14**). Our cocktail includes PE-Cy5-congugated antibodies against lineage markers, plus anti-mouse CD117 (c-Kit)-APC/Cy7, Flk2-Biotin, Sca-1 (Ly6A/E)-PE/Cy7, CD48-A700, CD150-PE and ESAM-APC (*see* Tables 1 and 2). We also include a 1:50 dilution of the rat IgG stock to prevent nonspecific Fc binding. Stain the equivalent compensation controls at this time. Incubate cells in the dark and on ice for 30 min.
2. Wash cells by adding 150 μl of SM and spinning at $900 \times g$ for 3 min.
3. Aspirate the supernatant and wash cells a second time by adding 200 μl of SM and spin cells at $900 \times g$ for 3 min.
4. Decant or aspirate the supernatant and resuspend pellet in 50 μl of SM containing a pre-titrated amount of Strepavidin-linked Brilliant Violet (BV)-605. Stain the equivalent compensation controls at this time. Incubate cells in the dark and on ice for 30 min.

### 3.5 Intracellular EdU/DAPI Staining

1. Wash cells by adding 150 μl of D-PBS containing 1% BSA and spin cells down at $900 \times g$ for 3 min. Repeat for a total of two washes, adding 200 μl of D-PBS containing 1% BSA per well for the second wash.
2. Aspirate the supernatant and fix cells by adding 100 μl of fixative (also called Component D) from the kit.

3. Incubate the cells in the plate for 15 min in the dark at room temperature (RT).
4. Wash cells by adding 100 μl of D-PBS containing 1% BSA and spin cells down at 900 × *g* for 3 min. Repeat for a total of two washes, adding 200 μl of D-PBS containing 1% BSA per well for the second wash.
5. Aspirate the supernatant and permeabilize cells by resuspending in 100 μl of 1× permeabilization/wash reagent (*see* **item 3** in Subheading 2.5). Incubate the cells for 15 min in the dark at RT.
6. Spin down cells at 900 × *g* for 3 min.
7. Aspirate the supernatant and resuspend the cells in 40 μl of the permeabilization/wash reagent. Once cells are fully resuspended, add 200 μl of the Click-IT reaction cocktail to each well, for a final volume of 240 μl per well. Stain the equivalent compensation controls at this time. Incubate the cells for 30 min at room temperature. Note that the volume of reaction cocktail we use is different than the kit instructions (*see* Table 3 for our reaction cocktail preparation for staining in plates). Also note that the manufacturer indicates this cocktail should be prepared in the order listed, and added to the sample within 15 min of preparation.
8. Spin down cells at 900 × *g* for 3 min.
9. Aspirate the supernatant and wash cells by adding 200 μl of permeabilization/wash reagent and spin down cells at 900 × *g* for 3 min.
10. Wash cells a second time by adding 200 μl of SM and spin down cells at 900 × *g* for 3 min.

**Table 3**
**EdU reaction cocktail reagent volumes for staining in 96-well plate**

| Component | Volume (per well) (μl) |
|---|---|
| D-PBS | 175 |
| Copper protectant (Component F) | 4 |
| Fluorescent dye picolyl azide | 1 |
| 1× Reaction buffer additive | 20 |
| Total Volume | 200 |

Reagent volumes required for the Click-IT reaction cocktail described in Subheading 3.5, **step 7**. Volumes shown are per well. Note that the manufacturer recommends reaction components to be added in the order listed. If performing EdU only staining (no Ki67), use the AlexaFluor 488 picolyl azide. If combining the staining, be sure to use the Alexa Fluor 647 picolyl azide

11. Aspirate the supernatant and resuspend cells in 200 µl of a 1 µg/ml DAPI solution prepared in D-PBS from the 1 mg/ml stock solution. Stain the equivalent compensation controls at this time.
12. Proceed to flow cytometry analysis. If instrument is not equipped to acquire samples from 96-well plates (e.g., using an HTS system on a BD instrument), combine the two wells per sample into one 5 ml tube for acquisition. Maintain samples in the dark and on ice until ready to acquire.

### 3.6 Intracellular Ki67/DAPI Staining

1. Wash cells by adding 150 µl of SM and spin down cells at 900 × *g* for 3 min. Repeat for a total of two washes, adding 200 µl of SM per well for the second wash.
2. Fix cells by resuspending in 100 µl of Cytofix/Cytoperm and incubate cells in the dark and on ice for 30 min.
3. Spin down cells at 900 × *g* for 3 min.
4. Aspirate supernatant and wash cells by resuspending in 200 µl of PermWash buffer. Spin down cells at 900 × *g* for 3 min.
5. Aspirate the supernatant and permeabilize the nucleus by resuspending in 100 µl of Permeabilization Buffer Plus. Incubate cells in the dark and on ice for 10 min.
6. Spin the cells at 900 × *g* for 3 min.
7. Aspirate the supernatant and wash cells by resuspending in 200 µl of PermWash buffer. Spin down cells at 900 × *g* for 3 min.
8. Re-fix cells by resuspending in 100 µl of Cytofix/Cytoperm and incubate cells in the dark and on ice for 5 min.
9. Spin the cells at 900 × *g* for 3 min.
10. Aspirate the supernatant and wash cells by resuspending in 200 µl of PermWash buffer. Spin down cells at 900 × *g* for 3 min.
11. Aspirate the supernatant and stain cells for Ki67 by resuspending in 50 µl of PermWash containing a pre-titrated amount of Ki67 FITC. Stain the equivalent compensation controls at this time. Incubate cells in the dark at RT for 30 min.
12. Wash cells by adding 150 µl of PermWash and spin down cells at 900 × *g* for 3 min.
13. Wash cells a second time by adding 200 µl of SM and spin down cells at 900 × *g* for 3 min.
14. Aspirate the supernatant and resuspend cells in 200 µl of a 1 µg/ml DAPI solution prepared in D-PBS from the 1 mg/ml stock solution. Stain the equivalent compensation controls at this time.

15. Proceed to flow cytometry analysis. If instrument is not equipped to acquire samples from 96-well plates (e.g., using an HTS system on a BD instrument), combine the two wells per sample into one 5 ml tube for acquisition. Maintain samples in the dark and on ice until ready to acquire.

### 3.7 Flow Cytometry Data Acquisition and Analysis

To set up the flow cytometer, specific controls are required to ensure optimal performance and discrimination of cell populations.

1. Compensation beads are added (one drop per well) to the 96-well plate at the same time as the experimental samples and stained with 1 μl of fluorochrome-linked antibodies for each fluorescent channel (excepting DAPI; see below). We typically use the antibodies in our cocktail to set our compensations (*see* **Note 9**). Beads are treated just as the experimental samples are, including being carried through washes, fixation and permeabilization steps to ensure that the fluorochromes on the compensation controls are treated similarly to experimental samples, since the treatments described above can lead to slight changes in emission characteristics (*see* **Note 15**).
2. To set up the flow cytometer, baseline PMT voltages for all channels including DAPI are first set, typically with negative fluorescence peaks of unstained splenocytes that have been fixed and permeabilized similar to the experimental samples, centered around 200 on the logarithmic scale.
3. DAPI-stained splenocytes are used to adjust the DAPI channel PMT voltages, as DNA content via DAPI staining is read on a linear scale. DAPI PMT voltages are adjusted in the linear scale to place the 2N DNA content peak (the majority of splenocytes) typically at or between 50K and 100K on the linear scale.
4. Unstained splenocytes, compensation beads, and DAPI-stained splenocytes are acquired and recorded on a logarithmic scale to generate the compensation matrix. DAPI-stained splenocytes are acquired on a logarithmic scale to allow the unstained control to be seen on scale.
5. Acquire experimental samples, with DAPI set back to a linear scale to analyze DNA content.
6. We recommend acquiring at least $2.5 \times 10^6$ events per sample, with $5 \times 10^6$ events being optimal (allowing one to acquire at least 1000 events in the phenotypic HSC gate). Events should be acquired at a fairly low rate (between 5 and 10K events/s) in order to ensure high-quality cell cycle data.
7. We analyze our data in FlowJo using a Mac platform. After data are exported and loaded into FlowJo, we check all parameters versus time for each sample to ensure data acquisition is consistent. Figure 1b shows our typical gating scheme for identifying

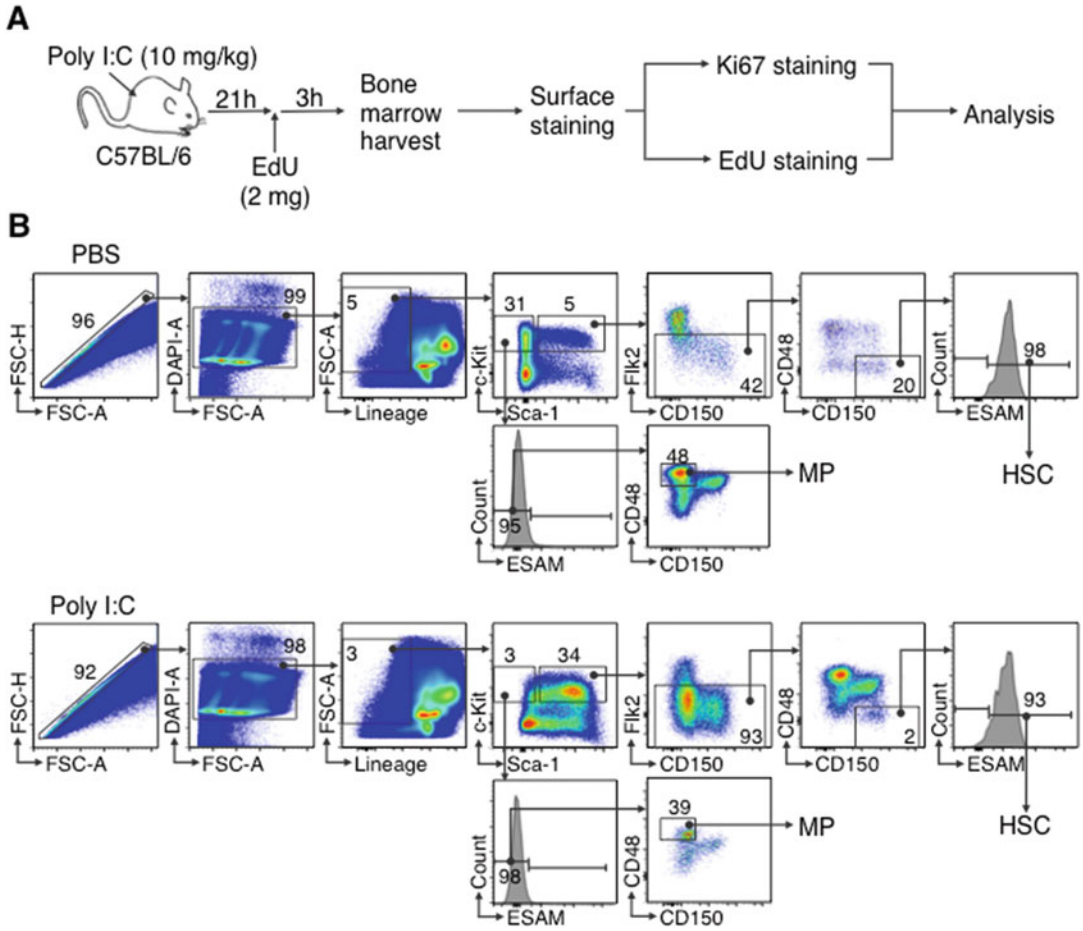


**Fig. 1** Gating strategy for HSC cell cycle analysis during inflammation. (**a**) Experimental scheme depicting poly I:C injection, EdU injection, and staining workflow for cell cycle analysis. (**b**) To identify HSC, we first include a geometry gate to exclude doublets, and use a FSC vs. DAPI gate to exclude apoptotic, anucleate, and >4N DNA content cells. We subsequently gate on $Lin^-$ cells, and then on c-Kit and Sca-1 to define the LSK compartment. From the LSK, we can identify MPP4 (LSK/$Flk2^+$), and within the $Flk2^-$ compartment we identify phenotypic HSC (LSK/$Flk2^-CD48^-CD150^+$) (*see* **Note 18**). Other populations in this compartment (not gated) include ST-HSC/ITRC (LSK/$Flk2^-CD48^-CD150^-ESAM^+$), MPP2 (LSK/$Flk2^-CD48^+CD150^+ESAM^+$), and MPP3 (LSK/$Flk2^-CD48^+CD150^-ESAM^+$). We also gate on a population of $Lin^-cKit^+CD48^+CD150^-$ myeloid progenitors (largely though not exclusively consisting of granulocyte/macrophage progenitors) The Sca-1 shift is notably evident in the poly I:C sample based on the increased frequency of phenotypic LSK, as well as the increased overall fluorescence intensity and decreased frequency of the $Lin^-$c-$Kit^+$ compartment. Contamination of MPs that have re-acquired Sca-1 is evident based on the sharp increase in $CD48^+CD150^-$ and $CD48^+CD150^+$ cells in the LSK/$Flk2^-$compartment, which are phenotypically identical to MPP2 and MPP3, except that they lack ESAM. Hence, we gate on $ESAM^+$ events within the LSK/$Flk2^-CD48^-CD150^+$ prior to cell cycle analysis to exclude MPs from the phenotypic HSC gate. The use of ESAM can allow for more reliable gating and cell cycle analysis of ST-HSC/ITRC (LSK/$Flk2^-CD48^-CD150^-ESAM^+$), MPP2 (LSK/$Flk2^-CD48^+CD150^+ESAM^+$), and MPP3 (LSK/$Flk2^-CD48^+CD150^-ESAM^+$), though some megakaryocyte progenitors also express CD150 and ESAM, and may not be entirely excluded from these compartments. Flk2 allows for identification of MPP4, though the $Flk2^+$ gate should be carefully drawn based on expression levels in $Sca\text{-}1^-$ MPs

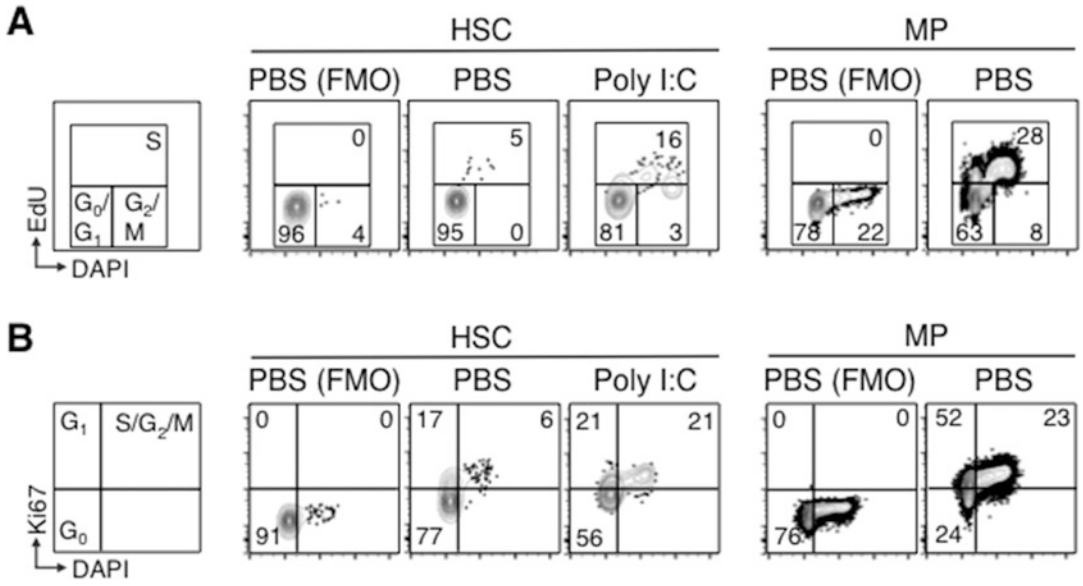


**Fig. 2** Cell cycle and proliferation analysis of HSCs. Using the gating scheme described in Fig. 1b, we can subsequently assess the cell cycle status of the HSC compartment in poly I:C-treated mice. For each staining, we show fluorescence-minus-one (FMO) controls for the HSC and MP compartments, which are critical for properly setting the positive and negative gates for EdU and Ki67. As MPs are actively cycling cells, we can use them as an internal positive control for each staining, as well as for setting the 2N and 4N DNA content gates. (**a**) By plotting EdU versus DAPI, we can identify proportions of cells in $G_0/G_1$, S, and $G_2/M$ phases of the cell cycle, thereby demonstrating an increase in actively proliferating (S-phase) HSCs in poly I:C-treated mice. Note the large proportion of $EdU^+$ MPs, functioning as an internal positive control for the staining. (**b**) Plotting Ki67 vs. DAPI allows for the specific discrimination of quiescent $G_0$ ($Ki67^-$/2N DNA) HSCs from HSCs in $G_1$ ($Ki67^+$/2N DNA) $Ki67^+$ cells with >2N DNA content comprise cells in $S/G_2/M$ phases of the cell cycle. In contrast to actively cycling MPs, the HSC compartment is predominantly quiescent at steady state, with elevated proportions of cells in cycle in poly I:C treated mice. Note that the boundary between $Ki67^-$ and $Ki67^+$ populations can be determined based on the vertex between the 2N DNA and 4N DNA populations in actively cycling MPs as shown

HSCs in control versus poly I:C-treated mice (*see* **Notes 15–17**). Representative cell cycle profiling of HSCs from PBS and poly I:C-treated mice by EdU/DAPI and Ki67/DAPI staining are shown in Fig. 2a, b.

8. We typically use this approach to analyze HSC cell cycle status in multiple individual mice at once, allowing the analysis of groups containing multiple biological replicates in one session.

## 4 Notes

1. All animal procedures described herein were conducted in accordance with protocols approved by the University of Colorado Denver Institutional Animal Care and Use Committee (IACUC).

2. This assay has been tested and used extensively in C57BL/6 mice. Certain mouse strains such as Balb/c do not express Sca-1, which may complicate identification of immature hematopoietic cells at least in steady-state condition.
3. Due to limited quality control by the manufacturer, Poly I:C from GE Healthcare should be carefully tested for specific biological activity prior to experimental use, particularly if it is being used as a type I IFN inducer. We routinely test new lots of Poly I:C on wild-type and *Ifnar1*$^{-/-}$ mice (e.g., JAX # 32045-JAX). Specifically, we assess by flow cytometry the degree to which Sca-1 expression increases in the phenotypic HSC compartment 24 h after a single injection of Poly I:C. Such shifts should be specific to wild-type mice but not *Ifnar1*$^{-/-}$ mice. While more expensive, Poly I:C from InVivoGen is more thoroughly tested for biological activity by the manufacturer. We have used the high molecular weight (HMW; cat. tlrl-pic) product successfully.
4. The cell cycle data shown in this chapter were acquired on a 3-laser (5V/4B/3R) FACSCelesta (Becton-Dickenson). Due to differences in laser power and optical benches among flow cytometers, the antibody panel we describe may not be optimal for all instruments. Antibody panels should be carefully titrated and optimized for individual instruments prior to use. We also recommend that titrations be performed on cells that are subsequently fixed and permeabilized in a similar manner as described in the protocol to ensure robust results, as some fluorochromes may not behave similarly in fixed conditions. Note that proper maintenance and quality control of flow cytometry instruments is crucial for good data. Our instruments are checked with QC beads on a daily basis and undergo rigorous cleaning between users. Note also that partial clogs, air bubbles, or low sheath fluid reservoir levels can dramatically impact the quality of data. Instruments should be checked for proper configuration, fluidics and optics operation and sheath fluid levels prior to data acquisition.
5. The surface marker cocktail described in this protocol is what we consider to be the minimum for robust identification of an HSC-enriched fraction in inflammatory conditions. Depending on instrument specifications, other surface markers to define HSCs and other progenitor populations (e.g., CD34, FcγR, CD105, etc.) can be added to address specific experimental objectives.
6. We have found that staining our samples in 96-well plates increases overall efficiency, particularly where multiple biological replicates (i.e., individual mice) are analyzed at the same time. Our flow cytometer is equipped with a high-throughput system (HTS) that acquires samples directly from

96-well plates, allowing the staining approach to easily interface with the HTS.

7. DAPI has an optimal excitation peak for the 355 nm (UV) laser line, but in our hands still yields bright fluorescence and good separation on the 405 nm (Violet) laser. Alternative products for DNA staining, such as Vybrant DyeCycle Violet, can also be used with instruments lacking a UV laser.
8. Multiple Ki67 antibody clones in several fluorochromes are commercially available. We tested the B56 clone conjugated to AlexaFluor 488, BV-421 and BV-786 as well as the 16A8 and SolA15 clones conjugated to FITC or PerCP-eFluor710 at dilutions ranging from 1:25 to 1:800. Head-to-head comparisons of the B56 and 16A8 clones showed superior separation of $Ki67^+$ cells relative to FMO with the 16A8 clone. BV dye-conjugated B56 antibodies did not yield markedly different performance relative to A488 in our hands.
9. We use DAPI-stained splenocytes along with unstained splenocytes to compensate for DAPI. For the remaining fluorophores, we find that compensation beads work very well in our analyses. Note that an antibody conjugated to either Alexa Fluor 488 or Alexa Fluor 647 will be needed to compensate for the EdU stain; and an antibody conjugated to BV-605 to compensate for the streptavidin. As an alternative to compensation beads, a common approach is to stain splenocytes with anti-B220 antibodies corresponding to each fluorochrome used. Ensure that all compensation controls (stained or unstained, beads or splenocytes) are subsequently fixed and permeabilized similarly to the samples, as these treatments can affect the fluorescence of the fluorochromes and scatter properties of the cells.
10. We and others have performed poly I:C treatments out to 30 days without noticing gross effects on animal health. We perform injections at the same time of day and alternate injections between the left and right sides of the abdomen to minimize inflammation at injection sites. While we have not observed effects on HSC activity related to injection alone, PBS-injected controls should be included in the experimental design. When performing kinetics experiments with multiple timepoints, we often stagger injection start points such that all animals are sacrificed and analyzed on the same day.
11. To combine the two stainings, stain first with Ki67 (FITC) followed by Edu (AlexaFluor 647) staining. Follow the protocol as described until the completion of Subheading 3.4. Proceed directly to Subheading 3.6 and perform **steps 1–12**. Next, go to Subheading 3.5 **step 5** and proceed with the following modification: Aspirate the supernatant and

resuspend in 200 μl of 1× permeabilization/wash reagent (*see* Subheading 2.5, **item 3** for preparation). No incubation is necessary and proceed directly **step 7**. At **step 8**, make sure to use the AlexaFluor 647 fluorescent dye picolyl azide. Perform all the subsequent steps until the end of the section.

12. Pro-inflammatory treatments such as poly I:C have the potential to induce bone marrow cell apoptosis or mobilization. It is critical to count and carry forward equivalent cell numbers for each sample into the staining, as variations in cell number can lead to variable brightness of individual stainings (particularly for DAPI), confounding interpretation.
13. To perform cell stainings in tubes, dispense $2 \times 10^7$ cells into a 5 ml tube for each sample and simply double the volumes indicated in subsequent steps. For wash steps when staining in tubes, we typically use 3 ml volumes. Perform centrifugations at $500 \times g$ for 5 min.
14. Complete resuspension of the cell pellet at every wash and staining step is critical for successful stainings. Resuspend pellets in the plate or tube by gently pipetting up and down several times and perform a visual check to ensure all cells are in suspension.
15. Optimally, two sets of compensation beads would be used for each staining to ensure best-practice compensation.
16. The careful use of scatter and geometry (doublet exclusion) gates can eliminate a large proportion of dead or clumped cells and/or debris. It may also be possible to include a fixable viability dye to ensure minimal interference of dead/dying cells in population identification the cell cycle analysis. To eliminate apoptotic cells, debris and polyploid cells (likely megakaryocytes) we plot DAPI against FSC, allowing removal of <2N and >4N DNA content outlier events.
17. Different inflammatory stimuli and disease conditions will result in different degrees of shift in Sca-1 expression, and thereby different levels of myeloid progenitor contamination. Type I or type II IFNs, or treatments that induce them, such as poly I:C or LPS, lead to significant and global increases in Sca-1 in progenitors and HSCs alike, akin to our observations in Fig. 1b. On the other hand, pro-inflammatory cytokines such as IL-1 induce minimal to no shift in Sca-1 expression in progenitors and HSCs. Thus, every model of inflammation should be individually evaluated for the extent to which reacquisition of Sca-1 by myeloid progenitors will occur.
18. In our staining scheme we retain Sca-1 since even under inflammatory conditions HSCs remain by definition Sca-1$^+$, and depending on the degree of shift in this marker, retaining Sca-1 allows us to gate out at least some proportion of MPs.

Gating with ESAM ensures the phenotypic HSC, ST-HSC/ITRC, MPP2, and MPP3 compartment remain relatively free of contaminating MPs, though we find that some phenotypic megakaryocytic progenitors (MkP) express ESAM and CD150 [25] and may not be completely excluded from the HSC gate. Likewise, we have noticed that other SLAM markers that enrich for HSC, such as CD229 or CD244 [26], also appear to have similar expression patterns between phenotypic HSC and MkP; this may represent a transient phenotypic state with subpopulations of HSCs expressing both marker sets as they differentiate into MkP [27]. Hence, it is always important when interpreting these data to regard phenotypic gates as "enriched" for specific populations, rather than exclusive for them. The ESAM gate can be used at multiple junctures in the analysis scheme; we prefer to incorporate it as shown in Fig. 1b for HSC cell cycle and proliferation analysis. We can also make use of a $Lin^-$ $cKit^+$ $ESAM^+$ or "LKE" gate rather than the LSK gate, with HSC, ST-HSC/ITRC, MPP2, and MPP3 falling within this gate while MPP4 remains within the $Lin^-$ $cKit^+$ $ESAM^-$ "LK" compartment.

## Acknowledgment

This work was supported by NIH grant K01DK98315 to E.M.P. We thank Biniam Adane and Brett Stevens for reagents and advice during the preparation of this chapter.

### References

1. Orkin SH, Zon LI (2008) Hematopoiesis: an evolving paradigm for stem cell biology. Cell 132:631–644. doi:10.1016/j.cell.2008.01.025
2. Pietras EM, Warr MR, Passegué E (2011) Cell cycle regulation in hematopoietic stem cells. J Cell Biol 195:709–720. doi:10.1083/jcb.201102131
3. Schepers K, Campbell TB, Passegué E (2015) Normal and leukemic stem cell niches: insights and therapeutic opportunities. Cell Stem Cell 16:254–267. doi:10.1016/j.stem.2015.02.014
4. Rossi L, Lin KK, Boles NC et al (2012) Less is more: unveiling the functional core of hematopoietic stem cells through knockout mice. Cell Stem Cell 11:302–317. doi:10.1016/j.stem.2012.08.006
5. Kiel MJ, Yilmaz ÖH, Iwashita T et al (2005) SLAM family receptors distinguish hematopoietic stem and progenitor cells and reveal endothelial niches for stem cells. Cell 121:1109–1121. doi:10.1016/j.cell.2005.05.026
6. Wilson A, Laurenti E, Oser G et al (2008) Hematopoietic stem cells reversibly switch from dormancy to self-renewal during homeostasis and repair. Cell 135:1118–1129. doi:10.1016/j.cell.2008.10.048
7. Cabezas-Wallscheid N, Klimmeck D, Hansson J et al (2014) Identification of regulatory networks in HSCs and their immediate progeny via integrated proteome, transcriptome, and DNA methylome analysis. Cell Stem Cell 15:507–522. doi:10.1016/j.stem.2014.07.005
8. Foudi A, Hochedlinger K, Van Buren D et al (2008) Analysis of histone 2B-GFP retention reveals slowly cycling hematopoietic stem cells. Nat Biotechnol 27:84–90. doi:10.1038/nbt.1517

9. Winkler IG, Barbier V, Wadley R et al (2010) Positioning of bone marrow hematopoietic and stromal cells relative to blood flow in vivo: serially reconstituting hematopoietic stem cells reside in distinct nonperfused niches. Blood 116:375–385. doi:10.1182/blood-2009-07-233437
10. Sun J, Ramos A, Chapman B et al (2014) Clonal dynamics of native haematopoiesis. Nature 514:322–327. doi:10.1038/nature13824
11. Busch K, Klapproth K, Barile M et al (2015) Fundamental properties of unperturbed haematopoiesis from stem cells in vivo. Nature 518:542–546. doi:10.1038/nature14242
12. Sawai CM, Babovic S, Upadhaya S et al (2016) Hematopoietic stem cells are the major source of multilineage hematopoiesis in adult animals. Immunity 45:597–609. doi:10.1016/j.immuni.2016.08.007
13. Pietras EM, Reynaud D, Kang Y-A et al (2015) Functionally distinct subsets of lineage-biased multipotent progenitors control blood production in normal and regenerative conditions. Cell Stem Cell 17:35–46. doi:10.1016/j.stem.2015.05.003
14. King KY, Goodell MA (2011) Inflammatory modulation of HSCs: viewing the HSC as a foundation for the immune response. Nat Rev Immunol 11:685–692. doi:10.1038/nri3062
15. Takizawa H, Boettcher S, Manz MG (2012) Demand-adapted regulation of early hematopoiesis in infection and inflammation. Blood 119:2991–3002. doi:10.1182/blood-2011-12-380113
16. Pietras EM, Mirantes-Barbeito C, Fong S et al (2016) Chronic interleukin-1 exposure drives haematopoietic stem cells towards precocious myeloid differentiation at the expense of self-renewal. Nat Cell Biol 18(6):607–618. doi:10.1038/ncb3346
17. Essers MAG, Offner S, Blanco-Bose WE et al (2009) IFNα activates dormant haematopoietic stem cells in vivo. Nature 458:904–908. doi:10.1038/nature07815
18. Ueda Y, Cain DW, Cain DW et al (2009) IL-1R type I-dependent hemopoietic stem cell proliferation is necessary for inflammatory granulopoiesis and reactive neutrophilia. J Immunol 182:6477–6484. doi:10.4049/jimmunol.0803961
19. Baldridge MT, King KY, Boles NC et al (2010) Quiescent haematopoietic stem cells are activated by IFN-gamma in response to chronic infection. Nature 465:793–797. doi:10.1038/nature09135
20. Pietras EM, Lakshminarasimhan R, Techner J-M et al (2014) Re-entry into quiescence protects hematopoietic stem cells from the killing effect of chronic exposure to type I interferons. J Exp Med 211:245–262. doi:10.1084/jem.20131043
21. Haas S, Hansson J, Klimmeck D et al (2015) Inflammation-induced emergency megakaryopoiesis driven by hematopoietic stem cell-like megakaryocyte progenitors. Cell Stem Cell 17:422–434. doi:10.1016/j.stem.2015.07.007
22. Matatall KA, Shen C-C, Challen GA, King KY (2014) Type II interferon promotes differentiation of myeloid-biased hematopoietic stem cells. Stem Cells 32:3023–3030. doi:10.1002/stem.1799
23. Ooi AGL, Karsunky H, Majeti R et al (2009) The adhesion molecule Esam1 is a novel hematopoietic stem cell marker. Stem Cells 27:653–661. doi:10.1634/stemcells.2008-0824
24. Salic A, Mitchison TJ (2008) A chemical method for fast and sensitive detection of DNA synthesis in vivo. Proc Natl Acad Sci U S A 105:2415–2420. doi:10.1073/pnas.0712168105
25. Barbier V, Nowlan B, Lévesque J-P, Winkler IG (2012) Flow cytometry analysis of cell cycling and proliferation in mouse hematopoietic stem and progenitor cells. Methods Mol Biol 844:31–43. doi:10.1007/978-1-61779-527-5_3
26. Oguro H, Ding L, Morrison SJ (2013) SLAM family markers resolve functionally distinct subpopulations of hematopoietic stem cells and multipotent progenitors. Cell Stem Cell 13:102–116. doi:10.1016/j.stem.2013.05.014
27. Pronk CJH, Rossi DJ, Månsson R et al (2007) Elucidation of the phenotypic, functional, and molecular topography of a myeloerythroid progenitor cell hierarchy. Cell Stem Cell 1:428–442. doi:10.1016/j.stem.2007.07.005

# Chapter 15

# A Facile, In Vitro 384-Well Plate System to Model Disseminated Tumor Cells in the Bone Marrow Microenvironment

**Johanna M. Buschhaus, Kathryn E. Luker, and Gary D. Luker**

## Abstract

Bone marrow disseminated tumor cells (DTCs) are dormant cancer cells that harbor themselves in a bone marrow niche for years after patient remission before potentially returning to a proliferative state, causing recurrent cancer. DTCs reside in bone marrow environments with physiologically important mesenchymal stem cells that are often negatively affected by chemotherapy treatments. Currently, there are very few models of DTCs that recapitulate their dormant phenotype while producing enough samples to accurately quantify cancer and surrounding stromal cell behaviors. We present a three-dimensional spheroid-based model system that uses dual-color bioluminescence imaging to quantify differential cell viability in response to various compounds. We successfully screened for compounds that selectively eliminated cancer cells versus supportive stromal cells and verified results with comparison to efficacy in vivo. The spheroid coculture system successfully modeled key aspects of DTCs in the bone marrow microenvironment, facilitating testing for compounds to selectively eliminate DTCs.

**Key words** Bioluminescence, Bone marrow, Breast cancer, Disseminated tumor cells, Dormancy, Spheroids

## 1 Introduction

Around 30% of breast cancer patients present with bone marrow (BM) disseminated tumor cells (DTCs) at the time of diagnosis [1]. These DTCs are usually in a non-proliferative state and present with possible immune escape and cancer stem cell phenotypes [2]. Undetectable by standard clinical imaging modalities, DTCs may remain dormant for years or decades before returning to an aggressive state [2, 3]. The phenomenon of tumor dormancy has not only been observed in breast cancer, but also in other epithelial cancers such as colon, lung, and prostate, thus expanding the clinical relevance of DTCs [2]. In breast cancer patients, these BM DTCs are associated with an increase in lymph node metastasis and more sizeable, higher histological grade, and hormone-receptor-negative

H. Daniel Lacorazza (ed.), *Cellular Quiescence: Methods and Protocols*, Methods in Molecular Biology, vol. 1686,
DOI 10.1007/978-1-4939-7371-2_15, 

tumors [1]. The patients harboring DTCs in their bone marrow at the time of initial surgery have a significantly higher risk of recurrent disease, skeletal metastases, distant disease, and death when compared to patients without BM DTCs [1–6].

Bone marrow is a specific niche that aids DTCs in maintaining a potential stem cell phenotype, surviving chemotherapy treatment, and withstanding various microenvironmental stresses [6]. The extracellular matrix, DTC-recruited bone marrow stromal cells, and bone marrow mesenchymal stem cells (MSCs) are fundamental aspects of this metastatic niche and increase the likelihood of DTC survival [7, 8]. MSCs have been shown to secrete exosomes containing assorted microRNAs that promote the dormant phenotype of DTCs [8]. The stem cell properties of MSCs also aid in restructuring the bone marrow niche to enable long-term DTC survival [9]. However, MSCs also provide vital support to hematopoietic stem cells (HSCs) by secreting various molecules [10]. As DTCs residing among MSCs are in a non-cycling state, they are often unaffected by chemotherapies whose mechanism of action targets proliferating cells [8, 11]. In fact, over 60% of BM DTC positive breast cancer patients who underwent neoadjuvant chemotherapy still contained DTCs after 12 months of treatment [12]. Such therapies are more likely to inadvertently harm MSCs whose elimination may lead to HSC death, in turn causing immune deficiency, a reduction in hematopoiesis, and hemorrhages [10]. At some point, dormant, protected DTCs must become aggressive to begin forming clinically detectable tumors [13]. Treatments that successfully eliminate DTCs while maintaining the health and vital function of MSCs, and in turn HSCs, remain an unmet clinical need.

There are currently very few models available to study DTCs and drug efficacy which encompass integral aspects of DTCs, such as extensive cell-cell adhesion in three-dimensional growth, inhomogeneous drug and nutrient distributions, and cancer cell quiescence [14]. Other groups have performed two-dimensional cell culture experiments to investigate the relationship between stromal and cancer cells, as well as the anticancer drug effects on the system [15, 16]. These models encompass aspects of an ideal system such as being high-volume, easy to execute, and readily analyzable. However, two-dimensional culture models fail to recapitulate many features of DTCs and their surrounding environment as cells are grown in a uniform, homogenous manner on plastic dishes. DTCs have also been modeled in an in vitro, three-dimensional gel coculture system that recapitulates breast cancer cells in both growth inhibitory and supportive bone marrow niches. This experimental system provides an accurate model for cancer cell quiescence but unfortunately prohibits bulk screening of cancer and stromal cell population viabilities [17].

The system to model DTCs in the bone marrow environment described in this protocol is simple, high-volume, and allows for multifaceted analysis of the tumor microenvironment. Human breast cancer cells and bone marrow stromal cells are plated in commercially available 384-well plates that form many uniform, healthy spheroids. Samples can be analyzed for the growth phase of breast cancer cells, differential drug effects on breast cancer cells and bone marrow stromal cells, and cancer cell outgrowth. The growth phase of individual cancer cells can be easily observed with fluorescence ubiquination-based cell cycle indicator (FUCCI) expressing cells. FUCCI markers express different colors depending on the cell's current cell cycle phase; red (G1), yellow (G1 to S transition), or green (S/G2/M) [18]. This dynamic mechanism verifies that breast cancer cells are truly in a growth-arrested phase and have the dormancy property fundamental to DTCs. Relative quantities of breast cancer cells and bone marrow stromal cells can be separately analyzed by dual-color bioluminescence imaging; a powerful tool that accurately measures relative cell numbers [19]. Cancer and stromal cells in the system are tagged with different bioluminescent proteins that emit light at two distinct wavelengths depending on cell type when treated with the same substrate. Consequently, growth of individual cell types over time can be easily monitored, which is useful in observing the effects of drug treatments on both cell types and identifying compounds that selectively eliminate the breast cancer cells over the bone marrow stromal cells. Colony outgrowth of plated spheroids allows detection of delayed cytotoxicity that prevents subsequent growth of cells. To verify the three-dimensional spheroid culture system's ability to recapitulate important aspects of DTCs and the bone marrow microenvironment, results were compared to in vitro, two-dimensional models and mouse models.

## 2 Materials

### 2.1 Molecular Biology

1. pCBR-Basic plasmid (for CBRed construct).
2. pCBG99-Basic plasmid (for CBG construct).
3. PCR primers: XbaI CBG99 forward 5′-ATTATCTAGAACCGCCATGGTGAAGCGTGAGAAAAATGTC-3′; XbaI CBG99 reverse 5′-ATTATCTAGACTAACCGCCGGCCTTCTCCAACAATTG-3′; XbaI CBR forward 5′-ATTATCTAGAACCGCCATGGTAAAGCGTGAGAAAAATGTC-3′; XbaI CBR reverse 5′-ATTATCTAGATTACTAACCGCCGGCCTTCACCAAC-3′
4. Lentiviral vector FUW.
5. Fluorescence ubiquination-based cell cycle indicators (*see* **Note 1**): FUCCI C mKO2-hCdt1(30/120)/pCSII-EF-MCS plasmid

and FUCCI D mAcGFPhGeminin(1/110)/pCSII-EF-MCS plasmid.

6. Enzymes, buffers, and equipment for PCR.
7. Restriction enzymes for DNA and ligations.

### 2.2 Cell Culture

1. Immortalized human bone marrow mesenchymal stem cell line HS-5 (HS-5).
2. Breast cancer cell line MDA-MB-231 (231).
3. Breast cancer cell line T-47D (T-47D).
4. Standard Fetal Bovine Serum (FBS).
5. Dulbecco's Modified Eagle Medium with high glucose and pyruvate (DMEM).
6. Penicillin Streptomycin Glutamine, 100×.
7. 0.25% Trypsin-EDTA, 1×.
8. Sterile Phosphate-Buffered Saline pH 7.4, 1×.
9. Miscellaneous desired cell culture supplies such as plasticware, incubators, and sterile pipettes.

### 2.3 Spheroid Coculture

1. 384-well low volume black round-bottom polystyrene NBS™ microplate, nonsterile.
2. Polystyrene universal microplate lid, sterile.
3. Spheroid medium: phenol-red free DMEM supplemented with 1% FBS, 0.1 nM β-Estradiol, penicillin and streptomycin (1×), glutamine, and sodium pyruvate (1×).
4. 10 nM stock solution of β-Estradiol (suitable for cell culture) in ethanol.
5. Sodium Pyruvate, 100×.
6. Multichannel pipettes with volumes from 1 to 200 μl.
7. Sterile pipette tips with low adherence.

### 2.4 Bioluminescence Imaging

1. High sensitivity bioluminescence imaging system (*see* **Note 2**).
2. Software compatible with bioluminescence imaging system for data quantification (*see* **Note 3**).
3. 15 mg/mL D-Luciferin, potassium salt, in sterile PBS. Filter solution through a 0.2 μm syringe filter and store at −20 °C until use.

### 2.5 Fluorescence Microscopy

1. Two-photon imaging system with variable laser power and compatible 25× objective (*see* **Note 4**).
2. Transfer and imaging (TRIM) plate (*see* **Note 5**).
3. Epifluorescence microscope with compatible 10× objective and red and green filter cubes (*see* **Note 6**).

### 2.6 Three-Dimensional Spheroid Treatment

1. Chemical compounds (*see* **Note 7**): Cisplatin, Doxorubicin, Paclitaxel, PD0325901.
2. Sterile ultrapure water, type 1 (Milli-Q™ water or similar).

### 2.7 Quiescence, Dissociation, and Colony Outgrowth from Spheroids

1. 6-well plates.

### 2.8 Cytotoxicity Assays in Two-Dimensional Culture

1. 96-well plate.

### 2.9 Animal Models of Bone Marrow Metastasis and Drug Treatment

1. Small animal shaver (Wahl compact cordless trimmer or similar instrument).
2. Depilatory solution such as Nair™.
3. 28- to 30-gauge insulin syringes for intraperitoneal and intracardiac injections.
4. Stereotaxic manipulator for intracardiac injections (optional).
5. Isoflurane.
6. Various desired surgical supplies.
7. Sterile 0.9% w/v NaCl solution.
8. Adult female NSG mice (*see* **Note 8**).
9. Chemical compounds (*see* **Note 7**): Doxorubicin (NDC-0069-3030-20 as clinical formulation, University of Michigan Hospital Pharmacy) and Trametinib (GSK112021).
10. Dimethyl sulfoxide (DMSO).
11. Solution of 1% carboxymethylcellulose (sodium salt, low viscosity) and 0.4% Tween® 80.
12. Flow Cytometer capable of exciting at 561 and 488 nm, such as BD FACS Aria II.

## 3 Methods

### 3.1 Construct and Maintain Stably-Expressing Cells

1. To generate stable cell lines constitutively expressing desired cell markers (*see* **Note 9**), use lentiviral transduction methods. Then, select those cells that are stably expressing desired markers. We refer readers to standard molecular biology texts for instructions on how to transfer reporters to lentiviral vectors and select for the stably-expressing cells. HS-5 cells were generated to stably express CBRed, 231 cells were generated to stably express CBGreen and FUCCI, and T-47D cells were generated to stably express CBGreen and FUCCI.

2. Before utilizing transduced cells in experiments, verify expression of the reporter in stable cell lines. Methods to do so include qRT-PCR or Western Blotting (refer to standard texts for techniques), fluorescence (flow cytometry or microscopy), or bioluminescence imaging assays (detailed below).
3. Maintain cells in appropriate culture medium as recommended by the supplier. For cells described in this section, we use DMEM supplemented with 10% FBS, penicillin, streptomycin, and glutamine (standard growth medium). Passage cells every 2–4 days by trypsinization and resuspension.

### 3.2 Spheroid Coculture Model

1. Sterilize 384-well plates (*see* **Note 10**) by UV radiation for 90 s.
2. For each spheroid, place cancer cells (*see* **Note 11**) along with CBRed HS-5 for a total of $3 \times 10^3$ cells per well in 25 μl of spheroid medium (*see* **Note 12**). These spheroids will grow to approximately 200–300 μm diameter. For 231 spheroids make the spheroid 1% 231 CBGreen and FUCCI. For T-47D cells, make the spheroid 5% T-47D CBGreen and FUCCI.
3. Distribute control wells throughout the plate to normalize for the effect of position on bioluminescence signaling. To decrease the amount of medium evaporation in experimental wells, fill the outermost wells of the plate with 25 μl of medium.
4. Maintain spheroids in long-term culture by carefully removing 20 μl of medium from each well and gently replacing used medium with 18 μl of a new spheroid medium using a 20 μl multichannel pipette to ease and quicken spheroid handling in the 384-well plates (*see* **Note 13**). Remove the medium from the wells by barely sticking the tips in the medium to avoid aspirating the spheroids and empty waste into a designated reservoir.

### 3.3 CBGreen and CBRed Bioluminescence Imaging

1. Capture signals from bioluminescence using a bioluminescence imaging system with optical filters to separate CBGreen and CBRed light emissions and analyze data using software compatible with the specific imaging system.
2. For spheroid imaging, gently remove 5 μl of the medium from each well of the 384-well plate. Quickly add 5 μl of a 1:4 dilution of 150 μg/mL luciferin (*see* **Note 14**) for a final luciferin dilution of 1:20 or 7.5 μg/ml of luciferin in each well.
3. For imaging standard two-dimensional culture systems, quickly add 10 μl of a 1:10 dilution of 150 μg/ml luciferin (*see* **Note 14**) to each well of the 96-well plate for a final luciferin dilution of 1:100, or 1.5 μg/ml of luciferin, in each well.
4. After adding luciferin, incubate cells at 37 °C for 5 min and place a single plate in the IVIS. Use medium binning, a

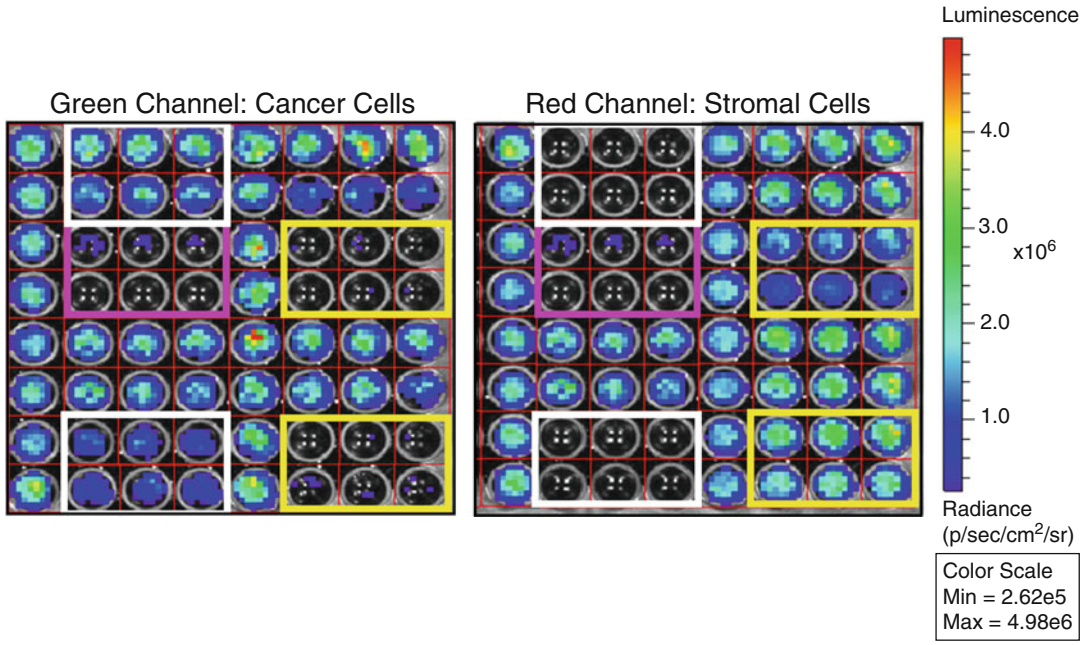


**Fig. 1** Dual-color bioluminescence imaging. Bioluminescence imaging of a 384-well plate section after treating spheroids with multiple different compounds. Cancer cell signals (CBGreen) and stromal cell signals (CBRed) are detected in the green and red channels, respectively. *Pink* bins show compounds toxic to both stromal and cancer cells, *white* bins show compounds that destroy stromal cells and not cancer cells, and *yellow* bins show compounds that eliminate cancer cells and not stromal cells. Scale bar depicts bioluminescence on a pseudo color scale with *red* and *blue* indicating high and low signaling, respectively

3–5 min exposure time for each channel, a 520 nm band pass filter for CBG imaging, and 680 nm band pass filter for CBR imaging settings to acquire images (Fig. 1). Separate signals using previously discussed methods (*see* **Note 15**).

### *3.4 Fluorescence Microscopy*

1. Using an upright Olympus FVE1000 MPE microscope with a 25× NIR corrected objective, acquire Z-stack slice sequences of spheroids. Two-photon microscopy has the benefit of minimal out of plane signaling and that both FUCCI proteins are excited at the same wavelength to decrease imaging time and photobleaching.
2. Since the microscope objective requires immersion in water, transfer spheroids to a TRIM plate to increase imaging efficiency and quality.
3. Use an excitation wavelength of 920 nm to excite both FUCCI proteins. FUCCI C protein emission is captured in the red channel (575–630 nm) and indicates the cell is in the G1 phase. FUCCI D protein emission is captured in the green channel (495–540 nm) and indicates the cell is in either S/G2/M phases (*see* **Note 1**).

4. Acquire 150 μm deep stacks of spheroid images with a 5 μm step size (30 images per spheroid). Two-photon signal decreases while imaging deeper into a spheroid and using the Olympus Bright-Z function helps compensate for this decrease in signaling. The Bright-Z function allows the user to adjust laser power and/or detector gain throughout a Z-stack for optimal imaging (unsaturated but maximized signals) throughout the spheroid. For optimal data analysis, keep spheroid image acquisition parameters consistent throughout a single experiment.
5. For two-dimensional culture experiments, use an Olympus IX70 epifluorescence microscope to easily visualize FUCCI markers. Signal is visible when using either red or green filter cubes.

### 3.5 Three-Dimensional Spheroid Treatment

1. Using the spheroid coculture model protocol, develop spheroids for 2 days before starting treatment with specified compounds and concentrations.
2. Compound preparation of various concentrations:
   (a) Dissolve cisplatin in sterile ultrapure water, type 1, to create concentrations between $10^{-1}$ and $10^{5}$ nM.
   (b) Dissolve doxorubicin in sterile ultrapure water, type 1, to create concentrations between 1 and $10^{5}$ nM.
   (c) Dissolve paclitaxel in sterile DMSO to create concentrations between $10^{-2}$ and $10^{3}$ nM.
   (d) Dissolve PD0325901 in sterile DMSO to create concentrations between $10^{-2}$ and $10^{3}$ nM.
3. On day 2, use two to four columns of the plate to measure preliminary bioluminescence of spheroids to help establish the growth curve before beginning compound treatment in the remaining wells (*see* **Note 16**).
4. Exchange compound-containing spheroid medium every other day using the same method as noted above.
5. Image spheroid bioluminescence after 8 days of treatment (Fig. 2). After imaging, exchange the medium in each well with 20 μl of medium three times to remove the majority (>99%) of remaining luciferin and compounds (*see* **Note 16**). In case of desired future cell-recovery, exchange medium in each will for a total of 6 days (two medium changes).

### 3.6 Quiescence, Dissociation, and Colony Outgrowth from Spheroids

1. Use the abovementioned "Spheroid coculture model" protocol to culture both types of cancer cell spheroids (231 CBGreen and FUCCI or T-47D CBGreen and FUCCI cells) and image for FUCCI markers 2 and 10 days after beginning culture. FUCCI reporters present orange when the cell is in the G1 phase and green when in the S/G2/M phases (*see* **Note 1**).

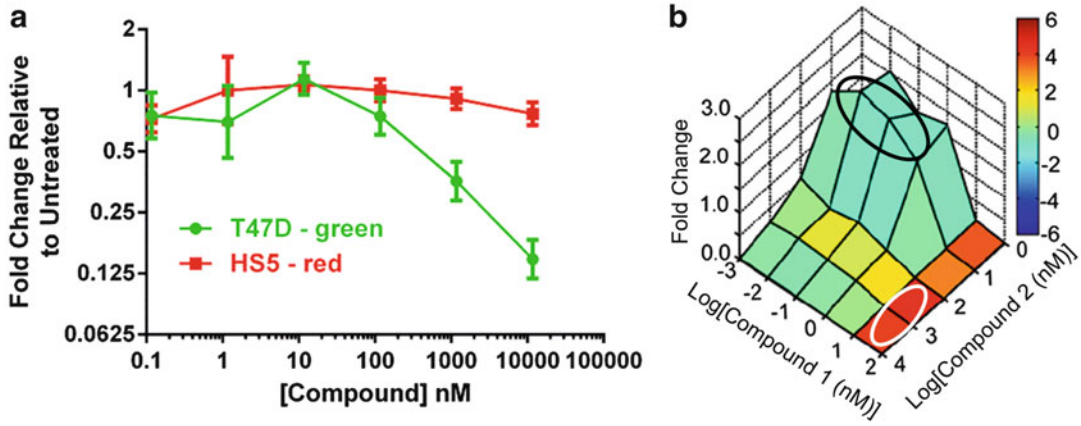


**Fig. 2** Cellular responses to compound treatments. (**a**) Drug response curves. Graph shows mean values ± SEM for bioluminescence fold change in response to varying compound concentrations for both T-47D cells (*green curve*) and HS-5 cells (*red curve*). Fold change was determined in comparison to untreated spheroids. Curves may be used to determine optimal drug dosing to differentially eliminate cancer cells over stromal cells. (**b**) Combinatorial drug dose response plot. Cancer cell fold change in response to compound combination treatments. Fold change was determined by normalizing bioluminescent image data of treated cells to control cells after 8 days of combination treatment. Color scale bar shows selectivity of compounds for eliminating cancer versus stromal cells. *Red* and *blue* depict highest and lowest selectivity, respectively. The *white circle* delineates optimal combination drug treatments for selectively eliminating cancer cells over stromal cells. The *black circle* shows combination treatment concentrations that do not inhibit cancer cell growth and kill stromal cells

2. As well as imaging on days 2 and 10, dissociate parallel spheroids of each condition on both days to analyze two-dimensional colony outgrowth.
   (a) Use a 200 μl pipette and tip to gently aspirate spheroids. Place spheroids undergoing the same treatment together into a well of a 6-well plate containing 2 ml of 1× PBS. Make sure that each condition has the same number of spheroids per well.
   (b) Once spheroids are collected, carefully aspirate PBS and add 0.2 ml of trypsin to each well.
   (c) Add 1.3 ml of growth medium per plate after spheroids are dissociated and gently swirl to evenly spread cells.
3. Image cells 1, 4, and 8 days after seeding cells with both epifluorescence, to visualize the growth phase of cells using FUCCI markers, and bioluminescence using the protocols described above. Replace medium on cells after bioluminescence imaging to reduce luciferin toxicity on cells and 6 days after seeding to maintain optimum nutrient concentrations. The higher rate of growth of the cancer cells in two-dimensional culture (versus three-dimensional culture) requires only analyzing CBGreen signaling.

### 3.7 Cytotoxicity Assays in Two-Dimensional Culture

1. Place a total of $1 \times 10^4$ cells per well with 100 μl growth medium in a 96-well plate. Use a mixture of 4% 231 CBG and FUCCI cells and 96% HS-5 CBR cells. Make sure that the cell types are mixed together well to create a homogenous coculture.
2. Grow cells for 24 h and subsequently treat cells with compounds for 72 h.
3. Prepare cisplatin, doxorubicin, and paclitaxel at an appropriate range of concentrations to create a cytotoxicity curve for two-dimensional cell culture conditions (*see* **step 2** in Subheading 3.5).
4. Use the bioluminescence imaging protocol detailed above to quantify drug toxicity.

### 3.8 Animal Models of Bone Marrow Metastasis and Drug Treatment (See Note 17)

1. Inject 100 μl of $1 \times 10^5$ 231 CBG and FUCCI cells suspended in 0.9% NaCl solution via intracardiac injection into the left ventricles of female NSG mice between 5 and 9 weeks old. Randomly assign mice to treatment and vehicle groups 3 days after cancer cell injection. Administer either: (a) a single intraperitoneal injection of doxorubicin (5 mg/kg, *see* **Note 18**), (b) five daily doses of trametinib by oral gavage (1 mg/kg, *see* **Note 19**), (c) combined treatment of doxorubicin and trametinib, or (d) vehicle controls.
2. 13 days after beginning treatment (e.g., 7 days after the last dose of trametinib or vehicle is given), humanely euthanize mice per institutional protocols.
3. Harvest bone marrow from the lower extremities of mice by flushing through the interior of the femur and tibia with PBS [20].
   (a) To quantify cancer cell growth, plate recovered bone marrow in a 10 cm tissue culture treated dish with standard growth medium. One week after plating bone marrow contents, use the bioluminescence imaging protocol described above to quantify growth of 231 cells.
   (b) To perform flow cytometry analysis of harvested bone marrow, keep each sample separate, centrifuge recovered bone marrow, and resuspend in 200 μl of PBS. For each sample, analyze $5 \times 10^5$ events using an appropriate flow cytometer.

## 4 Notes

1. The FUCCI construct used and described in these methods is not the most current and robust system available as it emits only red (G1) or green (S/G2/M) wavelengths. A newer

construct is commercially available [18] and emits at red (G1), yellow (G1 to S transition), or green (S/G2/M) wavelengths.

2. We used an IVIS Lumina Series III (Perkin Elmer, Waltham, MA) for all bioluminescence imaging.
3. We used Living Image 4.3.1 for all bioluminescence image processing.
4. We used an Olympus FVE1000 MPE microscope for all two-photon microscopy. Alternatively, confocal microscopy with lasers at 543 nm (red) and 488 nm (green) can be used. However, confocal microscopy does not excite both FUCCI proteins with the same wavelength. A 25× NIR corrected objective (XLPLN25XWMP, NA = 1.05, Olympus, Tokyo, Japan) was used in conjunction with the microscope.
5. We designed the TRIM (transfer, imaging, and analysis) plate to facilitate transfer and stabilization of spheroids for fluorescence microscopy. The protocol for fabricating the TRIM plate has been described previously [21].
6. We used an Olympus IX70 microscope for all epifluorescence imaging. Images were taken through custom red and green filter cubes (Olympus ©) using a 10× objective.
7. Cisplatin (NDC-0703-5748-11), doxorubicin (NDC-0069-3030-20), and paclitaxel (NDC-55390-304-50) were purchased as clinical formulations from the University of Michigan Hospital Pharmacy because the IACUC requires pharmaceutical grade drugs when possible for animal studies. Cell culture studies do not require pharmaceutical grade products and compounds may be purchased from other vendors.
8. NSG mice are used to promote the growth of human breast cancer xenografts. Although alternative strains of immunocompromised mice may be used, the growth of human breast cancer cells is deterred in less immunocompromised mice.
9. Cells stably expressing fluorescent and bioluminescent reporters are needed for long-term cell culture and animal studies. We employ lentiviral transduction to generate stably-expressing populations of cancer cells.
10. 384-well plates are used to culture spheroids because they are low-cost, easy to use, have low cell adhesion, and permit bulk experiments. The geometry of the well promotes quick spheroid growth (<24 h) and production of a single, uniform, stable, and reproducible spheroid per well.
11. Percentages of cancer cells are optimized to mimic relatively small numbers of DTCs in bone marrow and to read bioluminescence signal. There must be enough cancer cells to provide sufficient signal to be detected by imaging but not so many cells to produce detectable signal CBGreen signal in the

CBRed imaging filter window. The percentage of cancer cells per spheroid varies between cancer cell types due to differing growth rates of the T-47D and 231 cells.

12. Spheroid medium is formulated to match all but the serum content and phenol red in standard growth medium.
13. To avoid wasting tips, flush out the tips three times with sterile 1× PBS from a reservoir to remove medium from wells within the same experimental group. Use the multichannel pipette with new tips to collect medium from a reservoir (per experimental group) and gently add it to each well to avoid rupturing the formed spheroids.
14. Further dilute luciferin in sterile 1× PBS at the desired concentration before adding to spheroids or cells.
15. Images were taken with large binning and a 2 min exposure time. To gather both red and green signals, acquire images of the same plane using both 530–550 nm and 690–710 nm emission filters on the bioluminescence imaging system [22].
16. Leaving the luciferin on the cells is toxic and will skew results. Removing and diluting the medium also helps remove the compound from the system, which is desired as it is the end of the experiment.
17. All the animal procedures should be approved by the local IACUC (our protocol was approved by the University of Michigan Committee for the Use and Care of Animals).
18. Only a single dose of doxorubicin was administered because multiple doses are toxic to NSG mice. As doxorubicin was obtained already in solution from the University of Michigan Hospital pharmacy, commercial DMSO was used as a vehicle control.
19. Formulate trametinib for gavage [23] by dissolving it in sterile 100% DMSO and then diluting trametinib 1:9 in a sterile-filtered solution of 1% carboxymethylcellulose and 0.4% Tween-80.

## References

1. Braun S, Vogl FD, Naume B et al (2005) A pooled analysis of bone marrow micrometastasis in breast cancer. N Engl J Med 353 (8):793–802
2. Pantel K, Alix-Panabieres C (2014) Bone marrow as a reservoir for disseminated tumor cells: a special source for liquid biopsy in cancer patients. Bonekey Rep 3:584
3. Zhang X, Giuliano M, Trivedi M et al (2013) Metastasis dormancy in estrogen receptor-positive breast cancer. Clin Cancer Res 19 (23):6389–6397
4. Bidard FC, Vincent-Salomon A, Gomme S et al (2008) Disseminated tumor cells of breast cancer patients: a strong prognostic factor for distant and local relapse. Clin Cancer Res 14:3306–3311
5. Kim MY, Oskarsson T, Acharyya S et al (2009) Tumor self-seeding by circulating cancer cells. Cell 139(7):1315–1326

6. Kang Y, Pantel K (2013) Tumor cell dissemination: emerging biological insights from animal models and cancer patients. Cancer Cell 23 (5):573–581
7. Oskarsson T, Massagué J (2012) Extracellular matrix players in metastatic niches. EMBO J 31 (2):254–256
8. Ono M, Kosaka N, Tominaga N et al (2014) Exosomes from bone marrow mesenchymal stem cells contain a microRNA that promotes dormancy in metastatic breast cancer cells. Sci Signal 7(332):ra63
9. Frenette P, Pinho S, Lucas D et al (2013) Mesenchymal stem cell: keystone of the hematopoietic stem cell niche and a stepping-stone for regenerative medicine. Annu Rev Immunol 31:285–316
10. Cao J, Tao M, Yang P et al (2008) Effects of adjuvant chemotherapy on bone marrow mesenchymal stem cells of colorectal cancer patients. Cancer Lett 263(2):197–203
11. Braun S, Kentenich C, Janni W et al (2000) Lack of effect of adjuvant chemotherapy on the elimination of single dormant tumor cells in bone marrow of high-risk breast cancer patients. J Clin Oncol 18(1):80–86
12. Mathiesen RR, Borgen E, Renolen A et al (2012) Persistence of disseminated tumor cells after neoadjuvant treatment for locally advanced breast cancer predicts poor survival. Breast Cancer Res 14:R117
13. Cameron MD, Schmidt E, Kerkvliet N et al (2000) Temporal progression of metastasis in lung: cell survival, dormancy, and location dependence of metastatic inefficiency. Cancer Res 60(9):2541–2546
14. Mehta G, Hsiao A, Ingram M et al (2012) Opportunities and challenges for use of tumor spheroids as models to test drug delivery and efficacy. J Control Release 164(2):192–204
15. McMillin DW, Delmore J, Weisberg E et al (2010) Tumor cell-specific bioluminescence platform to identify stroma-induced changes to anticancer drug activity. Nat Med 16 (4):483–489
16. Weisberg E, Liu Q, Zhang X et al (2013) Selective Akt inhibitors synergize with tyrosine kinase inhibitors and effectively override stroma-associated cytoprotection of mutant FLT3-positive AML cells. PLoS One 8(2): e56473
17. Marlow R, Honeth G, Lombardi S et al (2013) A novel model of dormancy for bone metastatic breast cancer cells. Cancer Res 73 (23):6886–6899
18. Sakaue-Sawano A, Kurokawa H, Morimura T et al (2008) Visualizing spatiotemporal dynamics of multicellular cell-cycle progression. Cell 132(3):487–498
19. Cavnar S, Rickelmann A, Meguiar K et al (2015) Modeling selective elimination of quiescent cancer cells from bone marrow. Neoplasia 17(8):625–633
20. Stacer AC, Wang H, Fenner J et al (2015) Imaging reporters for proteasome activity identify tumor- and metastasis-initiating cells. Mol Imaging 14:414–428
21. Cavnar S, Salomonsson E, Luker K et al (2013) Transfer, imaging, and analysis plate for facile handling of 384 hanging drop 3D tissue spheroids. J Lab Auto 19(2):208–214
22. Coggins NL, Trakimas D, Chang SL et al (2014) CXCR7 controls competition for recruitment of β-arrestin 2 in cells expressing both CXCR4 and CXCR7. PLoS One 9(6): e98328
23. Kwong L, Costello J, Liu H et al (2012) Oncogenic NRAS signaling differentially regulates survival and proliferation in melanoma. Nat Med 18(10):1503–1510

# Chapter 16

# Distinguishing States of Arrest: Genome-Wide Descriptions of Cellular Quiescence Using ChIP-Seq and RNA-Seq Analysis

**Surabhi Srivastava, Hardik P. Gala, Rakesh K. Mishra, and Jyotsna Dhawan**

## Abstract

Regenerative potential in adult stem cells is closely associated with the establishment of—and exit from—a temporary state of quiescence. Emerging evidence not only provides a rationale for the link between lineage determination programs and cell cycle regulation but also highlights the understanding of quiescence as an actively maintained cellular program, encompassing networks and mechanisms beyond mitotic inactivity or metabolic restriction. Interrogating the quiescent genome and transcriptome using deep-sequencing technologies offers an unprecedented view of the global mechanisms governing this reversibly arrested cellular state and its importance for cell identity. While many efforts have identified and isolated pure target stem cell populations from a variety of adult tissues, there is a growing appreciation that their isolation from the stem cell niche in vivo leads to activation and loss of hallmarks of quiescence. Thus, in vitro models that recapitulate the dynamic reversibly arrested stem cell state in culture and lend themselves to comparison with the activated or differentiated state are useful templates for genome-wide analysis of the quiescence network.

In this chapter, we describe the methods that can be adopted for whole genome epigenomic and transcriptomic analysis of cells derived from one such established culture model where mouse myoblasts are triggered to enter or exit quiescence as homogeneous populations. The ability to synchronize myoblasts in $G_0$ permits insights into the genome in "deep quiescence." The culture methods for generating large populations of quiescent myoblasts in either 2D or 3D culture formats are described in detail in a previous chapter in this series (Arora et al. Methods Mol Biol 1556:283–302, 2017). Among the attractive features of this model are that genes isolated from quiescent myoblasts in culture mark satellite cells in vivo (Sachidanandan et al., J Cell Sci 115:2701–2712, 2002) providing a validation of its approximation of the molecular state of true stem cells. Here, we provide our working protocols for ChIP-seq and RNA-seq analysis, focusing on those experimental elements that require standardization for optimal analysis of chromatin and RNA from quiescent myoblasts, and permitting useful and revealing comparisons with proliferating myoblasts or differentiated myotubes.

**Key words** Quiescence, ChIP-seq, RNA-seq, Myoblasts, C2C12, $G_0$

H. Daniel Lacorazza (ed.), *Cellular Quiescence: Methods and Protocols*, Methods in Molecular Biology, vol. 1686,
DOI 10.1007/978-1-4939-7371-2_16, 

## 1 Introduction

Adult stem cells (ASC) differ from pluripotent stem cells (ESC or iPSC, here collectively referred to as PSC), which proliferate very rapidly and have a distinct cell cycle regulation. Therefore, while conditions that slow the proliferation of PSC lead to either multilineage differentiation or cell death, in somatic or adult stem cells, a third cell fate is possible: slowing proliferation can trigger a quiescence program, which permits reversible arrest. Thus, while adult stem cells are restricted in their capacity for differentiation compared to PSC, their capacity for self-renewal is strong, and facilitated by a tightly regulated program of quiescence. The benefits of entry into a quiescent state for an individual cell include resistance to genotoxic or nutritional stress [1–3], but for the tissue that harbors quiescent cells, this reserve population provides the important benefit of regeneration [4].

Earlier believed to be a passive withdrawal from the cell cycle in response to insufficient mitogenic stimulation and subsequent metabolic repression, the quiescent state is being redefined as an actively regulated state of temporary or reversible cell cycle arrest [3, 5, 6], with important implications for many stem cell types. Importantly, entry into quiescence is associated with active blocking of cell senescence and death [7–9]. Quiescence is evolutionarily ancient [10], and it is increasingly clear that highly conserved signaling pathways control activation of reversibly arrested cells [11, 12].

Adult stem cell populations from mammalian tissues such as the hematopoietic system (HSCs), epithelia, neuronal progenitors, hair follicles, and skeletal muscle (satellite cells) have been extensively studied to understand changes in cell state associated with differentiation, self-renewal, aging, and tissue repair [13–17]. Increasingly, these well-defined populations are also being used to study quiescence, whose regulation is critical for tissue homeostasis. Skeletal muscle tissue is well suited to a comparison of irreversible and reversible arrest since the terminally differentiated muscle fibers contain permanently post-mitotic nuclei, while the resident muscle stem cells are temporarily arrested until activated for regeneration [18].

There are several biological and technical challenges in studying the regulation of quiescence in vivo. First, locating the niche where quiescent cells are harbored requires a combination of unique markers of quiescence as well as those that define tissue-specificity. In the case of skeletal muscle, the niche is well defined between the basement membrane that surrounds each myofiber and its plasma membrane [19]. Thus, these satellite stem cells can be imaged in histological sections and on isolated myofibers, and excellent markers for defining both the niche and various stages of activation of the stem cell are available [20–22]. Second, stem cells are typically

present in very low numbers in vivo (for example, about $0.5–2 \times 10^5$satellite cells per mouse) [23, 24]. However, several surface markers or genetically encoded markers such as Pax3/7-gfp can be used for cell sorting by flow cytometry in sufficient numbers for molecular analysis [25–27]. By far the greatest hurdle to the study of quiescence at a genome-wide level in vivo is that isolation of dormant cells from their niche leads to alterations in the quiescent state of these cells: while disruption of the association with the myofiber does not immediately lead to proliferation, the transition from quiescence into the cell cycle takes only minutes and sets in motion a profound change of cellular state. Therefore, the freshly isolated previously dormant stem cell population while not yet dividing, no longer represents the "deeply quiescent" stem cell in vivo. Our approach to access deep quiescence has been to impose quiescence on proliferating populations of myogenic cells in culture, and study their entry into the dormant state as well as activation back into the cell cycle. Undoubtedly, this in vitro system carries a different set of caveats, including the substantial intrinsic differences between a cell line and the primary stem cell, and the altered signaling environment, but the benefits of controlled access to the genome of the essentially quiescent state are still useful. Until methods for isolating RNA and chromatin from quiescent stem cells fixed in situ become routine, the culture option for obtaining large populations of deeply quiescent cells will remain an attractive model.

Exit from the cell cycle into quiescence ($M/G_1$ to $G_0$ transition) is associated with decreased nuclear and metabolic activity and reduced cell size. Quiescence is completely reversible and quiescent cells in culture are viable, readily regaining their form and function upon activation, though the exact mechanisms by which the $G_0$ transcriptional program is reactivated remain unknown. We have previously described our laboratory protocol for an in vitro model for satellite cell quiescence using a C2C12 myoblast culture system [28] that allows comparison of the quiescent ($G_0$) state with proliferating myoblasts (MB) and terminally differentiated myotubes (MT). Both MT and $G_0$ represent nondividing states but are associated with distinct programs, i.e., cellular differentiation versus reversible arrest and it is of interest to delineate the genome-wide epigenetic changes that orchestrate the two programs using whole genome ChIP-seq and RNA-seq approaches. Contrasting these results with those from cycling myoblasts (MB) can provide useful insights into the common features of arrested cells and help define the switch between the quiescent and proliferative transcriptional programs.

Chromatin state is instrumental in controlling cellular function and identity by driving gene expression: each stage in a cell's development is tightly governed by epigenetic switches that regulate access to the transcriptional machinery. Epigenetic regulation

represents a dynamic mechanism for stem cells to respond to physiological and differentiation cues, and epigenetic marks likely define chromatin states associated with entry and exit into quiescence and its maintenance [29]. Histone modifications, DNA methylation and binding of chromatin proteins and remodelers are some of the critical epigenetic factors that specify chromatin state [30–32]. The presence of these marks at loci of interest can be detected by chromatin immunoprecipitation (ChIP) and concomitant changes to gene expression can be assayed by the investigation of the transcript profile. The widespread use of next-generation sequencing (NGS) technologies [33] downstream to chromatin and RNA-based techniques provides the ability for in-depth investigation of genome-wide changes in chromatin state.

Although the epigenome of a cell is informative of its gene expression potential, the functional output of transcription (mRNA level) provides direct estimate of gene expression. Before investigating the transcriptome profile of inactive quiescent cells for correlation with their epigenomic status and comparison across cell states, some key issues are worth consideration. RNA levels are linked to cellular physiology and vary not only across tissues but also within a given tissue or cell type [34, 35]. Moreover, cellular RNA levels change across development and cell cycle stages. Interestingly, the proportion of cells with 2n DNA content (interpreted as $G_0/G_1$ using cell cycle analysis), which display reduced levels of RNA, actually represent the $G_0$ population [34, 36, 37]. Moreover, the level of cellular RNA is tightly regulated and depends on cell size as well as cytoplasm to nuclear ratio [38, 39]. Although ribosomal RNA constitutes the bulk of cellular RNA (90–95%), the messenger RNA (mRNA) protein-coding RNA pool has been shown to vary the most with cell size [40–42] and stage of the cell cycle [43]. This varying cellular RNA content poses a challenge in global gene expression studies and interpretations drawn from these analyses. A recent study describes an approach to compare cell types with varying cellular RNA contents [44] by the addition of known exogenous control RNAs proportional to cell number, thereby minimizing bias.

In order to carry out gene expression profiling in quiescent cell types that vary in cellular RNA content, we have adopted key technical modifications prior to the standard NGS library preparation. Importantly, these help to account for the varying levels of RNA per cell between cell states, so that instead of equal amounts of total RNA, equal cell numbers are used to identify differentially expressed genes. Similar methods have been used in recent studies leading to overall conclusions that are strikingly different from those drawn when equal RNA is used [44, 45].

The methods to achieve the $G_0$, MB, and MT cell states and study their biology have already been outlined by Arora et al. [28], along with detailed descriptions of the culture methods used by our

lab to achieve reversible arrest. In this chapter, we focus on the methodology employed for whole genome ChIP- and RNA-seq assays on these three cellular states as a means to study the role of epigenetic regulation in setting and maintaining quiescence.

## 2 Materials

### 2.1 Cell Line

This method was originally developed for C2C12 mouse myoblasts [46–49]. Briefly *C2C12 myoblasts* (obtained originally from H. Blau, Stanford and subcloned in our lab), are maintained in growth medium (GM; DMEM + 20% FBS); differentiation is induced in low mitogen medium (DM: DMEM + 2% horse serum), for 5 days to form mature myotubes; synchronization in $G_0$ by suspension culture in 1.3% methylcelluose prepared in GM [28]. Quiescence can also be imposed on *human primary myoblasts* (isolated from muscle biopsies) [50, 51], or *mouse muscle satellite cells* purified from adult mice [52].

Regardless of the method used to generate quiescent myoblasts, a key set of control experiments that should accompany each genome-wide experiment is to establish that the cells are indeed quiescent as judged by: cell cycle status (flow cytometric confirmation of majority 2n population (>90%), low levels or absence of Cyclin mRNAs, repression of p21 mRNA/protein, induction of p27 mRNA/protein, and absence of BrdU incorporation) and myogenic status (induction of Pax 7 mRNA/protein, repression of MyoD, and absence of Myogenin).

In our experience, C2C12 myoblasts if treated vigilantly to ensure that stock cultures are routinely checked for absence of Myogenin positive cells, are extremely well behaved and enter quiescence robustly and homogeneously when cultured in suspension, readily exiting when replated on culture surfaces. However, primary human and mouse satellite cell cultures always retain a small population of triggered myoblasts which differentiate when exposed to quiescence-inducing conditions, and it is required to identify and remove that population from the analysis since it would skew the genomic profile.

### 2.2 Cell Culture Reagents

1. C2C12 growth medium (C2GM): Dulbecco's Modified Eagle Medium (DMEM, high glucose), 20% Fetal Bovine Serum, 1% Glutamax, 1% Penicillin-Streptomycin.
2. Phosphate Buffer Saline (PBS): Dissolve 200 mg of potassium chloride, 200 mg of potassium biphosphate, 8 g of sodium chloride, 1.15 g of disodium hydrogen phosphate in deionized water. Make up the volume to 1 l with deionized water.
3. Cell dissociation solution, non-enzymatic, 1×.

### 2.3 Chromatin Immunoprecipitation (ChIP) Reagents

1. Glycine: Dissolve 1.88 g in 10 ml of sterile nuclease-free water to get 2.5 M stock. Store at room temperature.
2. PMSF (phenyl methyl sulfonyl fluoride): Dissolve 174 mg in 10 ml of isopropanol to get 100 mM stock. It dissolves easily at room temperature by mixing and swirling. Store at −20 °C.
3. Protease inhibitor cocktail (PI): Dissolve 1 tablet (Roche) in 1 ml autoclaved milliQ water to get 50× stock.
4. RNase A: Dissolve 20 mg in 1 ml of autoclaved milliQ water to get 20 mg/ml stock. Store at −20 °C.
5. Proteinase K: Dissolve 10 mg in 1 ml of autoclaved milliQ water to get 10 mg/ml stock. Store at −20 °C.
6. ChIP dilution buffer with inhibitors: 0.01% SDS, 1.1% Triton-X 100, 1.2 mM EDTA, 16.7 mM Tris-HCl, pH 8.1, and 167 mM NaCl. Each time before use add 20 μl of 100 mM PMSF, 1 μl of 1 M DTT, and 40 μl of 50× PI to 2 ml of ChIP dilution buffer.
7. SDS lysis buffer: 1% SDS, 10 mM EDTA, and 50 mM Tris-HCl, pH 8.1. Add 50 μl of 100 mM PMSF, 2.5 μl of 1 M DTT, and 100 μl of 50× PI to 5 ml of lysis buffer.
8. LowCell# ChIP kit (Diagenode).
9. IPure kit (Diagenode).
10. NEBNext® DNA Library Prep kit for Illumina® (New England Biolabs).
11. NEBNext® Multiplex oligos for Illumina® (Index Primers set 1) (New England Biolabs).

### 2.4 RNA Isolation and RNA-seq

1. RNeasy Plus Mini Kit (Qiagen).
2. Agilent RNA 6000 Pico Kit on Agilent 2100 Bioanalyzer system.
3. DNA-free™ kit (Ambion).
4. RiboMinus™ Eukaryotic kit V2 (Ambion).
5. NEBNext® Ultra™ Directional RNA Library Prep Kit for Illumina® (New England Biolabs).
6. NEBNext® Multiplex oligos for Illumina®, index primers set 1 (New England Biolabs).
7. AMPure® XP Beads (Beckman Coulter).
8. Polypropylene microcentrifuge tubes, RNase and DNase free.
9. ERCC ExFold RNA Spike-In Mixes (Ambion).

## 3 Methods

### 3.1 Harvesting $G_0$ Cells

1. Suspend C2C12 cells in log phase of growth (not more than 70% confluency) at $1 \times 10^7$ cells per 100 ml suspension in a G250 bottle [28]. Mix gently to achieve a single-cell suspension.
2. After 48 h, harvest using a variation of the PBS wash method. At this time 99% of the cells are synchronized in $G_0$ phase.
3. Fill with pre-warmed PBS to the neck of the bottle, mix well, and spin in Sorvall at room temperature ($1250 \times g$) for 30 min (*see* **Note 1**).
4. Decant the supernatant slowly but completely until only about 5 ml of viscous solution remains. Cell pellet will be visible all over the base of the bottle after decanting. Dislodge pellet by pipetting PBS into the bottle and washing walls and base with repeated but gentle resuspensions.
5. Transfer cells from one bottle to two 50 ml falcon tubes. Fill with PBS to the top and centrifuge at $290 \times g$ for 10 min at room temperature. Slowly decant all the PBS, a good cell pellet should be visible. Repeat the PBS washes three times to remove all traces of the methylcellulose. Pool cells from both falcon tubes into one during the last wash.
6. Resuspend in 5 ml C2GM. Count cells. Up to 16 million cells may be obtained, though they may be difficult to count because of viscosity of leftover methylcellulose. Count in multiple aliquots and dilutions.
7. Add more C2GM medium such that cell density is one million cells per milliliter (usually achieved in 10 ml).

### 3.2 Harvesting MB and MT Cells

1. Remove all medium and wash plate with 10 ml PBS.
2. Add 2 ml cell dissociation solution and incubate at 37 °C for 10 min. Gently tap and shake the plates in between.
3. Collect cells with growth medium in a 15 ml falcon tube. Wash the plate well to release all the cells.
4. Count cells in C2GM as for $G_0$ cells.

### 3.3 Crosslinking Cells

1. Fix the cells by adding formaldehyde to the medium (typically 10 ml) reaching a final concentration of 1% and mix well by swirling the tube. Incubate at 37 °C for 10 min, mixing periodically (*see* **Note 2**).
2. Quench formaldehyde by adding 500 μl of 2.5 M Glycine to the 10 ml medium (final concentration 0.0125 M). Mix well.

3. Dilute by filling bottle with PBS and spin at 290 × *g* at room temperature for 5 min. A visible pellet should be seen. Decant carefully.
4. Add 10 ml of ice-cold PBS containing PMSF, DTT, and PI. Pipette PBS forcefully to break the pellet and mix well. Centrifuge at 290 × *g* at 4 °C for 5 min and decant. Repeat wash with ice-cold PBS (*see* **Note 3**).

### 3.4 Sonication to Shear DNA

1. Remove excess PBS and add 2 ml lysis buffer for ten million cells (200 μl per one million cells—this cell density should be kept constant). Mix well and incubate $G_0$ and MB for 15 min and MT for 45 min on ice.
2. Take out an aliquot as a non-sonicated sample (50–100 μl).
3. Sonicate 2–4 ml lysis buffer depending on the number of cells in a 50 ml falcon tube. For smaller volumes (1–2 ml), transfer cells in lysis buffer to a 15 ml falcon tube and proceed with the incubation on ice.
4. Sonication conditions have been standardized on Diagenode Bioruptor:

| | |
|---|---|
| $G_0$ | LOW power; 30 s ON; 90 s OFF, 40 cycles |
| MB | HIGH power; 45 s ON; 45 s OFF, 20 cycles |
| MT | HIGH power; 60 s ON; 60 s OFF, 25 cycles |

   Change ice every 5 cycles and avoid frothing or bubbling during sonication (*see* **Notes 4** and **5**).
5. Read DNA in Nanodrop to judge concentration of sonicated chromatin before preparing DNA. Sonicated samples can be stored at −80 °C in aliquots (typically 200 μl) to avoid repeated freeze-thaw.

### 3.5 Preparation of DNA to Confirm Sonication

1. Crosslink removal: Incubate for 8 h in 65 °C water bath with 5 M NaCl (200 mM final concentration).
2. RNase treatment: Add TE buffer (pH 8.0) and 20 mg/ml RNase A to a final concentration of 0.2 mg/ml. Incubate at 37 °C for 2 h (*see* **Note 6**).
3. Proteinase K treatment: Add 12 μl of 0.5 M EDTA, 24 μl of 1 M Tris-Cl (pH 6.5), and 12 μl of 10 mg/ml proteinase K (0.2 mg/ml final concentration) and incubate at 55 °C for 1 h.
4. DNA extraction: Add an equal volume of phenol:chloroform: isoamyl alcohol (25:24:1; PCI) and shake vigorously to mix. Spin at maximum speed (16,000 × *g*) for 10 min at room temperature and take the upper aqueous phase carefully into new tubes (*see* **Note 7**).

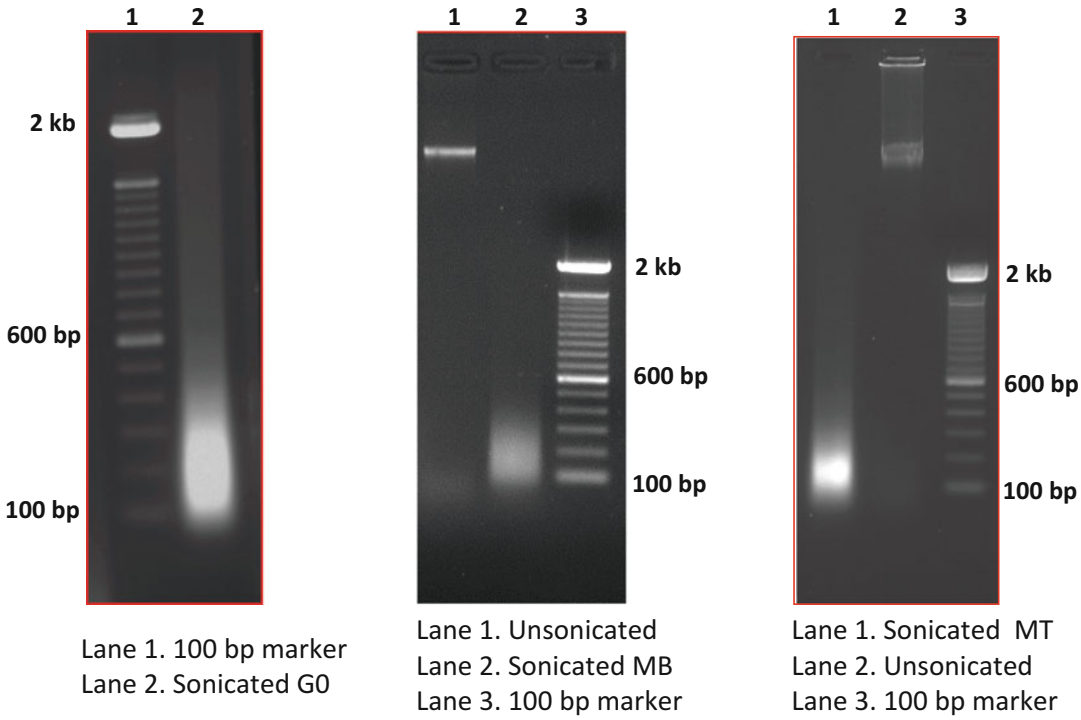


**Fig. 1** Sheared fragment sizes of isolated chromatin. Range of sonicated chromatin fragments from $G_0$, MB, and MT cells as checked on 1% agarose gel

5. DNA precipitation: Add sodium acetate (0.3 M final, pH 5.2), 2.5× the volume of absolute alcohol and 1 μl of 20 mg/ml glycogen. Mix and incubate at −80 °C for at least an hour.
6. Centrifuge at 16,000 × *g* for 20 min at 4 °C. DNA pellet should be visible; remove alcohol carefully and wash with 500 μl of 70% alcohol.
7. Centrifuge at 16,000 × *g* for 10 min at room temperature. Remove alcohol completely. Air dry and dissolve in 30 μl of TE.
8. Make sure the genomic DNA is well dissolved and check concentration.
9. Load on 1% agarose gel to confirm efficacy of sonication (Fig. 1). Aliquot chromatin in small volumes to avoid repeated freeze-thaw (*see* **Notes 4** and **5**).

### *3.6 Chromatin Immunoprecipitation (ChIP) for Low Cell Numbers*

This section is largely focused on investigating the chromatin state via ChIP for histone modifications. Since histones are highly abundant proteins, and the commercially available antibodies are of excellent specificity and purity, the protocols are very robust and provide very efficient pulldown. For transcription factors and other chromatin complexes with selective binding at fewer loci, and for which antibodies may not have comparable specificity, this protocol must be modified to enhance yield and efficiency.

In most cases, cell cultures yield sufficient material for regular ChIP-seq protocols. When cell number is not an issue, ChIP can be performed from one million cells per immunoprecipitation using standard protocols (*see* **Note 8**). However, this protocol does not give efficient enrichment in case of low cell number or difficulty in scaling up for a large number of ChIP experiments (Fig. 2). Here, we describe a low cell ChIP and purification protocol. This is especially useful in performing ChIP from $G_0$ cells and we find that this protocol provides enhanced antibody enrichment (Fig. 3).

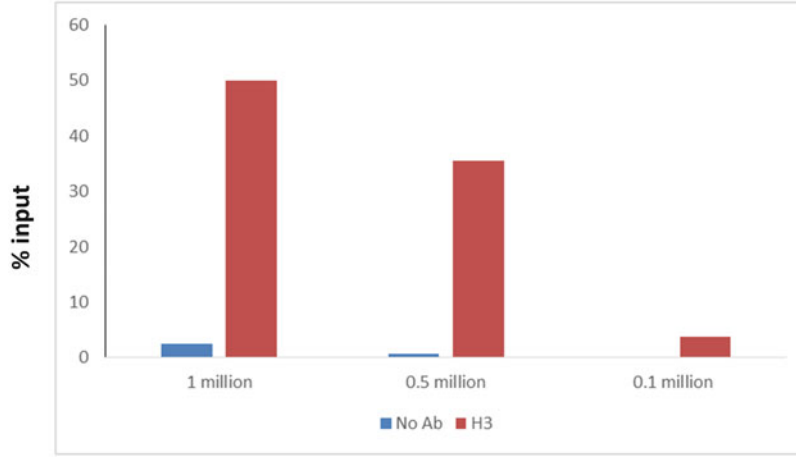


**Fig. 2** ChIP-qPCR with decreasing cell numbers. Real-time qPCR at myogenin promoter for histone H3 following ChIP with decreasing numbers of $G_0$ cells using the Upstate protocol. Lowering starting amount of chromatin drastically reduces enrichment levels, with 0.1 million cells indicating almost no enrichment

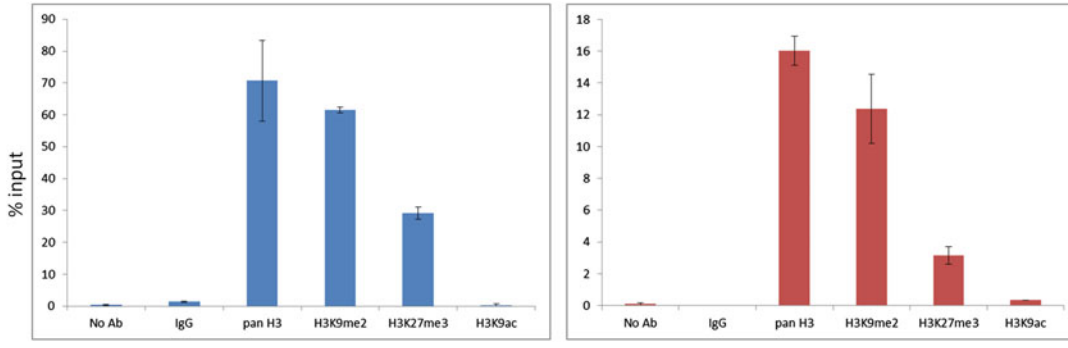


**Fig. 3** Comparison of LowCell ChIP versus ChIP from one million cells. Real-time qPCR at myogenin promoter (silenced in $G_0$) for histone H3 (positive control) and H3K9me2, H3K27me3 (repressive) and H3K9ac (activation) marks following ChIP with 25,000 $G_0$ cells using LowCell ChIP kit (*left panel*) and one million cells using the Upstate protocol (*right panel*). ChIP from low cell numbers shows efficient enrichment, with trends similar to those obtained from million cells. Error bars represent standard error of mean from two experiments

1. Perform cell lysis and DNA shearing (*see* Subheadings 3.3 and 3.4) Proceed with the ChIP protocol as per the manufacturer's instructions (LowCell ChIP kit) using 10,000 – 25,000 $G_0$ cells or approximately 1.5–2 μg chromatin per ChIP(*see* **Notes 9** and **10**).
2. Mix beads (11 μl per immunoprecipitate) with ice-cold buffer A (22 μl per immunoprecipitate), pipet well, and centrifuge at 500 × *g* for 5 min at 4 °C. Pipet out the buffer carefully and repeat wash.
3. Add 90 μl of ice-cold buffer A to 10 μl of washed beads in a 200 μl tube.
4. Add antibody and mix well. Incubate on a rotator at a slow speed in a cold room for 5 h (*see* **Note 11**).
5. Spin the sonicated chromatin at 16,000 × *g* for 10 min at 4 °C. Take the supernatant into fresh tubes on ice. Dilute the chromatin in ice-cold buffer A containing protease inhibitor (*see* **Note 12**).
6. Briefly spin the 200 μl tubes and place in a prechilled magnetic rack on ice. Allow beads to collect for 1 min and carefully pipet out the buffer without disturbing the antibody-coated beads.
7. Add 100 μl of chromatin to each antibody tube and mix gently by inversion away from the magnet. Incubate on a rotator at a slow speed in a cold room overnight.
8. Pellet the beads on the magnetic rack (prechilled) and discard the supernatant. Wash with 100 μl cold buffer A for 5 min on the rotator in the cold room (three times).
9. Wash similarly with 100 μl of cold buffer C.
10. DNA isolation for qPCR:
    (a) Pellet the beads on the magnetic rack and add 100 μl of DNA isolation buffer (containing 1 μl of 100× proteinase K). Resuspend beads and transfer to 1.5 ml centrifuge tubes.
    (b) For input DNA (10% of total immunoprecipitation), mix 10 μl of the diluted chromatin with 90 μl of the DIB + proteinase K and process along with the immunoprecipitation samples.
    (c) Incubate at 55 °C on a thermomixer for 15 min. Mix and incubate at 100 °C for 15 min.
    (d) Centrifuge at 16,000 × *g* for 5 min at 4 °C and transfer the supernatant to clean tubes.
    (e) Use this DNA for quantitative PCR analysis to confirm ChIP efficacy.

11. DNA isolation for sequencing: It requires additional purification using the iPure kit:
    (a) Pellet the beads on the magnetic rack and add 100 μl of elution buffer. Transfer resuspended beads to 1.5 ml centrifuge tubes.
    (b) For input DNA (10% of total immunoprecipitation), mix 10 μl of the diluted chromatin with 90 μl of the elution buffer and process along with the immunoprecipitation samples.
    (c) Incubate at 65 °C for 4 h on a thermomixer with gentle shaking.
    (d) Pellet the beads and collect the supernatant that contains immunoprecipitated DNA.
    (e) Add 2 μl of carrier DNA, 100 μl of isopropanol, and 15 μl of magnetic beads and incubate on a rotator for 1 h at room temperature.
    (f) Wash sequentially using 100 μl each of buffers 1 and 2 containing 50% isopropanol for 5 min.
    (g) Elute DNA twice with 25 μl elution buffer C at room temperature for 30 min.
    (h) Use eluted DNA for ChIP library preparation following the manufacturer's instructions.

## 3.7 ChIP-Sequencing

### 3.7.1 Library Preparation

1. Check immunoprecipitated DNA using a bioanalyzer to estimate abundance of fragments in the 200–300 bp size range. Typically, 60–80% of the fragments should fall in this size range. Use AMPure bead based size selection on input DNA to optimize the efficiency of size selection during the library preparation.
2. Use 20 ng of pull-down and input DNA to generate the sequencing library using NEBNext® DNA Library Prep kit for Illumina® along with NEBNext® Multiplex oligos for Illumina® (Index Primers set 1) as per the manufacturer's protocol. Perform cleanup using AMPure beads between each of the steps:
    (a) End Repair of Fragmented DNA
    (b) dA-Tailing of End Repaired DNA
    (c) Adaptor Ligation of dA-Tailed DNA
    (d) Cleanup of Adaptor Ligated DNA and follow up with size selection
    (e) PCR Enrichment of Adaptor Ligated DNA (*see* **Note 13**)
    (f) Check library quality on BioAnalyzer and by qPCR
    (g) Perform paired-end sequencing

*3.7.2 Analysis and Peak Calling*

The following pipeline can be adapted for identifying enrichment sites (*see* **Note 14**).

(a) Check sequencing quality (FastQC).

(b) Perform adapter trimming and removal of poor quality sequences (fastx_toolkit and TrimGalore).

(c) Align reads to *Mus musculus* reference genome (Bowtie2).

(d) Assess quality of IP (phantompeakqualtools) by UCSC and ChIPQC (R package).

(e) Tools such as MACS2 or SICER can be employed for peak calling depending on target (point source vs. broad domain).

(f) Perform differential binding analysis on the samples from the three cell states (DiffBind—R package).

(g) Annotate peaks with the nearest genes (ChIPSeeker—R package, HOMER).

(h) Proceed with Gene Ontology (GOStats, ClusterProfiler, DAVID, Panther, gProfiler) to identify potential networks involved in governing cell cycle exit and differentiation versus quiescence.

(i) Compare differentially enriched peaks of multiple antibodies across the three states at genes of interest using a genome browser (UCSC, IGV). Design primers for qPCR validations at selected loci.

(j) To facilitate easier comparison of chromatin state and transcriptional status at a large number of loci, we have developed a customized tool (C-State) that enables simultaneous visualization of multiple genes/genomic locations across chromosomes (Sowpati et al. (2017) C-State: An interactive web app for simultaneous multi-gene visualization and comparative epigenetic pattern search. BMC Bioinformatics, in press; website:http://www.ccmb.res.in/rakeshmishra/c-state/).

(k) Identify and filter genes containing specific epigenetic patterns such as active/repressed or bivalent domains (poised) and compare the profiles of selected gene subsets to document changes across the cell states (Fig. 4). Change in epigenetic marks can then be correlated with changes in transcriptome profile as outlined in the following sections.

## *3.8 Expression Profiling Using RNA-Sequencing (See Note 15)*

*3.8.1 Accurate Determination of Cell Number in Different States and RNA Isolation*

(a) Count trypsinized cell suspension of attached cultures (MB and MT) or suspension cells ($G_0$) three times (at two or more dilutions) with trypan blue exclusion to generate a live-cell count (*see* **Note 16**).

(b) Wash cells twice with cold PBS and lyse cells with 1 ml RLT plus buffer (buffer provided in the RNeasy Plus Mini Kit, Qiagen) containing β-mercaptoethanol.

(c) Vortex the lysate vigorously to shear genomic DNA and store at −80 °C until further processing.

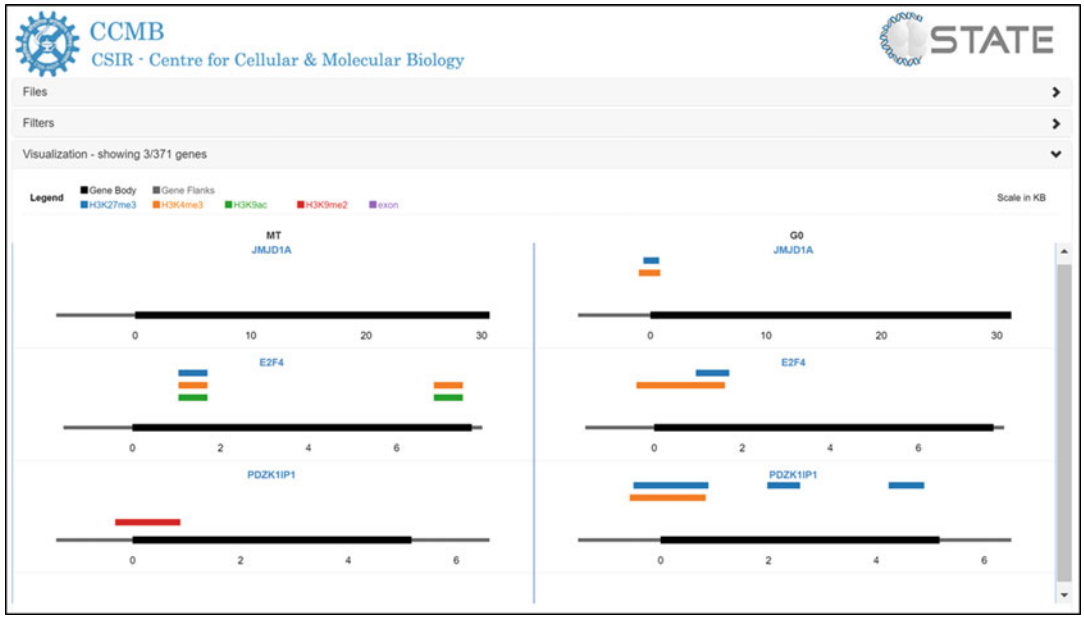


**Fig. 4** Custom visualization of enriched patterns for biological interpretation. C-State screenshot comparing bivalent domains at TSS of filtered and selected genes in $G_0$ (*right*) with MT (*left*). The target gene (indicated by its panel header) is shown as a *black bar* while enrichment peaks are shown as bar tracks above the gene, shaded according to the legend

(d) Isolate RNA using RNeasy Plus Mini Kit as per the manufacturer's protocol. Pass the lysate through a genomic DNA Eliminator spin column, add ethanol to the flow through, and apply to an RNeasy MinElute spin column (*see* **Note 16**).

(e) Elute RNA twice in 30 µl of water in low bind tubes and store in −80 °C. Visualize by bioanalyzer to check integrity and quantify accurately using Nanodrop and Qubit methods (*see* **Note 17**).

*3.8.2 RNA-seq Library Preparation*

(a) Verify the quality of RNA using BioAnalyzer.

(b) Use mean cell number (multiples of million) as a reference to add 3 µl 1:10 diluted ERCC spike-in RNA per millions cell to DNase-treated RNA proportional. ERCC mix1 is added to replicate set 1 and ERCC mix2 is added to replicate set 2 for each of sample MB, $G_0$, and MT (*see* **Notes 18** and **19**).

(c) Treat the spiked total cellular RNA with RNase-free DNase as per the manufacturer's protocol.

(d) Process 4 µg of the DNase-treated spiked RNA to remove ribosomal RNA and perform QC using BioAnalyzer. We use RiboMinus™ Eukaryotic kit V2. Verify the quality of RNA using BioAnalyzer and ensure removal of ribosomal RNA (Fig. 5). Repeat this step if needed.

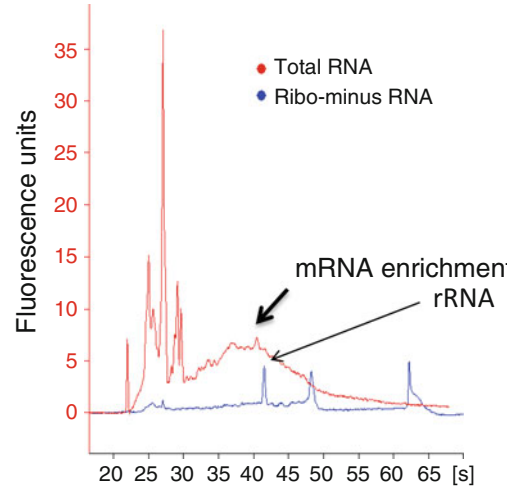


**Fig. 5** Representative Bioanalyzer profiles before and after ribosomal RNA depletion using Ribominus. The Bioanalyzer profiles of the MB show ribosomal peak presence in total RNA (*Blue trace*) and complete depletion in ribominus treated (*red trace*)

(e) Take equal amount of ribosomal depleted RNA (~250 ng) from various cell types for library preparation. The purified mRNA is used for cDNA synthesis and library preparation using NEBNext® Ultra™ Directional RNA Library Prep Kit for Illumina®.

(f) To ensure optimal quality the library should again be checked on BioAnalyzer (typically 200 bp fragments) and also verified by qPCR.

(g) Paired-end sequencing can be performed on the Illumina HiSeq1000 (or equivalent) platform.

*3.8.3 Post-sequencing Analysis (See Table 1)*

(a) Check sequencing quality (FastQC).

(b) Perform alignment of raw sequencing reads (TOPHAT). Add reference files of ERCC spike-in RNA to the mouse reference genome (*see* **Note 20**).

(c) Assess quality of alignment based on the proportion on reads mapping to various gene features (Fig. 6). Typically <2% reads should be from ribosomal RNA and more than 80% from gene coding regions.

(d) Normalization to equal cell numbers (*see* **Notes 21** and **22**). Funnel the output of TopHat into HTSeq-count package [53] to get read counts per gene for each of the samples using a reference annotation file. Normalize the read count per gene (including ERCC transcripts) using DEseq2 package [54]. Briefly, the sizeFactor is estimated for the subsampled Group B counts of ERCC spike-in RNA mix since

**Table 1**
**NGS Analysis tools for RNA-seq**

| Tools | Used for | Reference |
|---|---|---|
| Bowtie | Alignment | [56] |
| TopHat | RNA alignment | [57–59] |
| Cufflinks | RNA quantification | [58] |
| CummeRbund | Visualizations for Cufflinks | [60] |
| HTseq/Htcount and DEseq/Deseq2 | Quantification of RNA and normalization | [53, 54] |
| Seqmonk | Visualization and analysis of all NGS data | (http://www.bioinformatics.bbsrc.ac.uk/projects) |
| FastQC | Quality of raw Sequencing reads | http://www.bioinformatics. babraham.ac.uk/projects/f astqc/ |

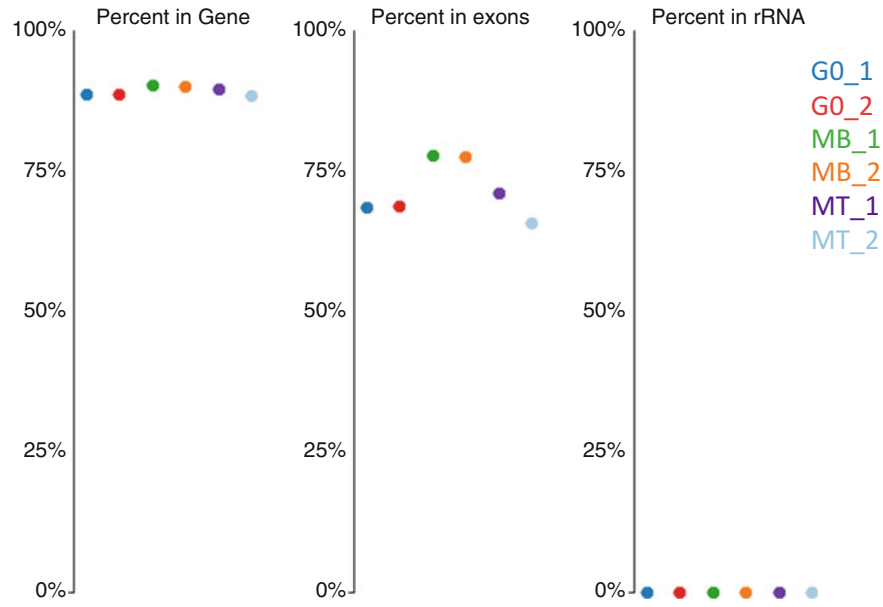


**Fig. 6** Mapping proportions. The plot shows the percentage of sequencing reads mapping to mm9 genome coordinates for all of the genes, exons, and rRNA

the group B genes (Unchanged group of 23 transcripts in ERCC spike in mixes) must not vary across all samples of both replicates. The calculated sizeFactor for each sample using Group B as reference gene set is further used to normalize other genes in the respective library including those in the other ERCC spike in mix groups (Groups A, C, D). This approach ensures that the RNA-seq libraries are scaled to

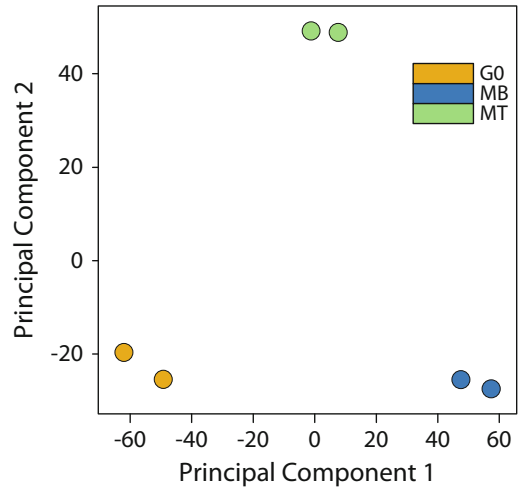


**Fig. 7** Heat map for ERCC transcript abundance. Cell number normalized and Equal RNA normalized samples Group B (mix1:mix2 = 1) and Group A (mix1: mix2 = 4)

reference spike-in controls, and not to the sequencing depth of the library.

*3.8.4 Example of Method Validations*

(a) *Comparison of effect of normalization of Group A and B genes.* The heatmap for ERCC transcripts for Group A (mix 1:2 = 4) and B (mix 1:2 = 1) genes carried out using Cufflinks (Total RNA normalization) and Deseq2 (cell number normalized) packages is shown in Fig. 7 (*see* **Note 23**). For cell number normalized data set, group A shows intensity values of mix 1 are 2× (log2 scale) that of mix 2 for all cell states and in group B, the values peak at 0 for all samples and replicates, since the normalization (DEseq package) was carried out using group B as a reference set. In contrast to Equal RNA normalization (Cufflinks) we find that in the $G_0$ samples, the mix set 1 or 2 has the maximum amount of intensity followed by MT and least in MB. This suggests that the proportion of spike-in RNA sampled in sequencing is $G_0$ > MT > MB. Similarly, the group A spike-in RNAs are expected to have twofold higher FPKM units in mix set 1 compared to mix set 2. When compared at $G_0$_1 and $G_0$_2 this twofold difference holds true (likewise for MB and MT), but the whole mix set 1 is always higher than its corresponding mix set 2. These results suggest that the total sequencing depth normalization method is accurate only when the total RNA content between the two states is comparable.

(b) *Effect of equal cell number normalization on replicates.* Principal component analysis (PCA) is plotted using the mouse genes and not the spike-in RNA (Fig. 8). For MB, $G_0$, and

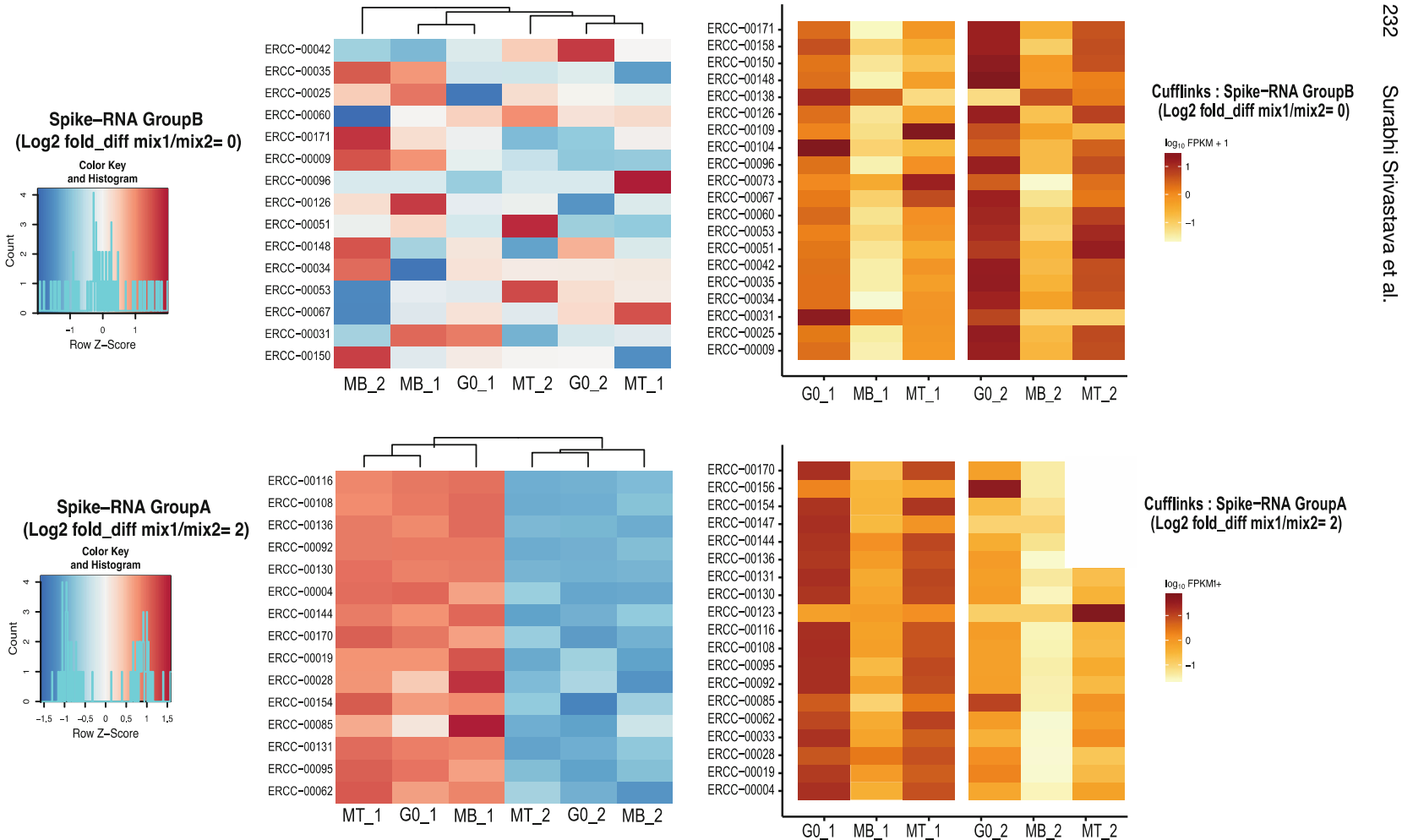


**Fig. 8** Effect of cell number normalization on variation with and across sample RNA (MB, $G_0$, MT). Principal component analysis plot for cell number normalized libraries (scatter plot of PC1 and PC2)

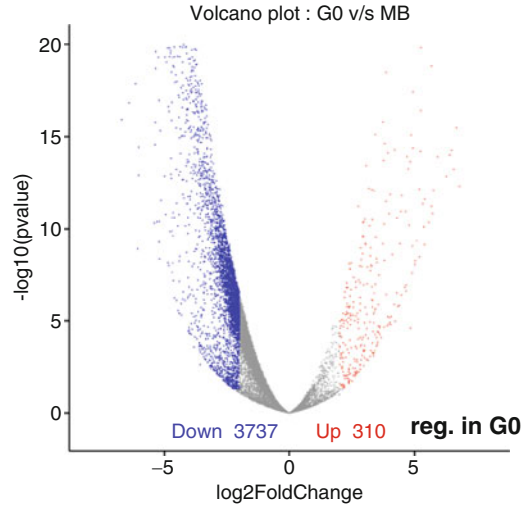


**Fig. 9** Differential gene expression—Volcano plots using cell number normalization. The log2 fold change ($G_0$ vs. MB) is plotted against *p*-value (negative log10). Upregulated (*red*) and downregulated genes (*blue*) are highlighted wherein the fold difference is >2 and *p*-value <0.05

MT samples, each of the two biological replicates cluster close to each other, whereas the cell states themselves are distinctly further apart.

(c) *Effect of normalization on Differential gene expression*. Using the cell number normalized RNA-seq expression datasets, volcano plots are generated using the log2 fold change and *p*-values (negative log10) for all the genes compared pair-wise for each comparison. The statistically significant de-regulated genes between the two states can be identified by setting a cutoff of >2-fold change and <0.05 *p*-value (Fig. 9).

(d) *Overlap of differentially regulated genes between Cufflinks and cell number normalization*. To compare the implications of normalization methods (Cufflink and cell number normalized) on differential gene expression and hence the biological interpretations, overlap of common differentially regulated genes is estimated (>2 log2 fold change and *p*-value <0.05) from these two methods. Size-adjusted Venn diagrams (BioVenn online tool) are generated. Representative Venn diagram for $G_0$ vs. MB comparison (Fig. 10).

## 4 Notes

1. Use cells in log phase of growth. Fully confluent plates should not be used for ChIP. Make sure brakes are off to ensure smooth centrifugation. Remove cups gently, with no jerks.

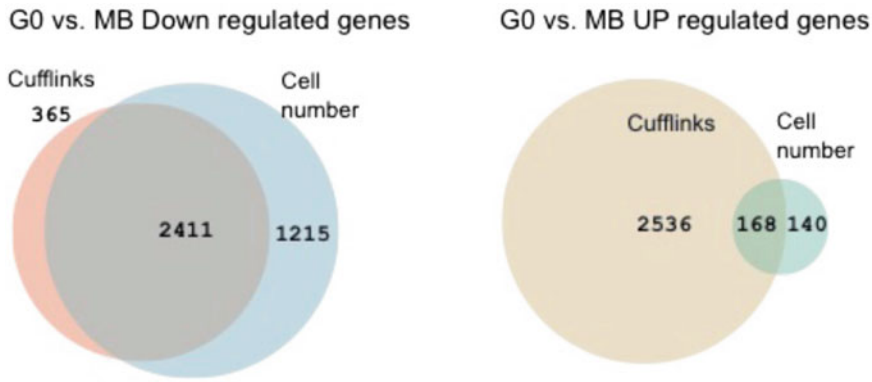


**Fig. 10** Overlap of differentially regulated genes between cufflinks and cell number normalization methods. Size-adjusted Venn diagrams showing overlap of genes between the two normalization methods for $G_0$ vs. MB. *Left panel* represents downregulated genes and *right panel* represents upregulated genes

2. In case ChIP has to be performed for some transcription factors or complexes with weaker binding to DNA, the fixation time can be increased to 30 min at 37 °C. The exact time needs to be determined empirically because over crosslinking can make the chromatin refractory to proper sonication. Color of the medium can change upon addition of formaldehyde.
3. Cells should be handled gently after fixation. Do not resuspend cells vigorously as they can adhere to the pipette.
4. The sonication conditions described here have been optimized for cultured C2C12 cells. When working with freshly isolated stem/progenitor cells, use a similar protocol to optimize sonication starting with the lowest power setting possible. Change in sonicator models or tubes can also lead to changes in the sonication quality. Hence, sonication needs to be checked and standardized to obtain average fragment size of 250 bp (range 100–500 bp). Sonication in the Diagenode Bioruptor is best performed in polypropylene 15 ml Falcon tubes rather than 1.5 ml Eppendorf tubes, which have proven more refractory to reproducible sonication in our hands.
5. Sonication should be checked on the input chromatin each time prior to library preparation using multiple amounts of sonicated sample on a 1% agarose gel to judge fragmentation range and quality of genomic DNA used. Sonicated samples can then be snap frozen and kept at −80 °C for long-term storage. Store chromatin in aliquots that can be used in a single experiment to avoid repeated freeze and thaw.

6. To dilute the SDS in the lysis and sonication buffer, we typically mix 200 μl of sonicated sample with 400 μl TE buffer. This is enough for subsequent reactions.
7. PCI is best used fresh and should not have low pH. Trace amounts of phenol can interfere with qPCR and library preparation; PCR MinElute (Qiagen) can be used for DNA isolation in such a case. Avoid using salmon sperm DNA as it will contribute background sequences and affect the reaction.
8. We typically pool immunoprecipitated DNA from three to four reactions (to obtain about 100 ng purified DNA) for ChIP-seq. Yields are significantly improved by replacing agarose beads with DynaBeads.
9. It is useful to have an estimate of the chromatin used as starting material. Harvested $G_0$, MB, and multinucleate MT cells can give diverse yields so we do not rely solely on cell numbers when performing the pulldown—we also ensure that the chromatin from all the cell states is in the same range for ChIP using the low cell protocol.
10. All the steps must be performed on ice and beads should not be allowed to dry. Leaving the beads for too long on the magnet can dry them out making the pellet hard to resuspend. Protein A or protein G beads should be selected depending on the antibody to be used.
11. The amount of antibody needs to be titrated for each experiment. Perform a pilot ChIP with 1, 2, and 3 μg of each antibody.
12. To dilute the SDS in the lysis and sonication buffer, the sheared chromatin should be diluted 8–10-fold in buffer A; adjust concentration of sheared chromatin accordingly.
13. Indexing of library is carried out at this step. Depending on required sequencing depth and per lane output of the sequencer multiplexing can be performed. If multiplex sequencing is carried out, only a fraction of library is primarily used to estimate the diversity and amount of PCR duplicates represented in the library. Number of PCR cycles used can be reduced if diversity of library is poor.
14. Use sonicated reverse crosslinked "input" DNA as control or baseline for peak calling after sequencing instead of sequencing mock immunoprecipitation.
15. Variation of RNA content between various cell types/cell states contributes to misinterpretation of gene expression profiles. To overcome this, we use a known quantity of exogenous RNA control (Spike-in) proportional to the cell number for each sample. Equal quantity of RNA is then used to carry out NGS as per kit instructions. mRNA enrichment is carried out

by depletion of ribosomal RNA as opposed to polyA pull-down methods, so that the transcriptome is representative of all RNA species: noncoding RNA, histone mRNA, RNA Polymerase III transcribed RNA species, and tRNA are not represented in the polyA pull-down approach [55]. Further, stranded or directional sequencing library kit is used for library synthesis. In this protocol, enriched mRNA undergoes biochemical treatment during library synthesis such that the orientation information of the DNA strand used as a template for mRNA synthesis by the cell is retained. This allows one to distinguish the RNA sequencing reads originating from overlapping genes and antisense transcripts, which can be extremely informative. The sequencing output is then normalized to known quantities of the spike-in RNA instead of total read counts, allowing the removal of any bias introduced due to improper sampling.

16. MT can pose a problem in accurate counting of the varying number of nuclei; therefore, nuclei should be isolated and counted after excluding dead cells. Genomic DNA eliminator column has binding capacity equivalent to four to five million cells (mouse genome). Use two columns if more than five million cells are used.
17. For RNA-seq, RNA quantification and quality check is done using Agilent RNA 6000 Pico Kit on Agilent 2100 Bioanalyzer system.
18. The ERCC RNA spike-in control mixes are pre-formulated 92 poly-adenylated transcripts (250–2000 nucleotides in length) from *E. coli*, whose exact molar concentrations are predetermined. The transcripts in Spike-In Mix 1 and Spike-In Mix 2 are present at defined Mix 1:Mix 2 molar concentration ratios, described by four subgroups (A–D). The concentrations of the transcripts span a $10^6$-fold range allowing their effective use in NGS platforms to detect even low abundance transcripts with higher confidence. These controls are available in two mixes (1 and 2). The transcripts in mix 1 and mix 2 represent at predefined mix1:mix2 molar ratios described by four subgroups (each containing 23 transcripts spanning $10^6$-fold concentration range, with approximately similar transcript size). The combination of mix 1 and mix 2 is useful to assess the accuracy of measurements in differential gene expression studies.
19. The dilution and amount of ERCC spike in control need to be adjusted so that the dynamic range 1–$10^6$ count of ERCC RNA can be represented in the sequencing output such that ERCC spike is contributed not more than 10% of ribosomal depleted RNA. The proportion of DNase-treated RNA per million used here would vary depending on cell types used.

20. ERCC FASTA files are online support files from manufactures. Use the strand option during alignment.
21. In the standard method transcripts are quantified using Cufflinks package. However, overlooking the use of ERCC spike in control can generate misinterpretation when analyzing $G_0$ cells. Hence, we compare with equal cell number as described.
22. ERCC spike in control can also be used to identify the lower detection limit for the cellular library. This is particularly important to identify low abundance transcripts with high confidence.
23. Tools used for generating heatmap: CummeRbund package for cufflink data set, and R tools for DEseq2 dataset.

## Acknowledgments

We gratefully acknowledge Divya Tej Sowpati for help with the bioinformatics analysis pipeline and development of custom visualization tools. HG was supported by doctoral fellowships from CSIR. The Mishra and Dhawan labs are supported by core funds from the Council of Scientific and Industrial Research to CCMB, and a collaborative grant from the Dept. of Biotechnology Indo-Australia Biotechnology Fund. JD also acknowledges funding from and the Dept. of Biotechnology Indo-Danish Strategic Fund, Indo-French Center for the Promotion of Advanced Research and from the Dept. of Biotechnology Institute for Stem Cell Biology and Regenerative Medicine.

### References

1. Cavallucci V, Fidaleo M, Pani G (2016) Neural stem cells and nutrients: poised between quiescence and exhaustion. Trends Endocrinol Metab 27:756–769. doi:10.1016/j.tem.2016.06.007
2. Daignan-Fornier B, Sagot I (2011) Proliferation/quiescence: when to start? Where to stop? What to stock? Cell Div 6:20. doi:10.1186/1747-1028-6-20
3. Cheung TH, Rando TA (2013) Molecular regulation of stem cell quiescence. Nat Rev Mol Cell Biol 14:329–340. doi:10.1038/nrm3591
4. Rumman M, Dhawan J, Kassem M (2015) Concise review: quiescence in adult stem cells: biological significance and relevance to tissue regeneration. Stem Cells Dayt Ohio 33:2903–2912. doi:10.1002/stem.2056
5. Coller HA, Sang L, Roberts JM (2006) A new description of cellular quiescence. PLoS Biol. doi:10.1371/journal.pbio.0040083
6. Yao G (2014) Modelling mammalian cellular quiescence. Interf Focus. doi:10.1098/rsfs.2013.0074
7. García-Prat L, Martínez-Vicente M, Perdiguero E et al (2016) Autophagy maintains stemness by preventing senescence. Nature 529:37–42. doi:10.1038/nature16187
8. Sousa-Victor P, Gutarra S, García-Prat L et al (2014) Geriatric muscle stem cells switch reversible quiescence into senescence. Nature 506:316–321. doi:10.1038/nature13013
9. Yanagida M (2009) Cellular quiescence: are controlling genes conserved? Trends Cell Biol 19:705–715. doi:10.1016/j.tcb.2009.09.006
10. Gray JV, Petsko GA, Johnston GC et al (2004) "Sleeping Beauty": quiescence in Saccharomyces cerevisiae. Microbiol Mol Biol Rev 68:187–206. doi:10.1128/MMBR.68.2.187-206.2004

11. Dhawan J, Laxman S (2015) Decoding the stem cell quiescence cycle–lessons from yeast for regenerative biology. J Cell Sci 128:4467–4474. doi:10.1242/jcs.177758
12. Rodgers JT, King KY, Brett JO et al (2014) mTORC1 controls the adaptive transition of quiescent stem cells from G0 to G(Alert). Nature 510:393–396. doi:10.1038/nature13255
13. Moore KA, Lemischka IR (2006) Stem cells and their niches. Science 311:1880–1885. doi:10.1126/science.1110542
14. Wagers AJ, Weissman IL (2004) Plasticity of adult stem cells. Cell 116:639–648. doi:10.1016/S0092-8674(04)00208-9
15. Yu H, Fang D, Kumar SM et al (2006) Isolation of a novel population of multipotent adult stem cells from human hair follicles. Am J Pathol 168:1879–1888. doi:10.2353/ajpath.2006.051170
16. Freter R, Osawa M, Nishikawa S-I (2010) Adult stem cells exhibit global suppression of RNA polymerase II serine-2 phosphorylation. Stem Cells 28:1571–1580. doi:10.1002/stem.476
17. Venezia TA, Merchant AA, Ramos CA et al (2004) Molecular signatures of proliferation and quiescence in hematopoietic stem cells. PLoS Biol 2:e301. doi:10.1371/journal.pbio.0020301
18. Dhawan J, Rando TA (2005) Stem cells in postnatal myogenesis: molecular mechanisms of satellite cell quiescence, activation and replenishment. Trends Cell Biol 15:666–673. doi:10.1016/j.tcb.2005.10.007
19. Mauro A (1961) Satellite cell of skeletal muscle fibers. J Biophys Biochem Cytol 9:493–495
20. Anderson J, Pilipowicz O (2002) Activation of muscle satellite cells in single-fiber cultures. Nitric Oxide Biol Chem 7:36–41
21. Zammit PS, Relaix F, Nagata Y et al (2006) Pax7 and myogenic progression in skeletal muscle satellite cells. J Cell Sci 119:1824–1832. doi:10.1242/jcs.02908
22. Moyle LA, Zammit PS (2014) Isolation, culture and immunostaining of skeletal muscle fibres to study myogenic progression in satellite cells. Methods Mol Biol Clifton N J 1210:63–78. doi:10.1007/978-1-4939-1435-7_6
23. Gromova A, Tierney M, Sacco A (2015) FACS-based satellite cell isolation from mouse hind limb muscles. Bio Protoc 5:e1558. doi:10.21769/BioProtoc.1558
24. Danoviz ME, Yablonka-Reuveni Z (2012) Skeletal muscle satellite cells: background and methods for isolation and analysis in a primary culture system. Methods Mol Biol Clifton N J 798:21–52. doi:10.1007/978-1-61779-343-1_2
25. Lagha M, Sato T, Regnault B et al (2010) Transcriptome analyses based on genetic screens for Pax3 myogenic targets in the mouse embryo. BMC Genomics 11:696. doi:10.1186/1471-2164-11-696
26. Sambasivan R, Yao R, Kissenpfennig A et al (2011) Pax7-expressing satellite cells are indispensable for adult skeletal muscle regeneration. Development 138:3647–3656. doi:10.1242/dev.067587
27. Liu L, Cheung TH, Charville GW, Rando TA (2015) Isolation of skeletal muscle stem cells by fluorescence-activated cell sorting. Nat Protoc 10:1612–1624. doi:10.1038/nprot.2015.110
28. Arora R, Rumman M, Venugopal N, et al (2017) Mimicking muscle stem cell quiescence in culture: methods for synchronization in reversible arrest. Methods Mol Biol 1556:283–302. doi: 10.1007/978-1-4939-6771-1_15
29. Srivastava S, Mishra RK, Dhawan J (2010) Regulation of cellular chromatin state: insights from quiescence and differentiation. Organogenesis 6:37–47
30. Hui Ng H, Bird A (2000) Histone deacetylases: silencers for hire. Trends Biochem Sci 25:121–126. doi:10.1016/S0968-0004(00)01551-6
31. Kaeser MD, Emerson BM (2006) Remodeling plans for cellular specialization: unique styles for every room. Curr Opin Genet Dev 16:508–512. doi:10.1016/j.gde.2006.08.001
32. Turner BM (2007) Defining an epigenetic code. Nat Cell Biol 9:2–6. doi:10.1038/ncb0107-2
33. Buermans HPJ, den Dunnen JT (2014) Next generation sequencing technology: advances and applications. Biochim Biophys Acta 1842:1932–1941. doi:10.1016/j.bbadis.2014.06.015
34. Darzynkiewicz Z, Evenson D, Staiano-Coico L et al (1979) Relationship between RNA content and progression of lymphocytes through S phase of cell cycle. Proc Natl Acad Sci U S A 76:358–362
35. Habets PEMH, Franco D, Ruijter JM et al (1999) RNA content differs in slow and fast muscle fibers: implications for interpretation of changes in muscle gene expression. J Histochem Cytochem 47:995–1004. doi:10.1177/002215549904700803
36. Darzynkiewicz Z, Evenson DP, Staiano-Coico L et al (1979) Correlation between cell cycle

duration and RNA content. J Cell Physiol 100:425–438. doi:10.1002/jcp.1041000306
37. Darzynkiewicz Z (1987) Cytochemical probes of cycling and quiescent cells applicable to flow cytometry. Springer, New York, NY
38. Poot M, Rizk-Rabin M, Hoehn H, Pavlovitch JH (1990) Cell size and RNA content correlate with cell differentiation and proliferative capacity of rat keratinocytes. J Cell Physiol 143:279–286. doi:10.1002/jcp.1041430211
39. Schmidt EE, Schibler U (1995) Cell size regulation, a mechanism that controls cellular RNA accumulation: consequences on regulation of the ubiquitous transcription factors Oct1 and NF-Y and the liver-enriched transcription factor DBP. J Cell Biol 128:467–483
40. Elliott SG, McLaughlin CS (1978) Rate of macromolecular synthesis through the cell cycle of the yeast Saccharomyces cerevisiae. Proc Natl Acad Sci U S A 75:4384–4388
41. Killander D, Zetterberg A (1965) Quantitative cytochemical studies on interphase growth. i. determination of DNA, RNA and mass content of age determined mouse fibroblasts in vitro and of intercellular variation in generation time. Exp Cell Res 38:272–284
42. Marguerat S, Bähler J (2012) Coordinating genome expression with cell size. Trends Genet 28:560–565. doi:10.1016/j.tig.2012.07.003
43. Benecke BJ, Ben-Ze'ev A, Penman S (1980) The regulation of RNA metabolism in suspended and reattached anchorage-dependent 3T6 fibroblasts. J Cell Physiol 103:247–254. doi:10.1002/jcp.1041030209
44. Lovén J, Orlando DA, Sigova AA et al (2012) Revisiting global gene expression analysis. Cell 151:476–482. doi:10.1016/j.cell.2012.10.012
45. Kouzine F, Wojtowicz D, Yamane A et al (2013) Global regulation of promoter melting in naive lymphocytes. Cell 153:988–999. doi:10.1016/j.cell.2013.04.033
46. Sachidanandan C, Sambasivan R, Dhawan J (2002) Tristetraprolin and LPS-inducible CXC chemokine are rapidly induced in presumptive satellite cells in response to skeletal muscle injury. J Cell Sci 115:2701–2712
47. Blau HM, Chiu CP, Webster C (1983) Cytoplasmic activation of human nuclear genes in stable heterocaryons. Cell 32:1171–1180
48. Yaffe D, Saxel O (1977) Serial passaging and differentiation of myogenic cells isolated from dystrophic mouse muscle. Nature 270:725–727
49. Milasincic DJ, Dhawan J, Farmer SR (1996) Anchorage-dependent control of muscle-specific gene expression in C2C12 mouse myoblasts. In Vitro Cell Dev Biol Anim 32:90–99
50. Sellathurai J, Cheedipudi S, Dhawan J, Schrøder HD (2013) A novel in vitro model for studying quiescence and activation of primary isolated human myoblasts. PLoS One 8:e64067. doi:10.1371/journal.pone.0064067
51. Cheedipudi S, Puri D, Saleh A et al (2015) A fine balance: epigenetic control of cellular quiescence by the tumor suppressor PRDM2/RIZ at a bivalent domain in the cyclin a gene. Nucleic Acids Res 43:6236–6256. doi:10.1093/nar/gkv567
52. Fukada S, Uezumi A, Ikemoto M et al (2007) Molecular signature of quiescent satellite cells in adult skeletal muscle. Stem Cells 25:2448–2459. doi:10.1634/stemcells.2007-0019
53. Anders S, Pyl PT, Huber W (2015) HTSeq—a Python framework to work with high-throughput sequencing data. Bioinformatics 31:166–169. doi:10.1093/bioinformatics/btu638
54. Anders S, McCarthy DJ, Chen Y et al (2013) Count-based differential expression analysis of RNA sequencing data using R and Bioconductor. Nat Protoc 8:1765–1786. doi:10.1038/nprot.2013.099
55. Cui P, Lin Q, Ding F et al (2010) A comparison between ribo-minus RNA-sequencing and polyA-selected RNA-sequencing. Genomics 96:259–265. doi:10.1016/j.ygeno.2010.07.010
56. Langmead B, Trapnell C, Pop M, Salzberg SL (2009) Ultrafast and memory-efficient alignment of short DNA sequences to the human genome. Genome Biol 10:R25. doi:10.1186/gb-2009-10-3-r25
57. Trapnell C, Pachter L, Salzberg SL (2009) TopHat: discovering splice junctions with RNA-Seq. Bioinformatics 25:1105–1111. doi:10.1093/bioinformatics/btp120
58. Trapnell C, Roberts A, Goff L et al (2012) Differential gene and transcript expression analysis of RNA-seq experiments with TopHat and Cufflinks. Nat Protoc 7:562–578. doi:10.1038/nprot.2012.016
59. Kim D, Pertea G, Trapnell C et al (2013) TopHat2: accurate alignment of transcriptomes in the presence of insertions, deletions and gene fusions. Genome Biol 14:R36. doi:10.1186/gb-2013-14-4-r36
60. Goff L, Trapnell C, Kelley D (2013) cummeRbund: analysis, exploration, manipulation, and visualization of Cufflinks high-throughput sequencing data. R package version 2.16.0

# Chapter 17

# Analysis of lncRNA-Protein Interactions by RNA-Protein Pull-Down Assays and RNA Immunoprecipitation (RIP)

**Holger Bierhoff**

## Abstract

Long noncoding RNAs (lncRNAs) have important roles in shaping chromatin by targeting chromatin-modifying enzymes to distinct genomic sites. This section covers two methods to analyze lncRNA-protein interactions. The RNA-protein pull-down assays use either bead-bound proteins to capture in vitro transcripts, or immobilized synthetic RNAs to bind proteins from cell lysates. In the RNA immunoprecipitation (RIP) assay, endogenous RNAs are co-immunoprecipitated with a protein of interest. Both the methods can be applied to material from proliferating and quiescent cells, thus providing insights into how lncRNA-protein interactions are altered between these two cellular states.

**Key words** lncRNA, Chromatin-modifying enzymes, Pull-down assay, Synthetic RNA, RNA immunoprecipitation

## 1 Introduction

Chromatin regulation by lncRNAs has been recognized as an important mechanism to adapt genome function to developmental programs and environmental cues [1, 2]. By guiding chromatin-modifying enzymes to distinct genomic loci, lncRNAs impact covalent modifications of DNA and histones, chromatin structure, chromatin accessibility, and gene expression [3, 4]. An example is the epigenetic silencing of genes coding for ribosomal RNA (rRNA) in quiescent mouse and human cells. Upon quiescence, the antisense lncRNA *PAPAS* recruits the histone methyltransferase Suv4-20h2 to the rRNA gene promoter, thereby inducing trimethylation of histone H4 at lysine 20 (H4K20me3), chromatin compaction, and transcriptional repression [5, 6]. We have characterized the interaction between *PAPAS* and Suv4-20h2 by RNA-protein pull-down assays in vitro and by RIP in vivo. Both methods complement one other as they provide information about different aspects of an interaction. While we have mapped the binding domains of *PAPAS* and Suv4-20h2 in RNA-protein pull-down

H. Daniel Lacorazza (ed.), *Cellular Quiescence: Methods and Protocols*, Methods in Molecular Biology, vol. 1686,
DOI 10.1007/978-1-4939-7371-2_17, 

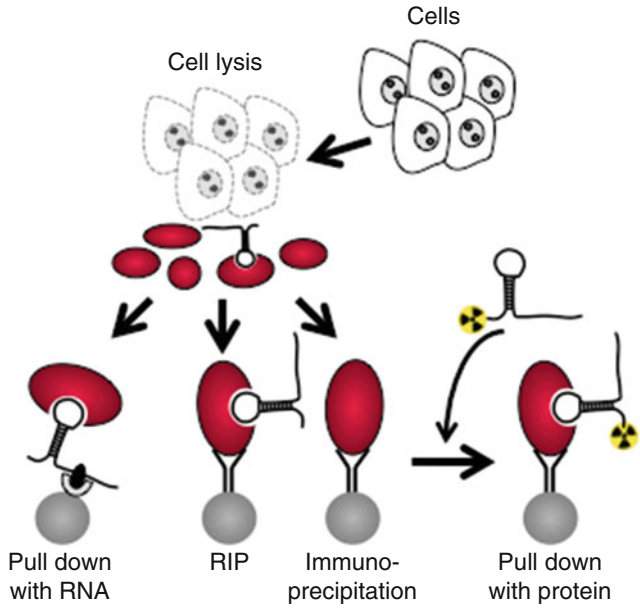


**Fig. 1** Schematic overview of the lncRNA-protein interaction assays described in this section. Initially, cells expressing the protein of interest are lysed. For RNA-dependent pulldown, the cell lysate is incubated with streptavidin beads coated with an in vitro synthesized, biotinylated lncRNA. For RNA immunoprecipitation (RIP), lncRNA is co-precipitated with the protein of interest from the cell lysate. To pull down lncRNAs in vitro, the immunopurified and immobilized protein is incubated with radiolabeled transcripts

assays, RIP experiments demonstrated the biological relevance of the interaction [56]. Moreover, both the methods can be easily conducted with standard laboratory equipment and can be readily adapted to certain experimental requirements and questions. For instance, Hämmerle et al. combined RNA-protein pulldowns with mass spectrometry to identify novel binding proteins for the lncRNA *HULC* [7]. In a recent study, RIP was combined with mild formaldehyde cross-linking to enhance efficiency of the RNA immunoprecipitation [8]. The combination of RIP with RNA deep sequencing (RIP-seq) allows the identification of an exhaustive list of lncRNAs interacting with a protein factor of interest, like it has been shown for the PRC2 complex [9].

In this section, three basic protocols are provided, two for RNA-protein pull-down assays with either the protein or the RNA immobilized and one for the RIP assay (Fig. 1).

## 2 Materials

Make sure that all buffers and solutions are free of RNase contaminations. Therefore, use only ultrapure water and autoclave solutions and lab ware if possible. For pipetting use filter barrier tips.

### 2.1 Protein Immunopurification from Cells

1. Cultured cells overexpressing the protein of interest.
2. Phosphate-buffered saline (PBS): dissolve 0.2 g of KCl, 0.2 g of $KH_2PO_4$, 1.15 g of $Na_2HPO_4$, and 8 g of NaCl in 1000 ml water, adjust pH to 7.4, store at 4 °C.
3. Cell lysis—immunoprecipitation (IP) buffer: 20 mM Tris-HCl, pH 8.0, 200 mM NaCl, 1 mM EDTA, 1 mM EGTA, 0.5% Triton X-100, 0.4 U/μl RNasin, protease inhibitor cocktail (*see* **Note 1**).
4. Antibody raised against the protein of interest.
5. Protein A/Protein G-coated agarose beads (*see* **Note 2**).

### 2.2 Synthesis of In Vitro Transcripts

1. Phage RNA polymerase (T7, T3, or SP6 RNA polymerase) (*see* **Note 3**).
2. Transcription-buffer (if not provided with the RNA polymerase): 200 mM Tris-HCl, pH 7.9, 30 mM $MgCl_2$, 50 mM NaCl, and 10 mM spermidine.
3. rNTP-Mix: 33 mM ATP, 33 mM CTP, 33 mM GTP.
4. [α-$^{32}$P]-UTP (10 μCi/μl, 800 Ci/mmol).
5. RNA Miniprep Kit.
6. 80% Formamide/0.05% bromophenol blue.
7. Native polyacrylamide gel.
8. Tris-Borate-EDTA (TBE) running buffer: dissolve 54 g Tris-base and 27.5 g boric acid in 980 ml water, add 20 ml 0.5 M EDTA, pH 8.0, store at room temperature in the dark.
9. Vacuum gel dryer.
10. Phosphor imaging system.

### 2.3 Immobilization of Biotinylated RNA for Protein Pull-Down

1. Biotin-16-UTP.
2. MEGAscript Transcription Kit (*Thermo Fisher Scientific*) (*see* **Note 4**).
3. B&W buffer 10 mM Tris-HCl, pH 7.5, 1 M NaCl, 1 mM EDTA.
4. Streptavidin-coated magnetic beads (*see* **Note 5**).
5. Benzonase (250 U/μl).
6. SDS sample buffer: 62.5 mM Tris-HCl, pH 6.8, 10% glycerol, 2% SDS, 2% 2-mercaptoethanol, 0.05% bromophenol blue.

### 2.4 Isolation of Immunoprecipitated RNA

1. Proteinase K buffer: 10 mM Tris-HCl, pH 8.0, 50 mM NaCl, 5 mM EDTA, 0.5% SDS.
2. 20 mg/ml Proteinase K.
3. 20 μg/μl Glycogen (*see* **Note 6**).
4. Monophasic guanidinium thiocyanate/phenol solution (e.g., Trizol) [10].

## 3 Methods

Carry out all the procedures at 4 °C (unless otherwise stated) and keep samples on ice between experimental steps.

### 3.1 RNA Pulldown with Immobilized Protein

#### 3.1.1 Protein Immunoprecipitation

1. Culture cells that express the protein for which you want to test the lncRNA-interaction. Culture conditions and amount of cells depend on the type of cells and the expression level of the protein of interest. Overexpression of the (epitope-tagged) protein, e.g., by transient transfection of cells, can facilitate the assay (*see* **Note 7**).
2. Remove the medium from cells and harvest in ice-cold PBS either by spinning down (suspension cells) or scraping with a rubber-policeman (adherent cells). Wash cells twice with ice-cold PBS, then take off the supernatant from the pellet.
3. Resuspend cells in Cell lysis/IP buffer (approximately 1 ml per $10^7$ cells) and homogenize by pipetting up and down for several times. Incubate for 1 h at 4 °C on a rotating wheel. Spin down precipitated chromatin and cell debris at 14,000 × *g* for 15 min at 4 °C. Transfer the supernatant to a fresh tube.
4. Add an appropriate amount of the antibody raised against your protein of interest. The amount depends on the protein abundance and the antibody affinity. Incubate for 4 h or overnight at 4 °C on a rotating wheel (*see* **Note 8**).
5. Prepare Protein A/Protein G-coated agarose beads by washing beads twice with 20–50 bead volumes Cell lysis/IP buffer. Resuspend beads as a 33% slurry (10 µl packed beads in 20 µl buffer) and add 30 µl per milliliter cell lysate containing antibody. Continue rotation for 1 h.
6. Spin down beads at 2000 × *g* for 30 s and remove the lysate. Wash beads three times with Cell lysis/IP buffer, using each time half of volume of the original lysate.
7. Store beads in 5 volumes of Cell lysis/IP buffer at 4 °C before continuing with pull-down assay.

#### 3.1.2 Synthesis of Radiolabeled RNA for Pulldown

1. Synthesize and radiolabel RNA by in vitro transcription in the presence of [α-$^{32}$P]-UTP. As a template, use a linearized plasmid (0.5–1 µg per reaction) or a PCR-product (50–100 ng per reaction) containing a phage promoter (T7, T3, or SP6) (*see* **Note 9**).

   For in vitro transcription add the template with 4 µl Transcription-buffer, 2 µl 100 mM DTT, 2 µl rNTP-Mix, 5 µl [α-$^{32}$P]-UTP, 0.5 µl RNasin (40 U/µl) and 20 U phage RNA polymerase in a total reaction volume of 20 µl. Incubate for 1 h at 37 °C (*see* **Note 10**).

2. Purify radiolabeled RNA using the RNA Miniprep Kit according to the manufacturer's recommendations. Elute RNA from the spin column with 50 µl of water.
3. Measure RNA labeling efficiency by Cerenkov scintillation counting of 1–2 µl of the eluate. For a more precise analysis, transcripts can be separated on a polyacrylamide gel in TBE. After transfer of the gel to cellulose paper and drying under vacuum, the transcript integrity and radioactivity can be assessed by phosphor imaging.

#### 3.1.3 Interaction Test Between Immobilized Protein and Radiolabeled RNA

1. Wash protein-coated beads (*see* Subheading 3.1.1) one more time with 5 volumes of Cell lysis/IP buffer and aliquot beads to PCR tubes (200 µl volume). The amount of beads might vary depending on the immunoprecipitation efficiency and the number of interaction assays you want to perform. However, use at least 5 µl of packed beads per tube for the pull-down assay (*see* **Note 11**).
2. Resuspend beads in a final volume of 50 µl Cell lysis/IP buffer per tube.
3. Dilute radiolabeled RNA (*see* Subheading 3.1.2) to a concentration of about 500,000 cpm/ml in Cell lysis/IP buffer (*see* **Note 12**).
4. Add 100 µl of diluted RNA to protein-coated beads (final reaction volume 150 µl) and add 40 U RNasin to the reaction. Resuspend beads by tapping the tube and immediately incubate tubes with rotation at room temperature for 30 min. Make sure that the beads do not settle to the bottom of the tube during the incubation (*see* **Note 13**).
5. Wash beads three times with 100 µl of Cell lysis/IP buffer.
6. Add 20 µl of 80% formamide/0.05% bromophenol blue to beads and elute RNA by incubating at 65 °C for 10 min. Spin down beads for 30 s at 2000 × *g* and transfer the supernatant to a new tube (*see* **Note 14**).
7. Run 50–100% of captured RNA together with 5% input RNA on a polyacrylamide gel, dry the gel, and analyze by phosphor imaging (Fig. 2a).

### 3.2 Protein Pulldown with Biotinylated, Bead-Bound RNA

#### 3.2.1 Immobilization of RNA

1. Synthesize RNA by in vitro transcription from a phage promoter-containing template (linearized plasmid or PCR-product) using Megascript Transcription Kit for the respective phage RNA polymerase according to the manufacturer's recommendations (a 20 µl reaction will yield approximately 100 µg of RNA, which is sufficient for ten pull-down experiments). Supply reactions with Biotin-16-UTP relative to UTP

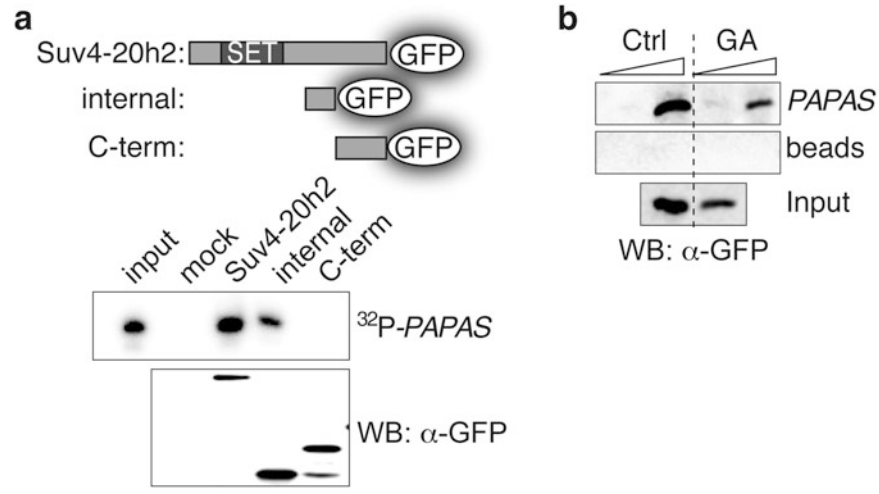


**Fig. 2** Pull-down assays to monitor the interaction between the histone methyltransferase Suv4-20h2 and the lncRNA *PAPAS*. (**a**) GFP-tagged full-length Suv4-20h2 or the truncated versions indicated in the scheme above (internal and C-terminal fragment) were overexpressed in cells and immunopurified. The amount of bead-bound proteins was analyzed by western blotting with anti-GFP antibodies (*lower panel*). Immobilized proteins were then incubated with radiolabeled *PAPAS*. Bound transcripts were eluted and analyzed by polyacrylamide gel electrophoresis and phosphor imaging, showing that full-length Suv4-20h2 and its internal domain, but not the C-terminal domain, bind to *PAPAS* (*upper panel*). (**b**) Pulldown with in vitro synthesized, biotinylated *PAPAS* immobilized on streptavidin beads. Two amounts of either empty beads (*middle panel*) or beads coated with *PAPAS (upper panel)* were incubated with lysates form Suv4-20h2-GFP expressing cells, growing normally (ctrl) or being growth arrested (GA) by hypotonic stress. Suv4-20h2-GFP bound to beads and in the input (*lower panel*) was monitored on western blots

so that every transcript is labeled two to three times with biotin (normally a Biotin-16-UTP/UTP ratio between 1/30 and 1/100 is sufficient, depending on the length and U content of the transcript) (*see* **Note 15**).

2. Purify RNA by phenol/chloroform extraction and precipitate with ammonium acetate. Dissolve RNA in water and determine RNA concentration with a spectrophotometer.
3. Incubate 10 μg RNA with streptavidin-coated magnetic beads (bead amounts will depend on their biotin-binding capacity) in B&W buffer overnight at 4 °C. Bind beads to magnet and measure RNA concentration of the supernatant to calculate how much RNA has been immobilized. Wash beads three times with 100 μl B&W buffer beads, followed by three washes with 100 μl Cell lysis/IP buffer. Store beads in Cell lysis/IP buffer on ice before continuing with pull-down assay (*see* **Note 16**).

*3.2.2 Protein Pull-Down from Cell Lysates*

1. Prepare lysates from cultured cells expressing the protein of interest (*see* **steps 1–4** in Subheading 3.1.1).

2. Remove Cell lysis/IP buffer from streptavidin beads coated with biotinylated RNA (approximately 10 μg) and add 1 ml of cell lysate. Allow RNA to protein binding by rotating for 1 h at room temperature.
3. Bind beads to magnet and take off the supernatant. Wash beads three times with 1 ml of Cell lysis/IP buffer.
4. Elute RNA-bound proteins by adding 30 μl of SDS sample buffer to the beads and heating at 95 °C for 5 min. Cool down samples for 1 min on ice, add 2 μl of Benzonase, and incubate for 20 min at room temperature. Heat again at 95 °C for 5 min. Immobilize beads on a magnet (*see* **Note 17**) and transfer the supernatant to a fresh tube.
5. Analyze pulldown of the protein of interest by western blotting (Fig. 2b).

### *3.3 RNA Immunoprecipitation (RIP)*

1. Immunoprecipitate the protein of interest from cell lysates as outlined in Subheading 3.1.1.
2. After washing, remove Cell lysis/IP buffer completely from the beads with the immobilized material and resuspend beads in 50 μl Proteinase K buffer. Add 2 μl of Proteinase K and incubate at 50 °C for 30 min. Keep the beads in the solution by orbital shaking (*see* **Note 18**).
3. Spin down beads at 2000 × *g* for 30 s and transfer the supernatant to a fresh tube. Add 1 μl of glycogen and 1 ml of monophasic guanidinium thiocyanate/phenol solution (e.g., Trizol). Isolate RNA according to the manufacturer's recommendations and monitor the presence of lncRNAs potentially binding to the protein of interest by RT-PCR or northern blotting.

## 4 Notes

1. You might need to modify the Cell lysis/IP buffer formulation according to the protein you are studying. For example, if working with a tightly chromatin-associated protein, extraction might be facilitated by higher salt concentrations and additional ultrasound treatment. However, extraction conditions should not harm the protein-RNA interaction. In case harsh extractions methods are required or interactions are very labile, cross-linking by formaldehyde or UV irradiation might be used [8, 11].
2. To bind different IgG subtypes from multiple species we use an equal mixture of Protein A/Protein G-coated agarose beads. Similar results should be obtained with recombinant Protein A/G beads (either agarose beads or magnetic beads). When

working with epitope-tagged proteins, beads covalently coupled to the antibody against the tag can also be used.

3. Many vendors provide phage RNA polymerases with an optimized buffer system. Make sure not to use a high-yield in vitro transcription kit, which is not suitable for radioactive labeling.
4. We have obtained transcript yields of 100 μg RNA per 20 μl reaction with the MEGAscript T7 Transcription Kit. However, high yield in vitro transcription kits from other vendors might perform equally well.
5. Use preferentially magnetic streptavidin-beads that have a diameter of 1 μm. Alternatively, streptavidin-coated agarose beads can be used.
6. As the amount of precipitated RNA is very low, glycogen is used as a carrier to facilitate precipitation. Glycogen conjugated to a dye facilitates visibility of the pellet, thereby preventing loss of RNA during precipitation.
7. The choice of the cell line and expression system strongly depends on the physiological question under investigation. High expression levels of recombinant proteins can be achieved by transient transfection of human HEK293T cells. However, non-transformed cells like fibroblasts might be more suitable for studies on cellular quiescence.
8. Usually, 1–5 μg of antibody is used per immunoprecipitation. Determine the optimal amount of antibody in a pilot experiment. For low affinity antibodies incubation with the lysate should be performed overnight. For high affinity antibodies or antibodies pre-coupled to beads the incubation should last only 4 h.
9. In our experience, in vitro transcription driven by T7 RNA polymerase gives very robust and reliable results. Transcription templates for RNAs in the range of 100–1000 nucleotides can be easily produced by PCR if the extended T7 promoter sequence 5′-GCTGAAATTAATACGACTCACTATAGGG-3′ is fused to the 5′ end of the forward primer.
10. If the yield of labeled transcript is low, extend the incubation time to 3 h and add additional 20 U of phage RNA polymerase to the reaction after 1.5 h. Low efficiency in transcription might also result from low UTP concentration (the concentration of [$\alpha$-$^{32}$P]-UTP in the reaction is 12.5 μM). In this case, supplement the reaction with 125 μM unlabeled UTP. Varying the amounts of unlabeled UTP can also be used to adjust the specific activity of different transcripts, e.g., if the content of U in the two transcripts differs fivefold, adding 5× more unlabeled UTP to the reaction for the U-rich transcript will equalize the specific activity of both transcripts.

11. It is hard to get a visible pellet at the tube bottom with <5 μl of agarose beads and thus beads might get lost during washing. If you want to use <5 μl of beads fill up the bead volume with "empty" beads. Alternatively, use magnetic beads that can be handled in very small amounts.
12. A concentration of about 500,000 cpm/ml for radiolabeled RNA is just a rough estimation. The amount of radiolabeled RNA will vary according to its specific activity and the optimal RNA concentration needs to be determined empirically.
13. To avoid beads of settling to the bottom of the PCR tube it is best to have them on a rotating wheel. For this you can put the PCR tubes in a 50 ml Falcon tube, which will be attached to the wheel, or you fix a PCR-rack to the wheel.
14. 80% formamide co-elutes RNA and proteins from the beads that can form complexes during polyacrylamide gel electrophoresis and might thus hinder migration of the RNA. If you face this problem, switch to elution by digestion with Proteinase K (*see* Subheading 3.3, **step 2**). Use 25 μl of Proteinase K buffer and 1 μl of Proteinase K. After digestion add an equal volume of 100% formamide/0.05% bromophenol blue for loading on the polyacrylamide gel.
15. The standard Megascript in vitro transcription reaction contains 7.5 mM of each unlabeled NTP. Using half of the concentration (3.75 mM) is still sufficient for transcription and reduces the amount of the expensive and low concentrated Biotin-16-UTP that needs to be added (e.g., adding 2 μl of 1 mM Biotin-16-UTP to the reaction will result in a final ~1/40 ratio between Biotin-16-UTP and unlabeled UTP).
16. Beads with biotinylated RNA should be used quickly for pulldown experiments to avoid the risk of RNA degradation. Coordinate preparation of cell lysates accordingly to keep the time between RNA immobilization and pulldown as short as possible.
17. Heating of magnetic beads in SDS sample buffer can reduce their binding to the magnet. If you face this problem, collect beads by spinning at 14,000 × *g* for 1 min and carefully take off the supernatant.
18. Incubate beads in a thermoblock with horizontal shaking function set to maximum speed. Gently resuspend beads first manually so that they do not get distributed on the wall of the tube. Then immediately transfer the tube in the thermoblock that is already shaking to prevent beads from settling down.

## Acknowledgments

This work was supported by the Thuringian country program ProExzellenz (RegenerAging—FSU-I-03/14) of the Thuringian Ministry for Research (TMWWDG).

### References

1. Guttman M, Rinn JL (2012) Modular regulatory principles of large non-coding RNAs. Nature 482(7385):339–346. doi:10.1038/nature10887
2. Rinn JL, Chang HY (2012) Genome regulation by long noncoding RNAs. Annu Rev Biochem 81:145–166. doi:10.1146/annurev-biochem-051410-092902
3. Quinodoz S, Guttman M (2014) Long noncoding RNAs: an emerging link between gene regulation and nuclear organization. Trends Cell Biol 24(11):651–663. doi:10.1016/j.tcb.2014.08.009
4. Roberts TC, Morris KV, Weinberg MS (2014) Perspectives on the mechanism of transcriptional regulation by long non-coding RNAs. Epigenetics 9(1):13–20. doi:10.4161/epi.26700
5. Bierhoff H, Schmitz K, Maass F, Ye J, Grummt I (2010) Noncoding transcripts in sense and antisense orientation regulate the epigenetic state of ribosomal RNA genes. Cold Spring Harb Symp Quant Biol 75:357–364. doi:10.1101/sqb.2010.75.060
6. Bierhoff H, Dammert MA, Brocks D, Dambacher S, Schotta G, Grummt I (2014) Quiescence-induced LncRNAs trigger H4K20 trimethylation and transcriptional silencing. Mol Cell 54(4):675–682. doi:10.1016/j.molcel.2014.03.032
7. Hammerle M, Gutschner T, Uckelmann H, Ozgur S, Fiskin E, Gross M, Skawran B, Geffers R, Longerich T, Breuhahn K, Schirmacher P, Stoecklin G, Diederichs S (2013) Posttranscriptional destabilization of the liver-specific long noncoding RNA HULC by the IGF2 mRNA-binding protein 1 (IGF2BP1). Hepatology 58(5):1703–1712. doi:10.1002/hep.26537
8. Hendrickson D, Kelley DR, Tenen D, Bernstein B, Rinn JL (2016) Widespread RNA binding by chromatin-associated proteins. Genome Biol 17:28. doi:10.1186/s13059-016-0878-3
9. Zhao J, Ohsumi TK, Kung JT, Ogawa Y, Grau DJ, Sarma K, Song JJ, Kingston RE, Borowsky M, Lee JT (2010) Genome-wide identification of polycomb-associated RNAs by RIP-seq. Mol Cell 40(6):939–953. doi:10.1016/j.molcel.2010.12.011
10. Chomczynski P, Sacchi N (1987) Single-step method of RNA isolation by acid guanidinium thiocyanate-phenol-chloroform extraction. Anal Biochem 162(1):156–159. doi:10.1006/abio.1987.9999
11. Ascano M, Hafner M, Cekan P, Gerstberger S, Tuschl T (2012) Identification of RNA-protein interaction networks using PAR-CLIP. Wiley Interdiscip Rev RNA 3(2):159–177. doi:10.1002/wrna.1103

# Chapter 18

# Analysis of MicroRNA-Mediated Translation Activation of In Vitro Transcribed Reporters in Quiescent Cells

**Syed I.A. Bukhari, Samuel S. Truesdell, and Shobha Vasudevan**

## Abstract

Quiescence (G0) is defined as an assortment of cell cycle arrested states that exhibit distinct properties. Leukemias harbor a subpopulation of G0 cells that can be enriched by growth factor deprivation or serum starvation. Target site reporters with shortened poly(A) tails show translation activation by microRNAs, via a noncanonical mechanism, when introduced into the nucleus of G0 cells. This is because recruitment by the activation causing FXR1a-microRNA-protein complex (FXR1a-microRNP) is nuclear and requires shortened poly(A) tails to avoid repressive factors and canonical translation. When introduced into the cytoplasm, target mRNAs and microRNAs are directed toward repression rather than translation activation. Leukemic cell lines are difficult to transfect but can be routinely nucleofected—where in vitro transcribed mRNA reporters and microRNAs are introduced into the nucleus of G0 leukemic cells. Nucleofection of a microRNA target reporter and either cognate, targeting microRNA, or control microRNA, into the nucleus of G0 cells, enables analysis of translation activation by microRNAs in G0. We discuss a modified protocol that we developed for transfection of mRNAs along with microRNAs to test translation regulation by microRNAs in G0 leukemic cells.

**Key words** MicroRNA, Noncanonical translation, Nucleofection, THP1 acute monocytic leukemia cell line, Quiescence, G0

## 1 Introduction

Quiescent (G0) cells are reversibly arrested cells, which are found in the body and in cancers [1–7]. Such cells show distinct properties [8], including resistance to harsh conditions [1, 2, 4, 5, 9–24]. Cells when subjected to specific stress conditions such as growth factor deprivation enter G0 transiently [3, 9]. G0 cells alter gene expression [14, 25–28]; in particular, at the translation level [29–31] where cells decrease canonical translation or protein synthesis [32, 33] and promote alternative, noncanonical modes of translation of specific genes that could enable G0 cell survival [29, 30]. We identified a noncanonical translation mechanism in G0 leukemic cells, which is mediated by microRNAs [29, 34–36]. MicroRNAs generally degrade mRNAs and repress their translation

H. Daniel Lacorazza (ed.), *Cellular Quiescence: Methods and Protocols*, Methods in Molecular Biology, vol. 1686,
DOI 10.1007/978-1-4939-7371-2_18, 

in proliferating cells, by base-pairing with specific sequences in mRNA 3′untranslated regions (UTRs) and by recruiting repressive factors to such mRNAs [37–42]. However, in G0 cells, microRNAs can activate translation of specific mRNAs by a noncanonical translation mechanism [29]. In G0 cells, microRNAs form a complex (microRNA-protein complex or microRNP) with RNA-binding proteins, FXR1a and AGO2, in the nucleus [34, 36, 42–45]. This specialized microRNP is recruited to the 3′ UTRs of specific target mRNAs that are unadenylated or possess a short poly (A) tail [29]. Short poly (A) tails avoid binding Poly (A) binding protein (PABP) that is involved in microRNA-mediated repression [37, 40], and in canonical translation that is decreased in G0 [32, 33]. Deadenylation of such target mRNAs in G0 cells is mediated by a cap-binding deadenylase protein called poly(A) ribonuclease (PARN) [29, 46, 47]. PARN becomes active in G0 cells and its binding to the 5′ cap is increased under these conditions [29, 46, 47]. PARN associates with FXR1a-microRNP that also interacts with p97/DAP5, an eIF4G paralog that brings in the 40S ribosomal subunit and mediates cap-dependent noncanonical translation of specific mRNAs in G0 cells, where canonical translation is reduced [29, 42, 48–51].

To study microRNA-mediated translation activation in G0 leukemic cells, we used luciferase reporter mRNAs bearing either a synthetic 3′UTR that possesses binding sites for a synthetic microRNA, or a specific gene 3′UTR bearing natural, endogenous microRNA-binding sites [52, 53]. Luciferase reporter mRNAs are synthesized by in vitro transcription, using T7 ultra mMESSAGE mMACHINE kit (Invitrogen™ Ambion™) with our modified protocol. The reporter mRNAs possessing gene-specific or synthetic microRNA target site 3′UTRs were generated with a 5′ Anti-reverse cap analog (ARCA) 7-methyl guanosine cap [54]. The reporter mRNAs were produced without a poly(A) tail to mimic the endogenous targets of activation that shorten their poly (A) tails to avoid PABP binding that can promote the repressive microRNP complex. The 3′ ends of the reporter mRNAs were protected by adding cordycepin (3′-deoxyadenosine analog of adenosine) that prevents transcript elongation and mRNA degradation [55].

Transfer of exogenous DNA or mRNA reporters allows us to study translation regulation in proliferating cells and upon their induction to G0. Many commercial methods have been developed to deliver exogenous DNA or RNA molecules into cultured cells. Nucleofection from Amaxa (now Lonza), an electroporation-based technology, allows for sufficient delivery of exogenous DNA or RNA molecules directly into the nucleus of a cell [56, 57 ]. Nucleofection [58] uses distinct sets of electrical parameters and buffers for each cell type to obtain high efficiency of transfection with low toxicity [57, 59]. Purified, in vitro transcribed reporter mRNAs along with their corresponding, targeting microRNAs can be

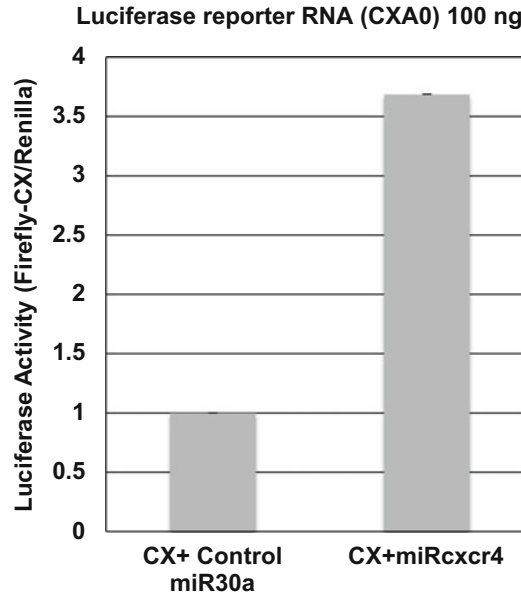


**Fig. 1** 100 ng of in vitro transcribed capped CX-Firefly luciferase mRNA—without a poly(A) tail (CXA0) and with cordycepin added at the 3′ end—was nucleofected along with 20 ng of renilla plasmid, and 500 pmol of miRcxcr4 or control miR30a, into $1 \times 10^6$ THP1 cells. After nucleofection, cells were grown in RPMI medium supplemented with 10% fetal bovine serum (FBS) for 24 h, and then shifted to G0 medium (RPMI medium without FBS) for 42 h before analysis of luciferase activity. More than three fold increase in the translation of CX-firefly luciferase is observed in the presence of cognate microRNA miRcxcr4 compared to control microRNA miR30a

nucleofected into the nucleus of cells of THP1 acute monocytic leukemic cell line.

In this chapter, we will outline nucleofection of reporter mRNAs along with their cognate or control microRNAs, to analyze microRNA-mediated translation activation in G0 leukemic THP1 cells. As an example, we show microRNA-dependent translation activation of in vitro transcribed CX-Firefly luciferase reporter mRNA in G0 THP1 cells (Fig. 1). CX-Firefly luciferase reporter mRNA is 5′ capped and unadenylated with four binding sites for the synthetic microRNA, miRcxcr4 [34, 53, 60]. CX-Firefly luciferase reporter mRNA, along with a control microRNA (miR30a), that does not bind the CX reporter 3′ UTR or a cognate microRNA (miRcxcr4) that can bind the 3′ UTR of the reporter mRNA, as well as Renilla luciferase reporter plasmid, were co-transfected by nucleofection. Renilla luciferase serves as a transfection and normalization control. Cells are allowed to grow in medium supplemented with serum for 24 h before being shifted to a medium without serum (G0 medium) for 42–48 h [29]. G0 cells are harvested for luciferase assay and translation efficiency is determined as the ratio of firefly luciferase activity normalized to renilla luciferase

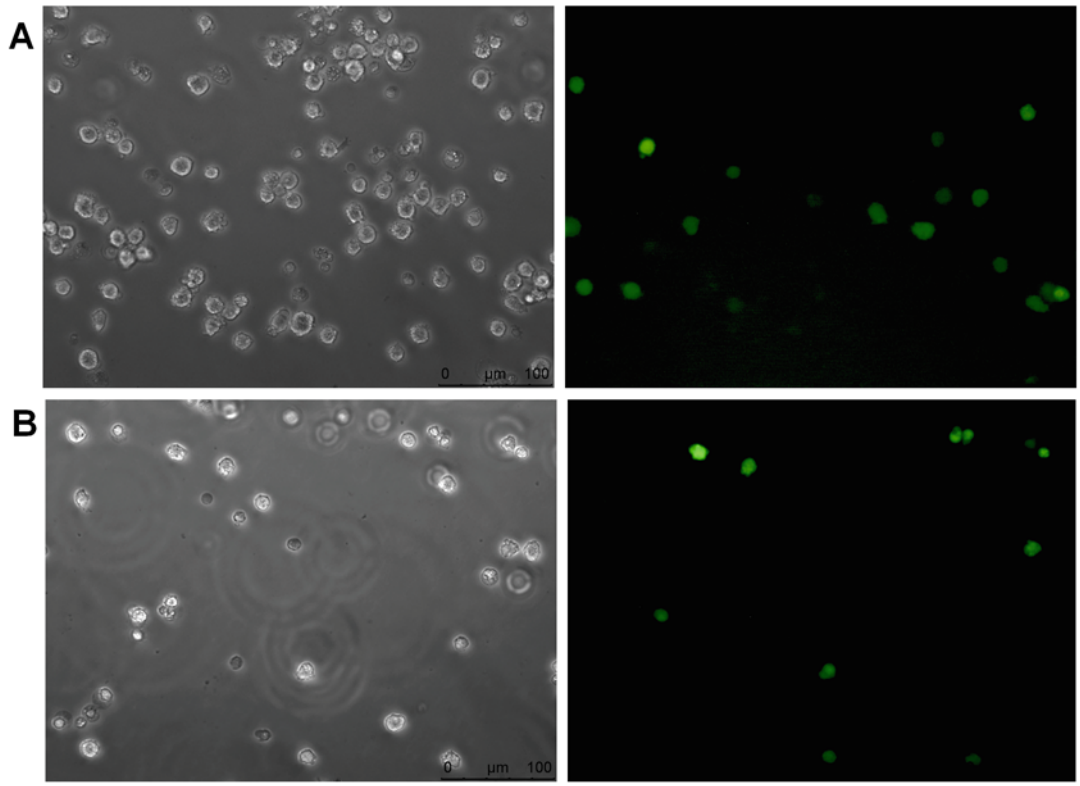


**Fig. 2** $1 \times 10^6$ THP1 cells were nucleofected with 2.0 µg of pmax-GFP, using Kit V and nucleofector device II from Lonza. Left and right panels show 20× phase-contrast image and green fluorescent protein (GFP) positive THP1 cells respectively (images captured using a Leica DMI-4000B fluorescence inverted microscope). (**A**) Nucleofection program U-001 for high cell viability was used and transfection efficiency of about 24% was observed. (**B**) Program V-001 for high nucleofection efficiency was used and transfection efficiency of about 40% was achieved

activity, and then further normalized for their RNA levels [29, 34]. Furthermore, to monitor the efficiency of transfection, THP1 cells are nucleofected with a GFP-expressing plasmid using the nucleofection protocol described here (Fig. 2). This protocol can also be used for nucleofecting siRNAs, LNAinhibitors, plasmid DNA that overexpress a gene of interest, or an shRNA to knock down a specific gene, and then monitor the effect on microRNA-mediated translation activation in G0 cells.

## 2 Materials

All reagents and solutions to be used for nucleofection should be warmed to room temperature (unless indicated otherwise) prior to use. RNAs stored at −80 °C or the frozen plasmid DNA to be used for nucleofection should be thawed on ice prior to use. Nuclease-free water should be used at all times.

### 2.1 Materials for In Vitro Transcription of Capped mRNA

1. T7 ultramMESSAGE mMACHINE transcription system kit from Invitrogen™ Ambion™ is used to in vitro transcribe RNA molecules from a linearized template DNA of interest.
2. Components of the kit used in our reaction are nuclease-free water, T7 Enzyme mix, 10× T7 reaction buffer containing salts, buffer, dithiothreitol, T7 2× NTP/ARCA comprising of 15 mM ATP, 15 mM CTP, 15 mM UTP, 3 mM GTP and 12 mM ARCA, and Turbo DNase I (2 U/μl).
3. CX-Firefly luciferase plasmid DNA described in [34, 35]—containing a T7 RNA polymerase promoter site upstream of the luciferase reporter sequence for in vitro transcription—at a concentration of 0.5 μg/μl in nuclease-free water.
4. ApaI restriction enzyme for linearizing the CX-Firefly luciferase reporter plasmid containing a T7 RNA polymerase promoter and corresponding buffer (New England Biolabs).
5. 1 mM Cordycepin (from Sigma).
6. 3 M sodium acetate, or 5 M ammonium acetate for precipitation.
7. 5× E-PAP buffer and enzyme (From Kit).
8. 25 mM $MnCl_2$ (From Kit).
9. Phenol:Chloroform (Prepared in the lab by mixing equal volume of saturated phenol with chloroform).
10. Ethanol, 100% (cold, −20 °C) and 70% (room temperature).
11. Glycogen.
12. Agarose gel.
13. 10× TAE electrophoresis buffer.
14. Ethidium bromide staining solution.
15. Nuclease-free water.

### 2.2 Materials for Nucleofection

1. Nucleofector II device from Lonza (Amaxa).
2. Nucleofector solution Kit V (tested and validated for usage for THP1 cells by Lonza).
3. Certified cuvettes supplied with the kit.
4. Plastic bulb pipettes supplied with the kit.
5. pmaxGFP plasmid supplied with the kit, in vitro transcribed firefly-luciferase reporter mRNA, renilla plasmid, and control or cognate microRNA duplex.
6. A 10 cm cell culture plate or a 6-well cell culture plate.
7. Pre-warmed RPMI1640 culture medium containing 2 mM glutamine, 100 μg/ml streptomycin, 100 U/ml penicillin, and 10% fetal bovine serum (Gibco/Invitrogen).

8. Appropriate number of THP1 cells ($1 \times 10^6$ cells per nucleofection reaction).

### 2.3 Materials for Transfection and Translation Analysis

1. pmaxGFP plasmid (supplied with nucleofection kit).
2. Dual-Luciferase® Reporter 1000 Assay System (Promega). Components of this kit are: Luciferase Assay Substrate (lyophilized), luciferase Assay Buffer II, Stop & Glo® Substrate (50×), Stop & Glo® Buffer, and Passive Lysis Buffer (5×).
3. Fluorescence microscope (Leica DMI-4000B).
4. Spectrophotometer—Nanodrop (ND1000 spectrophotometer).
5. TD 20/20 Luminometer (Turner Biosystems).
6. TRIzol® Reagent (Ambion by Life Technologies).
7. SuperScript™ III Reverse Transcriptase kit for cDNA synthesis (Invitrogen).
8. iTaq ™ Universal SYBR Green Supermix (BIO-RAD).
9. Real-time qPCR machine (Roche 480).

## 3 Methods

### 3.1 Plasmid DNA Template Linearization for In Vitro Transcription

1. Digest 5–10 μg of CX-Firefly luciferase reporter plasmid DNA described in [34] with ApaI restriction enzyme overnight at 25 °C in a 50–100 μl reaction volume. ApaI cuts downstream of the T7 promoter and the luciferase reporter sequence to be transcribed.
2. Extract the linearized plasmid with phenol:chloroform and precipitate the DNA with 3 M sodium acetate (1/10th of the reaction volume) and 100% (cold −20 °C) ethanol (2.5 times the reaction volume).
3. Mix well and incubate at −80 °C for minimum 1 hour and then centrifuge the tubes at maximum speed (12,000 × *g*) for 30 min at 4 °C. Remove the supernatant, wash the pellet with 70% ethanol at room temperature, and briefly spin the tubes again to collect and remove the residual fluid with a 0.2–10 μl pipette.
4. Air-dry the pellet on ice for 5 min and then resuspend the DNA to 1 μg/μl in nuclease-free water.
5. Run an aliquot (~0.5 μg) of the resuspended DNA on a 1% agarose gel to check the linearization of the plasmid.

### 3.2 Synthesis of In Vitro Transcribed Capped mRNA, Protected at the 3′ End by Cordycepin

1. Take out the frozen components of mMESSAGE mMACHINE T7 kit and thaw at room temperature. The RNA polymerase enzyme mix (that is stored in glycerol and not frozen) should be placed directly on ice.
2. After thawing the components, vortex the 10× T7 reaction buffer and the T7 2× NTP/ARCA to ensure thorough mixing.
3. Briefly centrifuge the tubes to collect the reagents at the bottom of the tube before opening to prevent loss or contamination of the reagents that may be present around the cap or rim of the tube.
4. Assemble the transcription reaction at room temperature and mix the reagents in the following order and amounts, for a 20 μl reaction volume:

   4 μl of nuclease-free water.

   10 μl of T7 2× NTP/ARCA.

   2 μl of 10× T7 Reaction Buffer.

   1 μg of 0.5 μg/μl linear template DNA.

   2 μl T7 enzyme mix.
5. Mix the reaction mixture thoroughly and then briefly centrifuge the tubes.
6. Incubate the reaction mixture at 37 °C for 2–4 h to achieve maximum yield.
7. To the reaction mixture, add 1 μl of TURBO DNase, mix by pipetting up and down gently, and then incubate at 37 °C for 15 min (*see* **Note 1**).
8. To 20 μl of mMESSAGE mMACHINE T7 ultra reaction, add 1.5 μl of cordycepin (1 mM final concentration), 20 μl of 5× E-PAP buffer, 10 μl of 25 mM $MnCl_2$, 43.5 μl of nuclease-free water, and 4 μl of E-PAP enzyme. Mix gently and incubate for 2 h at 37 °C.
9. After cordycepin addition, purify the in vitro transcribed RNA using phenol:chloroform. Add equal volume of saturated phenol:chloroform and vortex briefly (*see* **Note 2**).
10. Centrifuge the tubes at 12,000 × *g* for 15 min at 4 °C for phase separation.
11. Transfer the upper aqueous layer to a new tube (*see* **Note 3**).
12. Add 80 μl of 5 M ammonium acetate, 1 μl of glycogen as well 2.5 times the volume of the supernatant of 100% cold ethanol (−20 °C). Mix properly and incubate at −80 °C for 1 hour.
13. Centrifuge the tubes at maximum speed for 40 min.
14. Remove the supernatant and wash pellet with 1 ml of 70% ethanol (room temperature).

15. Briefly centrifuge the tubes to collect the residual ethanol and remove using a 10 μl pipette (*see* **Note 3**).
16. Air-dry the pellet on ice for 5 min and then resuspend the pellet in appropriate volume of nuclease-free water.
17. Run RNA on an agarose gel to check integrity and size of the RNA (*see* **Note 4**).
18. Measure the concentration of the RNA solution on a nanodrop (ND1000 spectrophotometer) at absorbance 260 nm.
19. Freeze and store the in vitro transcribed mRNA at −80 °C for further use.

#### 3.2.1 Synthesis of MicroRNAs

Synthetic microRNA (miRcxcr4) and control microRNA (miR30a) or a scrambled microRNA can be ordered as anti-sense (targeting microRNA) and sense RNA oligos that are modified with a 5′ phosphate. These RNA oligos are designed to base-pair with each other, with a bulge in the middle of the RNA oligos (at nucleotides (nt) 9–11 of the 19 nt oligos) [34, 61]. The anti-sense strand binds the target mRNA with imperfect base pairing.

1. Each of the individually synthesized sense and anti-sense microRNA strands is resuspended at 200 pmol/μl concentration in annealing buffer (10 mM potassium acetate and 1 mM EDTA), as described in [34, 61].
2. Measure resuspended anti-sense and sense microRNA strands and then mix in equimolar proportions.
3. Anneal mixed RNA oligos by heating the mixture to 95 °C for 5 min and allow to cool down slowly to room temperature for annealing of the sense and anti-sense strands.
4. Annealed microRNAs are nucleofected as duplexes as described in [3, 34, 53, 60].

### 3.3 Nucleofection of Plasmid DNA or In Vitro Transcribed mRNA along with MicroRNAs into THP1 Cells

#### 3.3.1 Culturing THP1 Cells [29]

1. THP1 cells from ATCC are thawed in RPMI-1640 culture medium, with 2 mM Glutamine, 100 μg/ml streptomycin, 100 U/ml penicillin, and 10% fetal bovine serum (FBS) added.
2. Cells should be allowed to recover after thawing for 2–3 days by incubating in a 37 °C humidified incubator supplied with 5% $CO_2$.
3. Passage cells at least two times prior to starting the experiment. Allow cells to reach an optimal density of $1 \times 10^6$ cells/ml in a T75 flask (30 ml per flask).
4. Replace the medium two to three times a week and maintain the cell density of $3–4 \times 10^5$ cells/ml every time the medium is changed.
5. Seed out $2 \times 10^5$ cells/ml and subculture for 2–3 days before nucleofection.

### 3.3.2 Nucleofecting THP1 Cells

1. Prepare the nucleofector mixed solution by mixing Nucleofector™ solution V and Supplement 1 solution, as instructed by Lonza. We prepare nucleofector mixed solution in a sterile 1.5 ml eppendorf tube by mixing 82 μl of Nucleofector™ solution V with 18 μl of Supplement 1 solution in a 4.5:1 ratio to make a total of 100 μl solution for a single nucleofection reaction (*see* **Note 5**).
2. Prepare a 10 cm plate with 10 ml of pre-warmed culture medium for every single reaction.
3. Count an aliquot of cells to determine the cell density.
4. For a single nucleofection, centrifuge $1 \times 10^6$ THP1 cells at 1000 rpm ($230 \times g$) in a microcentrifuge for 3–5 min. Remove the supernatant completely without disturbing the cell pellet (*see* **Note 6**).
5. Resuspend the cell pellet gently in the 100 μl prepared nucleofection solution at room temperature, following the instructions from Lonza (*see* **Note 7**).
6. Mix the resuspended cell suspension with 100–200 ng of in vitro transcribed CX-Firefly luciferase reporter mRNA, 500 pmoles of control microRNA or miRcxcr4, and 20 ng of renilla plasmid (*see* **Note 8**).
7. Transfer cell/nucleic acid suspension into the bottom of a certified cuvette (Lonza) using a plastic bulb pipette (Lonza). Close the cuvette with the cap (*see* **Note 9**).
8. Select the appropriate nucleofector program in the Nucleofector device II—for nucleofection of THP1 cells V-001 for high efficiency or U-001 for high viability, as recommended by Lonza (*see* **Note 10**).
9. Place the cuvette containing cells and nucleic acid suspension into the Nucleofector cuvette holder and apply the selected program, following the instructions from Lonza.
10. Take the cuvette out of the holder once the display shows OK, following the instructions from Lonza.
11. Add 200–300 μl of pre-warmed culture medium to the cuvette and carefully transfer the cell suspension into the prepared 10 cm culture plate using the plastic bulb pipette, as recommended by Lonza.
12. Incubate the nucleofected cells at 37 °C in a humidified incubator supplied with 5% $CO_2$ for 24–30 h, post nucleofection (*see* **Note 11**).
13. Change the medium to serum-free medium (G0 medium) and incubate the cells at 37 °C in a humidified incubator supplied with 5% $CO_2$ for 42–48 h until analysis.

14. For luciferase reporter assay, G0 cells should be harvested by centrifuging at 1500 rpm (530 × *g*) for 10 min at 4 °C. Remove the supernatant completely and resuspend cells in 50 μl of 1× passive lysis buffer (1 × PLB buffer) (*see* **Note 12**).
15. Freeze the cells resuspended in 1× PLB buffer at −80 °C overnight and ensure complete lysis of the cells.
16. Thaw the frozen samples and take out 10 μl of the sample for luciferase assay.
17. Measure firefly and renilla luciferase activity sequentially, as per the manufacturer's guidelines on a TD 20/20 luminometer, using an appropriate dual luciferase measurement program. First, add 100 μl of luciferase assay substrate to 10 μl of the sample, mix by pipetting and measure firefly luciferase activity using the dual luciferase program on the TD 20/20 luminometer. Firefly Luciferase activity is then quenched by adding 100 μl of Stop & Glo solution and renilla luciferase activity is measured.
18. Translation efficiency is calculated by normalizing the ratio of firefly luciferase activity to renilla luciferase and then further normalized to their RNA levels that were measured by qPCR as described in [29] (*see* **Note 13**).

## 4 Notes

1. Make sure to treat the transcription mixture with DNase at this step, as any DNA contamination will interfere with downstream steps.
2. Cordycepin is an adenosine analog and should be completely removed, as it inhibits polyadenylation and translation [55]. Remove all free nucleotides and ARCA completely, as unincorporated ARCA is also an inhibitor of translation.
3. The upper aqueous layer should be carefully transferred to new eppendorfs without any phenol contamination upon phenol: chloroform extraction. Remove all residual ethanol and dry the RNA pellet on ice. Residual ethanol or phenol contamination will impact the nanodrop readouts while measuring the RNA concentration and will affect the nucleofection efficiency as well.
4. Run the in vitro transcribed mRNA on a 1% TAE agarose gel to check RNA integrity and size. CX-Firefly luciferase mRNA will run around 2 kb (1.8 kb luciferase with an additional 150 nucleotides for miRcxcr4-binding sites).
5. The mixture of Nucleofector™ Solution V and Supplement 1 solution from the nucleofection kit (nucleofector mixed solution), is stable only for 3 months at 4 °C, according to the instructions from Lonza.

6. Cell numbers lower than the minimal recommended number could lead to an increase in cell death; cell numbers more than the recommended number could influence nucleofection efficiency, as recommended by Lonza [57].
7. Cells should not be left in the nucleofector solution for more than 15 min, as this may affect the nucleofection efficiency and decrease cell viability, as recommended by Lonza [57].
8. For a 100 μl reaction containing $1 \times 10^6$ cells, increasing nucleic acid concentrations for nucleofection more than recommended may lead to increased cell death, according to the instructions from Lonza [57].
9. Carefully transfer the cell suspension with nucleic acid to the bottom of the cuvette and avoid air bubbles that may decrease gene transfer efficiency, as instructed by Lonza. Cap of the cuvette should be closed every time to prevent spills or contamination, as instructed by Lonza [57].
10. Appropriate program should be selected based on the downstream requirement of the experiment. For high efficiency of gene transfer program V-001 should be selected and if more viable cells are required the program U-001 should be used, as recommended by Lonza.
11. After nucleofection, cells should be allowed to grow in medium supplemented with serum for more than 24 h to alleviate the stress induced by nucleofection [29].
12. 1× Passive lysis buffer (PLB) should be made fresh and if the cell lysate is to be used for Western blot analysis, appropriate amount of protease inhibitors should be added [29].
13. To measure firefly and renilla luciferase RNA levels, isolate RNA from the nucleofected samples dissolved in 1× PLB using TRIzol reagent. Prepare cDNA using random hexamer primers with superscript III kit following the manufacturer's instructions. Firefly luciferase mRNA levels can be measured by qPCR using Roche 480 real-time qPCR machine, following the manufacturer's instructions using primers; FF-F3: 5′-TTCCATCTTCCAGGGATACG-3′ and FF-R3: 5′-ATCCAGATCCACAACCTTCG-3′ and normalized to tRNA-Lys using primers; tRNA-Lys Forward: 5′-GCCCGGATAGCTCAGTCGGTAGAG-3′ and tRNA-Lys Reverse: 5′-CGCCCGAACAGGGACTTGAACCC-3′. Renilla mRNA levels are measured using primers; Renilla (Ren1) Forward; 5′-CCATGATAATGTTGGACGAC-3′ and Renilla (Ren2) Reverse; 5′-GGCACCTCCAACAATAGCATTG-3′ and normalized to tRNA-Lys. Normalized firefly and renilla mRNA levels were used to further normalize the firefly luciferase activity and renilla activity to obtain the translation efficiency [29, 34].

## References


1. Pardee AB (1974) A restriction point for control of normal animal cell proliferation. Proc Natl Acad Sci U S A 71(4):1286–1290
2. Aragon AD, Rodriguez AL, Meirelles O, Roy S, Davidson GS, Tapia PH, Allen C, Joe R, Benn D, Werner-Washburne M (2008) Characterization of differentiated quiescent and nonquiescent cells in yeast stationary-phase cultures. Mol Biol Cell 19(3):1271–1280. doi:10.1091/mbc.E07-07-0666
3. Coller HA, Sang L, Roberts JM (2006) A new description of cellular quiescence. PLoS Biol 4 (3):e83. doi:10.1371/journal.pbio.0040083
4. Ng SW, Mitchell A, Kennedy JA, Chen WC, McLeod J, Ibrahimova N, Arruda A, Popescu A, Gupta V, Schimmer AD, Schuh AC, Yee KW, Bullinger L, Herold T, Gorlich D, Buchner T, Hiddemann W, Berdel WE, Wormann B, Cheok M, Preudhomme C, Dombret H, Metzeler K, Buske C, Lowenberg B, Valk PJ, Zandstra PW, Minden MD, Dick JE, Wang JC (2016) A 17-gene stemness score for rapid determination of risk in acute leukaemia. Nature 540(7633):433–437. doi:10.1038/nature20598
5. Kreso A, Dick JE (2014) Evolution of the cancer stem cell model. Cell Stem Cell 14(3):275–291. doi:10.1016/j.stem.2014.02.006
6. Meacham CE, Morrison SJ (2013) Tumour heterogeneity and cancer cell plasticity. Nature 501(7467):328–337. doi:10.1038/nature12624
7. Crews LA, Jamieson CH (2013) Selective elimination of leukemia stem cells: hitting a moving target. Cancer Lett 338(1):15–22. doi:10.1016/j.canlet.2012.08.006
8. Bhola PD, Mar BG, Lindsley RC, Ryan JA, Hogdal LJ, Vo TT, DeAngelo DJ, Galinsky I, Ebert BL, Letai A (2016) Functionally identifiable apoptosis-insensitive subpopulations determine chemoresistance in acute myeloid leukemia. J Clin Investig 126 (10):3827–3836. doi:10.1172/JCI82908
9. Sang L, Coller HA, Roberts JM (2008) Control of the reversibility of cellular quiescence by the transcriptional repressor HES1. Science 321(5892):1095–1100. doi:10.1126/science.1155998
10. Tavaluc RT, Hart LS, Dicker DT, El-Deiry WS (2007) Effects of low confluency, serum starvation and hypoxia on the side population of cancer cell lines. Cell Cycle 6(20):2554–2562. doi:10.4161/cc.6.20.4911
11. Gupta PB, Onder TT, Jiang G, Tao K, Kuperwasser C, Weinberg RA, Lander ES (2009) Identification of selective inhibitors of cancer stem cells by high-throughput screening. Cell 138(4):645–659. doi:10.1016/j.cell.2009.06.034
12. Lemons JM, Feng XJ, Bennett BD, Legesse-Miller A, Johnson EL, Raitman I, Pollina EA, Rabitz HA, Rabinowitz JD, Coller HA (2010) Quiescent fibroblasts exhibit high metabolic activity. PLoS Biol 8(10):e1000514. doi:10.1371/journal.pbio.1000514
13. Lindeman GJ, Visvader JE (2010) Insights into the cell of origin in breast cancer and breast cancer stem cells. Asia Pac J Clin Oncol 6 (2):89–97. doi:10.1111/j.1743-7563.2010.01279.x
14. Salony SX, Alves CP, Dey-Guha I, Ritsma L, Boukhali M, Lee JH, Chowdhury J, Ross KN, Haas W, Vasudevan S, Ramaswamy S (2016) AKT inhibition promotes nonautonomous cancer cell survival. Molecular cancer therapeutics 15(1):142–153. doi:10.1158/1535–7163.MCT-15-0414
15. Dey-Guha I, Wolfer A, Yeh AC, GA J, Darp R, Leon E, Wulfkuhle J, Petricoin EF 3rd, Wittner BS, Ramaswamy S (2011) Asymmetric cancer cell division regulated by AKT. Proc Natl Acad Sci U S A 108(31):12,845–12,850. doi:10.1073/pnas.1109632108
16. Zheng X, Seshire A, Ruster B, Bug G, Beissert T, Puccetti E, Hoelzer D, Henschler R, Ruthardt M (2007) Arsenic but not all-trans retinoic acid overcomes the aberrant stem cell capacity of PML/RARalpha-positive leukemic stem cells. Haematologica 92(3):323–331
17. Li L, Bhatia R (2011) Stem cell quiescence. Clin Cancer Res: Off J Am Assoc Cancer Res 17(15):4936–4941. doi:10.1158/1078–0432.CCR-10-1499
18. Barnes DJ, Melo JV (2006) Primitive, quiescent and difficult to kill: the role of non-proliferating stem cells in chronic myeloid leukemia. Cell Cycle 5(24):2862–2866. doi:10.4161/cc.5.24.3573
19. Goldman J, Gordon M (2006) Why do chronic myelogenous leukemia stem cells survive allogeneic stem cell transplantation or imatinib: does it really matter? Leuk Lymphoma 47 (1):1–7. doi:10.1080/10428190500407996
20. Reed JC (1998) Molecular biology of chronic lymphocytic leukemia: implications for therapy. Semin Hematol 35(3 Suppl 3):3–13
21. Giles FJ, DeAngelo DJ, Baccarani M, Deininger M, Guilhot F, Hughes T, Mauro M, Radich J, Ottmann O, Cortes J (2008) Optimizing outcomes for patients with advanced disease

in chronic myelogenous leukemia. Semin Oncol 35(1 Suppl 1):S1–17.; quiz S18–20. doi:10.1053/j.seminoncol.2007.12.002

22. Krause A, Luciana M, Krause F, Rego EM (2010) Targeting the acute myeloid leukemia stem cells. Anti Cancer Agents Med Chem 10 (2):104–110
23. Besancon R, Valsesia-Wittmann S, Puisieux A, Caron de Fromentel C, Maguer-Satta V (2009) Cancer stem cells: the emerging challenge of drug targeting. Curr Med Chem 16 (4):394–416
24. Hanahan D, Weinberg RA (2011) Hallmarks of cancer: the next generation. Cell 144 (5):646–674. doi:10.1016/j.cell.2011.02.013
25. Le Tonqueze O, Kollu S, Lee S, Al-Salah M, Truesdell SS, Vasudevan S (2016) Regulation of monocyte induced cell migration by the RNA binding protein, FXR1. Cell Cycle 15 (14):1874–1882. doi:10.1080/15384101.2016.1189040
26. Sandberg R, Neilson JR, Sarma A, Sharp PA, Burge CB (2008) Proliferating cells express mRNAs with shortened 3′ untranslated regions and fewer microRNA target sites. Science 320 (5883):1643–1647. doi:10.1126/science.1155390
27. Mayr C, Bartel DP (2009) Widespread shortening of 3'UTRs by alternative cleavage and polyadenylation activates oncogenes in cancer cells. Cell 138(4):673–684. doi:10.1016/j.cell.2009.06.016
28. Cheung TH, Rando TA (2013) Molecular regulation of stem cell quiescence. Nat Rev Mol Cell Biol 14(6):329–340. doi:10.1038/nrm3591
29. Bukhari SI, Truesdell SS, Lee S, Kollu S, Classon A, Boukhali M, Jain E, Mortensen RD, Yanagiya A, Sadreyev RI, Haas W, Vasudevan S (2016) A Specialized Mechanism of Translation Mediated by FXR1a-Associated MicroRNP in Cellular Quiescence. Mol Cell 61(5):760–773. doi:10.1016/j.molcel.2016.02.013
30. Lee S, Truesdell SS, Bukhari SI, Lee JH, LeTonqueze O, Vasudevan S (2014) Upregulation of eIF5B controls cell-cycle arrest and specific developmental stages. Proc Natl Acad Sci U S A 111(41):E4315–E4322. doi:10.1073/pnas.1320477111
31. Loayza-Puch F, Drost J, Rooijers K, Lopes R, Elkon R, Agami R (2013) p53 induces transcriptional and translational programs to suppress cell proliferation and growth. Genome Biol 14(4):R32. doi:10.1186/gb-2013-14-4-r32
32. Sonenberg N, Hinnebusch AG (2009) Regulation of translation initiation in eukaryotes: mechanisms and biological targets. Cell 136 (4):731–745. doi:10.1016/j.cell.2009.01.042
33. Zoncu R, Efeyan A, Sabatini DM (2011) mTOR: from growth signal integration to cancer, diabetes and ageing. Nat Rev Mol Cell Biol 12(1):21–35. doi:10.1038/nrm3025
34. Vasudevan S, Tong Y, Steitz JA (2007) Switching from repression to activation: microRNAs can up-regulate translation. Science 318 (5858):1931–1934. doi:10.1126/science.1149460
35. Mortensen RD, Serra M, Steitz JA, Vasudevan S (2011) Posttranscriptional activation of gene expression in Xenopus laevis oocytes by microRNA-protein complexes (microRNPs). Proc Natl Acad Sci U S A 108 (20):8281–8286. doi:10.1073/pnas.1105401108
36. Truesdell SS, Mortensen RD, Seo M, Schroeder JC, Lee JH, LeTonqueze O, Vasudevan S (2012) MicroRNA-mediated mRNA translation activation in quiescent cells and oocytes involves recruitment of a nuclear microRNP. Sci Rep 2:842. doi:10.1038/srep00842
37. Jonas S, Izaurralde E (2015) Towards a molecular understanding of microRNA-mediated gene silencing. Nat Rev Genet 16 (7):421–433. doi:10.1038/nrg3965
38. He L, Hannon GJ (2004) MicroRNAs: small RNAs with a big role in gene regulation. Nat Rev Genet 5(7):522–531. doi:10.1038/nrg1379
39. Ameres SL, Zamore PD (2013) Diversifying microRNA sequence and function. Nat Rev Mol Cell Biol 14(8):475–488. doi:10.1038/nrm3611
40. Fabian MR, Sundermeier TR, Sonenberg N (2010) Understanding how miRNAs post-transcriptionally regulate gene expression. Prog Mol Subcell Biol 50:1–20. doi:10.1007/978–3–642-03103-8_1
41. Bartel DP (2009) MicroRNAs: target recognition and regulatory functions. Cell 136 (2):215–233. doi:10.1016/j.cell.2009.01.002
42. Bukhari SI, Vasudevan S (2017) FXR1a-associated microRNP: A driver of specialized non-canonical translation in quiescent conditions. RNA Biol 14(2):137–145. doi:10.1080/15476286.2016.1265197
43. Vasudevan S, Steitz JA (2007) AU-rich-element-mediated upregulation of translation by FXR1 and Argonaute 2. Cell 128 (6):1105–1118
44. Dube M, Huot ME, Khandjian EW (2000) Muscle specific fragile X related protein 1 isoforms are sequestered in the nucleus of

undifferentiated myoblast. BMC Genet 1:4. doi:10.1186/1471–2156–1-4

45. Siomi MC, Zhang Y, Siomi H, Dreyfuss G (1996) Specific sequences in the fragile X syndrome protein FMR1 and the FXR proteins mediate their binding to 60S ribosomal subunits and the interactions among them. Mol Cell Biol 16(7):3825–3832
46. Dehlin E, Wormington M, Korner CG, Wahle E (2000) Cap-dependent deadenylation of mRNA. EMBO J 19(5):1079–1086. doi:10.1093/emboj/19.5.1079
47. Korner CG, Wormington M, Muckenthaler M, Schneider S, Dehlin E, Wahle E (1998) The deadenylating nuclease (DAN) is involved in poly(A) tail removal during the meiotic maturation of Xenopus oocytes. EMBO J 17 (18):5427–5437. doi:10.1093/emboj/17.18.5427
48. Levy-Strumpf N, Deiss LP, Berissi H, Kimchi A (1997) DAP-5, a novel homolog of eukaryotic translation initiation factor 4G isolated as a putative modulator of gamma interferon-induced programmed cell death. Mol Cell Biol 17(3):1615–1625
49. Gradi A, Imataka H, Svitkin YV, Rom E, Raught B, Morino S, Sonenberg N (1998) A novel functional human eukaryotic translation initiation factor 4G. Mol Cell Biol 18 (1):334–342
50. Yamanaka S, Zhang XY, Maeda M, Miura K, Wang S, Farese RV Jr, Iwao H, Innerarity TL (2000) Essential role of NAT1/p97/DAP5 in embryonic differentiation and the retinoic acid pathway. EMBO J 19(20):5533–5541. doi:10.1093/emboj/19.20.5533
51. Sugiyama H, Takahashi K, Yamamoto T, Iwasaki M, Narita M, Nakamura M, Rand TA, Nakagawa M, Watanabe A, Yamanaka S (2017) Nat1 promotes translation of specific proteins that induce differentiation of mouse embryonic stem cells. Proc Natl Acad Sci U S A 114 (2):340–345. doi:10.1073/pnas.1617234114
52. Wu L, Fan J, Belasco JG (2006) MicroRNAs direct rapid deadenylation of mRNA. Proc Natl Acad Sci U S A 103(11):4034–4039
53. Doench JG, Sharp PA (2004) Specificity of microRNA target selection in translational repression. Genes Dev 18(5):504–511
54. Pasquinelli AE, Dahlberg JE, Lund E (1995) Reverse 5′ caps in RNAs made in vitro by phage RNA polymerases. RNA 1(9):957–967
55. Penman S, Rosbash M, Penman M (1970) Messenger and heterogeneous nuclear RNA in HeLa cells: differential inhibition by cordycepin. Proc Natl Acad Sci U S A 67 (4):1878–1885
56. Hohenstein KA, Pyle AD, Chern JY, Lock LF, Donovan PJ (2008) Nucleofection mediates high-efficiency stable gene knockdown and transgene expression in human embryonic stem cells. Stem Cells 26(6):1436–1443. doi:10.1634/stemcells.2007-0857
57. Maess MB, Wittig B, Lorkowski S (2014) Highly efficient transfection of human THP-1 macrophages by nucleofection. J Vis Exp 91: e51960. doi:10.3791/51960
58. Gresch O, Engel FB, Nesic D, Tran TT, England HM, Hickman ES, Korner I, Gan L, Chen S, Castro-Obregon S, Hammermann R, Wolf J, Muller-Hartmann H, Nix M, Siebenkotten G, Kraus G, Lun K (2004) New non-viral method for gene transfer into primary cells. Methods 33(2):151–163. doi:10.1016/j.ymeth.2003.11.009
59. Marchenko S, Flanagan L (2007) Transfecting human neural stem cells with the Amaxa Nucleofector. J Vis Exp 6:240. doi:10.3791/240
60. Doench JG, Petersen CP, Sharp PA (2003) siRNAs can function as miRNAs. Genes Dev 17(4):438–442
61. Vasudevan S (2012) Functional validation of microRNA-target RNA interactions. Methods 58(2):126–134. doi:10.1016/j.ymeth.2012.08.002

# Chapter 19

# Genome-Wide Identification of Transcription Factor-Binding Sites in Quiescent Adult Neural Stem Cells

**Shradha Mukherjee and Jenny Hsieh**

## Abstract

Transcription factors bind to specific DNA sequences and control the transcription rate of nearby genes in the genome. This activation or repression of gene expression is further potentiated by epigenetic modifications of histones with active and silent marks, respectively. Resident adult stem cells in the hematopoietic system, skin, and brain exist in a non-proliferative quiescent resting state. When quiescent stem cells become activated and transition to dividing progenitors and distinct cell types, they can replenish and repair tissue. Thus, determination of the position of transcription factor binding and histone epigenetic modification on the chromatin is an essential step toward understanding the gene regulation of quiescent and proliferative adult stem cells for potential applications in regenerative medicine. Genome-wide transcription factor occupancy and histone modifications on the genome can be obtained by assessing DNA-protein interaction through next-generation chromatin immunoprecipitation sequencing technology (ChIP-seq). This chapter outlines the protocol to perform, analyze, and validate ChIP-seq experiments that can be used to identify protein-DNA interactions and histone marks on the chromatin. The methods described here are applicable to quiescent and proliferative neural stem cells, and a wide range of other cellular systems.

**Key words** Chromatin sonication, DNA-protein crosslinking, ChIP-seq, ChIP-qPCR, Transcription factor genome-wide DNA occupancy, Genome-wide histone modification, Bioinformatics

## 1 Introduction

DNA-protein interactions are required for DNA replication, chromatin remodelers, transcriptional regulation, and DNA repair. The binding of transcription factors modulates and coordinates gene expression in response to external stimuli. Adult mammals have resident stem cells that predominantly exit in a resting non-proliferative quiescent state, which preserves the stem cell pool over the lifetime of the animal [1, 2]. In response to extrinsic and intrinsic factors, adult stem cells exit from quiescence and proliferate and differentiate into cells that maintain and repair the local tissue [3–7]. Adult resident stem cells provide an opportunity to harness them for regenerative medicine and stem cell therapy.

H. Daniel Lacorazza (ed.), *Cellular Quiescence: Methods and Protocols*, Methods in Molecular Biology, vol. 1686,
DOI 10.1007/978-1-4939-7371-2_19, 

Quiescent and proliferative adult stem cells possess distinct transcriptional profiles and epigenetic modifications, which govern distinct cell fate decisions [3, 4, 8]. Understanding the transcriptional regulatory network of DNA-protein interactions is essential to decipher the molecular basis of stem cell activation and differentiation in response to external stimuli.

Chromatin-immunoprecipitation (ChIP) gives us the capability to determine occupancy of proteins on DNA from intact cells in contrast to the earlier in vitro technique of electrophoretic mobility shift assays (EMSA) [9–11]. In ChIP, the protein (such as a transcription factor) is cross-linked to the DNA and then the DNA is fragmented mechanically by sonication or enzymatically using DNAse. The DNA fragment left bound to the protein is then pulled down with a specific antibody and when the chromatin-immunoprecipitated (ChIP-ed) DNA sequence is compared to genome sequence of the organism, it reveals the occupancy of the transcription factor. Thus, the size of DNA post-fragmentation determines the resolution of all ChIP methods, usually it is optimally maintained around 250–300 bp. The advances in the field of DNA-protein ChIP assays have primarily focused on developing better DNA fragmentation techniques and improved means to identify the chromatin-immunoprecipitated DNA.

Fragmentation of DNA or sonication of chromatin can be achieved by both enzyme-based methods and water bath-based methods. Among the water bath-based methods Bioruptor and Covaris sonicators are most popular. Bioruptor uses longer unfocused wavelengths without thermal control, while Covaris sonicators use shorter focused wavelengths with thermal control. As sonication efficiency and protein-DNA binding depends on temperature, Covaris sonicators that have thermal control are gaining popularity in the field [12]. The ChIP-on-chip method identifies protein DNA occupancy genome-wide using microarray technology with probes on the array representing only the promoter regions of the genome, as whole genome probe arrays are cost inhibitive [13]. The onset of next-generation sequencing, Solexa platform and Illumina HiSeq platform, allowed sequencing of all DNA with transcription factor occupancy across the genome without promoter bias [13].

In this chapter, we describe optimized methods for ChIP-seq and ChIP-qPCR in quiescent and proliferating adult hippocampal neural stem cells for the transcription factor REST, histone mark H3K27Ac, acetylation at the 27 lysine residue of the histone H3, and RNA Pol II. This protocol will be generally applicable to other types of biological cells and tissue. We also provide an overview of ChIP-seq data analysis.

## 2 Materials

### 2.1 Common Reagent Stocks

Buy commercially molecular grade or make in the laboratory.

1. PBS without $Ca^{2+}$ $Mg^{2+}$.
2. 8 M LiCl.
3. 1 M Tris–HCl, pH 8.0.
4. 1 M HEPES pH 6.8 to 8.2 adjust pH with KOH as required.
5. Tris-EDTA buffer (TE buffer).
6. 0.5 M EDTA and 0.5 M EGTA.

### 2.2 Preparation of Nuclei and DNA-Protein Crosslinking

1. 16% formaldehyde methanol. Once glass ampule is opened use within 1–2 weeks.
2. 10× Fixation buffer: Add 10 ml of 1 M HEPES pH 8.0, 4 ml of 5 N NaCl, 0.4 ml of 0.5 M EDTA, and 0.2 ml of 0.5 M EGTA to about 100 ml nanopure $H_2O$. Then, adjust volume to 200 ml with nanopure $H_2O$.
3. 1.25 M glycine (crosslinking quenching buffer): Dissolve 0.938 g of glycine in 10 ml nanopure $H_2O$.
4. Cell wash buffer B: Add 10 ml of 1 M HEPES-KOH pH 7.6, 5.6 ml of 5 M NaCl, 0.4 ml of 0.5 M EDTA pH 8.0, 20 ml of 100% Glycerol, 1 ml of 100% NP-40, 0.5 ml of 100% Triton-X100 to about 100 ml nanopure $H_2O$. Then, adjust volume to 200 ml with nanopure $H_2O$. Optional: add a tablet with protease inhibitors.
5. Cell rinse buffer C: Add 2 ml of 1 M Tris–HCl pH 8.0, 8 ml of 5 M NaCl, 0.4 ml of 0.5 M EDTA pH 8.0, 0.4 ml of 0.5 M EGTA pH 8.0 to about 100 ml nanopure $H_2O$. Then, adjust volume to 200 ml with nanopure $H_2O$. Optional: add a tablet with protease inhibitors.

### 2.3 Chromatin Shearing or Sonication

1. Sonication or shearing buffer D: Add 2 ml of 1 M Tris–HCl pH 8.0, 2 ml of 10% SDS, 0.4 ml of 0.5 M EDTA pH 8.0 to about 100 ml nanopure $H_2O$. Then, adjust volume to 200 ml with nanopure $H_2O$. Optional: add a tablet with protease inhibitors.
2. For Covaris sonication: Covaris milliTUBE 1 ml AFA fiber Part #520135 Covaris.

### 2.4 Chromatin Immunoprecipitation (ChIP)

1. Immunoprecipitation (IP) buffer or ChIP dilution buffer: To about 100 ml sonication or shearing buffer D add 20 ml of 10% Triton-X100 and 6 ml of 5 M NaCl. Then adjust volume to 200 ml with nanopure $H_2O$. Optional: add a tablet with protease inhibitors.

2. Low salt wash buffer I: Add 4 ml of 1 M Tris–HCl pH 8.0, 2 ml of 10% SDS, 1.6 ml of 0.25 M EDTA pH 8.0, 20 ml of 10% Triton-X100, 6 ml of 5 M NaCl to about 100 ml nanopure $H_2O$. Then adjust volume to 200 ml with nanopure $H_2O$. Optional: add a tablet with protease inhibitors.
3. High salt wash buffer II: Add 4 ml of 1 M Tris–HCl pH 8.0, 2 ml of 10% SDS, 1.6 ml of 0.25 M EDTA pH 8.0, 20 ml of 10% Triton-X100, 16 ml of 5 M NaCl to about 100 ml nanopure $H_2O$. Then adjust volume to 200 ml with nanopure $H_2O$. Optional: add a tablet with protease inhibitors.
4. LiCl wash buffer III: Add 2 ml of 1 M Tris–HCl pH 8.0, 20 ml of 10% Deoxycholate, 0.8 ml of 0.25 M EDTA pH 8.0, 20 ml of 10% NP-40, 12.8 ml of 8 M LiCl to about 100 ml nanopure $H_2O$. Then adjust volume to 200 ml with nanopure $H_2O$. Optional: add a tablet with protease inhibitors.
5. Mild wash buffer: Add 2.5 ml of 20% NP-40, 0.5 ml of 20% SDS, 0.8 ml of 0.5 M EDTA, 4 ml of 1 M Tris–HCl, 10 ml of 5 M NaCl to 100 ml of nanopure $H_2O$. Adjust volume to 200 ml with nanopure $H_2O$. Optional: add a tablet with protease inhibitors.
6. Elution buffer: Add 1 ml of 10% SDS and 84 mg of $NaHCO_3$ to nanopure $H_2O$ and make volume up to 10 ml.
7. No-stick SNAPLOCK microcentrifuge tubes: Eppendorf 1.5 ml tubes (e.g., Company Light Labs). Any other no-stick Eppendorf tubes may also be used.
8. Protein G Dynabeads or Protein A Dynabeads: Use Protein G Dynabeads for Rabbit host generated ChIP-grade antibody.
9. Magnetic rack for 1.5 ml eppendorf tubes.

### 2.5 DNA-Protein Reverse Crosslinking, DNA Isolation, and DNA Estimation of ChIP-ed DNA

1. Qiaquick PCR purification kit or general DNA isolation protocol.
2. DNA estimation kit Qubit (nano drop is not accurate for small amounts of DNA).

### 2.6 Determination of Sonicated DNA Size, Bioanalyzer Quality Check, and ChIP-seq

1. BIO-33062 EZ Ladder I: Any DNA ladder with range from 100 bp to 1 kb.

## 3 Methods

### 3.1 Preparation of Nuclei and DNA-Protein Crosslinking (Fig. 1)

#### 3.1.1 Cell Preparation and Crosslinking

1. Grow cells up to 80–90% confluency as a monolayer in a 10 cm plate.
2. Remove the medium and add 9 ml fresh medium (DMEM or medium in which the cells were growing) to a 10 cm plate. All the reagents are at room temperature in this step.
3. Add to above 1 ml of 10× Fixation Buffer A and 625 μl of 16% of methanol-free formaldehyde (1% final concentration). All reagents must be at room temperature in this step.
4. Place the cells on a shaker at room temperature and shake for 10 min to allow for efficient crosslinking (maximum 15 min).
5. Quench crosslinking by adding to above 10 ml volume 1.12 ml freshly prepared 1.25 M Glycine stock at room temperature and shake for 5 min (125 mM final concentration).
6. Completely aspirate the solution from the plate and wash twice with 10 ml of ice-cold PBS without $Ca_2^+$ and $Mg_2^+$ on a shaker at room temperature or 4 °C. First wash for 1 min and second wash for 3 min.
7. Harvest cells in fresh 5 ml or 10 ml ice-cold PBS by scrapping.
8. Spin down the pellet at 300 × *g* for 2 min at room temperature or 4 °C and discard the supernatant.

#### 3.1.2 Nuclei Preparation

1. Resuspend cell pellet of maximum 30 million cells in 10 ml of ice-cold cell wash buffer B.
2. Rotate at 4 °C on a rabbit-ear rotor for 10 min.
3. Spin down the nuclear pellet at 1500 × *g* for 2 min at room temperature or 4 °C and discard the supernatant.
4. Resuspend the nuclear pellet in 10 ml of ice-cold cell-rinse buffer C.
5. Immediately, spin down the nuclear pellet at 1500 × *g* for 2 min at room temperature or 4 °C and discard the supernatant.

### 3.2 Chromatin Shearing or Sonication (Fig. 1)

1. Resuspend maximum 15 million cells worth nuclear pellet in 1 ml sonication or shearing buffer D.
2. Rotate at 4 °C on a rabbit-ear rotor for 30 min or for a minimum of 10 min.
3. Covaris sonication: Now take the Covaris milliTUBE 1 ml AFA fiber to Covaris sonicator for sonication. One tube can be reused for up to 8 sonications (6 min 30 s each). Alternative option Bioruptor: Add 1 ml of sample to no-stick eppendorf and wrap cap with parafilm. Sonicate in ice-cold Bioruptor for

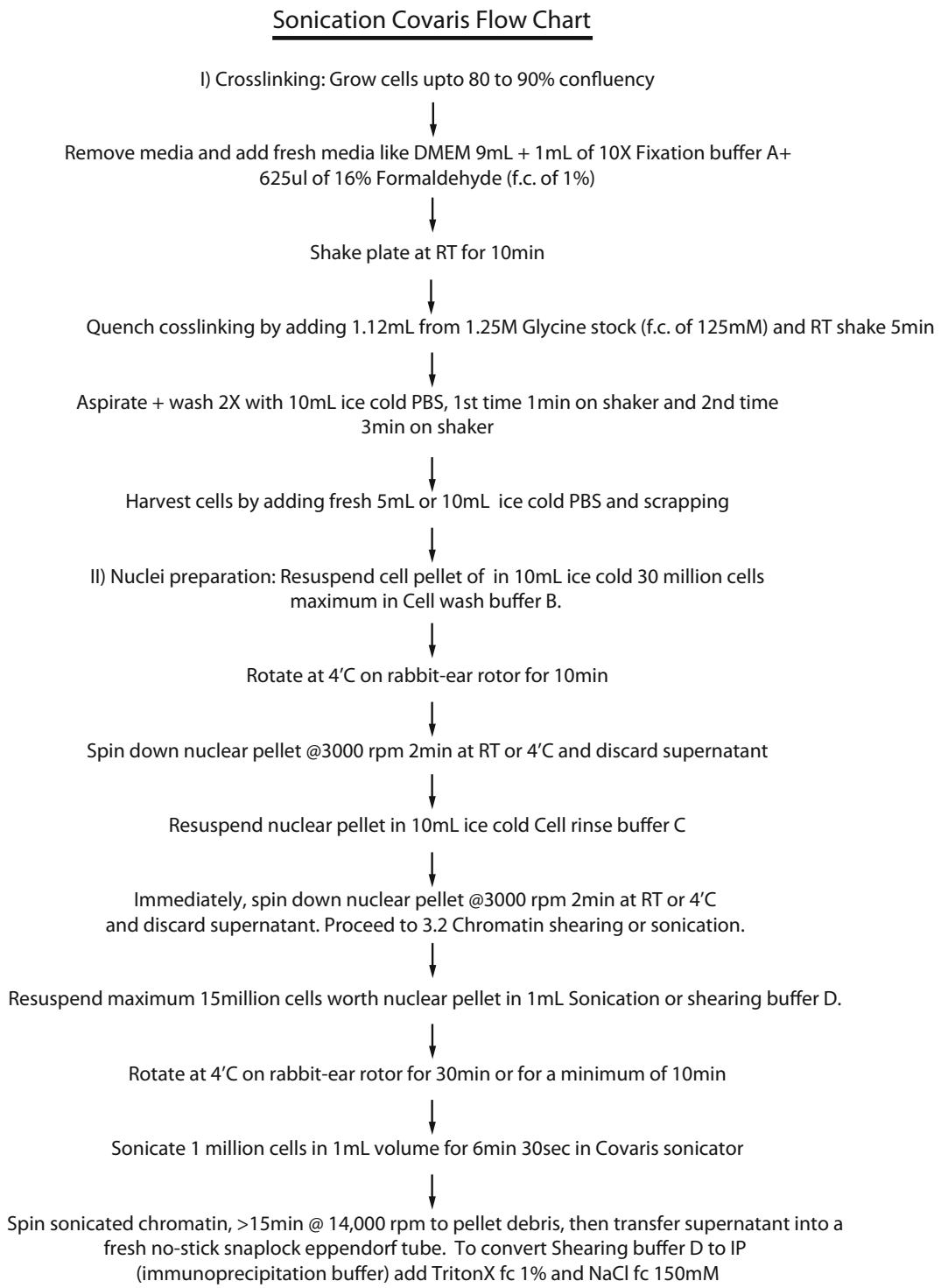


**Fig. 1** Flowchart of cell to sonication. Related to Subheading 3.1 preparation of nuclei and DNA-protein crosslinking and Subheading 3.2 chromatin shearing or sonication: Covaris sonication

five times 7 min each with 30 s on and 30 s off cycle. To maintain cold temperature, replace ice bath each time.

4. Covaris S-series sonicator settings: Duty cycle 5%, Intensity 4, Cycle per burst 200, Temperature 4 °C, Power mode frequency Sweeping, Degassing mode (default), AFA Intensifier (default), Water level (enough until base of black cap, use the Covaris black/white holder).
5. Sonicate 1 million cells in 1 ml volume for 6 min 30 s.
6. Spin sonicated chromatin, more than 15 min at 18,000 × *g* to pellet debris, then transfer the supernatant into a fresh no-stick snaplock eppendorf tube.
7. To convert shearing buffer D to IP (immunoprecipitation buffer) add Triton-X100 to 1% final concentration and NaCl 150 mM final concentration. Example: To 8.70 ml of sonicated chromatin solution add 1 ml of 10% Triton-X100 and 300 µl of 5 M NaCl.

### 3.3 Chromatin Immunoprecipitation (ChIP) (Fig. 2)

1. For each ChIP use 1 ml or 1.45 ml of the sonicated chromatin IP solution or 150–300 µg of chromatin (DNA concentration can be estimated using nano-drop DNA) and take out 5% input from it 50 µl or 72.5 µl, respectively (*see* **Note 1**).
2. Optional: If ChIP-seq or ChIP-qPCR shows high background, then preclear the above 1.45 ml or 1 ml sonicated chromatin IP sample with 20 µl of pre-washed Protein G Dynabeads by rotation on a rabbit-ear rotor for 1–2 h at 4 °C. Put the eppendorf on the magnetic rack and use the supernatant to proceed to the ChIP reaction in **step 3**. Pre-wash beads two times with 0.5% of BSA in PBS before three times with Covaris IP buffer washes as described in **step 5**.
3. Add 10 µl of preferably a ChIP-grade antibody (1 µg/µl) to the 1.45 ml of sonicated chromatin in IP or precleared sonicated chromatin in IP above and incubate at 4 °C on a rabbit-ear rotor overnight for up to 18 h and a minimum of 6 h.
4. For each ChIP use about 50 µl of Protein G Dynabeads.
5. Wash Protein G Dynabeads three times with Covaris IP buffer in 1.5 ml eppendorf tubes. Each wash is done by adding, 1 ml Covaris IP buffer and 4 min rotation in rabbit-ear at 4 °C. Then place the eppendorf tube on a magnetic rack for 1 min to allow beads to settle on the magnet. Pipette out and discard the supernatant and then add next wash 1 ml volume, take the tube out of the magnetic rack and invert seven times by hand to resuspend beads, then place in a rabbit-ear rotor and repeat the cycle (*see* **Note 2**).

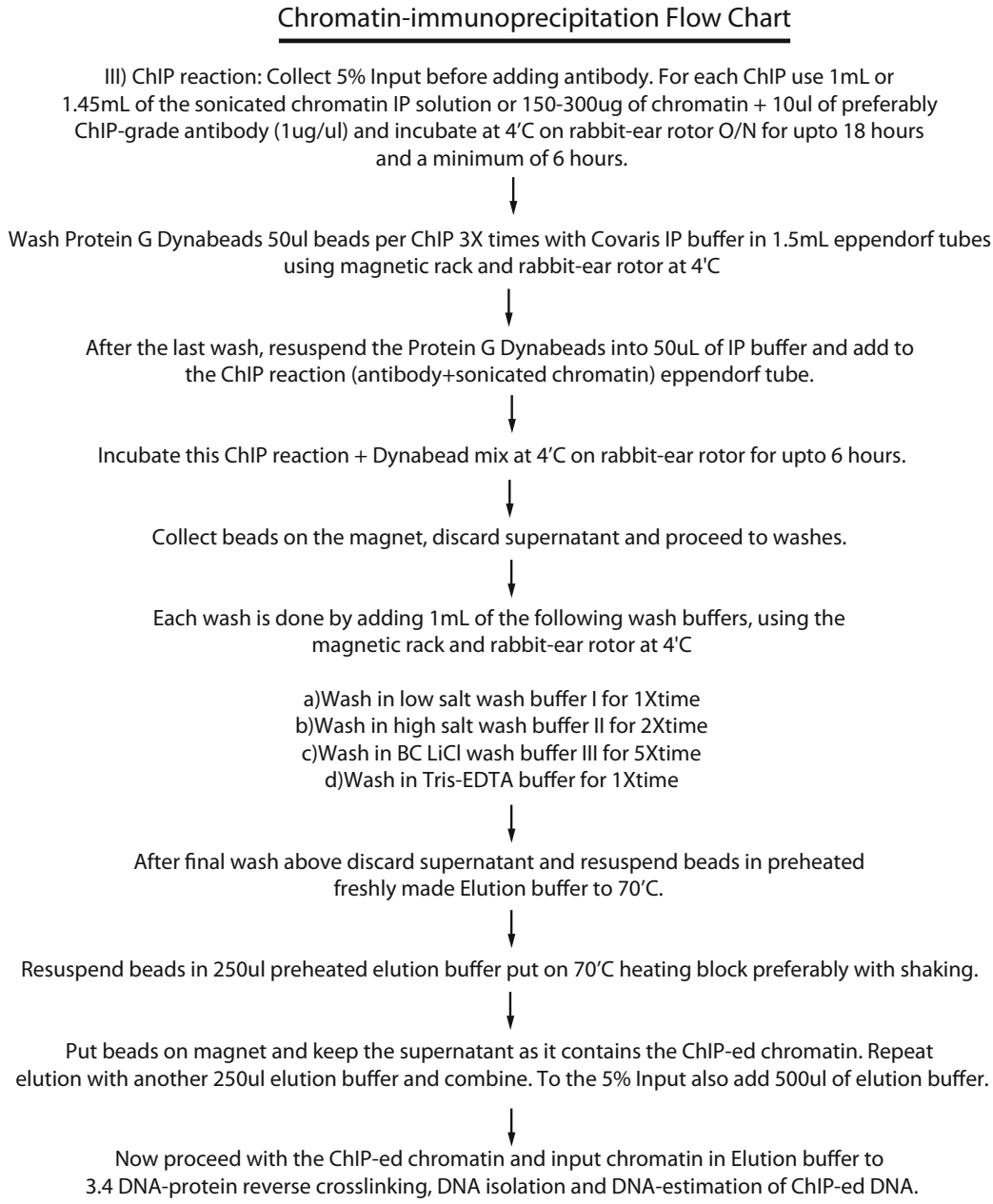


**Fig. 2** Flowchart of ChIP. Related to Subheading 3.3 Chromatin Immunoprecipitation (ChIP)

6. After the last wash, resuspend the Protein G Dynabeads into 50 μl of IP buffer and add to the ChIP reaction (antibody and sonicated chromatin) eppendorf tube from **step 2**.
7. Incubate this ChIP reaction and Dynabead mix at 4 °C on the rabbit-ear rotor for up to 6 h.

8. Collect beads on the magnetic rack, discard the supernatant, and proceed to washes. Each wash is done by adding 1 ml of the following wash buffers, using the magnetic rack and rabbit-ear rotor as described above in **step 4** (*see* **Note 3**).
   (a) Wash in low salt wash buffer I for one time.
   (b) Wash in high salt wash buffer II for two times.
   (c) Wash in BC LiCl wash buffer III for five times.
   (d) Wash in Tris-EDTA buffer for one time.
9. After final wash above discard the supernatant and resuspend beads in preheated freshly made elution buffer to 70 °C. Resuspend beads in 250 μl of preheated elution buffer and incubate in 70 °C heating block preferably with shaking. Then add beads on the magnetic rack and keep the supernatant as it contains the immunoprecipitated chromatin. Repeat elution with another 250 μl of elution buffer and combine the supernatants to get 500 μl of total eluted immunoprecipitated chromatin.
10. To the 5% input previously collected in **step 1**, similarly add 500 μl of elution buffer.
11. Now proceed with the ChIP-ed chromatin and input chromatin in elution buffer to the next step of DNA-protein reverse crosslinking, DNA isolation, and DNA estimation of ChIP-ed DNA.

### *3.4 DNA-Protein Reverse Crosslinking and Isolation of ChIP-ed DNA (Fig. 3)*

1. Make all volumes up to 500 μl by adding elution buffer. The 5% input and chromatin-immunoprecipitated DNA are already at 500 μl in elution buffer.
2. Reverse crosslinking: Add 11 μl of 5 M NaCl to the 500 μl DNA in elution buffer to get 0.3 M NaCl final concentration. Incubate on heating block overnight at 65 °C preferably with shaking.
3. RNA digestion: To the above reverse crosslinked DNA solution add 5 μl of RNAse to digest RNA. Incubate on a heating block for 1 h at 37 °C preferably with shaking.
4. Protein digestion: To the above reverse crosslinked and RNA digested DNA solution add 5 μl of Proteinase K to digest all proteins. Incubate on a heating block for 1–4 h at 55 °C preferably with shaking.
5. Purify and extract DNA using Qiaquick PCR DNA purification kit or any other DNA column purification and DNA extraction kit following the manufacturer's instructions. Steps are briefly described below for Qiaquick PCR DNA purification kit using buffers from the kit,

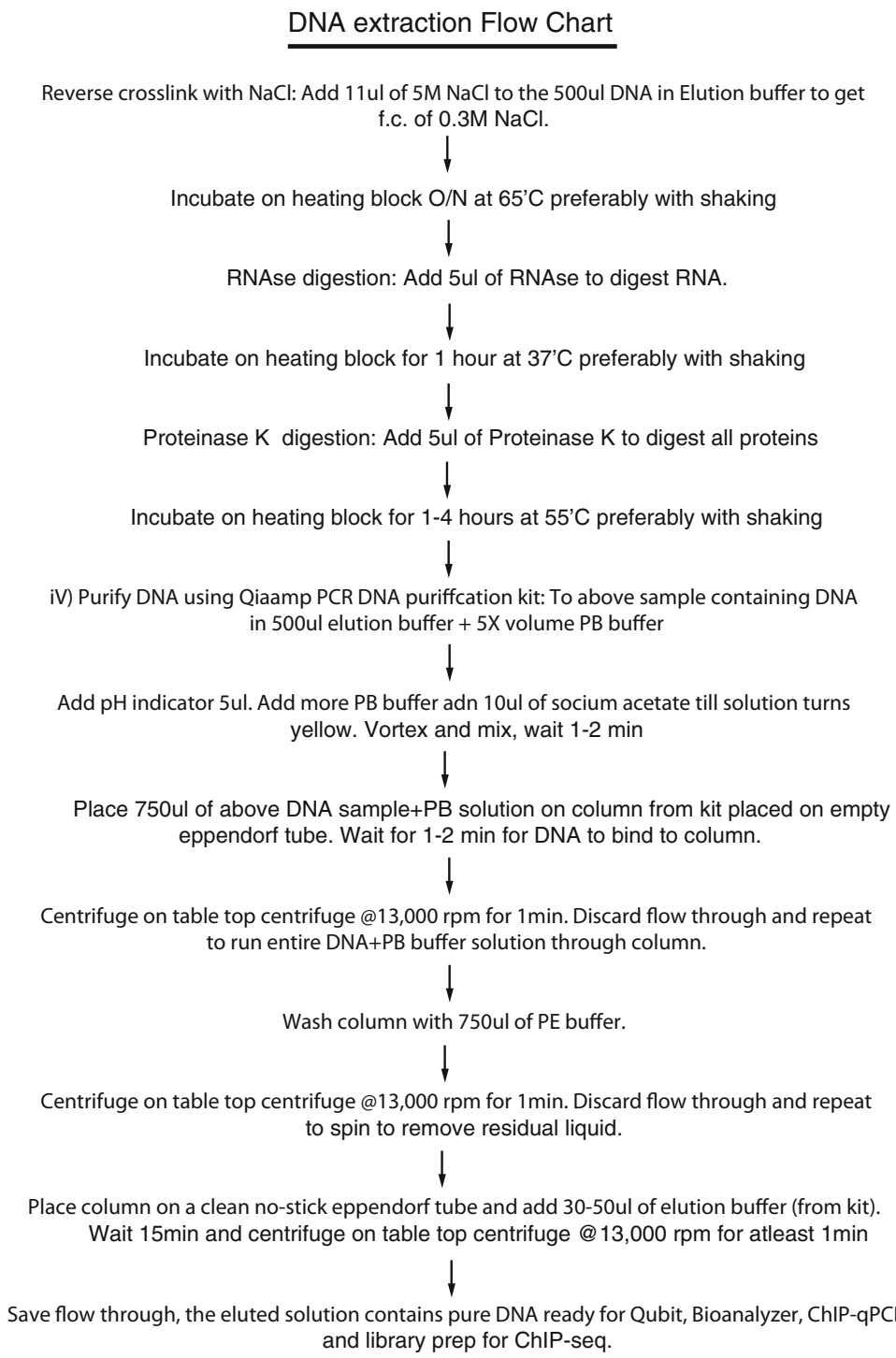


**Fig. 3** Flowchart of DNA extraction and purification. Related to Subheading 3.4 DNA-protein reverse cross-linking and isolation of chromatin-immunoprecipitated DNA

(a) To ~500 µl of DNA solution from **step 4**, add 5× its volume ~2500 µl PB buffer (buffer provided with the kit) and 5 µl of pH indicator. The solution should turn yellow, if orange add more PB buffer and/or 10 µl of 3 M sodium acetate until it turns yellow (*see* **Note 4**).

(b) Place 750 µl at a time of the above solution on the binding column that is placed on the empty eppendorf tube and wait for 1–2 min. Centrifuge at room temperature at 18,000 × *g* for 1 min and discard flow-through. Repeat for the remainder of the solution from step a.

(c) Add 750 µl of PE wash (buffer provided with the kit) buffer to column and centrifuge at room temperature at 18,000 × *g* for 1 min and discard flow-through.

(d) Centrifuge again on empty eppendorf to get rid of residual liquid from the column at room temperature at 18,000 × *g* for 1 min and discard flow-through.

(e) Put column on a no-stick eppendorf tube, add 30–50 µl of elution buffer from the kit to the column. Wait for 10–15 min and centrifuge at room temperature at 18,000 × *g* for 2 min.

(f) Discard column and save flow-through as it is pure eluted DNA from chromatin-immunoprecipitated DNA or 5% input samples.

6. Alternatively, purify and extract DNA by the kit-free Phenol/Chloroform method. This method usually gives lower yield than the described column-based method (*see* **Note 5**).

(a) Add 500 µl of phenol/chloroform equilibrated with TE buffer pH 8.0.

(b) Mix by vortexing.

(c) Centrifuge at room temperature at 18,000 × *g* for 10 min.

(d) Save the aqueous phase and add 500 µl of chloroform: isoamyl alcohol (24:1).

(e) Save the aqueous phase as it contains pure eluted DNA from chromatin-immunoprecipitated DNA or 5% input samples.

(f) Take aqueous phase into a new eppendorf tube and add 2 µl of glycogen, 50 µl of 3 M Sodium Acetate pH 5.2, and 900 µl of isopropanol. Mix well.

(g) Leave at −20 °C for 30 min to 1 h or overnight for DNA to precipitate.

(h) Centrifuge at 18,000 × *g* for 15–30 min at 4 °C to pellet DNA and discard the supernatant.

(i) Wash the pellet with 75% ethanol, centrifuge as above, and discard the supernatant. Air-dry the pellet but do not over dry.

(j) Resuspend DNA pellet in 50 μl of water.

7. DNA estimation: Input 5% DNA is usually >10 μg/μl in concentration that is reliably estimated by nanodrop. The chromatin-immunoprecipitated DNA from transcription factors is usually of a much lower concentration and amount (5–10 ng), so the concentration is estimated using Qubit following the manufacturer's instruction. Briefly,

   (a) Prepare a master mix for 200 μl buffer per sample and 1 μl of dye per sample in regular eppendorf. Vortex to mix.

   (b) Use Qubit eppendorf for this step. For samples, add 199 μl of master mix to 1–2 μl of sample. For kit standards, add 190 μl of master mix to 10 μl of standards.

   (c) Vortex to mix and incubate at room temperature in the dark for 2 min.

   (d) Now take readings on the Qubit machine for samples and standards in the Qubit eppendorf. Make sure the bottom of the Qubit eppendorf tube is clean. For standard readings, order is important, first read the first standard and then read the second standard.

   (e) Record the concentrations. Store these input and ChIP-ed DNA samples at 4 °C or lower temperatures until further use.

### *3.5 Determination of Sonicated DNA Size, Bioanalyzer Quality Check, and ChIP-seq (Fig. 4)*

1. DNA sonication size: Prepare a 1% agarose gel without ethidium bromide. Run ~200 ng of 5% input from the sample and the EZ-Ladder I until the 100 bp to 1 kb ladder bands are resolved in TAE buffer. Incubate gel in ethidium bromide TAE buffer with shaking at room temperature for 20 min to 1 h. Then visualize gel under UV, if bands not visible incubate longer in ethidium bromide TAE buffer. Save the ethidium bromide TAE solution to reuse. Smear of sonicated DNA size range from 100 to 500 bp is best with highest intensity in the 250 bp region.

2. DNA sonication size and concentration Bioanalyzer: Chromatin-immunoprecipitated DNA is usually a small amount (<200 ng), so to determine DNA size distribution of these samples use High Sensitivity Bioanalyzer assay (*see* **Note 6**). Submit 5% input samples diluted to pg/μl range to confirm DNA size range seen in 1% agarose gel above (optional). Follow the manufacturer's instruction or use sequencing core facility services.

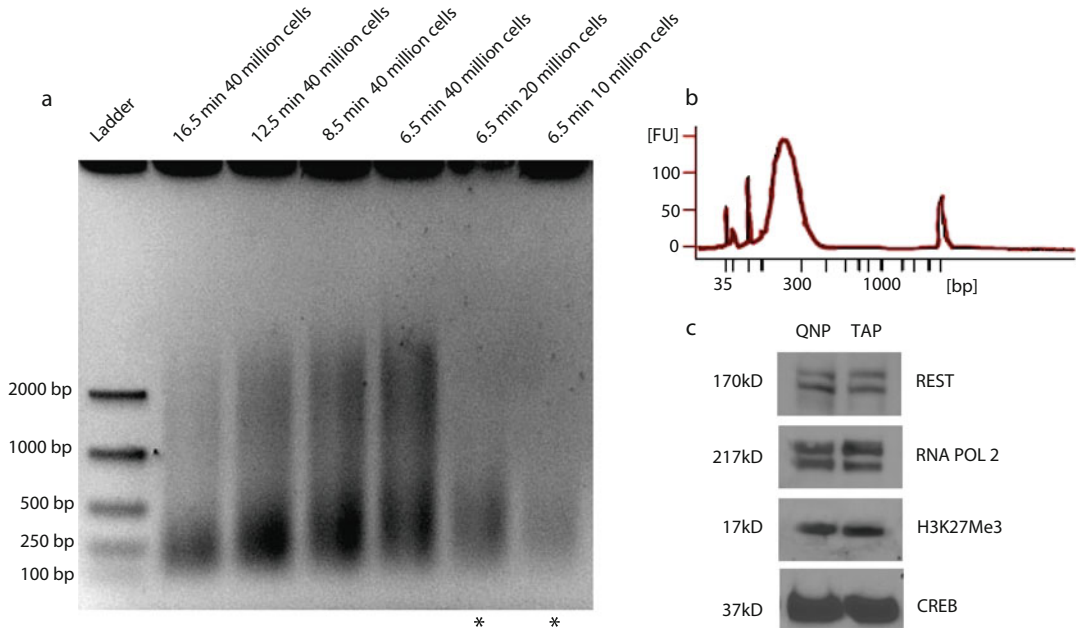


**Fig. 4** Sonication optimization, antigen retention, and bioanalyzer. (**a**) 1% Agarose gel electrophoresis shows sonication efficiency with varying time and cell number using Covaris sonication system and TAP (proliferating neural stem cells) from rats. Asterix indicates best sonication condition at 6.5 min and preparation from 10–20 million cells. (**b**) Bioanalyzer graph showing peak of ChIP-ed DNA at >300 bp after library preparation. (**c**) Western blots from sonication of 15 million cells for 6.5 min show efficient antigen retention for REST, RNA Pol 2, H3K27Me3, and CREB in QNPs (quiescent hippocampal neural stem cells) and TAPs from rat. Related to Subheading 3.5 determination of sonicated DNA size, Bioanalyzer quality check and ChIP-seq and Subheading 3.6 Sonication optimization and antigen retention

3. ChIP-qPCR validation of known binding sites is optional if there are some known targets for the transcription factor. Alternatively, ChIP-qPCR is performed on chromatin-immunoprecipitated DNA to validate ChIP-seq peaks (*see* Subheading 3.8).
4. Library preparation: Illumina's TruSeq ChIP library preparation kit or NEB Next Ultra II DNA Library Prep Kit for Illumina. Follow the manufacturer's instruction or use sequencing core facility services.
5. ChIP-seq: For sequencing at least 5–10 ng of chromatin-immunoprecipitated DNA is minimally required. Multiplex and run parallel ChIP reactions to get this amount of chromatin-immunoprecipitated DNA if necessary. Submit above ChIP-seq sample libraries for sequencing, preferably by Illumina HiSeq at 50 base single-end and at least 10–15 million reads per sample. Include 5% Input sample in the ChIP-seq run and IgG ChIP-ed DNA is optional.

### 3.6 Sonication Optimization and Antigen Retention (Fig. 4)

1. To optimize sonication settings, use recommended settings in Subheading 3.2 or default manufacturer's settings for the model of Covaris S or E series. Vary total time of sonication (e.g., 5, 6.5, 8.5, 12.5, 16.5 min) and number of cells (e.g., 0.5, 1, 2, 4, 6 million cells per ml) (*see* **Note 7**).
2. From the 1 ml sonication volume remove a 100 μl aliquot after each sonication trial time and replace the AFA covaris tube with fresh shearing buffer D to keep total volume of sonication always at 1 ml. Divide the 100 μl aliquot into two 50 μl parts, use one for DNA fragmentation and sonication check and the other part for antigen retention western blot.
3. DNA sonication or fragmentation: Use 50 μl of the 100 μl aliquot from **step 2**, make up to 500 μl with elution buffer or water and perform reverse crosslinking, RNAse digestion, and Proteinase K digestion as described in Subheading 3.4. Visualize fragments on 1% agarose gel as described in Subheading 3.5.
4. Antigen retention: To the other 50 μl of the 100 μl aliquot from **step 2** add 50 μl of elution buffer or water. Then add 5 M NaCl to a final concentration of 0.3 M. Incubate on heating block overnight at 65 °C preferably with shaking. Digest RNA using RNAse for 30 min to 1 h at 37 °C preferably with shaking. Now denature samples with LDS reducing buffer and perform western blot to probe with the same ChIP-grade antibody that will be used for ChIP in Subheading 3.4 (*see* **Note 8**).

### 3.7 ChIP-seq Bioinformatics Data Analysis, a Brief Overview (Figs. 5 and 6)

1. ChIP-seq run on Illumina or Solexa generates fastq read files. This section gives a brief overview of how to obtain occupancy of the protein on the DNA and other biologically relevant information from these raw reads. Alternately, ChIP-seq published data may be obtained from ENCODE https://www.encodeproject.org/ or NCBI GEO https://www.ncbi.nlm.nih.gov/geo/ and analyzed with the same pipeline described below.
2. Running platform and software installation: Web-based open resource platform Galaxy https://usegalaxy.org/ is a good starting point. For command line-based analysis, Mac users can use *Terminal* and Windows (UNIX operating system) users can use *cmd* or Cygwin or Ubuntu on Virtual box. For intense computing installing linux ubuntu operating system or cloud computing options may be considered. Many bioinformatics core host Galaxy cluster, which can be accessed through *Terminal* and *Putty* by Mac and Windows users, respectively. Local installation of the FastQC, Bowtie, SAMtools, and HOMER is required for ChIP-seq. For RNA-seq Tophat and

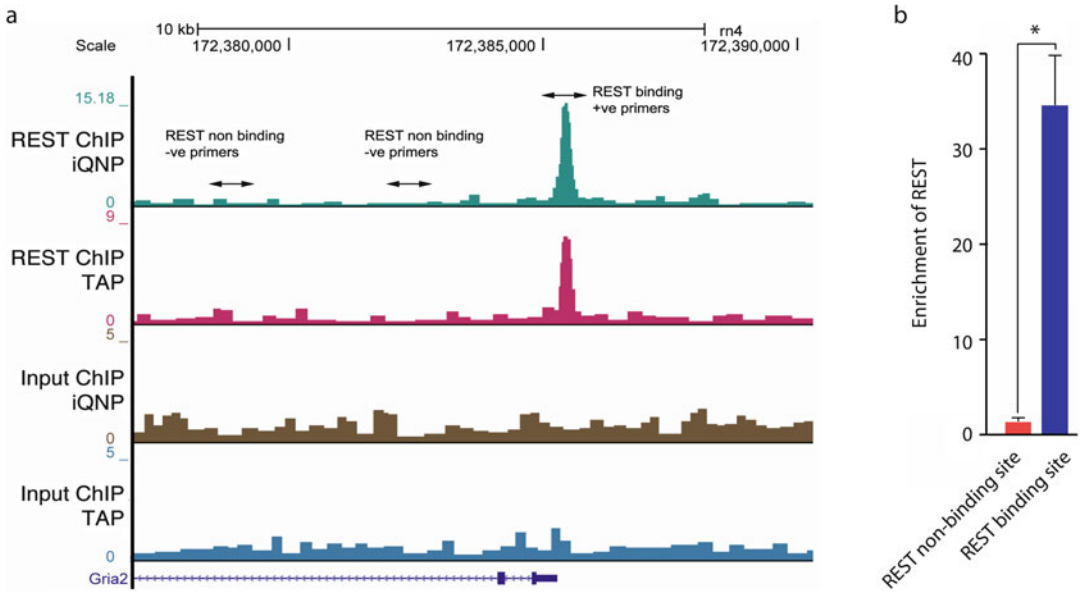


**Fig. 5** Gria2 UCSC view (with primer) and REST ChIP-qPCR. (**a**) UCSC genome browser view of REST ChIP-seq bedGraph file showing REST occupancy at Gria2 gene promoter. *Doublehead arrows* indicate region of genomic DNA suitable for primer design for positive binding and negative no binding sites. (**b**) ChIP-qPCR validation of REST binding peak at Gria2 promoter in TAPs. Related to Subheading 3.8 ChIP-qPCR primer design from ChIP-seq and Subheading 3.7 ChIP-seq bioinformatics data analysis, a brief overview

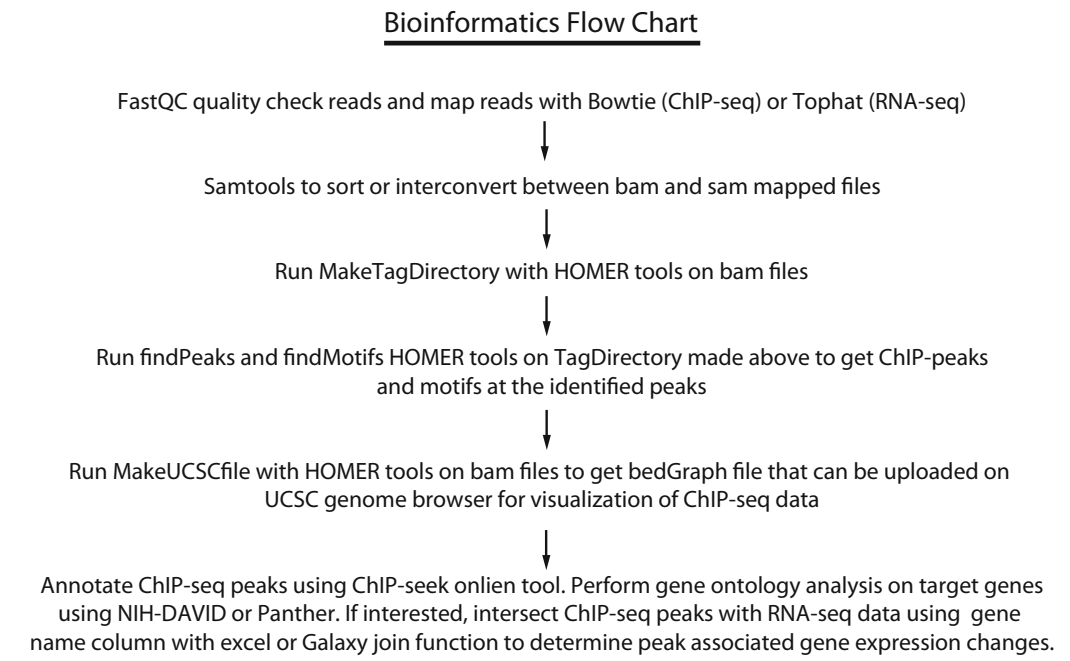


**Fig. 6** Flowchart of bioinformatics for ChIP-seq and RNA-seq intersection. Related to Subheading 3.7 ChIP-seq bioinformatics data analysis, a brief overview

Cuffdiff is also required. HOMER tools are described in detail on the website http://homer.salk.edu/homer/.

3. In the scripts below it is assumed that the software/packages are available in the path. If need be modify script to specify the path. Also, replace home in the scripts below with the home directory in use for running the pipeline. The script command lines are highlighted in gray.
4. *Quality check and mapping on genome.* The ChIP-seq fastq data after fastq quality check and *FastqGroomer* (tool to convert fastq file to fastqsanger) is mapped to the genome of the organism using Bowtie for ChIP-seq (or Tophat for RNA-seq) [14, 15]. The fastq dataset obtained from ENCODE or NCBI GEO can also be similarly run through fastq quality check and *FastqGroomer* [16–18]. ENCODE and NCBI GEO files are downloadable by ftp transfer in bam and fastq formats. The NCBI GEO fastq file is often available in the sra format, which can be converted to fastq with the command. Example:

```
#!/bin/sh
# request Bourne shell as shell for job
#$ -S /bin/sh
# run the fastq-dump on the specified sra file
/usr/local/bin/sratoolkit/bin/fastq-dump /home/example.sra
```

5. Bam files and sam files of mapped reads can be sorted and interconverted using samtools [19]. Example:

```
#!/bin/sh
# request Bourne shell as shell for job
#$ -S /bin/sh
# run the samtools on the specified bam file to sort bam
file by name
/usr/local/bin/samtools sort -n /home/example.bam /home/
example.name.sorted
```

Example:

```
!/bin/sh
# request Bourne shell as shell for job
#$ -S /bin/sh
# run the samtools on the specified bam file to convert bam to sam
/usr/local/bin/samtoolsview-h-o/home/example.name.sorted.sam
/home/example.name.sorted.bam
```

6. *Visualization of mapped ChIP-seq and RNA-seq data on UCSC genome browser.* To visualize the mapped reads on the UCSC genome browser, run HOMER tools makeTagDirectory and makeUCSCfile on bam files [20]. The resultant bedGraph file can then be uploaded and visualized on the UCSC genome browser as a custom track (create free UCSC genome browser login to save these tracks). Once the UCSC custom track is

created it can be used to visualize protein binding peaks and can be used for primer design (Fig. 6). This method can also be used on RNA-seq bam files to upload them on the UCSC genome browser.

Example:

```
#!/bin/sh
# request Bourne shell as shell for job
#$ -S /bin/sh
 # run the makeTagDirectory on the specified bam file have
 samtools in path if needed or change to sam or do interactively
 with bam
/usr/local/bin/homer/bin/makeTagDirectory /home/example-
TagDirectory /home/example.bam
```

Example:

```
#!/bin/sh
# request Bourne shell as shell for job
#$ -S /bin/sh
# run the makeUCSCfile on the specified tag directory
 /usr/local/bin/homer/bin/makeUCSCfile /home/exampleTag-
 Directory -o /home/exampleTagDirectory/exampleTagDirec-
 tory.ucsc.bedGraph
```

7. *ChIP-seq peak calling and motif analysis using HOMER*. There are several methods for ChIP-seq peak calling, such as MACS peak calling, Peak ranger and HOMER. Presently, described is the HOMER-based peak calling and HOMER motif analysis of peaks [20]. In the example below, for genome version input the same genome version that was used in mapping with Bowie or Tophat, in this example it is mouse mm9 genome.

   Example:

```
#!/bin/sh
# request Bourne shell as shell for job
#$ -S /bin/sh
 # run the findPeaks on the specified TagDirectory file
 both ChIP antibody and Input
# The output will show up in the home directory as did not
specify it for me its [smukherjee2@mb-galaxy ~]$
 /usr/local/bin/homer/bin/findPeaks /home/exampleTagDir-
 ectory -style factor -o example -i /home/exampleTagDir-
 ectory
```

   Example:

```
#!/bin/sh
# request Bourne shell as shell for job
#$ -S /bin/sh
# run the findmotifgenome on the above output homer peak file
```

```
/usr/local/bin/homer/bin/findMotifsGenome.pl /home/exam-
plemotif.txt genome version /home/example/results -prepar-
sedDir /home/example/preparsed/
```

8. To obtain a global average view of ChIP peak enrichment over input ngs.plot can be useful [21]. This is however not an essential step for detailed annotation of peaks and assignment to genes.
9. *Annotation of ChIP-seq peaks and intersection with RNA-seq.* To annotate ChIP peaks bed file use ChIP-seek, http://chipseek.cgu.edu.tw/. The input bed file should contain the peak genomic coordinates in the format chrN:start-end [22]. From the result summary, download peak location pie chart (global distribution of peaks on different regions of the genome) and annotation table file (each peak assigned to nearest gene).
10. Other useful resources for ChIP-seq peak annotation are

    http://sartorlab.ccmb.med.umich.edu/software
    http://broad-enrich.med.umich.edu/
    http://manticore.niehs.nih.gov/pavis2/
11. To determine the gene expression changes associated with ChIP-seq protein-DNA occupancy. First, *Cuffdiff* analysis is performed on RNA-seq bam files generated by using Tophat (**step 4**) [23, 24]. Second, the output Cuffdiff file is intersected or joined with the ChIP-seq gene annotated file from ChIP-seek above (**step 9**) by gene name. This join function can be performed on excel or on Galaxy using the *Join two dataset function*.
12. The resultant file contains protein-DNA interactions and associated gene expression changes. This dataset of upregulated and downregulated genes associated with transcription factor occupancy is very useful for biological interpretation of the data and hypothesis generation. These "target gene" lists can now be used to perform gene ontology using NIH DAVID gene ontology or panther gene ontology or gene ontology analysis tools [25–28].
13. Additional tool: To convert between genomes of species or within species, use UCSC LiftOver, https://genome.ucsc.edu/cgi-bin/hgLiftOver. The input file to be converted should be a bed format file of peak genomic coordinates.

### 3.8 ChIP-qPCR Primer Design from ChIP-seq (Fig. 5)

1. The ChIP-ed DNA from Subheading 3.4—reverse crosslinked, RNAse and Proteinase K treated, isolated and purified with Qiaamp PCR purification kit, concentration from Qubit—can be directly used for ChIP-qPCR. Use about 250–500 pg of chromatin-immunoprecipitated DNA per qPCR reaction. For input normalization use same amount per qPCR reaction as

chromatin-immunoprecipitated DNA (i.e., about 250–500 pg of 5% input or 1% input).

2. Binding site primer: Design qPCR primers around the center of the known binding site or if validating ChIP-seq at highest point, usually at the center of ChIP-seq-binding peak. For internal control and internal normalization, design qPCR primers around sites 3 kb or further away from the binding site or ChIP-seq peak at a region of nonbinding or non-ChIP-seq peak. Additional controls that can be included are IgG and specific antibody chromatin-immunoprecipitated DNA from cells where the antigen being used to pull down has been knockdown or knockout.
3. The qPCR primers should cover 120–200 bp amplicon size on genomic DNA sequence. Primers can be designed using default parameters a NCBI Primer blast tool, https://www.ncbi.nlm.nih.gov/tools/primer-blast/, IDT Primer quest tool https://www.idtdna.com/Primerquest/Home/Index, http://bioinfo.ut.ee/primer3-0.4.0/primer3/input.htm, http://www.bioinformatics.nl/cgi-bin/primer3plus/primer3plus.cgi or any other software.
4. To validate primers, run a dilution series with 5% or 1% input sample, 1:2, 1:5, 1:10, 1:100. An efficient primer should give a straight line for Ct vs concentration plot and R2 value >90%, at least within 1:2, 1:5, 1:10 of 5% or 1% input dilution series.
5. With validated primers run the qPCR reaction (ChIP-qPCR) with SYBR green using standard protocol or manufacturer's instruction on ABI or Biorad qPCR instruments. Applied Biosystems 7000 detection system using Biorad iTaq Universal SYBR green supermix (172-5124). Example of a typical reaction mixture, 1 μl of fordward primer (10 μM stock), 1 μl of reverse primer (10 μM stock), 12.5 μl of SYBR green (+ROX or other quenchers), 0.5 ng DNA and nano-pure water up to 25 μl.
6. Normalize ChIP-qPCR signal on binding site primer with 5% or 1% input or IgG ChIP-qPCR using Delta Ct (δCt) method. Similarly, normalize to nonbinding site primer signals using the δCt method. Enrichment of at least twofold of antibody ChIP-ed signal over input or IgG or nonbinding site indicates real binding (*see* **Note 9**). Calculate the δCt value using formula,

$$\delta Ct = (\mathrm{Ct}(5\%\mathrm{Input}) - \mathrm{Ct}(\mathrm{ChIP})) \text{ or } \delta Ct = (\mathrm{Ct}(\mathrm{IgG}) - \mathrm{Ct}(\mathrm{ChIP}))$$

Next, calculate the fold enrichment from the δCt values using the formula, fold enrichment = 2(−δCt).

## 4 Notes

1. For all immunoprecipitations done from the sonicated chromatin IP solution in **step 7** in Subheading 3.2, only one 5% input is required. Proceed to ChIP after ensuring sonication efficiency with 5% input for every experiment even when sonication conditions have been optimized.
2. Optional: If ChIP-seq or ChIP-qPCR shows high background, wash beads twice with 0.5% BSA in PBS before the three times with Covaris IP buffer washes.
3. Alternatively, wash only with mild wash buffer for five times if target protein does not bind strongly with DNA.
4. Yellow color indicates the solution is at the correct pH for optimal binding of DNA to the column in the next step.
5. It should be OK to use for histone modifications and polycomb complexes as these have many binding sites on the chromatin, unlike transcription factors for which the column-based method is preferred for higher yields.
6. The sensitivity of Bioanalyzer is in pg/μl range and thus 1 ng of chromatin-immunoprecipitated DNA in 5 μl of elution buffer is sufficient to accurately detect size range of pulled down ChIP-ed DNA and accurately measure concentration, to confirm Qubit concentration estimation.
7. Avoid over sonication of samples as it will reduce DNA size and antigen retention; hence, it will reduce the ChIP signal.
8. This experiment probing antigen retention is good to do during optimization of sonication conditions, to ensure that efficient DNA fragmentation occurs without loss of the antigen being used to pull down the DNA in ChIP.
9. Decreased enrichment of chromatin-immunoprecipitates signal over input or IgG by at least twofold should occur in knockout or knockdown samples of protein being used for ChIP. This validates the specificity of the antibody being used for ChIP.

## Acknowledgments

We thank Stephen Johnson, Ralf Kittler, Francois Guillemot, Jane Johnson, Victor Corces, Sean Goetsch, Bradford Casey, Mark Borromeo, Derek Smith, Tulip Nandu, Xin Liu, Caelin Potts, and Benjamin Nelson for helpful advice on the ChIP-seq project. We also thank the UT Southwestern Medical Center next-generation sequencing core facilities (McDermott sequencing core for library preparation of samples, Illumina HiSeq ChIP-sequencing and

bioinformatics support. Genomics and Microarray core facility for Bioanalyzer,). Jose Cabrera for graphical support. The ChIP-seq work was supported by US National Institutes of Health grants (R01NS093992, R01NS089770, R01NS081203, and K02AG041815), American Heart Association 15GRNT25750034, Department of Defense W81XWH-15-1-0399, and a grant from the Texas Institute for Brain Injury and Repair.

## References

1. Rezza A, Sennett R, Rendl M (2014) Adult stem cell niches: cellular and molecular components. Curr Top Dev Biol 107:333–372. doi:10.1016/B978-0-12-416022-4.00012-3
2. Cheung TH, Rando TA (2013) Molecular regulation of stem cell quiescence. Nat Rev Mol Cell Biol 14(6):329–340. doi:10.1038/nrm3591
3. Fukada S, Uezumi A, Ikemoto M, Masuda S, Segawa M, Tanimura N, Yamamoto H, Miyagoe-Suzuki Y, Takeda S (2007) Molecular signature of quiescent satellite cells in adult skeletal muscle. Stem Cells 25 (10):2448–2459. doi:10.1634/stemcells.2007-0019
4. Venezia TA, Merchant AA, Ramos CA, Whitehouse NL, Young AS, Shaw CA, Goodell MA (2004) Molecular signatures of proliferation and quiescence in hematopoietic stem cells. PLoS Biol 2(10):e301. doi:10.1371/journal.pbio.0020301
5. Hsieh J (2012) Orchestrating transcriptional control of adult neurogenesis. Genes Dev 26 (10):1010–1021. doi:10.1101/gad.187336.112
6. Ma DK, Marchetto MC, Guo JU, Ming GL, Gage FH, Song H (2010) Epigenetic choreographers of neurogenesis in the adult mammalian brain. Nat Neurosci 13(11):1338–1344. doi:10.1038/nn.2672
7. Blanpain C, Fuchs E (2009) Epidermal homeostasis: a balancing act of stem cells in the skin. Nat Rev Mol Cell Biol 10 (3):207–217. doi:10.1038/nrm2636
8. Martynoga B, Mateo JL, Zhou B, Andersen J, Achimastou A, Urban N, van den Berg D, Georgopoulou D, Hadjur S, Wittbrodt J, Ettwiller L, Piper M, Gronostajski RM, Guillemot F (2013) Epigenomic enhancer annotation reveals a key role for NFIX in neural stem cell quiescence. Genes Dev 27(16):1769–1786. doi:10.1101/gad.216804.113
9. Garner MM, Revzin A (1981) A gel electrophoresis method for quantifying the binding of proteins to specific DNA regions: application to components of the Escherichia coli lactose operon regulatory system. Nucleic Acids Res 9 (13):3047–3060
10. Mahony S, Pugh BF (2015) Protein-DNA binding in high-resolution. Crit Rev Biochem Mol Biol 50(4):269–283. doi:10.3109/10409238.2015.1051505
11. Furey TS (2012) ChIP-seq and beyond: new and improved methodologies to detect and characterize protein-DNA interactions. Nat Rev Genet 13(12):840–852. doi:10.1038/nrg3306
12. Pchelintsev NA, Adams PD, Nelson DM (2016) Critical parameters for efficient sonication and improved chromatin immunoprecipitation of high molecular weight proteins. PLoS One 11(1):e0148023. doi:10.1371/journal.pone.0148023
13. Ho JW, Bishop E, Karchenko PV, Negre N, White KP, Park PJ (2011) ChIP-chip versus ChIP-seq: lessons for experimental design and data analysis. BMC Genomics 12:134. doi:10.1186/1471-2164-12-134
14. Hung JH, Weng Z (2016) Mapping short sequence reads to a reference genome. Cold Spring Harb Protoc 2017(2):prot093161. doi:10.1101/pdb.prot093161
15. Ghosh S, Chan CK (2016) Analysis of RNA-Seq data using TopHat and cufflinks. Methods Mol Biol 1374:339–361. doi:10.1007/978-1-4939-3167-5_18
16. Droop AP (2016) fqtools: an efficient software suite for modern FASTQ file manipulation. Bioinformatics 32(12):1883–1884. doi:10.1093/bioinformatics/btw088
17. Cock PJ, Fields CJ, Goto N, Heuer ML, Rice PM (2010) The sanger FASTQ file format for sequences with quality scores, and the Solexa/Illumina FASTQ variants. Nucleic Acids Res 38 (6):1767–1771. doi:10.1093/nar/gkp1137
18. Blankenberg D, Gordon A, Von Kuster G, Coraor N, Taylor J, Nekrutenko A, Galaxy T (2010) Manipulation of FASTQ data with

galaxy. Bioinformatics 26(14):1783–1785. doi:10.1093/bioinformatics/btq281

19. Li H, Handsaker B, Wysoker A, Fennell T, Ruan J, Homer N, Marth G, Abecasis G, Durbin R, Genome Project Data Processing S (2009) The sequence alignment/map format and SAMtools. Bioinformatics 25 (16):2078–2079. doi:10.1093/bioinformatics/btp352
20. Heinz S, Benner C, Spann N, Bertolino E, Lin YC, Laslo P, Cheng JX, Murre C, Singh H, Glass CK (2010) Simple combinations of lineage-determining transcription factors prime cis-regulatory elements required for macrophage and B cell identities. Mol Cell 38 (4):576–589. doi:10.1016/j.molcel.2010.05.004
21. Shen L, Shao N, Liu X, Nestler E (2014) ngs.plot: Quick mining and visualization of next-generation sequencing data by integrating genomic databases. BMC Genomics 15:284. doi:10.1186/1471-2164-15-284
22. Chen TW, Li HP, Lee CC, Gan RC, Huang PJ, Wu TH, Lee CY, Chang YF, Tang P (2014) ChIPseek, a web-based analysis tool for ChIP data. BMC Genomics 15:539. doi:10.1186/1471-2164-15-539
23. Trapnell C, Williams BA, Pertea G, Mortazavi A, Kwan G, van Baren MJ, Salzberg SL, Wold BJ, Pachter L (2010) Transcript assembly and quantification by RNA-Seq reveals unannotated transcripts and isoform switching during cell differentiation. Nat Biotechnol 28 (5):511–515. doi:10.1038/nbt.1621
24. Trapnell C, Roberts A, Goff L, Pertea G, Kim D, Kelley DR, Pimentel H, Salzberg SL, Rinn JL, Pachter L (2012) Differential gene and transcript expression analysis of RNA-seq experiments with TopHat and cufflinks. Nat Protoc 7(3):562–578. doi:10.1038/nprot.2012.016
25. Thomas PD, Campbell MJ, Kejariwal A, Mi H, Karlak B, Daverman R, Diemer K, Muruganujan A, Narechania A (2003) PANTHER: a library of protein families and subfamilies indexed by function. Genome Res 13 (9):2129–2141. doi:10.1101/gr.772403
26. Zhang B, Kirov S, Snoddy J (2005) WebGestalt: an integrated system for exploring gene sets in various biological contexts. Nucleic Acids Res 33(Web Server issue):W741–W748. doi:10.1093/nar/gki475
27. Wang J, Duncan D, Shi Z, Zhang B (2013) WEB-based GEne SeT analysis toolkit (WebGestalt): update 2013. Nucleic Acids Res 41 (Web Server issue):W77–W83. doi:10.1093/nar/gkt439
28. Huang da W, Sherman BT, Lempicki RA (2009) Systematic and integrative analysis of large gene lists using DAVID bioinformatics resources. Nat Protoc 4(1):44–57. doi:10.1038/nprot.2008.211

# Chapter 20

# Study Quiescence Heterogeneity by Coupling Single-Cell Measurements and Computer Modeling

**Jungeun Sarah Kwon, Xia Wang, and Guang Yao**

## Abstract

Single-cell measurements combined with mathematical modeling and computer simulations are powerful tools for understanding and exploring dynamical behaviors of gene networks and cellular functions that they control. Here, we describe experimental and computational methods to study cellular quiescence and its heterogeneity at the single-cell level.

**Key words** Cell cycle, Quiescence, Heterogeneity, Fluorescent protein reporter, DNA content, Click-iT EdU assay, Ordinary differential equation (ODE), Deterministic simulation, Stochastic simulation

## 1 Introduction

Quiescence is often considered the "G0" phase outside the cell cycle. It is however not a uniform resting state but with considerable heterogeneity [1, 2]. Even a population of isogenic cells induced to quiescence by the same experimental condition can exhibit significant cell-to-cell variations in their growth responses. Furthermore, as cells remain quiescent for longer durations, they move progressively "deeper" into quiescence and display an elongated pre-replication phase upon growth stimulation [3–5]. Quiescent cells can also move to a shallower state(s), demonstrated recently as the "$G_{Alert}$" state and "primed" quiescence in muscle and neural stem cells [6, 7]. Dysregulation of quiescence depth can lead to hyper- or hypo-proliferative diseases including cancer and aging [8]. Despite its importance, control mechanisms underlying cellular quiescence and its heterogeneity are poorly understood, due to the lack of an integrated mechanistic framework and effective investigation techniques.

Here, we describe experimental and computational techniques to study quiescence heterogeneity. Experimentally, cells can be brought into quiescence by serum starvation or contact inhibition

H. Daniel Lacorazza (ed.), *Cellular Quiescence: Methods and Protocols*, Methods in Molecular Biology, vol. 1686,
DOI 10.1007/978-1-4939-7371-2_20, 

[1]. Then, quiescence heterogeneity can be investigated by observing how a population of quiescent cells responds to growth stimulation [9, 10]. In particular, the proportion of cells, and their speed, in exiting quiescence and reentering the cell cycle can be measured using fluorescent gene reporters and/or BrdU/EdU incorporation assays over time [9–11]. Furthermore, molecular mechanisms underlying quiescence control can be probed by measuring the dose-dependent effects of ectopically expressed candidate gene(s). Such dose-dependent effects can be measured in a single-transfection/infection experiment, taking the advantage of naturally occurring variations (typically ~3 orders of magnitude) in the vector-delivery efficiency associated with transient transfection (e.g., electroporation) and viral infection [12, 13].

Experimental data and observations can be integrated, explained, and used to make further predictions, using mathematical models and computer simulations. It has been suggested that the heterogeneous quiescent state and its transition to proliferation upon growth stimulation is controlled by a Cyclin/cdk-Rb-E2F gene network, which functions as a bistable switch to convert graded and transient growth signals into an all-or-none E2F activation [9, 14–17]. In this chapter, we briefly describe how to simulate gene responses to serum withdrawal and stimulation using an Rb-E2F mathematical model in COPASI and MATLAB simulators [18]. We further show how to investigate the influences of model parameters (reflecting the rate constants of protein synthesis, degradation, and modification) and their variations on the heterogeneity of quiescence entry and exit. We demonstrate the procedures in both deterministic simulations and stochastic simulations that consider cell-to-cell variations due to intrinsic and extrinsic noise [19, 20].

## 2 Materials

All the reagent solutions are stored at 4 °C unless otherwise noted.

### 2.1 Cell Culture

1. Cell lines: Rat embryonic fibroblasts (REF52 cells) [21] and a single-cell clone (REF/E23 cells) derived from REF52 containing a stably integrated E2F-d2GFP reporter [9].
2. Culture medium: Dulbecco's Modified Eagle Medium (DMEM) containing 10% Bovine Growth Serum (BGS).
3. Serum-starvation medium: DMEM containing 0.02% BGS. Make fresh before use.
4. Trypsin-EDTA (0.05%).
5. Dulbecco's Phosphate-Buffered Saline (DPBS).
6. Cell culture plates (150 mm, 6-well, 12-well).

### 2.2 Propidium Iodide (PI) Staining of DNA Content

1. Preparing nuclear isolation medium (NIM) buffer: 0.5% BSA and 0.1% NP-40 in DPBS.
2. PI-staining buffer: NIM buffer containing 10 μg/ml PI and 100 μg/ml RNase A. Make fresh before use.

### 2.3 Measurement of Quiescence Heterogeneity Using Flow Cytometry

1. Cell fixation buffer (for fluorescent protein reporter): 1% paraformaldehyde (methanol-free) and 3% BGS in DPBS.
2. Click-iT EdU assay kit for flow cytometry (Thermo Fisher Scientific, including reagents described below).
3. EdU (5-ethynyl-2′-deoxyuridine), 10 mM stock solution in DMSO, store at −20 °C.
4. Click-iT EdU fixative: 4% paraformaldehyde in DPBS.
5. 1× Click-iT saponin-based permeabilization and wash reagent (PB): 10× stock solution provided. Make 1× dilution in DPBS containing 1% BSA.
6. Prepare Click-iT reaction cocktail: for each sample, add 250 μl of cocktail mix containing 218.75 μl of DPBS, 5 μl of 100 mM CuSO4, 1.25 μl of fluorescent dye azide, and 25 μl of Click-iT EdU buffer additive (1×). Prepare according to the manufacturer's protocol and use within 15 min of preparation.

### 2.4 Measurement of Dose-Dependent Effects of Quiescence-Modifier Genes with OneElectroporation

1. Plasmid vector (≥1 μg/μl) expressing the gene of interest and a fluorescent protein reporter, or fluorescently labeled siRNA.
2. Neon Electroporation system, electrolytic (E2) buffer, resuspension (R) buffer, Neon Tips (Thermo Fisher Scientific).

### 2.5 Computer Modeling

1. A computer with Windows, Mac, or Linux system.
2. Install COPASI software (free download from http://copasi.org/).
3. Install licensed MATLAB software (Mathworks).

## 3 Methods

All cell culture work should be conducted in a certified tissue culture hood. Use sterilized pipettes, tubes, culture plates, and follow aseptic techniques. Pre-warm the culture medium in a 37 °C water bath prior to cell culture experiments. Store the culture medium at 4 °C after use. The cells are incubated at 37 °C in 5% $CO_2$. The methods described here apply to rat embryonic fibroblast (REF52) cells and can be readily adapted to other cell types.

### 3.1 Induce Cellular Quiescence by Serum Starvation or Contact Inhibition

1. Culture and maintain cells under an actively growing condition (*see* **Note 1**).
2. Serum starvation: Trypsinize and split cells into 6-well culture plates to achieve 30–50% confluence (*see* **Note 2**). Let cells reattach to the plate and recover in the culture medium (2 ml/well) overnight. Wash the cells twice with 1 ml DMEM. Culture the cells in the serum-starvation medium for 2 days or longer (*see* **Note 3**).
3. Contact Inhibition: Trypsinize and split cells in 12-well culture plates to achieve 200–300% confluence in the culture medium (1 ml/well) for 2 days or longer (*see* **Note 4**).
4. Evaluate quiescent cell population by PI staining of DNA content (*see* **Note 5**): Collect the cells by trypsinization (for contact inhibited cells, *see* **Note 6**). Centrifuge the cells in a microcentrifuge tube at 835 × *g* for 3 min. Remove the supernatant and resuspend the cell pellet in PI-staining buffer (*see* **Note 7**). Store cell suspension in 4 °C protected from light. Measure the PI-stained DNA content using a flow cytometer.

### 3.2 Measurement of Quiescence Heterogeneity Using E2F Reporter Cells or Click-iT EdU Assay

1. Induce cellular quiescence in E2F reporter cells (REF/E23) or other cells by serum starvation or contact inhibition (*see* Subheading 3.1).
2. Stimulate cells with a serum gradient by switching cells to culture medium containing varying serum concentrations (*see* **Note 8**). Include EdU in the culture medium at a final concentration of 1 μM if the cells are subject to EdU assay.
3. Harvest cells by trypsinization at varying time points after serum stimulation (*see* **Notes 9** and **10**).
4. In each harvested sample, measure the percentage of cells that exit quiescence as indicated by the E2F-ON state and/or positive EdU incorporation (*see* **Note 11**).
5. Measure the E2F-ON cell percentage: Resuspend the cells in 300 μl of cell fixation buffer and store in 4 °C, protected from light. Measure E2F-GFP reporter activity using a flow cytometer (Fig. 1A).
6. Measure the percentage of EdU-positive cells: Perform the Click-iT EdU Assay according to the modified manufacturer's protocol (*see* **Note 12**).
7. Briefly, fix the cells in 200 μl of Click-iT fixation buffer for 15 min at room temperature, protected from light.
8. Resuspend cell pellet in 500 μl of permeabilization buffer (PB).
9. Spin cells down at 835 × *g* for 3 min.

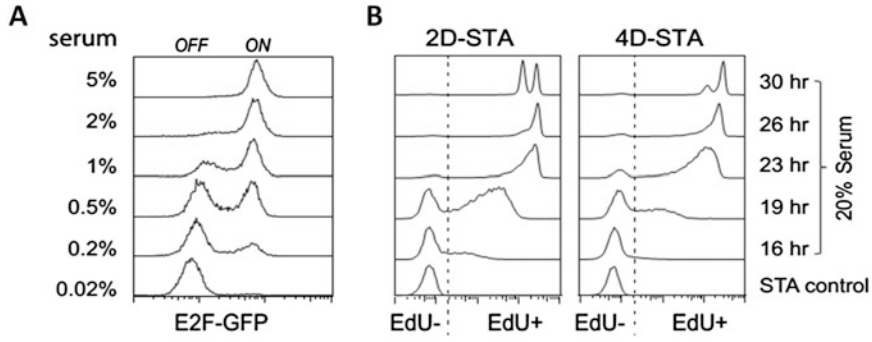


**Fig. 1** Quiescence heterogeneity measured using E2F reporter cells and EdU assay. (**A**) E23 cells were serum starved for 2 days and stimulated with serum at indicated concentrations. E2F-d2GFP reporter activity was measured using flow cytometry 24 h after serum stimulation (reproduced from Ref. [9]). (**B**) E23 cells were serum starved for 2 or 4 days (2D- and 4D-STA, respectively), and stimulated with 20% serum. Cells were harvested at indicated time points and subject to Click-iT EdU assay. EdU intensity was measured using flow cytometry. Higher EdU intensity indicates being closer to the completion of S-phase of the cell cycle (e.g., compare 2D- and 4D-STA cells at the 19th hour after serum stimulation). EdU intensity in the cell reduces by half after cell division (*see* the 30th hr). Each histogram in **A** and **B** represents the distribution of GFP or EdU intensity from approximately 10,000 cells

10. Resuspend cell pellet in 250 μl of Click-iT reaction cocktail. Incubate at room temperature for 30 min, protected from light.
11. Wash cell twice with 500 μl of PB. Resuspend cell pellet in 300 μl of PB and store in 4 °C, protected from light.
12. Run samples on a flow cytometer (Fig. 1B).

### *3.3 Measurement of Dose-Dependent Effects of a Quiescence-Modifier Gene with a Single Electroporation Delivery*

1. Prepare the plasmid vector expressing the gene of interest and a fluorescent protein reporter, or prepare fluorescently labeled siRNA (*see* **Note 13**).
2. Trypsinize actively growing cells, wash cells once with PBS, and resuspend cells at a concentration of $10^6$ cells per 100 μl of resuspension buffer.
3. Add 10 μl of plasmid DNA (10 μg) or siRNA (*see* **Note 14**) to 100 μl of cell suspension and gently mix.
4. Set up the Neon electroporator. Place a Neon tube in the chamber and add 3 ml of E2 buffer. Set the electroporation parameters (for REF52 cells: 1800 V with one 20 ms pulse).
5. Attach a Neon tip (100 μl) to the pipette. Pipet and mix the cell suspension with plasmid/siRNA a few times (*see* **Note 15**). Insert the neon pipette into the Neon tube.
6. Press "Start" on the electroporator and wait for a few seconds. Once electroporation is complete, mix cells with pre-warmed culture medium and transfer to cell culture plates (*see* **Note 16**).

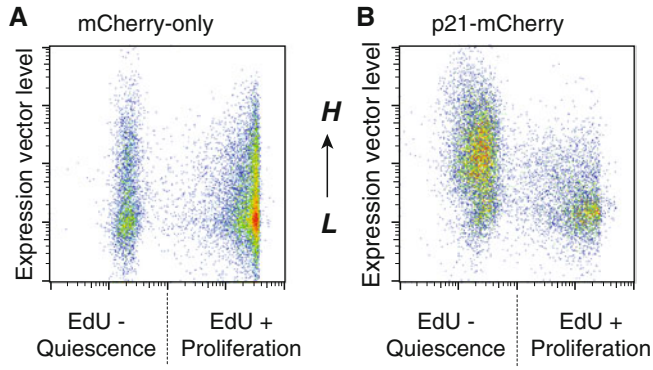


**Fig. 2** Measure dose-dependent effects of a quiescence modifier delivered by a single electroporation. E23 cells were transfected using Neon electroporator with expression vectors of mCherry (**A**) or p21 and mCherry (5:1, co-transfection) (**B**). Cells were recovered overnight in culture medium and induced to quiescence by serum starvation for 2 days. Cells were subsequently stimulated with 3% serum and subject to Click-iT EdU assay and flow cytometry after 32 h. (**B**) The level of p21 expression vector introduced in individual cells was indicated by the intensity of co-transfected mCherry (and the correlation between p21 and mCherry protein levels was verified by immunoflow cytometry, data not shown). With increasing p21 expression (from low/L to high/H), the percentage of cells that were able to respond to 3% serum stimulation and exit quiescence was quickly reduced (compared to that in the mCherry-only transfection control), indicating deeper quiescent states of the affected cells

7. After recovery in culture medium for overnight to a day, induce cells to quiescence by serum starvation or contact inhibition (*see* Subheading 3.1, **steps 2** or **3**).
8. Measure the influence of ectopic gene expression or siRNA on cellular quiescence (*see* Subheading 3.2), with the introduced "dose" of ectopic plasmid or siRNA in individual cells indicated by the intensity of co-introduced fluorescent protein reporter or fluorescent label (Fig. 2).

### *3.4 Modeling Quiescence Control Using Deterministic Simulation in COPASI*

1. Download COmplex PAthway SImulator (COPASI) from http://copasi.org/and install it in your computer (*see* **Note 17**).
2. Import a curated model from BioModels Database (https://www.ebi.ac.uk/biomodels) or create your own in the "Model" module (*see* **Note 18**). Here, we use a curated Rb-E2F bistable model as an example. Download the model from http://www.ebi.ac.uk/biomodels-main/BIOMD0000000318. In "Download SBML," choose SBML L2 V4 (curated), save and import the model into COPASI.
3. Under the Tasks menu, select Time Course. Define the Duration of model simulation (use 24 h in this example, Fig. 3A).
4. Select "Output Assistant" and choose "Concentrations, Volumes, and Global Quantity Values" under Plots, then click "Create."

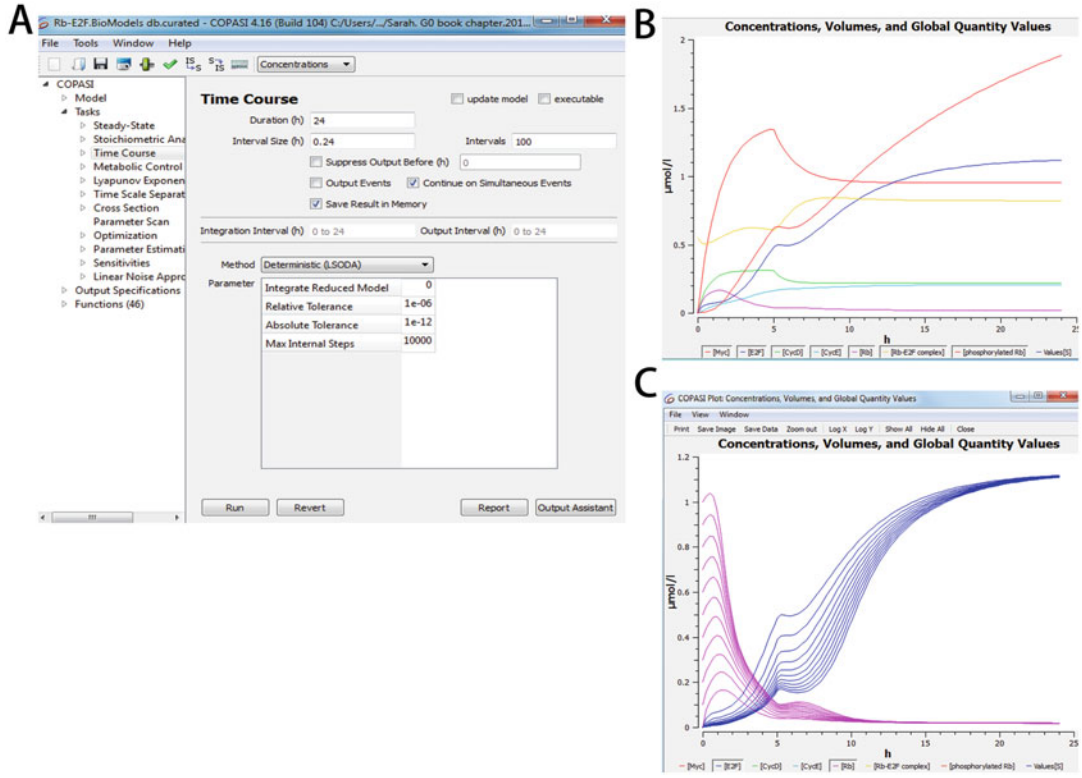


**Fig. 3** Deterministic simulation of the Rb-E2F model in COPASI. (**A**) Time-course simulation interface. Note that the duration was set to 24 (h), and all other settings were default. "Output Assistant" is at the lower right corner. (**B**) Time-course simulation of gene expression in the Rb-E2F network in quiescent cells, responding to a serum pulse (20% for 5 h, dropping to 1% afterward). (**C**) Simulated time-course expression of Rb (*pink curves*) and E2F (*blue curves*) with the initial concentration of Rb scanned from 0 to 1 μM with 10 intervals

5. Click "Run" in the Time Course module and observe the plot of the simulation result (Fig. 3B).
6. Evaluate the effects of varying model parameters on simulated gene activities using Parameter Scan: Under the Tasks menu, select Parameter Scan and click "Create." Select the parameter (s) to be scanned (e.g., the Initial Concentrations of Rb in Species). Define the scanned range of parameter value (e.g., min and max for [Rb]_0 = 0 and 1, respectively). Click "Run" and observe the plotted simulation result (Fig. 3C). Export the simulation result by selecting "Save Data" in the plot window.

### *3.5 Modeling Quiescence Control Using Stochastic Simulation in MATLAB*

1. Install MATLAB® (MathWorks) in your computer.
2. Open a new script editor file (*.m).
3. Create a stochastic Rb-E2F model [22, 23] based on its ODE model (*see* Subheading 3.4), which represents the continuous states of the Rb-E2F gene network (*see* **Note 19**).

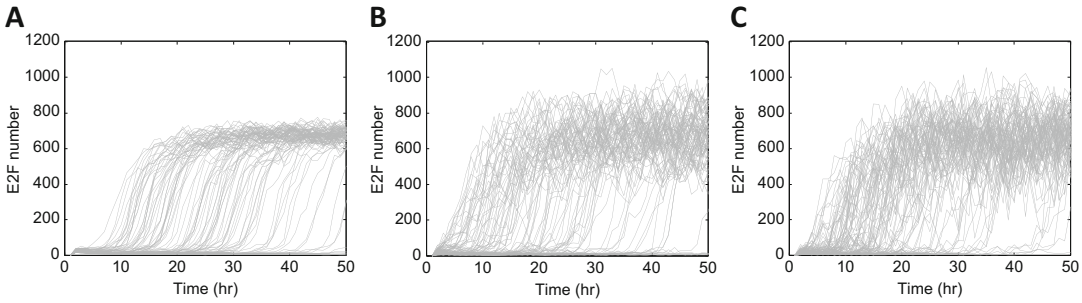


**Fig. 4** Stochastic simulation of the Rb-E2F model. Stochastic simulation of the E2F molecule number change over time in quiescent cells upon stimulation with serum (1%). Intrinsic noise ($\sigma$) and extrinsic noise ($\delta$) were set to $\sigma = 0.1$, $\delta = 10$ (**A**), $\sigma = 0.8$, $\delta = 10$ (**B**), and $\sigma = 0.1$, $\delta = 40$ (**C**), respectively. Results from 100 simulations are shown in each panel. Larger noise led to a relatively quicker E2F activation and a larger variation of E2F molecule number at the E2F-ON state (in cells with E2F activated), but did not significantly affect the mean E2F molecule number at the E2F-ON state

4. Determine the duration of simulation (model time, T), and the number of time steps (N). The time interval ($\Delta t$) is determined by T/N (*see* **Note 20**).
5. Convert the units of model parameters and concentrations of species defined in the ODE model to molecule numbers, using the system size ($\Omega$) and Avogadro constant ($\mathrm{Na} = 6.02 \times 10^{23}\ \mathrm{mol}^{-1}$) (*see* **Note 21**).
6. Save the script editor file. Solve the model numerically by Euler–Maruyama (EM) method in MATLAB at the time interval defined in **step 4** above (*see* **Note 22**) with predefined intrinsic and/or extrinsic noises (*see* **Note 23**).
7. Repeat the simulation (**step 6**) for a desired number of times using the loop control statement, with each simulation representing a single independent cell.
8. Output the simulated time evolution of molecule numbers for each species to a data file (e.g., csv/Excel/txt format).
9. Plot the time evolution of molecule numbers for the species of interest (Fig. 4).

## 4 Notes

1. Change the culture medium every 2–3 days. Do not let cell grow into confluency. Split cells into new culture plates when cells approach high density.
2. Avoid over-trypsinization of cells to ensure a healthy cell population under serum starvation. Wash cells first with DPBS, then add room-temperature trypsin, and incubate at room temperature for ~5 min. Monitor progress under a microscope.

Once most cells are rounded up (not detached), aspirate excess trypsin and leave only a thin layer of trypsin to cover cells. Tap the plate gently against a solid surface to dislodge most cells. Quench remaining trypsin with serum-containing culture medium, and pipet cells into single-cell suspension.

3. Increasing the culture duration under serum starvation will drive cells into deeper quiescence (*see* Subheading 1).
4. For REF52 cells, 300% confluence corresponds to $4 \times 10^5$ cells per well in a 12-well culture plate. The higher the plating density, the quicker the cells enter contact inhibition-induced quiescence. Alternatively, cells can be plated at sub-confluency in a culture medium and allowed to grow into confluence after several days. Increasing the culture duration after cells reach contact inhibition will drive cells into deeper quiescence (*see* Subheading 1).
5. A quiescent cell population exhibits 2n DNA content, distinct from a cycling cell population displaying 2-4n DNA content. Quiescence can also be confirmed with the E2F-OFF state (Fig. 1A, 0.02% serum) and negative EdU incorporation (Fig. 1B, STA control).
6. Contact inhibited cells at high cell density are difficult to be trypsinized. For harvesting, incubate cells with trypsin at 37 °C instead of room temperature and for a longer duration than stated in **Note 2**.
7. It helps to first loose and disperse the cell pellet with a pipet tip before resuspending to ensure that cells are thoroughly mixed with the PI-staining buffer.
8. For serum-starved cells, stimulate cells with varying serum concentrations ranging from 0.02% to 10%. For contact inhibited cells, stimulate cells with serum ranging from 10% to 50%.
9. The typical time points for measuring E2F reporter are between 15 and 30 h (before cell division) depending on the concentration of serum used to stimulate quiescent cells. For EdU assay, cells can be harvested after cell division if necessary since the EdU+ cells are well separated from EdU− cells even after cell division.
10. E2F-GFP reporter activity can also be tracked in individual single cells using time-lapse fluorescence microscopy, in which cells will not be harvested but observed continuously at different time points.
11. Deep quiescent cells are slower to exit quiescence compared to shallow quiescent cells. Meanwhile, a higher percentage of cells will exit quiescence when stimulated with serum at a higher concentration. At a given time point following stimulation at a given serum concentration, a smaller percentage of deep vs. shallow quiescent cells will exit quiescence.

12. EdU is a thymidine analog that gets incorporated into cellular DNA during S phase of the cell cycle, and can be selectively labeled and detected by Click-iT chemistry.
13. The fluorescent protein reporter (e.g., GFP, mCherry) will serve as the transfection indicator of the quiescence-modifier gene in individual cells. The gene of interest and fluorescent protein reporter can be fused directly or through a self-cleaving 2A peptide cassette [24] to generate a protein-level fusion, or via IRES sequence to generate a transcriptional fusion. They can also be co-transfected using two separate expression vectors. When necessary, the expression correlation at the single-cell level between the modifier gene and the fluorescent protein reporter can be confirmed using immunoflow cytometry.
14. Use high-quality plasmid DNA (A260/280 $\geq$ 1.8) in deionized water or TE buffer. The volume of plasmid DNA should not exceed 10% of the total transfection volume. For siRNA, its concentration should be 100–250 μM in the transfection mix (and 10–200 nM in final cell culture medium).
15. Avoid air bubbles when pipetting, as air bubbles can cause arcing during electroporation that kills cells.
16. The culture medium should not contain antibiotics to maximize the viability of electroporated cells.
17. COPASI is a computer simulation program for analysis of biochemical and gene regulatory networks. A list of computer simulation programs can be found at http://systems-biology.org/software/simulation/
18. Refer to the online COPASI manual (http://copasi.org/Support/User_Manual/) or tutorials (http://copasi.org/Support/Video_Tutorials/) for model creation and other tasks and features in COPASI.
19. A stochastic differential equation (SDE) model was derived from the deterministic ODE model based on the chemical Langevin equation (*see* Eq. 3 below). For example, given the ODE for Myc activity,

$$\frac{\mathrm{d}M}{\mathrm{d}t} = \frac{k_{\mathrm{M}} S}{K_{\mathrm{S}} + S} - d_{\mathrm{M}} M \tag{1}$$

we have the SDE for Myc,

$$\frac{\mathrm{d}M}{\mathrm{d}t} = \frac{k_{\mathrm{M}} S}{K_{\mathrm{S}} + S} - d_{\mathrm{M}} M + \sigma\gamma\sqrt{\frac{1}{\mathrm{d}t}}\left(\sqrt{\frac{k_{\mathrm{M}} S}{K_{\mathrm{S}} + S}} - \sqrt{d_{\mathrm{M}} M}\right) + \delta\omega\sqrt{\frac{1}{\mathrm{d}t}} \tag{2}$$

The chemical Langevin equation describes the time evolution of molecular counts of reacting chemical species [25]:

$$X_i(t+\tau) = X_i(t) + \sum_{j=1}^{M} \nu_{ji} a_j[X(t)]\tau + \sigma \sum_{j=1}^{M} \nu_{ji} \left(a_j[X(t)]\tau\right)^{1/2} \gamma + \delta\omega\tau^{1/2} \quad (3)$$

where $X_i(t)$ denotes the molecule number of species $i (i = 1, \ldots, n)$ at time t, and $X(t) = (X_1(t), \ldots, X_n(t))$ with $X(t)$ being the system state at time t. Therefore, the time evolution of the system is measured based on the rates $a_j[X(t)]$ $(j = 1, \ldots, M)$ with the corresponding change of molecule number $i$ described in $v_{ji}$. In this equation, the first two terms represent deterministic kinetics, the third and fourth terms represent intrinsic (reaction-dependent) and extrinsic (reaction-independent) noise. $\gamma$ and $\omega$ are temporally uncorrelated, statistically independent random variables which follow normal Gaussian distribution with mean 0 and variance 1. COPASI program introduced in Subheading 3.4 also provides algorithms to perform stochastic simulation, but it does not allow the change of noise levels.

20. In this simulation example (Fig. 4), we set T = 50 h, N = 50,000, so $\Delta t = 50/50{,}000 = 0.001$.
21. The copy number of species $y_i = x_i \times Na \times \Omega$. Here, $x_i$ is the concentration of species i in ODE model. For example, with the initial concentration of protein A in the ODE model being 2.65 nM = $2.65 \times 10^{-9}$ M, we set the cell volume as $10^{-12}$ L, and thus the initial molecular number of protein A in SDE is $[A] = 2.65 \times 10^{-9} \times 6.02 \times 10^{23} \times 10^{-12} = 1595$ molecules/cell.
22. MATLAB uses numerical integration to calculate the current model state from the state at the previous time point. Generally, decreasing the time interval (i.e., increasing the number of time steps) improves the accuracy of simulation results, which meanwhile takes longer time to complete.
23. σ and δ in Eq. 3 are scaling factors to control the degrees of intrinsic and extrinsic noise, respectively. In this example (Fig. 4), we set σ = 0.1 or 0.8, and δ = 10 or 40 as indicated, respectively.

## Acknowledgment

This work was supported by grants from the NSF (DMS-1463137 and DMS-1418172, to G.Y.), NIH (GM-084905, a T32 fellowship to J.S.K) and the NSF of China and Anhui Province (Grant No. 31500676 and 1508085SQC202, to X.W.).

## References


1. Coller HA, Sang L, Roberts JM (2006) A new description of cellular quiescence. PLoS Biol 4 (3):e83. doi:10.1371/journal.pbio.0040083
2. Yao G (2014) Modelling mammalian cellular quiescence. Interface Focus 4:20130074
3. Augenlicht LH, Baserga R (1974) Changes in the G0 state of WI-38 fibroblasts at different times after confluence. Exp Cell Res 89 (2):255–262
4. Owen TA, Soprano DR, Soprano KJ (1989) Analysis of the growth factor requirements for stimulation of WI-38 cells after extended periods of density-dependent growth arrest. J Cell Physiol 139(2):424–431. doi:10.1002/jcp.1041390227
5. Yanez I, O'Farrell M (1989) Variation in the length of the lag phase following serum restimulation of mouse 3T3 cells. Cell Biol Int Rep 13(5):453–462
6. Rodgers JT, King KY, Brett JO, Cromie MJ, Charville GW, Maguire KK, Brunson C, Mastey N, Liu L, Tsai CR, Goodell MA, Rando TA (2014) mTORC1 controls the adaptive transition of quiescent stem cells from G0 to G (alert). Nature 510(7505):393–396. doi:10.1038/nature13255. nature13255 [pii]
7. Llorens-Bobadilla E, Zhao S, Baser A, Saiz-Castro G, Zwadlo K, Martin-Villalba A (2015) Single-cell transcriptomics reveals a population of dormant neural stem cells that become activated upon brain injury. Cell Stem Cell 17(3):329–340. doi:10.1016/j.stem.2015.07.002. S1934-5909(15)00301-X [pii]
8. Hanahan D, Weinberg RA (2000) The hallmarks of cancer. Cell 100(1):57–70
9. Yao G, Lee TJ, Mori S, Nevins JR, You L (2008) A bistable Rb-E2F switch underlies the restriction point. Nat Cell Biol 10 (4):476–482
10. Dong P, Maddali MV, Srimani JK, Thelot F, Nevins JR, Mathey-Prevot B, You L (2014) Division of labour between Myc and G1 cyclins in cell cycle commitment and pace control. Nat Commun 5:4750
11. Stewart-Ornstein J, Lahav G (2016) Dynamics of CDKN1A in single cells defined by an endogenous fluorescent tagging toolkit. Cell Rep 14(7):1800–1811. doi:10.1016/j.celrep.2016.01.045. S2211-1247(16)30023-7 [pii]
12. Wong JV, Yao G, Nevins JR, You L (2011) Viral-mediated noisy gene expression reveals biphasic E2f1 response to MYC. Mol Cell 41 (3):275–285. doi:10.1016/j.molcel.2011.01.014. S1097-2765(11)00041-4 [pii]
13. Wong JV, Yao G, Nevins JR, You LC (2011) Using noisy gene expression mediated by engineered adenovirus to probe signaling dynamics in mammalian cells. Methods Enzymol 497:221–237. doi:10.1016/B978-0-12-385075-1.00010-X
14. Yao G, Tan C, West M, Nevins JR, You L (2011) Origin of bistability underlying mammalian cell cycle entry. Mol Syst Biol 7:485. doi:10.1038/msb.2011.19. msb201119 [pii]
15. Tyson JJ, Baumann WT, Chen C, Verdugo A, Tavassoly I, Wang Y, Weiner LM, Clarke R (2011) Dynamic modelling of oestrogen signalling and cell fate in breast cancer cells. Nat Rev Cancer 11(7):523–532. doi:10.1038/nrc3081. nrc3081 [pii]
16. Aguda BD, Tang Y (1999) The kinetic origins of the restriction point in the mammalian cell cycle. Cell Prolif 32(5):321–335
17. Novak B, Tyson JJ (2004) A model for restriction point control of the mammalian cell cycle. J Theor Biol 230(4):563–579
18. Hoops S, Sahle S, Gauges R, Lee C, Pahle J, Simus N, Singhal M, Xu L, Mendes P, Kummer U (2006) COPASI–a COmplex PAthway SImulator. Bioinformatics 22(24):3067–3074. doi:10.1093/bioinformatics/btl485. btl485 [pii]
19. McAdams HH, Arkin A (1997) Stochastic mechanisms in gene expression. Proc Natl Acad Sci U S A 94(3):814–819
20. Hasty J, Pradines J, Dolnik M, Collins JJ (2000) Noise-based switches and amplifiers for gene expression. Proc Natl Acad Sci USA 97(5):2075–2080. doi:10.1073/pnas.040411297
21. Logan J, Nicolas JC, Topp WC, Girard M, Shenk T, Levine AJ (1981) Transformation by adenovirus early region 2A temperature-sensitive mutants and their revertants. Virology 115(2):419–422
22. Lee T, Yao G, Bennett DC, Nevins JR, You L (2010) Stochastic E2F activation and reconciliation of phenomenological cell-cycle models.

PLoS Biol 8(9):e1000488. doi:10.1371/journal.pbio.1000488

23. Srimani JK, Yao G, Neu J, Tanouchi Y, Lee TJ, You L (2014) Linear population allocation by bistable switches in response to transient stimulation. PLoS One 9(8):e105408. doi:10.1371/journal.pone.0105408. PONE-D-14-22009 [pii]
24. Szymczak AL, Workman CJ, Wang Y, Vignali KM, Dilioglou S, Vanin EF, Vignali DA (2004) Correction of multi-gene deficiency in vivo using a single 'self-cleaving' 2A peptide-based retroviral vector. Nat Biotechnol 22 (5):589–594. doi:10.1038/nbt957
25. Gillespie DT (2000) The chemical Langevin equation. J Chem Phys 113(1):297–306. doi:10.1063/1.481811

# INDEX



H. Daniel Lacorazza (ed.), *Cellular Quiescence: Methods and Protocols*, Methods in Molecular Biology, vol. 1686,
DOI 10.1007/978-1-4939-7371-2, © Springer Science+Business Media LLC 2018

## G



## H



## I



## K



## L



## M



## N



## O



## P



## Q

## R



## S



## T



## V



## W



## Y